Univerzita Karlova v Praze

1. lékařská fakulta

Charles University in Prague

First faculty of Medicine

Studijní program: Biomedicína

Studijní obor: Fyziologie a patofyziologie člověka

Msc. Karina Vargová

Role onkogenní mikroRNA-155 a proto-onkogenu *MYB* u chronické lymfatické leukémie

The Role of oncogenic microRNA-155 and proto-oncogen *MYB* in chronic lymphocytic leukemia

Disertační práce

Ph.D. Thesis

Školitel/Supervisor: Doc. MUDr. Tomáš Stopka, Ph.D.

Prague 2013

Prohlášení:

Prohlašuji, že jsem závěrečnou práci zpracovala samostatně a že jsem řádně uvedla a citovala všechny použité prameny a literaturu. Současně prohlašuji, že práce nebyla využita k získání jiného nebo stejného titulu.

Souhlasím s trvalým uložením elektronické verze mé práce v databázi systému meziuniverzitního projektu Theses.cz za účelem soustavné kontroly podobnosti kvalifikačních prací.

Declaration:

I hereby declare that I have written this PhD Thesis with help of the cited work. The text of this Thesis was not used to apply for other degree than this. I herby agree with electronic deposition of this Thesis and any validations of its originality.

V Praze/In Prague, 21.08.2013

Mgr. Karina Vargová

Podpis/Signature

Identifikační záznam:

VARGOVÁ, Karina. *Role onkogenní mikroRNA-155 a proto-onkogenu MYB u chronické lymfatické leukémie. [The Role of oncogenic microRNA-155 and proto-oncogen MYB in chronic lymphocytic leukemia].* Praha, 2013. 170s, 2 přílohy. Doktorská práce (Ph.D.). Univerzita Karlova v Praze, 1. lékařská fakulta, Ústav patologické fyziologie, Praha. Školitel: Stopka, Tomáš.

ACKNOWLEDGEMENT

I am cordialy thankful to my Ph.D. mentor Dr. Tomáš Stopka for his overall support, endless scientific enthusiasm, and experimental guide as well as scientific discussions.

I thank to all members of our laboratory for their outstanding collaboration, for excellent working atmosphere, discussions and advice. Especially to Vít Pospíšil, Juraj Kokavec, Pavel Burda, Nikola Čuřík, Vojtěch Kulvait, Tomáš Zikmund, Jarmila Vargová (Podskočová), Petra Vlčková (Bašová), Martina Dluhošová (Kapalová), Hanka Hušková and Nina Dusílková as well as to others including Pavel Klener, Magda Klánová, Bokang Calvin Maswabi, Jan Molinský, Filipp Savvulidi and Luděk Šefc.

I would like to acknowledge help with clinical data and patients donation of Professor Marek Trněný, Dr. Petra Obrtlíková, Dr. Adela Berková (General Faculty Hospital) and Dr. Jiří Zavadil (NYU) for excellent collaborative bioinformatics research.

I also thank to Professor Emanuel Nečas, former Head of the Institute of Pathological Physiology, and current Head of the Institute Dr. Martin Vokurka, for their continuous support.

My special acknowledge goes to my colleague and close friend Erika Kužmová for her help with proof-reading of the text and discussions.

On a personal note, I am fortunate to be surrounded by loving family and friends. My deepest gratitude goes to my parents and brother Richard for their support and encouragement during my whole studies.

My profound gratitude goes to my beloved partner Filipp for his endless support, discussions and love.

CONTENT

ABSTRAKT (CZ)

B-buněčná lymfocytární chronická lymfatická leukémie (B-CLL) představuje nádorové onemocnění, pro které je význačná akumulace B-buněk v periferní krvi, kostní dřeni, lymfatických uzlinách a slezině v důsledku poruchy programované smrti. Klinický průběh B-CLL je značně heterogenní, což dokazuje i fakt, že u některých pacientů toto onemocnění rychle progreduje, zatímco jiní pacienti přežívají několik let bez nutnosti léčby. I když se onemocnění charakterizuje stanovováním několika prognostických parametrů, jež jsou typické pro B-CLL, chybí spolehlivá indikace začátku včasné terapie. Z popsaného důvodu je v současnosti velice intenzivně studována nejenom biologická role malých nekódujících RNA (tzv. mikroRNA), ale také spojitost těchto molekul se vznikem a průběhem leukemických onemocnění včetne B-CLL. Proto jsme se zaměřili na studium miR-155, která reguluje diferenciaci buněk krvetvorby, zánětlivých reakcí a produkci protilátek. Zvýšená exprese miR-155 se objevuje v leukemogenezi, kde se předpokládá, že má vliv na zástavu buněčné diferenciace a narušení normální funkce B-buněk. Naše výsledky potvrdily zvýšenou expresi jejího primárního transkriptu miR-155 a také maturované formy u pacientů s B-CLL. Analýza expresních dat kohorty 239 pacientů s B-CLL naznačuje, že vzorky pacientů s nepříznivou prognózou vykazují signifikantně vyšší hladiny obou forem miR-155 s nimiž prokazatelně souvisí nízké hladiny proteinu PU.1 oproti kontrolám. Domníváme se, že jedním z mechanizmů vzniku leukémie by mohla být nižší exprese proteinu PU.1 zapříčiněná vysokou hladinou miR-155. Naše výsledky dále ukazují, že transkripční faktor, proto-onkogen MYB z rodiny E-box proteinu se přímo váže do promotorové oblasti genu pro miR-155 - *MIR155HG*, čímž stimuluje jeho transkripci. V oblasti vazebních míst pro MYB jsme detekovali přítomnost chromatinových značek: H3K9Ac a H3K4Me3. Funkční *in vitro* eseje s primárními buňkami pacientů s B-CLL dále prokázaly vzájemný negativní vztah mezi miR-155 a PU.1, a pozitivní vztah mezi MYB a miR-155. Na základě našich výsledků jsme vytvořili pracovní model pro B-CLL, kde MYB stimuluje transkripci miR-155, který následně snižuje produkci PU.1 v B-CLL buňkách. U 20% měřených vzorků B-CLL byl prokázán výše uvedený vztah. Úspěšnost léčby B-CLL spočívá v jejím správném zahájení. Zjistili jsme, že zvýšená exprese miR-155 koreluje s agresivitou B-CLL. Můžeme shrnout, že měření exprese molekul miR-155, MYB a PU.1 u pacientů s B-CLL by tedy mohlo být vhodným nástrojem pro detailnější charakterizaci onemocnění, které by dále umožnilo včasné zahájení terapie.

KLÍČOVÁ SLOVA: B-CLL, terapie, mikroRNA, mRNA, miR-155, MYB, PU.1, genová exprese, leukemie, chromatinové modifikace, DNA, protein.

ABSTRACT (EN)

Chronic lymphocytic leukemia (B-CLL) represents a disease of mature-like B-cells. Due to failed apoptosis but also due to enhanced proliferative signals, the leukemic B-cells accumulate in the peripheral blood, bone marrow, lymph nodes and spleen. The clinical course of B-CLL is very heterogeneous; in some patients B-CLL progresses very rapidly into an aggressive form. Such patients need therapy sooner while in other patients with indolent B-CLL the onset of therapy takes years. Several standard prognostic and disease progression markers are used for disease staging and monitoring, however a reliable marker that will suggest when to start therapy is unknown. Expression of small, non-coding microRNAs is often deregulated and represent important prognostic markers in variety of cancers including leukemia. Hence in our study we concentrated to miR-155, an important molecule regulating differentiation of hematopoietic cells, inflammation process and antibody production. Its aberrant expression was described in Hodgkin`s as well as in non-Hodgkin`s lymphoma, including indolent lymphoproliferations like B-CLL. Our results confirmed elevated levels of both, primary miR-155 transcript and mature form of miR-155 in our B-CLL patient samples (N=239). The aberrant expression of miR-155 in B-CLL samples associated with unfavorable prognosis. Moreover, we also observed elevated miR-155-mediated decrease of its direct target – PU.1 in B-CLL cells that is important regulator of B-cell maturation. Next, we demonstrated that proto-oncogen MYB directly binds at the promoter region of the miR-155 gene - *MIR155HG* and stimulates its transcription. This coincided with enrichement of activated epigenetic marks: hypermethylated histone H3K4 residue and spreaded hyperacetylation of H3K9 at the *MIR155HG* promoter. Our *in vitro* functional assays on the primary B-CLL cells and Raji cell line confirmed the negative relationship between miR-155 and PU.1 and positive relationship between MYB and miR-155. We also have shown that unfavorable prognosis of B-CLL associates with low expression of miR-150 (inhibitor of Myb) and high expression of MYB mRNA. Based on above-mentioned results, we created working model of relationship between miR-155, MYB and PU.1 that can be applied to around 20% of more aggressive B-CLL patients. The success of therapy of B-CLL patients depends on the accurate start of the therapy. Our data also indicate that the levels of miR-155 in B-CLL patients associate with the disease progression and can be used to predict therapy onset. We conclude that measurement of miR-155, MYB and PU.1 expression associates with B-CLL progression and could help in making valuable clinical decisions.

KEY WORDS: B-CLL, therapy, microRNA, mRNA, miR-155, MYB, PU.1, gene expression, oncogene, chromatin modifications, DNA, protein.

LIST OF ABBREVIATIONS

ABC/GC	activated B-cell like/germinal center (type of DLBCL)
ADAR	adenosine deaminase
AGO-1-4	argonaut family proteins 1-4
AID (AICDA)	activation-induced cytidine deaminase
ALL	acute lymphoblastic leukemia
ALV	avian leukosis virus
AML	acute myeloid leukemia
AMV	avian myeloblastosis virus
AP-1	activator protein 1
APL	acute promyelocytic leukemia
ARS2	arsenate resistance protein 2
ATM	ataxia-telangiectasia mutated
AVG	average
BCL2	B-cell lymphoma 2
BCL6	B-cell lymphoma 6
B-CLL	B-cell chronic lymphocytic leukemia
BCR	B-cell receptor
BIC	B-cell Integration Cluster
bp	base pair
BSA	bovine serum albumine
Btk	Bruton`s tyrosine kinase
CD38	cluster of differentiation 38
cDNA	complementary DNA
c-Fos	cellular FBJ murine osteosarcoma viral oncogene homolog
CLP	common lymphoid progenitor
CML	chronic myeloid leukemia
ChIP	chromatin immunoprecipitation
DBD	DNA binding domain
DGCR8	DiGeorge syndrome critical region gene 8
DLBCL	diffuse large B-cell lymphoma
DMSO	dimethyl sulfoxide
DNA	deoxyribonucleic acid
dNTPs	deoxynucleotide triphosphates
DSMZ	Deutsche Sammlung von Mikroorganismen und Zellkulturen GmbH
ES	enrichment score
ETS family	E twenty-six family proteins
FACS	Fluorescence Activated Cell Sorting
FADD	Fas-associated protein with death domain
FBS	fetal bovine serum
FC	fold change
FCR	Fludarabine-Cyclophosphamide-Rituximab
FISH	Fluorescence *in situ* hybridization
FITC	Fluorescein isothiocyanate
FosB	FBJ murine osteosarcoma viral oncogene homolog B
FOXP3	forkhead box P3

FUS	fused in sarcoma
GAPDH	glyceraldehyde 3-phosphate dehydrogenase
GSEA	gene set enrichment analysis
H2A	histone H2A
H3	histone H3
H3K4Me3	H3K4 methyl3
H3K9Ac	H3K9 acetyl
HIF1A	hypoxia inducible factor 1A
Hsa	*Homo sapiens*
HSC	hematopoietic stem cell
HSPCs	hematopoietic stem progenitor cells
hrs	hours
IFNα/β	interferon α/β
IFNγ	interferon γ
IgM	immunoglobulin M
IgVH	immunoglobulin heavy chain variable
IL-2	interleukin-2
IMDM	Iscove's Modified Dulbecco's Medium
IRAK3	interleukin-1 receptor-associated kinase 3
Kb	kilo base
kDa	kilo Dalton
KRAS	Kirsten rat sarcoma viral oncogene homolog
KSHV	Kaposi's sarcoma-associated herpesvirus
LMP-1	latent membrane protein
MAD2, 4	mitotic arrest deficient, yeast, homolog-like 2, 4
MAFB	v-maf musculoaponeurotic fibrosarcoma oncogene homolog B
MAP3K7	mitogen-activated protein kinase kinase kinase 7
MBL	monoclonal B-cell lymphocytosis
MCL	mantle cell lymphoma
MGB	minor groove binder
min	minutes
miRNA	microRNA
miRNA-155	microRNA-155
miR-155	microRNA-155
MIR155HG	miR-155 Host Gene
mmu	*Mus musculus*
MOI	multiplicity of infection
mRNA	messenger RNA
MYB	v-myb myeloblastosis viral oncogene homolog
MYC	v-myc avian myelocytomatosis viral oncogene homolog
NES	normalized enrichment score
NFκB	nuclear factor kappa B
NFQ	non-fluorescent quencher
NHL	non-Hodgkin`s lymphoma
nM	nano molar
NRD	negative regulation domain
Nt	nucleotide

ORF	open reading frame
OS	overall survival
P/S	penicillin/streptomycin
PABP	poly(A)-binding protein
PACT	protein activator of PKR
PBMC	peripheral blood mononuclear cells
PBS	phosphate buffered saline
PI	propidium iodide
PI3K	phosphoinositide 3-kinase
pre-miRNA	precursor microRNA
pri-miRNA	primary transcript of microRNA
RISC	RNA induced silencing complex
RNA	ribonucleic acid
RS	Richter`s syndrome
RT-qPCR	reverse transcription quantitative polymerase chain reaction
SATB1	special AT-rich Binding protein-1
SEM	standard error of the mean
Sfpi1(Pu.1)	spleen focus forming virus proviral integration oncogene (*Mus musculus*)
SHIP1	inositol polyphosphate-5-phosphatase
SHM	somatic hypermutation
siRNA	small interfering RNA
SLL	small lymphocytic leukemia
SMAD2, 4	Sma- and Mad-related protein 2,4
SPI1 (PU.1)	spleen focus forming virus proviral integration oncogene (*Homo sapiens*)
STAT3	signal transducer and activator of transcription 3
stRNA	small temporal RNA
TAD	transactivation domain
TF	transcription factor
TGF-β	tumor growth factor β
Th	therapy
TLR	Toll-like receptor
TRBP	ribonucleo protein
tRNAs	transfer RNA
TSS	transcription start site
UTR	untranslated region
WHO	World Health Organisation
wt	wild type
ZAP-70	zeta associated protein about 70kDa

Motto:

The success of therapy of B-CLL patients depends on the accurate start of the therapy.

1. INTRODUCTION

1.1 Characterization, diagnosis, progression and therapeutic tools of B-cell chronic lymphocytic leukemia (B-CLL)

1.1.1 What is B-CLL?

B-CLL represents slow-growing leukemia characterized by an accumulation of leukemic, mature appearing B-cells in the bone marrow, lymph nodes, spleen and in the peripheral blood [1,2]. The WHO classification characterizes B-CLL as leukemia of mature B-cells [3]. Accumulation of leukemic B-cells is due to imbalance between emerging and apoptosis of B-cells. As a result of failed apoptosis, most B-CLL cells are arrested in G0/G1 [4]. The high number of lymphocytes in B-CLL patients is caused not only by the prolonged survival of B-cells with failed apoptosis, but also by proliferating of subset B-cells in proliferative centers in lymph nodes and bone marrow [5,6]. Messmer *et al.* showed that B-CLL represents a non-static disease where cells displayed dynamic cellular kinetics: some cells proliferate and some die [7]. The stimulation of endothelial cells and T-cells activates B-CLL cells to divide and reinforces their resistance to apoptosis. The B-CLL cells are then released from proliferative centres into peripheral blood where they start to express markers of activation (CD154, IL-2, CD38). Activated B-CLL cells are further attracted by chemokines back into tissues and proliferative centres [8]. Normal healthy B-cells originate from bone marrow and mature in the lymph nodes where they are specialized to fight infections by producing antibodies. Leukemic B-cells grow out of control, accumulate in the bone marrow and in peripheral blood and overgrow healthy normally functioning blood cells [9]. It is under intensive study how the normal B-cell transforms into the leukemic cell. *In vitro* studies on the primary leukemic cells help to understand the pathogenesis of leukemia in more detail.

The etiology of B-CLL is still unclear and actively discussed. The identification of the cellular origin of B-CLL is essential to elucidation of the pathobiology of leukemia development. In most B-CLL cases, the disease manifests initially as a precursor phase, called monoclonal B lymphocytosis (MBL), characterized by asymptomatic monoclonal or oligoclonal proliferation of CD5+ B-cells. The primary leukemogenic event in B-CLL might involve self-renewing hematopoietic stem cells. Thus, the accumulation of leukemic events in B-CLL cells begins at the HSC stage [10]. Moreover, Goldin *et al.,* described that B-CLL

precedes MBL with higher frequency in the hereditary form of B-CLL [11]. The MBL shares some similarities with B-CLL, as for example chromosomal aberrations [11,12]. Acquisition of chromosomal aberrations as deletion of 11q22-23, 17p13, 13q14 or trisomy of chromosome 12 appears to be the secondary driver of B-CLL development [10,13]. Chromosomal aberrations and microenvironment stimuli influence selection and expansion of the B-CLL malignant clone [14].

The study of small non-coding, regulatory microRNAs in the molecular pathogenesis and development of B-CLL dramatically increased in the last decade [15]. Croce`s research group [16] showed the first evidence that miRNAs are involved in the pathogenesis of B-CLL. Authors found that decreased expression of miR-15-16 cluster associates with frequent deletion of chromosome 13q14 in B-CLL cells [16]. The recently published data showed that miRNAs as: miR-21, miR-150, miR-155, miR-181b, miR-34, miR-29 are differentially expressed in B-CLL [16–18]. The recent evidence suggests that miRNAs could be used as biomarkers for B-CLL prognosis and progression [19,20].

1.1.2 Epidemiology of B-CLL

B-CLL belongs to the most common leukemia in the Western world and affects mainly elderly population with a median age around 70 years. Rarely, B-CLL developes in the individuals under 50 years [21]. In contrast, in Asian population B-CLL arise with very rare frequency [22]. Further, in males B-CLL develops with significantly higher prevalence (the male:female ratio is 2:1) [23]. In the hereditary form of B-CLL the incidence of B-CLL or another lymphoid neoplasm is three times higher as in general population [24]. The highest risk of B-CLL development display siblings of the same gender, especially sons where mother was affected with leukemia [25].

1.1.3 Diagnosis of B-CLL

Typical symptoms of B-CLL include weight loss (≥10%) within 6 month; fevers of >38°C for more than 2 weeks without evidence of infection; night sweats; extreme fatique [26]. Among the B-CLL symptoms there are also presented signs of B-CLL as lymphadenopathy (common at the initial phase of B-CLL); painless splenomegaly; hepatomegaly; lessions on skin (macules, papules, ulcers, blisters)[27]; glomerulonephritis have occasionally been

described. However, in 25% of B-CLL cases, above described symptoms and signs are not present [26].

The diagnosis of B-CLL follows criteria:

A: Peripheral blood analysis

To be diagnosed as B-CLL positive, patient must display more than 5000 of B lymphocytes in 1µl of peripheral blood (lymphocytosis) in duration of 3 months. The clonallity of the leukemic B-cells must be confirmed by presence of typical B-CLL surface markers detected by flow cytometry: CD5/CD23/CD19/CD20. The B-CLL cells display reduced levels of IgM, IgD and CD79b as compared to normal B-cells [2]. Strict immunophenotyping of CD5+ B-cells by flow cytometry confirms the suspected diagnosis of B-CLL and helps to distinguish B-CLL from other lymphoproliferative disorders. The CD5+ B-CLL cells differ in presence of CD23, CD22 surface markers from MCL (mantle cell lymphoma) where these markers are missing [21,28]. Elevated level of B2 microglobulin in serum represents another blood abnormality in B-CLL; it is associated with poor prognosis [26].

In the typical blood smear of leukemic B-CLL cells, mature appearing small to medium size B-cells with a compact and visible cytoplasm are clearly detected (Figure 1.1). Nucleus is dense with partially aggregated chromatin and with hard to recognize nucleolus. A small part of B-cells (~10%) may be twice larger with clearly visible nucleolus: these cells are designated as prolymphocyte like cells (Figure 1.2).

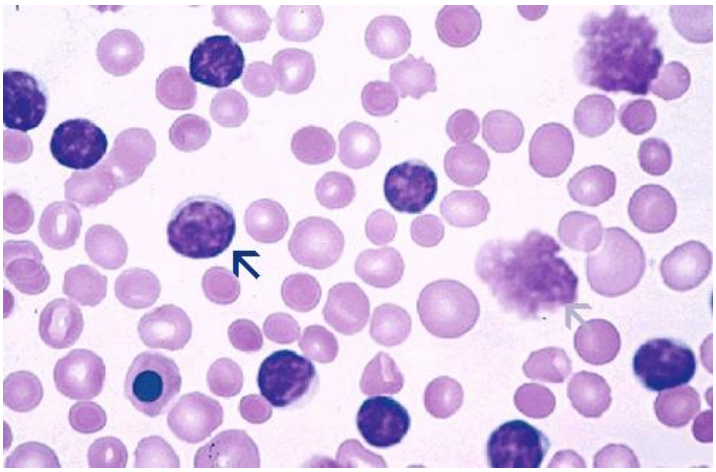

Figure 1.1: Typical blood smear of B-CLL cells (adapted from Brandon Guthery and Nasir Bakshi, 2007 - http://moon.ouhsc.edu/kfung/jty1/HemeLearn/HemeCase/PB-001-Ans.htm]). Dark blue arrow indicates typical B-CLL cell and gray arrow indicates “smudge cell”, that is very often seen in B-CLL blood smear.

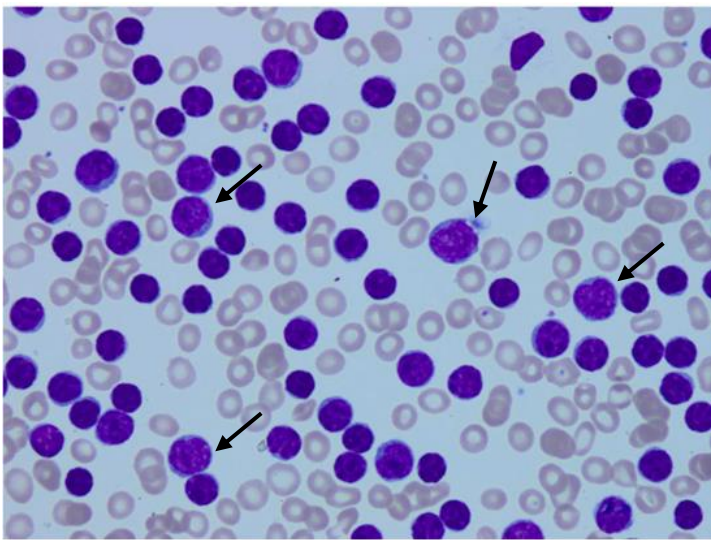

Figure 1.2: Blood smear of B-CLL with prolymphocytes like cells (adapted from [18]). Black arrows indicate prolymphocytes.

B: Bone marrow aspiration, biopsy

The bone marrow examination usually shows more than 30% of mature B-cells. The pattern of marrow infiltration (diffuse, non-diffuse) reflects disease progression, provides prognostic information [2]. The bone marrow examination is accessory parameter for B-CLL diagnosis.

C: Mutational status of IgVH genes and expression of prognostic markers CD38 and ZAP-70

The process of somatic hypermutation introduces mutations in the variable segments of immunoglobulin variable heavy chain gene (**IgVH**). The proliferating B-CLL cells display mutated IgVH gene as these cells undergo somatic hypermutation in the germinal centers. In contrast, B-CLL cells with unmutated IgVH genes derived from pre-germinal centers [29]. The IgVH gene is considered as „mutated“ when shows <98% homology to germ line. The „unmutated“ IgVH is then when the homology to germ line is >98% [30,31].

Determination of presence **ZAP-70** [32] and CD38 on the B-CLL cells [33] allows to predict the prognosis of asymptomatic patients. ZAP-70 (zeta association protein; 70kDa) is member of family Syk protein tyrozin kinases. The normal B-cells do not express ZAP-70 while the normal T and NK cells express ZAP-70. B-cell receptor enhances expression of ZAP-70 on B-CLL cells [34]. ZAP-70 binds on the CD3-zeta and by this engagement activates T-cells [35] Activated T-cells then differentiate, proliferate and secrete a number of cytokines. The estimated cutt-off level of B-cells is usually 20%. Unfortunatelly this method is not well

standardized [28], moreover by measuring of the expression ratio of ZAP-70 on T-cells/B-CLL cells improves the prognostication and prediction of B-CLL clinical course [36]. ZAP-70 represents a rather surrogate prognostic marker in addition to IgVH mutation status and CD38 expression [37].

Measurement of **CD38** surface marker expression on B-CLL cells reflects the situation occuring inside the cell while CD38 represents an indicator of cellular activity (dividing and growing cells). This is a reason why a such CD38+ B-CLL clone is rather associated with the poorer prognosis [38]. Generally, the cut-off for CD38 positivity varies from 7-30% [39]. The percentage of CD38+ cells together with expression of ZAP-70 on B-CLL cells provides even stronger prognostic value as each marker separately [40].

D: Molecular cytogenetic: an optional prognostic test

Evaluation of chromosomal abnormalities by molecular genetics fluorescence *in situ* hybridization (FISH) helps to predict prognosis of B-CLL progression [28]. The hierarchical model described by Döhner *et al.,* defines five prognostic categories in B-CLL (1. deletion of 13q14 as a sole aberration; 2. trisomy of 12 chromosome; 3. deletion of 11q22-23; 4. deletion of 17p13; 5. normal karyotype). The most frequent chromosomal abnormality represents loss of **13q14.3** region with prevalence 55% [13]. This cytogenetic aberration associates with favorable prognosis [13].

The second chromosomal abnormality represents trisomy of long arm of 12 chromosome **(t12q)** with prevalence around 12% in B-CLL patients [13]. This chromosomal aberration represents intermediate risk in B-CLL prognosis [13].

The third chromosomal aberration represents deletion of chromosome **11q22-23** with prevalence 18% in B-CLL patients and associates with poor prognosis [13]. This deleted region includes ataxia-telangiectasia mutated (*ATM*) gene which is mutated in 30% of B-CLL cases and represents sign of rapid disease progression [13,41].

The fourth chromosomal aberration represents deletion of chromosome **17p13** with prevalence 7% [13]. The deleted region contains gene *TP53*: the guardian of the cell genome. B-CLL patients with deleted 17p13 chromosome have most likely deleted or mutated gene *TP53* and predispose to poor prognosis [42].

The last category represents normal karyotype [13].

1.1.4 Clinical staging of B-CLL

Standard methods for assessment of B-CLL prognosis represent Rai and Binet staging system. These staging systems are based on the results from physical examinations and blood tests [43,44].

The **Rai staging system** (Kanti R. Rai, USA) defines three categories of risk disease: low, intermediate and high [2].

Low risk: lymphocytosis with leukemic cells (>30%) in blood and/or in bone marrow (Rai stage 0)

Intermediate risk: lymphocytosis; enlarged lymph nodes; splenomegaly and/or hepatomegaly (Rai stage I-II)

High risk: anemia (Hg<11g/dl) or thrombocytopenia (Rai stage III-IV)

The **Binet staging system** (Jacques-Louis Binet, France) is based: on A) area of presented enlarged lymph nodes (>1cm) or organomegaly (categories: A-C), B) on presence of anemia or thrombocytopenia (categories: 1-5):

A) Area of presented enlarged lymph nodes:

1. Head and neck.
2. Axillae.
3. Groins.
4. Palpable spleen.
5. Palpable liver.

B) Anemia or thrombocytopenia:

A: Hg 100g/L or more; platelets $100x10^9$/L or more

B: Hg 100g/L or more; platelets $100x10^9$/L or more; organomegaly

C: Hg <100g/L; platelets $<100x10^9$/L; irrespective to organomegaly

1.1.5 Progression and transformation of B-CLL

Small lymphocytic leukemia (SLL) shows very similar manifestation as B-CLL. SLL is clinically defined by presence of lymphadenopathy, clonal marrow infiltration, but with absence of peripheral blood lymphocytosis and cytopenia. Number of B-cells in the peripheral blood should not exceed 5000 per μL. The SLL diagnosis needs to be confirmed by histopathological evaluation of lymph nodes [2].

B-CLL/SLL could transform into more aggressive non-Hodgkin lymphoma (NHL) called Richter's syndrome (RS) [45]. RS develops with frequency 5-7% and is mostly represent as diffuse large B-cell lymphoma (DLBCL) [46]. Patients with RS have a very poor prognosis [46]. The molecular mechanism leading to RS transformation from B-CLL is unknown.

1.1.6 Conventional and novel therapeutic tools of B-CLL

The manifestation of B-CLL is very heterogeneous. One third of B-CLL patients do not need therapy and survive for years; in another third of B-CLL patients the indolent course of disease progresses; the remaining third of B-CLL patients exhibits aggressive onset at the beginning and needs immediate therapy [29]. In many patients, typical symptoms or signs of B-CLL do not manifest; in this case, the B-CLL is revealed simply by routine blood test. Standard treatment of B-CLL is based on "watch and wait" strategy with controls of blood counts and clinical examinations over a period of 3-6 months [26]. Therapy to B-CLL patients is applied when the symptoms are visible and the disease progresses rapidly [2,26]. We can split the chemotherapy components into several groups [2]:

A: Cytostatic agents.

From the purine analogues, the Fludarabine monotherapy is by far the most used and studied as it shows the best results: 7-40% of complete remission rate and overall survival (OS) 66 month [47]. Nowadays, the standard first line of therapy B-CLL patients in good condition without comorbidities is considered combination of Fludarabine, Cyclophosphamide and Rituximab (FCR). This combined therapy represents very effective treatment as 95% of treated patients responded and from 50-70% showed complete remission [48,49]. Among the most common side effects of this therapy belong toxicity, neutropenia, lymphopenia with an increased risk of secondary bacterial infections [50]. In elder patients and patients with comorbidity is more likely used an alternative therapy protocol FCR-lite, where the toxicity is lower [50]. For patients where the alkylating agents had failed or patient relapsed after second-line of Fludarabine therapy is applied monotherapy with Alemtuzumab. It is a recombinant, monoclonal antibody against the CD52 antigen. The main use of Alemtuzumab monotherapy was found in "high risk" patients with deleted 17p chromosome or with mutated *TP53* gene [50]. Another monotherapy alternative for elderly patient with comorbidity is Chlorambucil (alkylation agents), mainly for its low toxicity and low cost. The side effects (cytopenia; myelodysplasia; secondary acute leukemia) and low

complete remission (CR) rate are the main disadvantages of Chlorambucil monotherapy. Chlorambucil in combinations with anti-CD20 antibodies based therapy such as Rituximab shows better results [51].

B: Agents targeting B-cell receptor (BCR) signaling.

Signaling through BCR supports survival of B-CLL cells [52]. BCR signaling needs interaction with different tyrosine kinases: Bruton`s tyrosine kinase (Btk), spleen tyrosine kinases (Syk); Src family of tyrosine kinase and PI3K [53]. Therefore, novel drugs are based on the inhibition of BCR signaling e.g. inhibitors of Btk [54]. Ibrutinib inhibits Bruton`s tyrosine kinase and induce apoptosis of B-CLL and lymphoma cells [55]. In a recent study, in which Ibrutinib was orally administered to the patients with relapsed or refractory B-cell lymphoma and B-CLL, it was demonstrated that Ibrutinib is well tolerated and induces significant objective responses (16% of patients with complete remission)[56].

C: BCL-2 inhibitors.

Pro-apoptotic proteins the members of Bcl-2 family represent key regulators of apoptosis [57]. ABT-199 inhibitor selectively inhibits the growth of BCL-2 dependent tumors *in vivo* and spares human platelets. In patients with refractory B-CLL, administration of ABT-199 resulted in lysis of tumor cells [58].

D: Immunomodulatory drugs.

Lenalidomide with its anti-angiogenic, anti-neoplastic properties was primarily used for treatment of myelodysplastic syndrome and multiple myeloma [59,60]. Lenalidomide therapy is also applied to the treatment of B-CLL patients. In 4 year study of Lenalidomide as initiating therapy (cohort of 60 B-CLL patients), drug administration resulted in tumor flare reaction with overall survival 82%. Treatment with Lenalidomide was also associated with sustained (36 months or longer) normalization of the absolute number of circulating T-cells (CD3+) and the percentage of CD4+ and CD8+ cells [61].

1.2 Introduction to the microRNAs

1.2.1 Discovery, nomenclature of microRNAs

The microRNAs were discovered in 1993 by Lee *et al.,* in *Caenorhabditis elegans* animal model [62]. This class of small non-protein coding single stranded RNAs (~19-23 nucleotides in length) is now very intensively studied. MiRNAs work as negative post transcriptional regulators of gene expression. MiRNAs, endogenously produced RNAs are evolutionary conserved among all four kingdoms - *Animalia, Plants, Funghi* and *Viruses*. Due to the role of small RNAs in controlling the proper timing of development, were firstly named as small temporal RNAs (stRNA) [63] and later renamed to microRNAs [64].

One of the first discovered miRNAs were lin-4 (*lineage*) and let-7 (*lethal*) in 1993 by Lee *et al.* in worms *Caenorhabditis elegans* [62]. These miRNAs inhibition mechanism involves sense and anti-sense interactions of RNAs. The lin-4 inhibits translation of *LIN-14* that is responsible for correct timing during the first larval stage and let-7 regulates correct timing and development from the last larval stage to the adult stage [65].

Nowadays, identification of miRNAs exploits methods as subclonning, *de novo* sequencing studies and bioinformatics approaches. Prediction programs use the conservation of miRNAs within species. Variety miRNA databases were developed: miRBASE [66], miRNA map [67], microRNA [68], coGemiR [69], miRGEN [70]and deepBase [71]. In publications, computationally predicted miRNA target programs/databases are used: Targetscan [72], Pictar [73], Tarbase [74], microRNA [68], Diana-microT [75], miRecords [76]and Starbase [77]. Recently, the most used miRNA database – „miRBase“ issued the version 19 [78] which contains 1600 human microRNAs and their number is still rising up.

Terminology of miRNAs distinguishes the precursor miRNA from the mature miRNA. Precursor miRNA is referred to as “hsa-pre-miR-X” while mature as “hsa-miR-X” (where X represents a number in line of discovery). The prefix of three letters refers to the origin of organism (e.g. hsa = *Homo sapiens*, mmu = *Mus musculus*). If there exists a difference in few bases in the sequence of mature miRNA, after numeric value X the letters a, b or c are added (e.g. hsa-miR-106a; hsa-miR-106b). To specify which arm of the hairpin structure is processed from the precursor miRNA, specification 3p (from 3` arm) and 5p (from 5` arm) are used (e.g. hsa-miR-155-3p or hsa-miR-155-5p). By processing of both strands from pre-miRNA, than the less abundant is named as miR-X*. The mature miRNA can result from two

genomic loci, then the numeral suffix after X is added (e.g. hsa-miR-181a-1 or e.g. hsa-miR-181a-2) [79,80]. In addition, some miRNAs do not follow such nomenclature (e.g. let-7).

1.2.2 Biological function of microRNAs

The cell fate is under tight control of miRNAs that regulate apoptosis, cell cycle, proliferation or differentiation of cells. Primarily, miRNAs negatively regulate gene expression. MiRNA binds to the 3' untranslated region (3` UTR) of its target mRNA and based on the level of complementarity, the mRNA degradation (*Plants*) or inhibition of translation (*Animalia*) is executed [81]. Besides negative regulation of gene expression, some miRNAs could also promote translation of ribosomal RNA [82].

One miRNA can regulate several target mRNAs and on the other hand, several miRNAs can regulate one mRNA target [83,84]. The cluster miRNAs as hsa-miR17-92 cluster are processed from one primary transcript that is later spliced into several mature miRNAs. The single miRNAs as miR-155 are transcribed from one primary transcript of host gene. It was estimated that 10–30% of genes are regulated by miRNAs. It is thus not surprising, that miRNAs are involved in cancer development where they are differentially expressed. It is known, that microRNAs are deregulated during leukemia and tumor development [85]. Important role of microRNAs in tumor genesis is supported by the fact that microRNAs are frequently located at the genomic loci amplified in tumors [86]or the loci that frequently undergo genetic mutation: breaks or deletions [87]. Genes encoding microRNAs and their regulatory regions are often located in vicinity of viral integrations, that leads to deregulation of their expression [88]. MicroRNAs are important for normal development as documented by the genetic inactivation of several components of microRNA metabolism, resulting in absolute phenotype of early embryonic lethality [89].

1.2.3 Biogenesis of microRNAs

Genes that encode miRNAs are localized on the sex and somatic chromosomes with the exception of Y chromosome [79]. MicroRNA genes are mainly localized in the chromosomal loci that are predisposed to the deletions or amplifications [90]. The miRNAs are transcribed from RNA transcripts of independent genes or from introns of protein coding genes. MiRNAs can be then divided into three categories depending on their genomic location: 1) exonic

miRNAs in non-coding genes; 2) intronic miRNAs in non-coding genes and 3) intronic miRNAs in protein-coding genes [91].

Biogenesis of microRNAs (Figure 1.3) starts in the cell nucleus and continues in the cytoplasm. The processing of miRNAs requires RNA polymerase II [92] but some miRNAs as miR-515-1, miR-517a, miR-517c and miR-519a-1 could be transcribed also by polymerase III [93]. The first product is the primary transcript - **pri-miRNA** that is usually several kilobases long with a typical hairpin structure (Figure 1.3). The endonuclease - RNase III called Drosha digests pri-miRNA. This process is followed by adding three phosphates (3P) at the 5'end on which further binds 7-methyl-guanosine (m^7G; also called a cap). This cleavage step is important as determines the sequence of the mature miRNA and generates the optimal conditions for further processing of pri-miRNA [94].

The second product arising during the biogenesis of miRNA is precursor-miRNA (pre-miRNA) originated from pri-miRNA. The **pre-miRNA** (~70-100nt long) arises by digesting of the one strand by enzyme Drosha and its cofactor DGCR8 (DiGeorge syndrome Critical Region gene 8; dsRNA binding protein). DGCR8 cofactor binds as the molecular anchor to the double-stranded RNA and recognizes the pri-miRNA flanking sequences where undergo subsequent cleavage of stem-loop mediated by the ribonuclease Drosha. Drosha cleaves in approximately 11bp from the junction between the flanking sequences and the stem-loop. Such non-symmetric cleavage leaves two unpaired nucleotides at the 3'OH end [95]. Drosha complex consists of several factors "accessory components" as EXSR1, FUS, ribonucleoproteins and DEAD-box helicases. These "accessory components" may function as the enhancers of fidelity and activity of miRNA processing by Drosha [96,97]. Processing of pri-miRNA to the pre-miRNA is a critical step while defines the mature miRNA sequences (Figure 1.3).

Besides the canonical miRNA biogenesis there exists also an alternative biogenesis of miRNA called mirtron pathway (Figure 1.3). The **mirtron** is a short intron with hairpin structure. This pathway uses mRNA splicing mechanisms. After lariat (structure that originates from intron of mRNA during splicing and processing of mRNA/miRNA) releasing the intron by self generates pre-miRNA, however with shorter length as in canonical pre-miRNA pathway, since lack of lower stem of 1 helical turn that typically recruits and mediates cleavage by Drosha/DGCR8 complex [98]. Cleavage step by Drosha does not occur in the mirtrone pathway [99]. The miRNAs originated by mirtron pathway are miRNAs with

regulatory function as well as miRNAs that are made up by the canonical biogenesis pathway (Figure 1.3).

The nuclear protein, **Exportin-5** (Ran-GTP receptor) guides transport of pre-miRNA from the nucleus into the cytoplasm. This boundary of pre-miRNA with Exportin-5 ensures two flanking nucleotides on the 3'end of pre-miRNA. RNaseIII (Dicer) cleaves the terminal hair loop of pre-miRNA and give rise to the temporarily present double strand duplex of **miRNA:miRNA*** (~21-23nt). Dicer together with its co-factor TAR RNA binding protein (TRBP) regulates processing and liberation of miRNA:miRNA* duplex. Strand with strongest boundary to the 5'end of miRNA:miRNA* duplex is then incorporated into so called miRNP (ribonucleoprotein) or **RISC** complex (RNA Induced Silencing Complex). The miR* strand plays role in the pathogenesis of some diseases and acts in regulating signaling events [100]. Only the active RISC* complex could bind the mature miRNA and transport it to its target mRNA. The mechanism of miRNA acting lies in guiding the active RISC* complex to the 3`UTR of the target mRNA through "seed sequence". The "seed sequence", usually 6-8nt long is responsible for the correct boundary of miRNA on the 3'end of the target mRNA [101]. The key components of RISC are Argonaut proteins 1-4 (**AGO1-4**). All four proteins stabilize the RISC complex, but only AGO-2 has "slicer" activity (slicer activity=cleavage) [102,103]. AGO proteins interact also with proteins of RISC complex: GW182 (glycine-tryptophan protein of 182KDa) [103]. GW182 than further interacts with poly (A) binding protein (PABP) and together recruit deadenylases – to proceed the final step of mRNA deadenylation [104].

Inhibited targeted mRNA together with miRNA and catalytic components of RISC (AGO1-4) are then collected into the **P bodies** [81]. The P bodies (**p**rocessing) are subcellular compartments that serve in mRNA turnover. In P bodies' proceeds decapping, degradation of unwanted mRNAs and storage of mRNA until needed for translation. P bodies also act on aiding in translational repression by miRNAs [105,106]. Some miRNAs after entering P bodies are not degraded but rather utilized for re-initiation of translation [107].

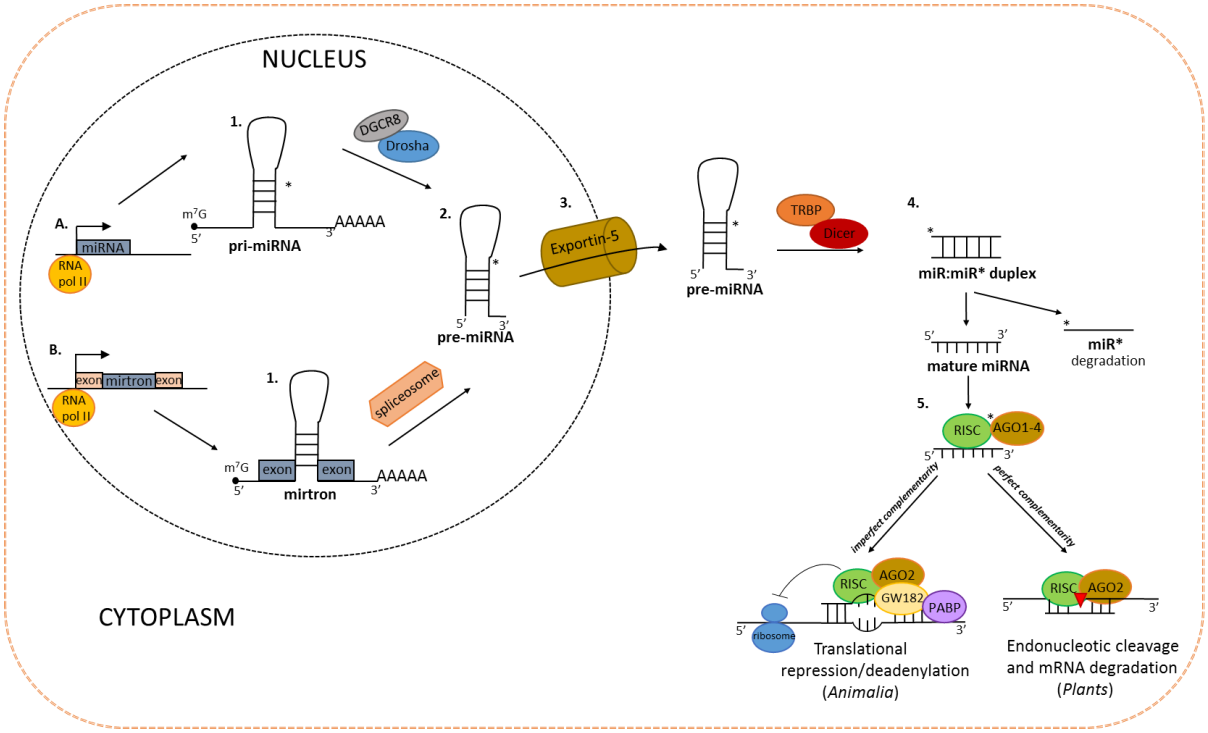

Figure 1.3: Biogenesis of miRNA (adapted and modified from Breving K and Esquela-Kercher A, 2009[102]; Iorio MV and Croce CM, 2011[108]; Okamura K *et al.*, 2007[109]; Krol J *et al.*, 2010[103]). Biogenesis of miRNAs starts in the cell nucleus and proceeds in the cytoplasm. There are two pathways of biogenesis miRNAs: A) Canonical and B) Alternative mirtron pathway. A) In the canonical pathway, the first step is generation of long primary transcript pri-miRNA by polymerase II/III. The pri-miRNA transcript contains cap at 5`end and polyA tail at the 3`end. In the second step, digestion of pri-miRNA by RNAse III-Drosha together with DGCR8 gives rise the precursor - pre-miRNA. B) In the alternative mirtron pathway, the first step is generation of mirtron-encoded by introns. Mirtron hairpins are spliced and debranched in spliceosome to gives rise to pre-miRNA. From this step, both pathways share further steps of generation the mature miRNA. Pre-miRNA is in the third step exported from the nucleus to the cytoplasm by Exportin-5. In the cytoplasm the second RNAse III – Dicer together with TRBP further process pre-miRNA. In the next step short existing miR:miR* duplex arise. The mature miRNA originates from the guided strand - with the strongest boundary to the RISC complex and more stable; the miR* strand is usually degraded (but could also play some biological role). Mature miRNA is further loaded into RISC complex mediated by AGO1-4 proteins. In that step, the mature miRNA becomes ready for action: translational repression/deadenylation (in Animals) or mRNA degradation (in Plants).

1.2.4 Regulation of the microRNA biogenesis

Proper timing and precise regulation of miRNAs expression are required for maintaining cell and tissue homeostasis [110].

Both miRNAs and mRNAs have complex promoters regulated by transcription factors, enhancers, silencing elements and by chromatin modifications [107,111]. Transcription of miRNAs genes is regulated at the promoter level by: A) Binding of transcription factors, B) Chromatin modifications (Figure 1.4). Direct binding of transcription factors (TF) positively

or negatively regulates miRNA expression. TF c-MYC stimulates expression of miR-17-92 cluster by direct binding at conserved sequence upstream of miR-17-92 host gene [112]. Expression of miRNAs is regulated also by chromatin modifications, 5-10% of mammalian miRNAs are regulated epigenetically. The tumor suppressor miR‑124a is unmethylated in normal cells but undergos methylation in cancer cells [113].

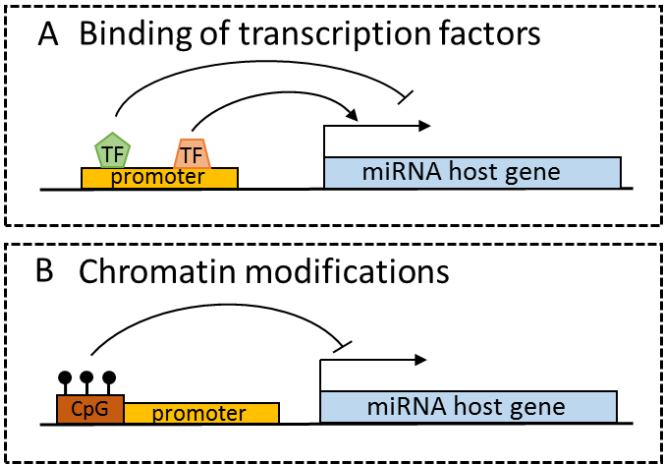

Figure 1.4: Regulation of miRNAs transcription: Transcription of miRNA genes could be positively or negatively regulated by: A) Binding of transcription factors or B) Chromatin modifications. A) Direct binding of TF (transcription factor) at miRNA host gene promoter could positively or negatively regulate the miRNA host genes expression. B) Methylation of CpG at the miRNA host gene promoter region negatively regulates expression of miRNA.

It was shown that processing of miRNAs is regulated by: 1) protein cofactors, 2) protein-protein interactions or 3) through direct interactions with pri-miRNA [114]. Each step of the biogenesis of miRNA is tightly regulated alike the regulation of mRNA maturation. The first regulatory step occurs at the processing of **pri-miRNA**. For example, SMAD proteins and p53 protein enhances the maturation of pri-miRNAs through interaction with protein p68 – a component of the Drosha microprocessor complex [115,116]. An autoregulation of miRNAs was recently described - e.g. the let-7 promotes processing of its primary transcript [117]. Such a regulatory feedback loops are very common in miRNAs and it was postulated that they are critical for maintenance of balance between the levels of the Drosha-DGCR8 complex and their substrate [118]. It was described that processing of pri-miR-155, pri-miR-21 and let-7 by Drosha is enhanced by arsenite-resistance protein 2 (ARS2), a component of the nuclear cap binding complex. The low expression or depletion of ARS2 inhibits processing of pri-miRNA-155 [119].

The second level of regulation miRNA maturation occurs at pre-miRNA stage. The processing of **pre-miRNA** is mediated not only by Dicer but also by other cofactors as TRBP and PACT (protein activator of PKR). These two cofactors enhance the specificity of cleavage and promote stability of the Dicer-pre-miRNA complex [120]. Translocation of processed pre-miRNA from the cell nucleus into the cytoplasm mediates the nuclear pore complex called Exportin-5 [94]. Exportin-5 together with pre-miRNAs may shuttle also tRNAs (transfer RNAs). Therefore, pre-miRNAs and tRNAs compete for transport by Exportin-5 [94]. Another regulation of pre-miRNA maturation proceeds during interaction of Dicer with Exportin-5, thus overproduction of Dicer mRNA or pre-miRNA could work as negative or positive feedback loop [121]. The processing of Dicer is negatively regulated by viral miRNA – e.g. miR-BART6-5p encoded by Epstein-Barr virus [122]. Another negative regulation of pre-miRNA processing respectively export of pre-miRNA represents post-transcriptional process RNA editing mediated by adenosine deaminases (ADAR) [103]. ADAR proteins catalyze conversion of adenosine to inosine what affects base pairing and structural properties of RNA transcripts [123]. ADARs regulate both Drosha-mediated and Dicer-mediated cleavage and prevent the export of pre-miRNAs [103].

Mutations in the sequences of pre-miRNAs or mature miRNAs influence further miRNA processing, stability and target selection. Mutations in the pre-miRNA and miRNA sequences originate from changes at the DNA coding sequences and from RNA posttranscriptional modifications [124,125]. The single substitutions of base pairs (C to T) in the sequence of pre-miR-15a and pre-miR-16-1 abolish processing of these two miRNAs in B-CLL patient samples [126].

Briefly, regulation at the pri-miRNA level by interactions with proteins/cofactors results in different expression of miRNAs. Changes at the base pairs in pre-miRNA and/or mature microRNA sequences alter processing and/or selection of target mRNAs.

1.2.5 miRNAs are involved in pathogenesis of B-CLL

For the first time Calin *et al.,* described the link between B-CLL and miRNAs. Authors desribed significant down regulation of the microRNA **cluster miR-15-16** (miR-15a and miR-16-1) in B-CLL patient samples. MiR-15-16 cluster is localized in the 13q14 chromosomal region that is often deleted in B-CLL [16]. Klein *et al.,* described on the mouse model, that deletion of 13q14 region with *DLEU2*/miR-15a/miR-16-1 leads to clonal B-cell

lymphoproliferations similarly as in B-CLL patient cells. Moreover, they proved that deletion of cluster miR-15-16 accelerates proliferation of B-cells by enhanced transition of cells from G0/G1 to S phase [127]. Thus, miR-15-16 cluster plays important role in pathogenesis of B-CLL [128,129]. Another consequence of the deletion 13q14 chromosomal region is elevated production of an anti-apoptotic protein – BCL2, thus absence of miR-15-16 cluster increases resistance of B-CLL cells to the apoptosis. On the other hand, in the normal B-cells, presence of miR-15-16 cluster acts as tumor suppressor gene while it inhibits expression of *BCL2* gene and drives cells to apoptosis [130]. While the BCL2 is in majority of B-CLL patient samples overexpressed, it makes BCL2 molecule a potential target in B-CLL therapy. Recent work by Masood A *et al.,* showed that an inhibitor of BCL2 (AT-101) induces apoptosis in B-CLL cells [131].

It is described that several miRNAs are deregulated in B-CLL cells [90,130,132]. The **miR-34a/b/c cluster** is the one among them. To the frequent chromosomal aberrations in B-CLL belongs loss of the long arm of chromosome 11 and deletion of the short arm of chromosome 17. The miR-34a/b/c cluster is localized on these two chromosomes. The miR-34 cluster downstream regulates the expression of *TP53* gene that suggests on link between chromosomal deletions (11q, 17p chromosomes) and expression of miR-34a/p53 during B-CLL progression [133]. Fabbri *et al.,* shown that p53 binds at miR-34b/c cluster and thereby stimulates expression of miR-34b/c cluster in B-CLL [134]. Interestingly, in B-CLL patient cells with deletion or mutation of *TP53* gene the levels of miR-34 cluster decreased. Based on this knowledge, measurement of levels miR-34a could distinguish between the high and low risk B-CLL patients. The B-CLL patient samples with high risk expressed lower levels of miR-34a, displayed shorter time to treatment and shorter doubling time of lymphocytes in comparison to the low risk B-CLL patient samples. Moreover, it was described that low expression of miR-34a due to deletion or mutation of *TP53* gene positively correlates with Fludarabine resistance of B-CLL cells [135]. MiR-34a induces cell cycle arrest and apoptosis in the primary B-CLL cells. The cell cycle and apoptosis are in cooperation with p53 – this suppose an existence of positive feedback loop between miR-34a and p53 protein.

Patients with deletion of 17p chromosome (encoding *TP53* gene) are clinically described as patients with high risk B-CLL. It was shown that B-CLL cells of patients with high risk expressed elevated levels of **miR-21**. Moreover, the B-CLL patients with elevated expression of miR-21 displayed shorter overall survival (12 months) in comparison to the

patients with low miR-21 expression (24 months). Therefore, measurement of miR-21 levels could be in the future used as the marker for overall survival of B-CLL. The statistical analysis based on the cytogenetic data has shown that expression of miR-21 is a marker of an early stage of B-CLL [136].

Fulci *et al.,* described three-fold increased levels of **miR-150** in the peripheral blood and lymph nodes of B-CLL patients [17]. The RNA *in situ* staining of leukemic cells showed very clear staining of miR-150 in the outer site of the proliferation centers of leukemic cells in the lymph nodes [137]. Moreover, expression of miR-150 correlates with poor prognosis as the B-CLL patient cells with unmutated IgVH expressed less miR-150 as IgVH mutated B-CLL cells [17,137].

Decreased expression of **miR-181b** in B-CLL cells overal correlates with worse prognosis of B-CLL. Patients with low levels of miR-181b had higher probability of requiring treatment and display shorter overal suvival (5 months) as patients with higher miR-181b expression (14 months). Moreover, the B-CLL cells with deletion of short arm of chromosome 17 expressed less miR-181b as cells without this deletion. Based on this data the low miR-181b expression has become an unfavorable prognostic marker of B-CLL [19,136]. The B-CLL patient cells with unmutated IgVH expressed lower levels of miR-181b as mutated IgVH cells [138].

Different expression pattern of members **miR-17-92 cluster** appears to be another sign of B-CLL. This cluster encodes six different microRNAs (miR-17p, 18a, 19a, 19b-1, 20a, 92a). Moreover, the miRNA-17-92 cluster regulates proliferation of B-cells and Ig rearrangement as it is highly expressed in progenitor B-cells [139,140]. Expression of miR-92, a member of miR-17-92 cluster was increased in the lymph nodes of B-CLL patient samples. Other members as miR-20a and miR-19b-1 were highly expressed in the peripheral blood of B-CLL patients [137]. The ChIP analysis has shown that the transcription factor MYC stimulates expression of miR-17-92 cluster in B-CLL [112].

The most studied microRNA in B-CLL represents a multifunctional oncogenic microRNA - **miR-155**. The elevated levels of miR-155 were detected in Hodgkin [141,142] and non-Hodgkin lymphomas including B-CLL [17,130,143,144]. The aberrant expression of miR-155 represents sign of more aggressive course of the disease [143,145]. The recent data shows on the potential usage of miR-155 as a prognostic marker in distinguishing between two types of DLBCL forms (ABC/GC) [146]. Based on this information, the measurement of miR-155 levels during

disease progression could be potentially used as a marker of B-CLL progression. Very recently, a prognostic value of miR-155 as marker of B-CLL progression was confirmed [20]. Authors shown an association between elevated levels of miR-155 in plasma of B-CLL patients and progression of B-CLL from MBL [20].

1.3 Characterization of microRNA-155 and its role in B-cells and leukemia

1.3.1 Overview of microRNA-155/*BIC/MIR155HG*

MiR-155 is encoded by non-protein coding gene *BIC* identified by Tam as the B cell Integration Cluster while *BIC* gene represents frequent site for integration of the avian leukosis virus (ALV) [147]. *BIC* gene lacks an extensive open reading frame (ORF) and contains three exons that form 13kb region within the human chromosome 21q21.3 (Figure 1.5). *BIC* gene does not code any protein-coding gene. The secondary structure of *BIC* gene conserved sequences formed hairpins with imperfectly base paired stem loops. Taken together, *BIC* functions as non-protein coding RNA [147]. The human BIC cDNA is in 83% identical with the mouse BIC cDNA, moreover mature human (hsa) miR-155 differs from mouse (mmu) miR-155 only in a single nucleotide in non seed sequence [148]. The *BIC* gene is now designed as *MIR155 Host Gene* (*MIR155HG*).

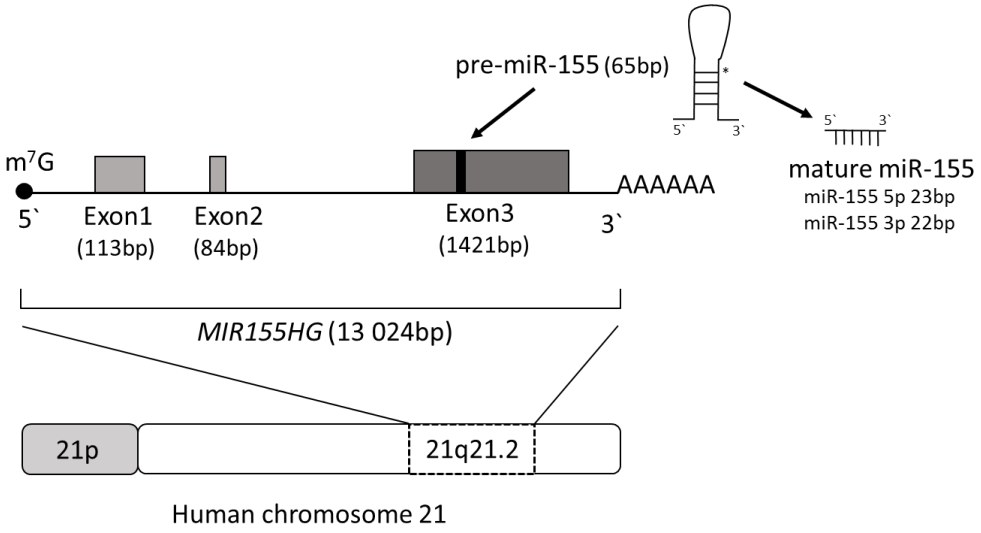

Figure 1.5: Structure of the *MIR155HG/BIC* gene (NC_000021.8). *MIR155HG (BIC)* is localized on the 21q21.2 chromosomal locus. The full length of *MIR155HG* spans 13024 bp that contains three exons. The exon 3 encodes precursor pre-miR-155 (1421 bp). After two endonuclease cleavage steps (by endonuclease Drosha and Dicer) arise the mature miR-155 (adapted and modified from Tam W, 2001[148] and http://www.ncbi.nlm.nih.gov/gene/114614).

The **biogenesis of miR-155** follows canonical miRNA pathway, this process begins in the cell nucleus and continues in the cytoplasm (for details see also Figure 1.3). The primary transcript of miR-155 – pri-miR-155 (13 024nt) is transcribed from *MIR155HG* or *BIC* gene by polymerase II (Figure 1.3 and 1.5). The precursor miR-155 - pre-miR-155 (65nt) originates from the pri-miR-155 by enzymatic cleavage mediated by endonuclease Drosha. This pre-miR-155 is further enzymaticaly cleaved by Dicer endonuclease to give rise two mature miR-155 - miR-155 5p (23nt) and miR-155 3p (also called miR-155*) (22nt) (Figure 1.5) [149]. The major product represents miR-155 5p that is also the most studied in different cells and tissues including hematopoietic and immune system. However, the minor product, miR-155 3p is less known and it seems that these two products tightly cooperate [100]. Authors described opposite cooperation between these two miRNAs in regulation of IFNα/β (interferon α/β) production in human dendritic cells. Here the miR-155 5p acts as negative regulator and miR-155 3p as positive regulator of production IFNα/β. Their opposing functions are explained by their different mRNA targets: miR-155 3p targets IRAK3 (Interleukin-1 Receptor-associated kinase 3) and miR-155 5p targets TAB2 (TGF-β activated kinas 1/MAP3K7 binding protein 2) [100].

MiR-155 (5p) represents a **multifunctional microRNA**, while it involves in the various physiological as well as in the pathological processes (reviewed in [150,151]). In the normal human hematopoietic stem-progenitor cells (HSPCs) miR-155 maintains early **hematopoietic stem cells** (HSCs) at an early stem-progenitor stage by blocking their further maturation into myeloid, lymphoid and erythorid lineage. The transducing of miR-155 into erythroid K562 cell line as well as into human CD34+ bone marrow cells resulted in decrease of megakaryocytic differentiation and less formation of myeloid and erythroid colonies [152]. The northern analysis revealed that miR-155 expresses all hematopoietic tissues [153]. Maturation of **B-cells** is under control of miR-155 [154,155]. O`Connell has found that permanent expression of miR-155 can increase number of immature granulocytes. Moreover, the increased levels of miR-155 led to the **granulocytes and monocytes** expansion, similarly to the myeloid proliferations as AML [156]. Vigorito and Xiaochun studied the role of miR-155 in **immunity** [157,158] and **inflammation** [159]. Trotta *et al.,* described that miR-155 acts as positive regulator of IFNγ production by natural killer cells [160]. The positive functioning of miR-155 on the **inflammation process** underlines also fact that the atherosclerotic plaques and pro-inflammatory **macrophages** displayed high expression of

miR-155 that results in inhibition of inflammatory responses and lipid uptake [161]. It has been described that miR-155 involves in pathogenesis of **autoimmune diseases** as rheumatoid arthritis, multiple sclerosis and systemic lupus erythematosis [162]. MiR-155 attenuates **apoptosis** via targeting FADD (Fas-Associated protein with Death Domain) [163]. Haasch *et al.,* demonstrated a strong up regulation of miR-155 expression in CD3/CD28 activated T-cells, suggesting a possible role for miR-155 in **T-cell** activation [164]. Role of miR-155 in the **cardiovascular disorder** support evidence that during the acute inflammatory phase of viral myocarditis the increased expression of miR-155 was specifically localized in the infiltrating macrophages and T-cells [165]. Presence of miR-155 is required for CD8+ T-cell responses to both virus and cancer [166]. MiR-155 is involved also in the development of different types of solid tumors as **breast cancer** [167,168], **lung cancer** [85], **colon cancer** [85] and **cervical cancer**[169]. It was described that miR-155 is over-expressed in **acute myeloid leukemia** (AML) [170] and in **acute lymphocytic leukemia** (ALL) [171]. In practically all **B-cell lymphoproliferations** (Hodgkin's and non-Hodgkin's lymphoma, primary mediastinal B-cell lymphoma, diffuse large B-cell lymphoma (DLBCL)) including **B-CLL** microRNA-155 is aberrantly expressed [17,141,144,149,172–174].

Above-mentioned physiological and pathological processes including leukemia/cancer underlines the wide range of miR-155 functioning.

1.3.2 Role of miR-155 in normal and leukemic B-cells

The B-cell development is regulated by transcriptional factors that are modulated by microRNAs [154]. Deregulated expression of miRNAs and transcription factors are key events in pathogenesis of B-cell malignancies [175].

During the normal lymphopoiesis the highest level of miR-155 express germinal center cells, intermediate level HSCs and the lowest mature B-cells [152]. In the hematopoietic stem cells, miR-155 functions as blocker of hematopoietic differentiation along all lineages including lymphoid lineage [152]. The normal healthy, germinal center B-cells express aberrant levels of miR-155. In the germinal centers occurs maturation of antibodies and generation of memory B-cells in T-cell dependent antibody responses. As the Hodgkin`s lymphoma originate from the germinal center cells, the sustained up regulation of miR-155 is due to block of lymphocyte maturation [175].

MiR-155 is required for production of antibodies that documents reduced secretion of IgG in B-cells of miR-155 deficient mice. This impaired antibody production is due to defect in differentiation of plasmablast cells and reduced proportion of germinal center B-cells. Another reason of reduced antibody production in miR-155 deficient mice is failure of BCR signaling [157]. Thai *et al.,* described that reduced expression of miR-155 leads to reduced cytokine production [176].

It was described that miR-155 does not implicates in the somatic hypermutation (SHM) [157]. In contrast, Teng *et al.,* showed that aberrant expression of miR-155 negatively regulates AID (activation-induced cytidine deaminase) expression in B-cells. AID is involved in somatic hypermutation, gene conversion and class-switch recombination of immunoglobulin genes. Authors showed that absence of AID mediated by miR-155 inhibition resulted in imperfect maturation of B-cells [177].

It has been reported that direct target of miR-155 is *SHIP1* (Src homology-2 domain-containing inositol 5-phosphatase 1) gene that regulates differentiation of B, T-cells and macrophages [178]. The Ship1 knockout mice displayed spontaneous germinal center formation and antibody class-switching [179].

During B-cell maturation the presence of miR-155 is necessary for activation of B-cell receptor (BCR): important for antibody production [141,180,181]. The B-CLL cells with high expression of miR-155 displayed higher capacity for BCR signaling [34].

The last stage of B-cell development occurs in the peripheral lymphoid tissues where miR-155 is expressed by centroblasts and activated B-cells, necessary for normal B-cell development [154].

1.3.3 Mouse models of miR-155

Until now it was generated four main miR-155 transgenic mouse models with either enhanced [182] or deficient miR-155 expression [157,176,183]. More information about mechanism of miR-155 acting in immune system may help to understand its role in leukemic process.

In the miR-155 over-expressing transgenic mice ("Eμ–mmu-miR-155" mouse model), pre-leukemic stage with polyclonal B-cell expansion and splenomegaly developed initially (after 3 weeks) [182]. Later, after seven month, pre-leukemic stage progressed into high-grade B-cell lymphoma that is direct evidence of miR-155 functioning as activator of leukemia development [182].

Vigorito *et al.,* confirmed importance of miR-155 in antibody production in germinal centers [157]. MiR-155 deficient mice had reduced proportion (50%) of germinal center B-cells that led to reduced production of high affinity antibodies. Interestingly, authors firstly thought that impaired antibody production is result of dysfunctioning of somatic hypermutation affected by miR-155. The further experiments showed that miR-155 does not affect somatic hypermutation that occurs in germinal center B-cells (SHM) [157]. Failure of antibody production is due to block in differentiation of plasmablast B-cells (stage of B-cells between plasma and mature B-cells) and in reduced production of cytokines. This was confirmed also by other groups of researchers as Thai and Rodriguez [176,183]. Moreover, the miR-155 deficient mice produced less amount of IgM and switched antigen specific antibodies after immunization with pathogen – *Salmonella typhinurium*. The evidence that miR-155 regulates also T-cells represents its strong up regulation in activated T-cells [176]. Rodriguez *et al.,* also proved that dendritic cells failed efficiently activate T-cells [183].

As the miR-155 bears the potential to be therapy-targeted molecule, Babar *et al.*, generated miR-155 Cre-loxP tetracycline controlled knock-in mouse model (miR-155^{LSLtTA}). In these mice, the transcription of miR-155 can be deactivated by doxycycline, thus it provides "TET OFF" system with temporal controlling of miR-155 transcription. MiR-155 ^{LSLtTA} mice developed after five month disseminated lymphoma with enlarged lymph nodes and splenomegaly. Surprisingly, mice with such miR-155 induced lymphoma after doxycycline treated food displayed within two days reduced lymph nodes and in 2 weeks the lymphoid organs were as in normal, healthy mice [184].

To summarize, over expression of miR-155 leads to high grade B -cell lymphoma and miR-155 knockout mice model showed on a marked impairment of miR-155 in T- and B-cell function. The knock-in mouse model gave strong evidence that miR-155 is inductor of B-cell leukemia. Moreover, miR-155 regulates homeostasis of immune system, thus it makes potentially very powerful therapy tool.

1.3.4 Transcriptional regulation of *MIR155HG*

Similarly as mRNA genes, also miRNA host genes are regulated by transcription factors and chromatin modifications [102,111]. Aberrant expression of miR-155 in the immune cells and hematopoietic cells usually results in cancer, leukemia and autoimmune disorder [162].

As miR-155 represents a common target of a broad range of inflammatory mediators and regulators of immune homeostasis, it is not surprising that inflammatory molecules and members of inflammatory pathways can activate the transcription of *MIR155HG*.

It is described that **IFNγ** (Interferon γ), **TNFα** (tumor necrosis factor α), Toll-like receptor (**TLR**) ligands positively regulate *MIR155HG* expression [185,186]. Van den Berg *et al.,* find an putative NFκB binding site in -371 to -362bp upstream of the transcription start site of *MIR155HG* [141].

TGF-β induces *MIR155HG* transcription through binding of **SMAD4** to the promoter region. Thus, miR-155 is a direct transcriptional target of the TGF-β/Smad4 pathway which activation promotes invasion and metastasis of breast cancer [167].

Another molecule that mediates inflammatory responses in the immune system and induces cytokines represents AP-1. Mathematical and bioinformatical analysis of the promoter *MIR155HG* gene resulted in the identification of **AP-1** (activator protein-1) binding sites -40nt upstream of the first exon *MIR155HG* [141]. It was confirmed later also by reporter assay [187]. B-cells carry out its function through B-cell receptor (BCR). Activated BCR signaling induces expression of transcription factors c-Fos, FosB, and JunB, members of AP-1 family. Transcription factor AP-1 enhances the miR-155 expression through activated BCR and complex of transcription factors (FOS/Jun). The mutation in AP-1 binding site decreased activity of MIR155HG promoter and impaired BCR signaling [187].

Several transcription factors regulate expression of *MIR155HG*. One of them is ***FOXP3*** (Fork-head box P3) a regulator of Tregs (T regulatory cells). In the breast cancer cells, *FOXP3* functions as tumor suppressor gene [188]. Over expression of FOXP3 stimulates *MIR155HG* transcription. MiR-155 by this feed-forward regulatory loop inhibits expression of its direct target: chromatin-remodeling transcription factor ***SATB1*** (Special AT-rich Binding Protein homeobox 1) that implicates in metastasis of breast cancer cells [189].

Very recently, it was described, that regulator of cell proliferation and survival, ***STAT3*** (Signal transducer and activator 3) activates *MIR155HG* expression in B-CLL cells. STAT3 binds to GAS-like elements at the position -709 and -700nt of *MIR155HG* promoter region results in stimulation of *MIR155HG* transcription [190].

The viral proteins and viral microRNAs could also activate transcription of miR-155 in the leukemic cells. Infection by Epstein-Barr virus (**EBV**) stimulates proliferation of B-cells. EBV infection induces expression of viral microRNAs (miR-BART and miR-BHRF) which enhances

the expression of cellular microRNAs. The EBV infected B-cells express high levels of miR-155 [191,192]. EBV encodes latent membrane protein-1 (LMP-1), a functional homologue of the tumor necrosis factor receptor family, contributes to EBV's oncogenic potential through activation of nuclear factor κ B (**NFκB**). In the EBV infected B-cells LMP-1 activates transcription of *MIR155HG* through NFκB and AP-1 [191]. Authors identified the second NFκB binding site at position -1697nt from TSS of *MIR155HG*. By recruiting both NFκB binding sites (-1150 and 1697nt from TSS) mediate LMP-1 elevated levels of miR-155 [187,191]. Aberrant expression of miR-155 in the EBV infected B-cells reprograms these cells into rapidly dividing cells and evoke the EBV latency [192]. The *MIR155HG* transcription is stimulated also by the oncogenic herpes virus - Kaposi's sarcoma-associated herpes virus (KSHV) [193,194].

MiR-155 expression is regulated also epigenetically. Chang S *et al.,* described the BRCA1-mediated silencing of *MIR155HG* promoter in breast cancer cells. Authors found that BRCA1 recruits HDAC2 complex at the *MIR155HG* promoter [168]. Therefore is the *MIR155HG* promoter epigenetically silenced through deacetylation of H2A and H3 histones. Silencing of BRCA1 results in increased miR-155 expression [168].

As the miR-155 is in leukemic or cancer cells aberrantly expressed, the transcription factors and inflammatory molecules positively regulate its host gene transcription. The *MIR155HG* is negatively regulated by HDAC2. Viral infection (EBV) contributes to miR-155 expression likewise. Anti-miRNA therapy could be then orientated on inhibition of miR-155 either itself or its activators.

1.3.5 Relationship between miRNA-155 and its direct target PU.1

In silico prediction showed that PU.1 transcription factor belongs among miR-155 target genes. Vigorito *et al.,* validated that miR-155 directly targets PU.1 mRNA in the miR-155 deficient mouse model in which the mRNA and protein levels of PU.1 were increased. The 3`UTR of PU.1 mRNA contains phylogenetically conserved 9nt complementary to miR-155 seed region (9nt) (Figure 1.6). PU.1 rescue experiment *in vitro* on the primary B-cells resulted in impaired IgG production and increased proportion of IgM [157]. The luciferase reporter assay confirmed this targeting of PU.1 by miR-155. After transfection of miR-155 mimic into PU.1 luciferase reporter, the luciferase expression of PU.1 reporter was inhibited

[157]. Together these data confirm that PU.1 decreasment is mediated by elevated level of miR-155.

It was described that over expression of miR-155 leads to decrease of both mRNA and protein level of PU.1 in primary B-CLL cells [144].

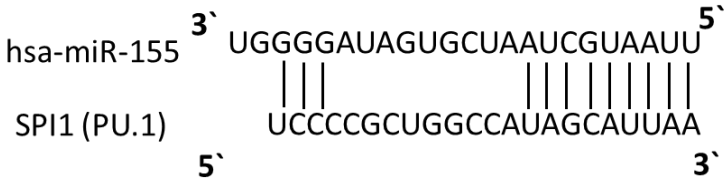

Figure 1.6: The complementary base-pairing between miR-155-5p and the human *SPI1* (spleen focus forming virus proviral integration oncogene) (also known as *PU.1*) mRNA. The miR-155-5p binding site is located 46-53 base pairs downstream from the SPI1 mRNA stop codon. The "seed sequence" base-pairing is represented by 9nt (adapted from miRBASE[78]).

It was described that LMP-1 mediated miR-155 over expression resulted in 2-fold decrease of protein level of PU.1 in EBV negative cell line DeFew [191].

PU.1 also known as *SPI1* (spleen focus forming virus proviral integration oncogene) is a member of ETS family [195,196]. PU.1 controls differentiation of common myeloid and lymphoid progenitor cells through regulation of transcription factors [197]. Importance of PU.1 in hematopoiesis underlined PU.1 mouse model (*Sfpi1*$^{-/-}$) where the null mutation of Sfpi1 resulted in perinatal lethality and failure in generation of B-cells, macrophages and neutrophils [198]. PU.1 acts as oncogene and as tumor suppressor gene [195,196]. Interestingly, different level of PU.1 defines the cell stage during the differentiation. The low level of PU.1 favors in the development of granulocytes and high in the development of monocytes [199]. In the B-cell, the high levels of PU.1 are observed in germinal center B-cells, while PU.1 level decreases with maturation [200]. Reduced levels of PU.1 in precursor cells leads to leukemia in mice and humans and also predict poor prognosis [201–204]. Additional data from our lab suggest that PU.1 low mice (PU.1$^{ure/ure}$) develop after three months acute myeloid leukemia (AML) with aberrant expression of miR-155 and Myb [205].

Hematopoietic transcription factor PU.1 regulates differentiation of both lymphoid and myeloid cell lineages. The highest levels of PU.1 in B-cell line are expressed in germinal center B-cells and with maturation PU.1 expression decreases. Reduced levels of PU.1 in leukemia are mediated by aberrant expression of miR-155.

1.4 Characterization of E-box protein MYB and its role in B-cells and leukemia

1.4.1 Characterization of E-box protein MYB

MYB gene is a cellular homolog of viral *v-MYB* (v-myeloblastosis viral oncogene). It is a founding member of E-box (enhancer box) family transcription factors. *MYB* is a part of genome of two avian myeloblastosis viruses: avian myeloblastosis virus (AMV) and E26 virus [206]. These viruses induce acute avian leukemia [206]. The E-box family includes also *MYBL1* (also called *A-MYB*), *MYBL2* (also called *B-MYB*), *MYC*, *N-MYC* and the viral *v-MYB* genes. Each member plays different role and is expressed by different tissues and cells [207]. The *MYB* gene transcribes from chromosomal locus 6q22-23. Schematic map of *MYB* gene structure shows figure 1.7. *MYB* contains DNA binding domain (DBD), transactivation domain (TAD) and terminal negatively regulated domain (NRD) [208]. Product, MYB protein (75kDa) functions as DNA binding protein through its binding sequence AACG/TG [209]. The *MYB* gene contains 15 exons, of which some undergo alternative splicing [210] (Figure 1.7). The alternative splicing forms (9A, 10A) showed higher transcriptional and transforming potential [210].

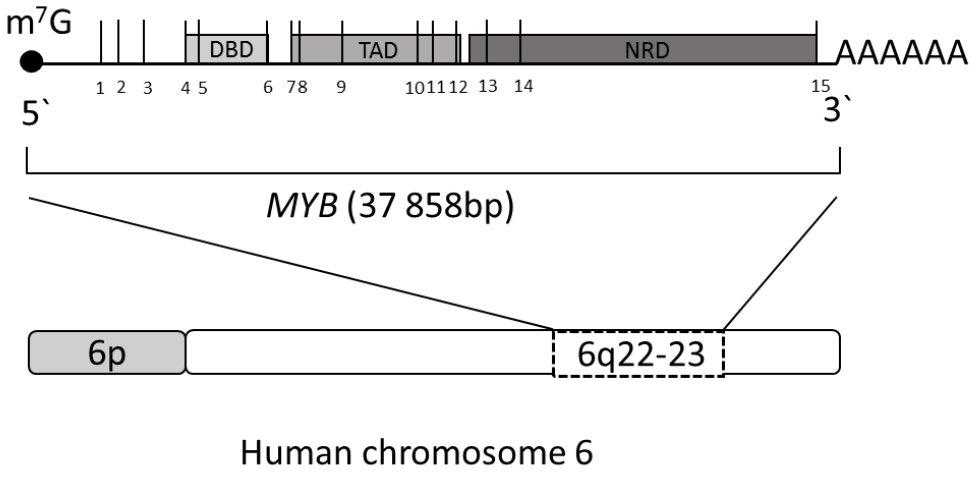

Figure 1.7: Structure of *MYB* gene (NC_000006.11). The *MYB* gene contains three domains: DNA binding domain (DBD) (blue box), central transactivation domain (TAD) (orange box) and terminal negatively regulated domain (NRD) (green box). Human *MYB* spans 37 858bb long mRNA transcript that contains 15 exons (black lines) (adapted and modified from Pattabiram DR and Gonda TJ, 2013 ; O`Rourke JP *et al.*, 2008 [208,210] http://www.ebi.ac.uk/s4/summary/molecular?term=MYB&classification=9606&tid=synENSMUSG00000019982).

The key biological function of MYB transcription factor (TF) lies in the maintaining of proliferative potential in progenitor cells. Downregulation of MYB leads to cell differentiation. MYB participates on G2/M cell cycle transition in hematopoietic cells by

direct stimulation of cyclin B1 expression [211]. Moreover, the MYB expression is associated with leukemogenesis. Expression of MYB can be activated by itself and by structural alterations and/or genomic rearrangements [212].

1.4.2 Role of MYB in normal and leukemic B-cells

MYB is required for self-renewal in B-cells, T-cells and common lymphoid, myeloid progenitors. The expression of MYB is highest in the long term HSC and its production reduces with maturation of B-cells [213]. During the early B-cell development, presence of MYB i s crucial for transition from pro-B to pre-B-cells [214]. Loss of MYB causes a partial block during B-cell development at the pro-B to pre-B cell transition that result in greatly decreased output of new B-cells from the bone marrow. Furthermore, absence of Myb prevents normal B-cell homeostasis due to decreased splenic B-cell survival [215]. MYB is required for survival and accumulation of CD19+ pro B-cells in the peripheral blood [214]. Impaired B-cell lymphopoiesis due to loss or mutated MYB is related with defect in IL-7 signaling [213]. The cytokine IL-7 regulates pro-B and pre-B cell transition [216].

Role of MYB in B-cell malignancies is much less known and studied while MYB was firstly found as inducer of myeloid leukemia in chicken [206]. There are some studies where aberrant expression of MYB resulted in acute lymphoid leukemia in humans [217] and childhood lymphoid leukemia [218,219]. It was described that elevated levels of MYB in subset of B-CLL cells (40%) enhanced the expression of miR-155 [144]. The Sarvaiaya *et al.*, studied knockdown of MYB in the pre-B-ALL leukemic cells. They found that inhibition of MYB decreases the expression of BCL2 – the anti-apoptotic protein and a target of *MYB*. It resulted in increased apoptosis of pre-B-ALL leukemic cells and sensitivity to chemotherapy [219].

1.4.3 Transcription factor MYB and its role in leukemia

MYB is a driver of leukemogenesis that underscores its identification as inducer of avian myeloid leukemia [206].

In the human T-cell acute lymphoid leukemia (T-ALL) Clappier *et al.*, identified genomic alterations as reciprocal translocation t(6;7)(q23;q34) and duplication of MYB loci. In these cases, the expression of MYB was much higher as in cases without genomic

alterations [220]. Similar results shown Lahortiga *et al.*, that the aberrant MYB expression in T-ALL associates with duplication of MYB. The knockdown of MYB expression initiates differentiation of T-cells [221].

O`Rourke and Ness described that minor change in the MYB structure by alternative splicing gives MYB stronger transforming potential. There is a difference in the expression of alternative transcripts in different hematopoietic cells. Truncated variant of MYB (exon 9A) in human pediatric B-cell ALL, T-ALL and AML samples displayed higher expression and higher oncogenic activity. Thus MYB and its alternative splicing forms strongly contribute to the leukemogenesis [210].

The increased expression of MYB mRNA [222] mediated by low expression of miR-150 was described in chronic myeloid leukemia (CML) [223]. In subset of primary B-CLL cells we detected elevated expression of MYB mRNA [144].

The aberrant expression of MYB in T-ALL, AML is associated with translocation or duplication of *MYB* gene.

1.4.4 Mouse models of Myb

The null Myb mouse model underscores importance of *MYB* gene in hematopoiesis. Homozygous mutant Myb mice at 15 day of gestation showed abnormal phenotype characterized by 10-fold decreased hematocrit; low number of multipotent hematopoietic progenitor cells and as well as myeloid and non-nucleated erythrocytes. These mice die at day 15 due to anemia [224].

The Myb null mouse model confirmed importance of MYB in the B-cell development. These mice displayed 65% decrease of pre-B-cells, 50% decrease of new pre-B-cells in the bone marrow and reduced production of IgM. Loss of Myb causes a partial block during the B-cell development at the pro-B to the pre-B cell transition. Myb is mainly important for maintenance of pre-B-cells and signals through the pre-BCR and IL-7R. The absence of Myb negatively affects also the number of splenic B and follicular B-cells due to decreased bone marrow cells output [215]. Moreover, Myb deficiency increase the number of apoptotic B-cells, probably mediated by decreased level of Bcl2 – a target of *Myb* [215].

Greig *et al*., described another mouse model with Myb deficiency. The bone marrow analysis by flow cytometry showed reduced amount of immature and mature CD19+ B-cells. In absence of Myb, mice displayed B lymphopenia with reduced response to IL-7. Authors

demonstrated that conditional deletion of Myb in B-cell progenitors completely abolished B-cell development, thus Myb is required for normal development of common lymphoid progenitor cells (CLPs) as well as for committed B-cell progenitors. Data from microarrays showed that Myb is required for induction of expression several lymphoid genes as *Sfpi1, Ikzf1, Tcfe2a* within multipotent progenitor cells [225].

Waldron *et al.,* tested the role of Myb in the pathogenesis of $p190^{BCR/ABL}$ dependent B cell leukemia in Myb deficient transgenic mouse model. Interestingly, loss of one copy of Myb suppresses the leukemogenic potential of B-cells isolated from $p190^{BCR/ABL}$ transgenic mice. Similarly, knockdown of Myb in $p190^{BCR/ABL}$ expressing human B-cell leukemia lines (Z-181, SUP-B15) resulted in reduced proliferation and colony formation B-cells [226].

These data on mouse models collectively show on the critical role of Myb in the regulation of multiple stages of B-cell development, especially in the pro-B to pre-B cell transition.

1.4.5 miR-150 a target of *MYB* gene in leukemia

Among the top 10 predicted targets of miR-150 belongs *MYB* gene that is critical for B-cell development as described above (Targetscan[72]). MiR-150 is highly B-cell specific microRNA [227]. Xiao *et al.*, validated this computational prediction by luciferase reporter assay in HEK293 cell line where miR-150 targeted MYB. Authors identified three miR-150 putative binding sites at 3`UTR of MYB mRNA. In addition, the enhanced MYB expression in miR-150 deficient B-cells confirmed that miR-150 directly regulates MYB at protein level. This direct relationship was further documented by transfection of progenitor B-cells with mimic-miR-150 that resulted in dose dependent decrease of MYB levels and led to partial block of B cell development with reduced B-cells [228].

Interestingly, in the Bürkitt lymphoma B-cell lines (Daudi, Raji, BJAB, Ramos) the expression of miR-150 is very low. The restoration of miR-150 expression by its stable transfection leads to decreased level of MYB and to terminal differentiation of B-cells. Moreover, elevated level of miR-150 resulted in reduced proliferation of cells that suggest to tumor suppressor role of miR-150 [229].

MYB represents an evolutionary conserved target of miR-150 that is confirmed by highly evolutionary conserved seed region of miR-150 at MYB [230].

2. INTRODUCTION TO THE THESIS

To the mostly used prognostic markers of B-CLL belong expression of ZAP-70, CD38, IgVH status and detection of chromosomal abnormalities by FISH [39]. These markers help to evaluate the status of B-CLL and to predict disease progression [39]. Used prognostic markers are not sufficient in answering following questions: 1) When to start with the therapy? 2) Will the patient respond to the therapy well?

Since the development of leukemia is a multistep process where any step can be deregulated, more detailed knowledge of regulators of the leukemic process in B-CLL is needed. Transcription factors as PU.1 and MYB are involved in regulation of the normal and pathologic hematopoiesis [212,231]. While the transcription factors may regulate each other a tight relationship between transcription factors and miRNAs was recently identified [232]. The role of miRNAs during the leukemic process and moreover the potential role of miRNAs in prognosis and therapy is at present very intensively studied. Fulci *et al.,* described that B-CLL cells express high levels of miR-155 and miR-150 [17]. Moreover, elevated levels of miR-155 inhibit the expression of PU.1 in B-CLL in comparison to the normal healthy B-cells [17,157].

Recent data show the potential usage of miR-155 as prognostic marker in the breast cancer [233]. High expression of miR-155 correlates with higher tumor grade and advanced disease stage [233]. Application of the antisense miR-155 inhibits cell growth, enhances apoptosis and increases sensitivity of the breast cancer cells to the therapy [233]. Based on this information, the measurement of miR-155 levels during disease progression could be similarly used as a marker of B-CLL progression as well.

During the B-cell development, MYB is required for transition from pro-B to pre-B-cells and for survival of accumulated pro-B-cells [214]. The expression of MYB in the hematopoietic cells differs: the highest levels of MYB are in immature, actively dividing cells and the lowest ones in the mature, differentiated cells [212,234]. It was described that MYB is involved in acute myeloid [235] and chronic myeloid leukemia [223], mixed lineage leukemia [236] and in acute lymphoblastic leukemia [219] but not described in B-CLL yet. *MYB* gene was described among the top 10 target genes of miR-150 [228], so we also considered existence of relationship between expression of miR-150, MYB and B-CLL progression.

2.1 Hypothesis

The expression level of oncogenic miR-155 is elevated in hematologic malignancies including B-CLL. The direct target of miR-155 is a key hematopoietic transcription factor PU.1. The miR-155 inhibits PU.1 as a negative post-transcriptional regulator and this leads to progressive blockade of differentiation and leukemogenesis. We hypothesize that MYB proto-oncogene is highly expressed in B-CLL, and that MYB directly promotes the elevation of miR-155 expression level in B-CLL. This might be caused by direct binding of MYB at the promoter region of *MIR155HG* and by this way stimulates the transcription of *MIR155HG* in B-CLL. The detection of high MYB expression levels may be used as the reliable prognostic marker of B-CLL together with miR-155 or miR-150. Moreover, the rescue of PU.1 expression may turn off the leukemic process and may be used as a therapeutic tool in the future.

2.2 Aims of the Thesis

1) To determine whether levels of oncogenic miR-155, miR-150 and transcription factors MYB, PU.1 are related to oncogenesis of B-CLL and to delineate their relationship with the B-CLL disease-prognosis, presence of progression characteristics including ZAP-70, CD38, IgVH and Rai stage and to the therapy response.

2) To determine if proto-oncogene MYB binds to the promoter region of *MIR155HG* and if it stimulates transcription of the *MIR155HG* in B-CLL. To functionally validate direct relationship between MYB, miR-155 and PU.1 in B-CLL cells from patients and in Raji cell line by *in vitro* functional assays.

3) To determine the miR-155 and MYB target genes deregulation in B-CLL in comparison to the normal B-cells using the global microarray approach.

2.3 Specific aims of the Thesis

1) To determine whether levels of oncogenic miR-155, miR-150 and transcription factors MYB, PU.1 are related to oncogenesis of B-CLL and to delineate their relationship with the B-CLL disease-prognosis, presence of progression characteristics including ZAP-70, CD38, IgVH and Rai stage and to the therapy response.

The success of therapy of B-CLL patients is in the proper timing of the therapy. Our aim was to determine the levels of miR-155 in B-CLL patients and test whether there is any correlation between elevated levels of miR-155 and the disease progression (Rai stage, ZAP-70, CD38, IgVH). To answer the question if the expression of miR-155 could be used as reliable prognostic marker, we measured the levels of miR-155 in B-CLL patients in different stages of the disease. MiRNAs negatively regulate transcription of targeted mRNAs. The direct target of miR-155 is a key hematopoietic transcription factor PU.1. Reduced levels of PU.1 were reported to cause leukemia and lymphoma. Here we determined the mRNA and protein levels of PU.1 in B-CLL patient B-cell samples. We also asked if the expression of MYB could be used together with miR-155 as reliable prognostic marker of B-CLL. We measured the mRNA and protein level of MYB in B-CLL patient samples during different

disease stages. Since the miR-150 is a potent inhibitor of MYB, we measured expression level of miR-150 in B-CLL cells in relation with Rai stage and prognostic markers.

2) To determine if proto-oncogene MYB binds to the promoter region *of MIR155HG* and if it stimulates transcription of the *MIR155HG* in B-CLL. To functionally validate direct relationship between MYB, miR-155 and PU.1 in B-CLL cells from patients and in Raji cell line by *in vitro* functional assays.

Transcription factors play crucial role in the development of leukemia. Here we focused on the role of a member of the E-box family - *MYB*. Firstly, we asked whether the mRNA of MYB is increased in B-CLL. Next, we set to verify MYB binding at the *MIR155HG* promoter region and asked if MYB influences transcription of *MIR155HG* in B-CLL. We performed chromatin immunoprecipitation assay of primary B-CLL cells to test if MYB binds at the promoter region of *MIR155HG*. We transfected constructs with mutated or unmutated MYB binding site into HeLa cells and measured the luciferase activity. We asked whether the studied molecules: MYB, miR-155 and PU.1 are in close and mutual relationship within B-CLL. We aimed to verify the relationship between MYB, miR-155 and PU.1 by *in vitro* functional assays using the primary B-CLL cells and lymphoblastic cell line Raji. Here we manipulated the levels of MYB or miR-155 and determined the outcome as well as rescued the levels of PU.1.

3) To determine the miR-155 and MYB target genes deregulation in B-CLL in comparison to the normal B-cells using the global microarray approach.

We performed the microarray analysis on B-CLL patient samples and normal healthy controls to determine if the target genes of miR-155 and MYB are deregulated. Further, by gene set enrichment analysis and by additional tools for prediction of target genes we asked if miR-155 and MYB targeted genes are differentially expressed within B-CLL microarray data.

3. MATERIAL AND METHODS

3.1 Material

3.1.1 Biological material

3.1.1.1 Primary B-CLL patient samples and normal healthy controls

The B-CLL patient samples were collected in the period from 2007 until 2012. The patient cohort included overall 239 peripheral blood samples of 210 B-CLL patients from two medical clinics in the Czech Republic: 1) General Faculty Hospital in Prague (under leadership of prof. MUDr. Marek Trněný and in close cooperation with MUDr. Tomáš Stopka, Ph.D and MUDr. Petra Obrtlíková Ph.D) and 2) Medical Faculty and University Hospital in Brno (by kind collaboration with prof. MUDr. Jiří Mayer, CSc. prof. RNDr. Šárka Pospíšilová, Ph.D and MUDr. Marek Mráz, Ph.D). Total number of all patient samples obtained from General Faculty Hospital in Prague was 210 where 23 patient samples were provided two times and three patient samples were provided three times during the study. 71 samples of these 210 patient samples were separated as peripheral blood mononuclear cells (PBMCs) by Ficoll-Paque and 157 samples CD19+ B-CLL cells were separated by Rosette separation kit (Table 3.1). The plasma was collected from all patients in parallel with peripheral blood, but for this Thesis only ten plasma samples were used (Table 3.1). All patient samples (N=41) from Medical Faculty and University Hospital in Brno were separated for CD19+ B-cells by Rosette separation kit (Table 3.1). The patient cohort consists of 142 men and 68 women (Table 3.2). The patient`s age ranged from 36 to 95 years with median age 65. All patients signed a written consent in accordance with the ethical guidelines.

Diagnostic and prognostic evaluation of patients was done in both medical institutes based on WHO guidelines (http://ncicll.com/ and [28]). The B-CLL diagnosed in 196 cases out of the 210 patients. B-CLL transformation into Richter's syndrome observed in 14 cases (Table 3.2). Based on the prognostic and cytogenetic data, our patient cohort represents a typical B-CLL population (Table 3.2). The distribution (Nr; %) of patients and patient samples based on the mutation status of IgVH, expression of ZAP-70, CD38 and cytogenetic aberrations are shown in table 3.2. Distribution of patients on Rai staging system as follows: Rai stage 0 (N=42; 20%), Rai stage I (N=47; 23%), Rai stage II (N=46; 22%), Rai stage III (N=19;

9%) and Rai stage IV (N=54; 26%) (Table 3.2). 49% of patients were treated during the study (Table 3.2). For detailed clinical and expression information of patient samples please see section 10. Supplement; Supplemental table: 10.1 and 10.2.

The B-CLL patient samples were used for following experimental methods: isolation of total RNA (including miRNA) (N=239); measurement of protein level by western blot (N=5); chromatin immunoprecipitation (ChIP) (N=15); microarrays (N=12); transient transfections (N=2); transduction (N=1); DNA sequencing (N=2).

The cohort of normal healthy donors included overall 22 peripheral blood samples collected in the period from 2009 until 2010 on the Institute of Hematology and Blood Transfusion in Prague. PBMCs were isolated from 10 samples and CD19+ B-cells were separated from 12 samples. Control cohort consisted of 20 males and 2 women; age of donors ranged from 20 to 43 years with median age 31. From all donors written consents in accordance with the ethical guidelines were obtained. The detailed information about the control samples are in section 10. Supplement; Supplemental table 10.3.

The control patient samples were used for following experimental methods: isolation of total RNA (including miRNA) (N=22); measurement of protein level by western blot (N=1); chromatin immunoprecipitation (ChIP) (N=8); microarrays (N=5); transient transfections (N=5); DNA sequencing (N=1).

Table 3.1: Distribution of patient samples and the sample origin.

Medical Institution	PBMCs	CD19+	Plasma
Prague (N=198)	71	157*	10
Brno (N=41)	0	41	0

*From General Faculty Hospital in Prague were donated in total 198 B-CLL patient samples of the peripheral blood including 10 plasma samples. From 30 patient samples were separated PBMCs and also CD19+ B-CLL cells. From Medical Faculty and University Hospital in Brno were donated in total 41 B-CLL patient samples separated for CD19+ B-cells.

Table 3.2: Clinical and biological characteristics of the B-CLL patient cohort.

Parameter	CLL patients (N=210) No (%)					CLL samples (N=239)* No (%)				
Epidemiological data:										
Age at sample providing (median)	36-95 (65)					36-95 (65)				
Gender (Female/Male)	68 (32%) / 142 (68%)					76 (32%) / 163 (68%)				
Prognostic markers:										
IgVH status	**mutated**		**unmutated**			**mutated**		**unmutated**		
	48 (26%)		134 (74%)			60 (30%)		141 (70%)		
ZAP-70	**positive**		**negative**			**positive**		**negative**		
	118 (61%)		76 (39%)			135 (61%)		85 (39%)		
CD38	**positive**		**negative**			**positive**		**negative**		
	100 (48%)		108 (52%)			113 (48%)		123 (52%)		
Disease progression and transformation:										
Rai stage	**0**	**I**	**II**	**III**	**IV**	**0**	**I**	**II**	**III**	**IV**
	42 (20%)	47 (23%)	46 (22%)	19 (9%)	54 (26%)	44 (19%)	53 (22%)	55 (23%)	23 (10%)	60 (26%)
Richter's syndrome (DLBCL/MCL)	**DLBCL**		**MCL**			**DLBCL**		**MCL**		
	11 (5%)		3 (1%)			14 (6%)		3 (1%)		
Cytogenetics:										
Low risk (del13q14)	69 (33%)					78 (33%)				
Intermediate risk (trisomy of 12 chromosome, normal karyotype)	51 (25%)					63 (27%)				
High risk (del11q22-23/del17p13)	14 (7%) / 9 (4%)					20 (9%) / 9 (4%)				
Therapy:										
Therapy prior study	84 (40%)					92 (39%)				
Therapy during study	103 (49%)					124 (52%)				
Overall survival (OS) from dg to last follow up:	**died / alive**					**died / alive**				
OS <5 years	26 (54%) / 113 (70%)					27 (54%) / 138 (73%)				
OS 5-10 years	15 (31%) / 34 (21%)					15 (30%) / 35 (19%)				
OS >10 years	7 (15%) / 15 (9%)					8 (16%) / 16 (9%)				

*23 patients provided two samples and 3 patients provided three samples during the study (2007-2012).

3.1.1.2 Cell lines

The cell lines were obtained from DSMZ (Deutsche Sammlung von Mikroorganismen und Zellkulturen GmbH). Cultivation conditions and media were according DSMZ guidelines.

Raji (#ACC 319) cell line was established from the left maxilla of a 12-year-old African boy with Burkitt`s lymphoma in 1963. Raji cell line was classified as risk category 1 according to the German Central Commission for Biological Safety (ZKBS) [237].
Morphologically, the cells are round, growing in suspension, partly as single cells or in clusters. The cells were cultured in IMDM medium supplemented with 10% FBS, 1% of P/S (Penicillin/Streptomycin) in density of about $0.5x10^6$ cells/mL at 37°C with 5% CO_2. Doubling time of Raji cells is 24-36 hours. Saturated Raji cell culture was splited at ratio 1:4 twice a week. Raji cells were frozen in medium containing 70% of RPMI-1640 medium, 20% FBS and 10% DMSO at aliquots of approximately $3x10^6$ cells per cryotube.

HeLa (#ACC 57) cell line was established from the epithelioid cervix carcinoma of a 31-year-old Afro-American woman (Henrietta Lacks) in 1951. Later the diagnosis changed into adenocarcinoma [238].
Morphologically, the cells are epithelial-like cells growing in monolayer. HeLa cells were cultured in RPM1-1640 medium supplemented with 10% FBS, 1% of P/S in density of about $1\text{-}2x10^6$ cells/mL at 37°C with 5% CO_2. Doubling time of HeLa cells was around 48 hours. Confluent HeLa cell culture was split 1:4 to 1:6 every 3-5 days using trypsin. HeLa cells were frozen in medium containing 70% of RPMI-1640 medium, 20% FBS and 10% DMSO at aliquots of approximately $1x10^6$ cells per cryotube.

NB4 (#ACC 207) cell line was established from the bone marrow of a 23-year-old woman with acute promyelocytic leukemia (APL = AML FAB M3) in second relapse in 1989. Cells carry the t(15;17) PML-RARA fusion gene [239].
Morphologically, the cells are round, growing in suspension. NB4 cells were cultured in RPM1-1640 medium supplemented with 10% FBS, 1% of P/S in density of about $1x10^6$ cells/mL at 37°C with 5% CO_2. Doubling time of NB4 cells was around 35-45 hours. Saturated NB4 cell culture was splited at ratio 1:2, 1:3 once a week. NB4 cells were frozen in

medium containing 70% of RPMI-1640 medium, 20% FBS and 10% DMSO at aliquots of approximately $7x10^6$ cells per cryotube.

3.1.2 Chemicals and buffers

3.1.2.1 Chemicals

Name	Cat #	Company
Acetic acid 99% p.a.	457311	Penta
Albumin, from bovine serum (BSA)	A2153	Sigma-Aldrich
Annexin V FITC	556419	BD Biosciences
Annexin V 10x diluted Binding Buffer	20090907ANXVBB	BD Biosciences
anti-miR miRNA inhibitor negative control#1	AM17010	Ambion
Bradford Reagent	E530	Amresco
Briliant Blau R 250	3862.2	Carl Roth GmbH
CL-XPosure Film (Clear Blue X-ray Film)	34090	Thermo Scientific
Deoxycholic acid (sodium salt)	0613	Amresco
Dimethylsulfoxid (DMSO)	D06502	p_lab
DL-Dithiotherotol (DTT)	0281	Amresco
DMRIE-c	10459-014	Invitrogen
ECL Plus Western Blotting Detection System	RPN2132	GE Healthcare
EDTA	27270	Sigma-Aldrich
EGTA	0732	Amresco
Ethanol 99% p.a.	028621	Penta
Fetal Bovine Serum (FBS)	10270	Gibco, Invitrogen
Ficoll-Paque PREMIUM gradient	17-5442-03	GE Healthcare
Formaldehyde 37% solution	252549	Sigma-Aldrich
Glycine	0167	Amresco
Glycerol	0854	Amresco
Glycogen RNA grade (20mg/mL)	R0551	Fermentas
Chloroform p.a.	256921	Penta
HEPES	0485	Amresco
hsa-miR-155 anti-miRNA inhibitor	AM12601	Ambion

hsa-miR-155 mimic	AM17100	Ambion
jetPEI	101-10-101-10N	Baria
iBlot Gel Transfer Stacks, PVDF, Mini	IB4010-02	LifeTechnologies
Igepal CA-630	I8896	Sigma-Aldrich
IMDM medium	BE12-722F	Lonza
Isopropylalkohol p.a.	593001	Penta
Linear Acrylamide (5mg/ml)	AM9520	Invitrogen
MEM non-essential amino acids (100x)	M714	Sigma-Aldrich
Methanol HPLC	21230-12500	Penta
negative control#1 siRNA	4457289	Ambion
Nuclease eliminator	E891	Amresco
NuPAGE 10% Bis-Tris Gel 1.5mm x 10 well	NP0335BOX	LifeTechnologies
NuPAGE LDS Sample Buffer (4x)	NP0007	LifeTechnologies
NuPAGE MOPS SDS Running Buffer (20x)	NP0001	Life Technologies
OPTI-MEM medium	31985	Gibco, Invitrogen
Penicillin/Streptomycin (P/S) (100x)	15070063	Gibco, Invitrogen
Phosphate Buffered Saline (PBS) (10x)	L1835	Biochrom AG
Polybrane (8mg/ml)	H9268	Sigma-Aldrich
Ponceau S	P3504	Sigma-Aldrich
Precision Protein Dual Color Standards	161-0374	BIO-RAD
Propidium iodid (PI)	P4170	Sigma-Aldric
Protease Inhibitor Cocktail	P8340	Sigma-Aldrich
Protein-A-agarose	P7786	Sigma-Aldrich
Protein-G-Agarose	P4691	Sigma-Aldrich
Ribonuclease A	R4642	Sigma-Aldric
RPMI-1640 medium	R7388	Sigma-Aldrich
siRNA MYB	sc-29855	Santa Cruz
Sodium dodecyl sulfate	M107	Amresco
Sodium chloride	0241	Amresco
Steady-Glo Luciferase Assay System	E1910	Eastport (Promega)
SYBRgreen Master Mix	4368702	LifeTechnologies
TaqMan Universal master Mix II	4427788	LifeTechnologies

Tris-Hcl Ultrapure grade	0234	Amresco
Triton X-100	0694	Amresco
TRIzol reagent	15596-018	Invitrogen
Trypsin (0.25%)	15050	Gibco, Invitrogen
Trypan blue solution (0.4%)	T8154-100mL	Sigma-Aldrich
Tween 20	0777	Amresco
Universal Probe Library (UPL) set	4683633001	ROCHE

3.1.2.2 Buffers and solutions

Buffers and solutions	**Content (final concentrations)**
RIPA lysis buffer (WB)	50mM Tris-Hcl; pH 8,0; 137 mM NaCl; 1% Igepal CA-630; 0.5% Deoxycholic acid sodium salt; 0.1% SDS; Protease Inhibitor Cocktail (dilution 1:1000)
11% Formaldehyde solution (ChIP)	11% formaldehyd; 0.1M NaCl; EDTA(pH 8.0); 1mM EDTA; 0,5mM EGTA; 50mM HEPES (pH 8.0)
Lysis buffer (ChIP)	50mM HEPES-KOH (pH 7.5); 140mM NaCl; 1mM EDTA; 10% glycerol; 0.5% Igepal CA-630; 0.25% Triton X-100
Lysis buffer II (ChIP)	1mM EDTA (pH 8.0); 0.5mM EGTA (pH 8.0); 10mM Tris-Hcl (pH 8.0); 200mM NaCl
Lysis buffer III (ChIP)	1mM EDTA (pH 8.0); 0.5mM EGTA (pH 8.0); 10 mM Tris-Hcl (pH 8.0)
Paro´s IP buffer (ChIP)	0.02% SDS; 2% Triton X-100; 4mM EDTA (pH 8.0); 40mM Tris-Hcl (pH 8.0); 300mM NaCl

Paro´s washing buffer I (ChIP)	0.1% SDS; 1% Triton X-100; 2mM EDTA (pH 8.0); 20mM Tris-Hcl (pH 8.0); 50mM NaCl
Paro´s washing buffer II (ChIP)	0.1% SDS; 1% Triton X-100; 1% EDTA (pH 8.0); 20mM Tris-Hcl (pH 8.0); 500mM NaCl
Buffer for Proteinase K (ChIP)	0.5% SDS; 25mM EDTA (pH 8.0); 10mM Tris-HCl (pH 8.0); 100mM NaCl
MACS buffer (MACS separation)	0.5% BSA; 2mM EDTA in 1xPBS with Ca^{2+}, Mg^{2+} (pH 7.2)
NH_4Cl solution (Erythrocytes lysis)	8.34g NH_4Cl + 1g NaCl + 0.037g EDTA filled up 1L of ddH_2O and sterilized. Stored at 4°C for one month.

3.1.2.3 Commercially kits

Name	**Cat #**	**Company**
Anti-FITC MicroBeads	130-048-701	MACS, Miltenyi Biotech
GeneChip HG-U133 Plus 2.0 Array	900467	Affymetrix
Human B cell line nucleofection kit	VPA-1001	Lonza
miRNAeasy kit	217004	Qiagen
hsa-miR-150 (ID:0000473)	4427975	LifeTechnologies
hsa-miR-155 (ID:0002623)	4427975	LifeTechnologies
hsa-pri-miR-155 (ID:Hs03303349_pri)	4427975	LifeTechnologies
RNA Nano chips	5067-1511	Agilent Technologies
RNU44 (ID: 0001094)	4427975	LifeTechnologies
RosetteSep B cell enrichment kit	15064	Stem Cell Technologies
TaqMan microRNA Reverse Transcription Kit	4366596	LifeTechnologies
3'-IVT Express Kit	901228	Affymetrix

3.1.2.4 Antibodies

Name	Cat #	Method	Company
Anti-Actin HRP-conjugated (clone I-19)	sc-1616	WB	Santa Cruz
Anti-CD19 FITC (clone HIB19)	302206	FACS	Biolegend (Luvil)
Anti-H3K4methyl	ab1012	ChIP	Abcam
Anti-H3K9acetyl	07-353	ChIP	Merck Millipore
Anti-v-Myb/MYB (clon EP769Y)	ab45150	ChIP, WB	Abcam
Anti-PU.1 (clone T-21)	sc-352	WB	Santa Cruz
Normal Rabbit IgG	NI01	ChIP	Merck Millipore

3.1.2.5 Plasmids

Name	Cat#	Company
pcDNA	kindly provided by M. Dvořák, Institute of Molecular Genetics in Prague	
pmaxGFP	as part of nukleofection kit	Lonza
pGL4.17	E6721	EastPort Promega
PU.1-IRES-GFP	expressing lentivirus kindly provided by Prof. A.I. Skoultchi, New York	
MYB (wt)	kindly provided by M. Dvořák, Institute of Molecular Genetics in Prague	

(Generic vector maps of plasmids are in the section 10. Supplement; Supplemental material: 10.1).

3.1.3 Instruments

Name	Company
Amaxa nucleofector Device II	Lonza
BD FACS Aria IIu cell sorter	BD Biosciences
BD FACS Canto II fluorescence analyser	BD Biosciences
Bioanalyzer 2100	Agilent Technologies
Cellometer Auto T4	Bioscience
Digital sonifier cell disruptor M500	Branson
Genetic Analyzer 3500	Life Technologies
iBlot Gel Transfer System	Life Technologies
Mastercycler Gradient	Eppendorf
Sirius Luminometer	Berthold
Spectrophotometer ND-1000	NanoDrop Technologies
7900HT Fast Real-time PCR System	Life Technologies

3.1.4 Programs

Name	Method	Company
Chromas 2.33	DNA sequencing	Technelysium Pty Ltd
FACSDiva software v.6.3	flow cytometry	BD Biosciences
GeneSpring GX10 software	microarrays	Agilent Technologies
GraphPad Prism (version 5) software	RT-qPCR	GraphPad Software Inc.
Scion Image software Beta 4.0.2	WB	Scion Corporation
ProbeFinder Version 2.45	RT-qPCR	ROCHE
TIGR MeV4 4.0.01	microarrays	TM4 Microarray Software

3.2 Methods

3.2.1 Isolation of primary B-cells and plasma

3.2.1.1 Isolation of peripheral blood mononuclear cells (PBMCs) by Ficoll – Paque

The PBMCs were isolated from 71 peripheral blood samples (from General Faculty Hospital in Prague) from B-CLL pacients by Ficoll-Paque PREMIUM gradient.
Briefly, anti-coagulated peripheral blood was diluted with sterile 1xPBS, carefully layered on the Ficoll-Paque PREMIUM solution and centrifuged. Differential migration of cells during the centrifugation results in the formation of layers that contain different cell types (Figure 3.1). The PBMCs are found in the interlayer after centrifugation- seen as “foggy ring”, recovered from this interlayer by short washing step (100g, 6min, 4°C) with a 1xPBS that removes any platelets, rest of Ficoll-Paque PREMIUM and plasma.

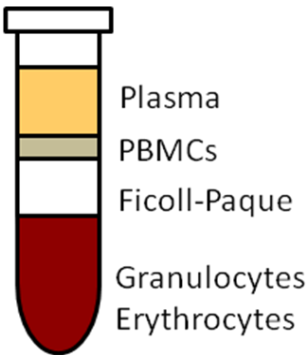

Figure 3.1: Scheme of separated fractions of blood cells by Ficoll-Paque PREMIUM. After centrifugation of peripheral blood on the Ficoll-Paque PREMIUM layer the PBMCs – B, T lymphocytes and ~1% of monocytes, platelets were found in the interlayer between the plasma and the Ficoll-Paque PREMIUM. On the top of the erythrocytes pellet were granulocytes.

With the separated B-CLL/SLL patients PBMC cells was done one or more of the following experimental procedures: 1) cryopreservation: frozen in the freezing medium (90% FBS + 10% DMSO) for 24-48hrs and for the long storage in the liquid nitrogen; 2) transient transfections (N=2) or transduction experiments (N=1); 3) Isolation of mRNA/miRNA for expression profile (N=71) or 4) Microarray profiling (N=12).

The primary PBMCs were cultured one week for maximum (for transient transfections and transduction) *in vitro* in IMDM medium supplemented with 20% FBS, 1% of MEM non-essential amino acids and 1% of P/S at 37°C in humidified atmosphere with 5% of CO_2.

3.2.1.2 Isolation of CD19+ B-cells by RosetteSep kit

The CD19+ B-cells were isolated from 198 peripheral blood samples of B-CLL patients (157 patients samples were from General Faculty Hospital in Prague and 41 from Medical Faculty and University Hospital in Brno) and as well from 12 normal healthy controls from Institute of Hematology and Blood Transfusion in Prague (Table 3.1).

The method of separation the CD19+ B-cells by commercially available Rosette Sep kit is based on the principle involves contacting a sample containing nucleated cells and red blood cells with an antibody composition which allows immunorosettes of the nucleates cells and the red blood cells to form. Briefly, immunorosettes form by crosslinking of B-cell enrichment antibody cocktail with the unwanted cells through multiple erythrocytes. Immunorosettes are targeted for removal with tetramer antibody complexes recognizing CD2, CD3, CD16, CD36, CD56, CD66b and glycophorin A on the erythrocytes. The unwanted cells are than pelleted with the free erythrocytes by centrifugation over a density medium Ficoll-Paque PREMIUM. Desired cells are not labeled with the antibody cocktail and are collected as a highly enriched population at the interlayer between the plasma and the Ficoll-Paque PREMIUM density medium (Figure 3.2).

The purity of separation was confirmed by flow cytometry using anti CD19 FITC antibody. The purity exceeded 93%. The viability of separated cells measured by Trypan blue and Cellometer Auto T4 was more than 90%.

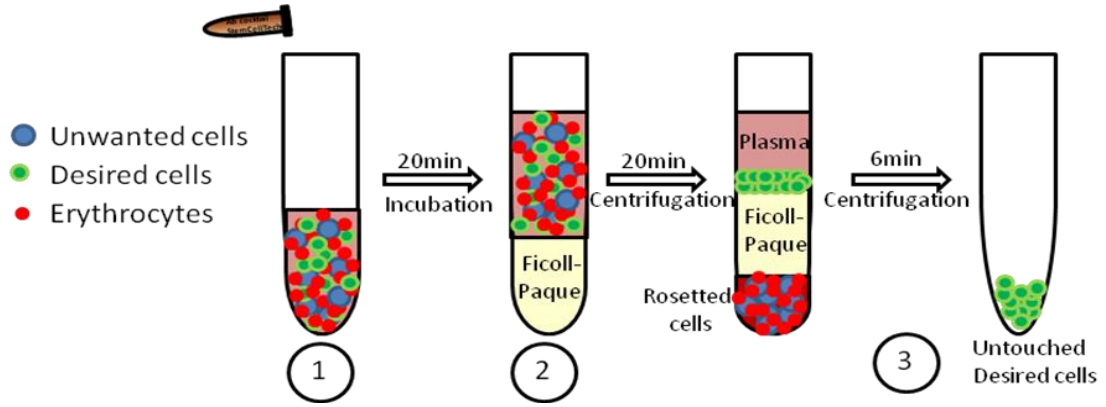

Figure 3.2: Scheme of RosetteSep procedure. During the first step the unwanted cells from whole blood bound to the erythrocytes by using special antibody cocktail. Than the suspension incubated for 20 minutes at room room temperature (RT). During the second step the suspension is loaded on the Ficoll-Paque layer and centrifugated for 20 minutes, RT. The unwanted cells pellet along with the erythrocytes. During the third step enriched CD19+ B-cells are collected. The scheme was adapted from the Stem Cell Technologies: http://www.stemcell.com/en/Products/All-Products/RosetteSep-Human-B-Cell-Enrichment-Cocktail.aspx.

3.2.1.3 Plasma separation

The plasma of 10 B-CLL patient peripheral blood samples was obtained by centrifugation at 2000rpm for 10min at 4°C. The miRNAs from plasma samples were isolated by miRNA easy kit following the manufacturer's instructions (see section miRNA isolation). Plasma samples were stored at -80°C.

3.2.1.4 Lysis of erythrocytes by ammonium chloride (NH_4Cl)

The membranes of erythrocytes are effectively permeable to NH_4Cl. The erythrocytes lysis occurs due to unbalanced osmotic pressure. The peripheral blood samples from the normal healthy donors (N=10) were lysed by ammonium chloride (15minutes; 37°C) prior the magnetic separation of CD19+ B-cells.

3.2.1.5 Magnetic separation of CD19+ B-cells by MACS magnetic beads

After erythrocytes lysis, the CD19+ B-cells were isolated by magnetic beads separation. In the first step, the cells were stained with FITC-labeled anti-CD19 antibody. In the second step, anti-FITC magnetic beads were bound to the CD19+ (FITC stained) cells. The third step was magnetic separation of CD19+ cells labeled with magnetic beads on the MACS columns in the magnetic field, where non-labeled cells goes through the column, and labeled cells stay inside the column. Labeled cells were than collected from column.

3.2.2 Flow cytometry analysis (FACS)

3.2.2.1 Control measurements for CD19 purity after MACS separation

The purity of magneticaly enriched CD19+ B-cells was confirmed by flow cytometry (FACS). The cell viability and apoptosis was measured by propidium iodide (PI) and AnnexinV staining. The purity of MACS isolated cell population exceeds 93% and cell viability exceeds 90%. The separated CD19+ B-cells were further proceeded for RNA/miRNA isolation (N=10).

3.2.2.2 Propidium iodide (PI) staining

PI is a membrane non-permissible dye that is generally excluded from viable cells. PI will stain necrotic and late apoptotic cells with compromised membranes. In dead (or apoptotic) cells, PI binds to the double stranded DNA by intercalating between the base pairs. 1µL of PI was added per sample directly before FACS analysis.

3.2.2.3 AnnexinV staining

AnnexinV belongs to family of calcium-dependent phospholipid-binding proteins. AnnexinV marks mid to late stage apoptotic cells by labeling phosphatidyl serine (PS). Under normal physiologic conditions, PS is predominantly located in the inner site of the cell membrane. After initiation of apoptosis, PS is translocated on the outer surface of the cell membrane. This phenomen is used for the detection of apoptotic cells by fluorescently labeled antibodies to AnnexinV.

Briefly, cells were harvested and washed with 1xPBS and binding buffer. Stained with FITC conjugated AnnexinV for 10-15 minutes at room temperature, in dark. After AnnexinV staining, cells were washed with binding buffer and analysed by flow cytometry within one hour.

3.2.3 Transient transfections and transduction

3.2.3.1 Transfection of primary B-CLL cells by lipofection reagent DMRIE-c

Primary PBMC cells isolated from 2 B-CLL patient samples were transfected with following molecules: 1) siRNAs MYB (pool of three target specific siRNAs) and negative control #1 siRNA; 2) hsa-miR-155 anti-miRNA Inhibitor and miRNA inhibitor negative control #1; 30) pmaxGFP plasmid (2µg). The pmaxGFP plasmid was used for optimization of transfections - to find the final and most efficient concentration of desired oligonucleotides.

Transfection reagent DMRIE-c (1,2-dimyristyloxypropyl-3-dimethyl-hydroxy ethyl ammonium bromide and cholesterol) represents a liposomal component that forms complexes with nucleic acids (RNA, DNA). DMRIE-c is efficient for transfections of mammalian cells, particularly lymphoid suspension cells.

The confluency of cells was around 80%. Cells were washed with the serum and antibiotics-free medium OPTI-MEM prior to transfection. The siRNA against MYB (30nM) or anti-miR-155 (40nM) as well as negative controls (added in the same final concentrations as the concentrations of specific siRNA MYB/anti-miR-155) were mixed with DMRIE-c and OPTI-MEM medium. Transfection suspension was added to the cell suspension and incubated in humidified atmosphere with 5% CO_2 at 37°C for 5 hours. After 5hrs of incubation with transfection reagents the equal volume of cultivation IMDM medium was added to the cells. The transfection efficiency was controlled by fluorescence activity of pmaxGFP, efficacy of B-CLL cells was around 60%. Transfected cells were harvested after 48 hrs (MYB siRNA) or 96 hrs (anti-miR-155). Total RNA was extracted and RT-qPCR was performed (see section RNA isolation and RT-qPCR).

3.2.3.2 Transfection of HeLa cells by lipofection reagent JetPEI

Into HeLa cells were transfected MYB (wt; mutated MYB binding sites) and control pcDNA plasmids by lipofection reagent JetPEI (linear polyethilenimine). The confluence of HeLa cells prior to transfection was around 60%. Transfection reaction contained plasmid DNA, jetPEI solution and NaCl solution. The transfection reagents were mixed and incubated for 25 minutes at room temperature to form the complexes. The formed complexes were added to the HeLa cells by slow pippeting. HeLa cells were incubated in the humidified

atmosphere with 5% CO_2 at 37°C. After 48 hrs, the HeLa cells were harvested and lysates for luciferase assay and for western blot were prepared.

3.2.3.3 Transfection of Raji cells by Amaxa nucleofector

Raji cells were transfected with following molecules: 1) MYB siRNAs (pool of the three target specific siRNAs) and siRNA negative control#1; 2) mimic hsa-miR-155 and miRNA negative control#1; 3) hsa-miR-155 anti-miRNA Inhibitor and miRNA inhibitor negative control#1; 4) MYB and control pcDNA plasmids. The pmaxGFP plasmid was used for optimization of transfections - to find the final and most efficient concentration of desired oligonucleotides.

The Raji cells were transfected by nucleofector Amaxa with Human B-cells nucleofection kit. 24 hrs prior to transfection the cell number was determined, cells were seeded in the ~70% of confluency in 6 well plates and cultured until transfection in IMDM medium with FBS, but without antibiotics. On the next day, the cultured Raji cells were centrifuged and washed once with 1xPBS. Two million of Raji's cells were mixed with the nucleofection solution and transfected with oligonucleotides of hsa-miR-155 (40nM and 100nM final concentration), anti-miR-155 (40nM and 100nM final concentration/well), siRNA MYB (30nM and 100nM final concentration/well), MYB and control pcDNA plasmids (0.2µg and 2µg/well) and co-transfected with pmaxGFP plasmid (2µg/well) provided with the transfection kit. The program M-013 was used for transfection as recommended. After nucleofection the cells were immediately transferred into warmed up culture medium (37°C) and incubated in humidified atmosphere with 5% CO_2 at 37°C. Transfected cells were harvested after 24 hrs for mimic hsa-miR-155 transfection and 48 hrs for transfection of siRNA MYB, anti-miR-155, plasmid MYB. The transfection efficiency was controlled by fluorescence microscopy by fluorescence activity of pmaxGFP. The transfection efficacy was ~70%. The RNA was extracted and RT-qPCR was performed.

3.2.3.4 Transduction of primary B-CLL cells with lentivirus

Primary PBMC cells from B-CLL patient sample (P40) were infected with either GFP expressing plasmid or *PU.1*-IRES-GFP expressing lentivirus. Infection of primary B-CLL cells was performed with MOI=3 [MOI=multiplicity of infection; means the ratio of infectious agents (e.g. virus) to infection targets (e.g. cell)]. After 48 hrs, the GFP positive infected cells were sorted out (Fluorescence activated cell sorting, BD FACS AriaIIu), and cultured for 24 hrs in the IMDM medium supplemented with 10% of FBS and 1% of MEM non-essential amino acids in humidified atmosphere with 5% CO_2 at 37°C. The viability of infected cells was determined by PI and AnnexinV staining (see PI and AnnexinV staining).

3.2.4 Luciferase reporter assay

To test the putative MYB binding site at the promoter region of *MIR155HG* the mutated region in MYB binding site was subcloned into pGL4.17 plasmid. The mutated region originated from the region of MYB binding site (E-box1) localized at -397nt to – 335nt from TSS. It was deletion of 5nt CCACC in forward direction and deletion of 5nt GGTGG in reverse direction (Figure 3.3). The MYB “wt” and MYB “mutated” plasmids were transiently transfected into HeLa cells by transfection reagent jetPEI (see also section transfection). The HeLa cells were harvested 48hrs post transfection. Following the manufacturer`s instruction the luciferase assay was performed.

The luciferase activity was measured using Dual Luciferase Assay on Sirius luminometer with the collection time 10 seconds. The values of luciferase activity were normalized to the protein content relative to the signal of transfected cells with the empty reporter vector pGL4.17.

Scheme of DNA sequence of *MIR155HG* with CpG islands and putative MYB binding sites

- CpG -33 to 349bp (relative to TSS)
- MYB binding motif (AACT/G) -399 to -394bp (E-box 1)
  209 to 215bp (E-box 2)
  1201 to 1207bp (E-box 3)
- Primers for ChIP and sequencing

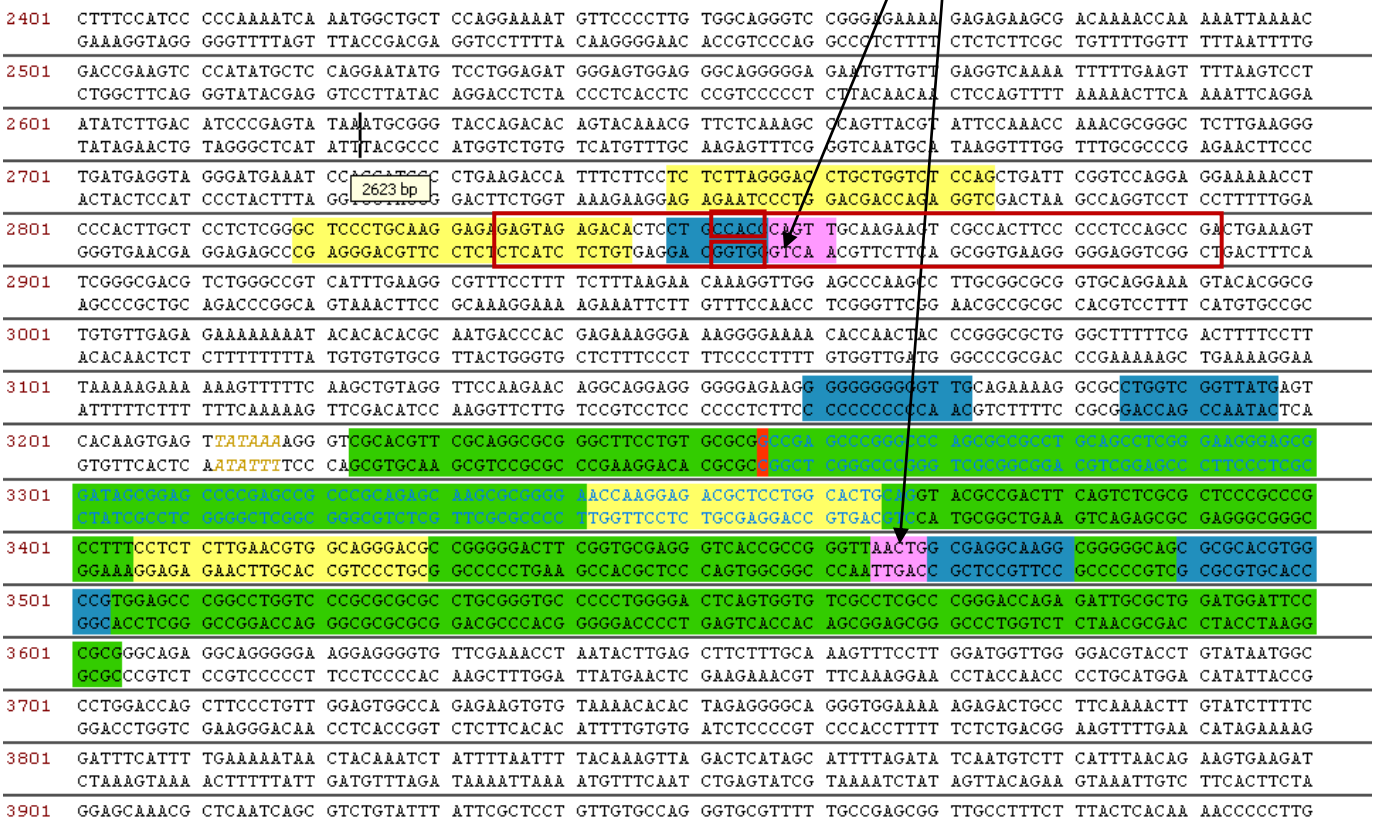

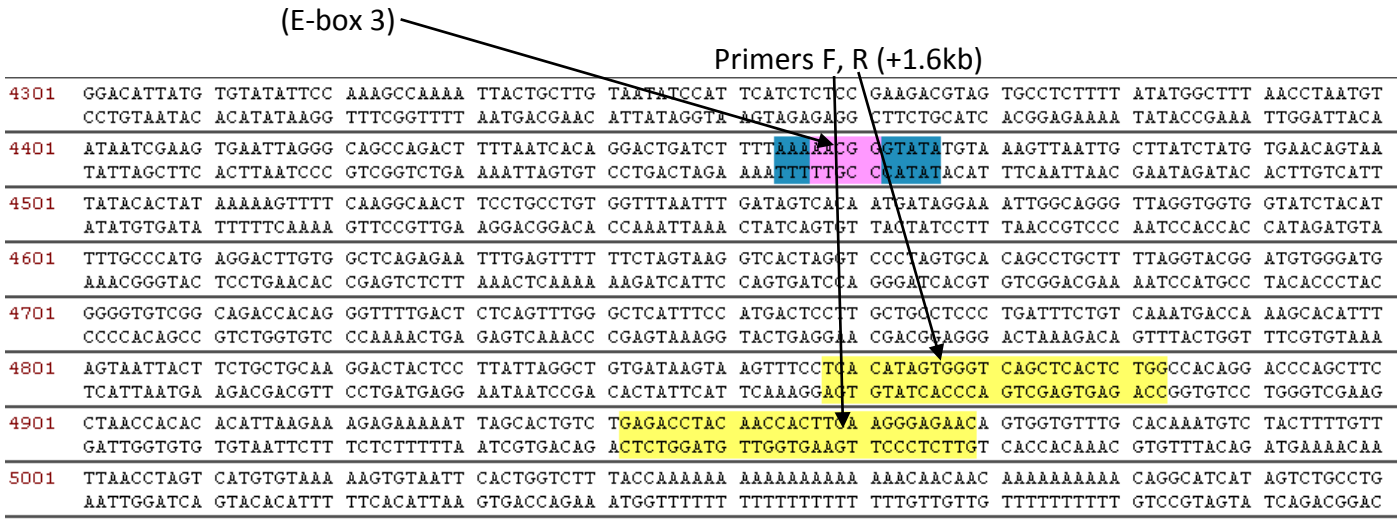

Figure 3.3: Scheme of DNA sequence of *MIR155HG* with CpG islands and putative MYB binding sites. The scheme shows the DNA sequence of *MIR155HG* with highlighted E-box sequences (blue) and putative MYB binding sites (E-box 1, 2, 3 (pink)), CpG islands (green color), TSS (red), primers for ChIP: -0.5kb, +0.1kb, +1.6kb from TSS (yellow), TATA box (-44bp; dark yellow). The DNA sequence of *MIR155HG* (NT_000021.8) was obtained from GenBank database and further worked out in the program Vector NTI suite 9.

Sequences of primers for subcloning of wt versus mutated MYB binding site into pGL4.17 plasmid:

(Oligonucleotides containing the putative MYB binding site (in bold and italic) and oligonucleotides with mutation/deletion of putative MYB binding site (E-box 1) are highlighted in gray color:

Primer 1F (wt) (in the region of E-box 1 (red box))
TCGAGTC GACACTCCTGCCACC***CAGTT***GCAAGAAGTCGCCACTTCCCCCTCCAGCCGA

Primer 1R (wt) (in the region of E-box 1 (red box))
AGCTTCGGCTGGAGGGGGAAGTGGCGACTTCTTGC***AACTG***GGTGGCAGGAGTGTC GAC

Primer 2F (mut) (in the region of E-box 1 (red box)) with deletion of CCACC
TCGAGTC GACACTCCTG***CAGTT***GCAAGAAGTCGCCACTTCCCCCTCCAGCCGA

Primer 2R (mut) (in the region of E-box 1 (red box)) with deletion of GGTGG
AGCTTCGGCTGGAGGGGGAAGTGGCGACTTCTTGC***AACTG***CAGGAGTGTC GAC

3.2.5 Western blot

Primary PBMC cells of B-CLL patient samples (N=5) and NB4, HeLa cells were lysed and sonicated. Denatured cell lysates were loaded on the Bis-Tris gel. The gels were dry-blotted by iBlot Gel Transfer System. Prior to overnight incubation with primary antibody the membranes were blocked by non-fat milk in PBS/Tween 20. The membrane was washed with PBS/Tween 20 and incubated with the secondary antibody HRP-conjugated. For visualization of bands the ECLPlus Western Blotting Detection System and X-ray films were used. As a loading control antibody the anti-Actin HRP-conjugated antibody was used. The optical density of protein bands was measured by Scion Image software.

3.2.6 Chromatin immunoprecipitation (ChIP)

Chromatin from $10x10^6$ primary PBMCs cells (isolated from B-CLL patients samples, N=15 and normal healthy B-cells (N=8)) was cross-linked with 1% formaldehyde for 10 minutes at room temperature. Subsequently cells were lysed by a set of lysis buffers to isolate the nuclei from cells that were resuspended in 2ml of low-salt buffer and sonicated (45% intensity, 500 cycles of 2 seconds, in ice-ethanol cooling bath) with a Branson Sonic Dismembrator equipped with a microtip to yield 200bp to 400bp DNA fragments [240,241]. ChIP was performed using the following antibodies: antibodies against H3K9Ac, H3K4Me3, MYB and isotypic normal rabbit IgG as a control nonspecific antibody. DNA extracted from the immunoprecipitates was used as template for SYBRGreen based qPCR reactions. Specific occupancy on DNA ("percentage of input") was defined as a copy number of a specific DNA fragment in each immunoprecipitate compared with the copy number of that DNA fragment within 1/100 input dilution used for immunoprecipitation (1% input DNA). The control antibody values were subtracted from the values obtained using the specific antibodies.

The quantitative PCR was performed on the 384 well plates in the real time PCR machine and samples were runned in duplicates. The single qPCR reaction composed of 8µL=1µL of DNA + 0.4µ of 20µM primers (F+R) + 4µL of SYBRgreen Master Mix + 2.6µL of sterile ddH_2O.

The sequence of primers used for qPCR amplification of precipitated DNA were as follows:

putative MYB binding site 1 (E-box 1):
MIR155HG (-0.5kb) F: TCTCTTAGGGACCTGCTGGTCTCCAG
MIR155HG (-0.5kb) R: TGTCTCTACTCTCTCCTTGCAGGGAGC

putative MYB binding site 2(E-box 2):
MIR155HG (+0.1kb) F: ACCAAGGAGACGCTCCTGGCACTG
MIR155HG (+0.1kb) R: CGTCCCTGCCACGTTCAAGAGAGG

putative MYB binding site 3 (E-box 3):
MIR155HG (+1.6kb) F: TCACATAGTGGGTCAGCTCACTCTGG
MIR155HG (+1.6kb) R: GTTCTCCCTTGAAGTGGTTGTAGGTCTC

Program for SYBRgreen based qPCR:

50°C 2min, 95°C 10min, 95°C 15sec, 60°C 1min, 95°C 15sec, 60°C 15sec, 95°C 15sec for 40 cycles.

Presence of chromatin modifications of histones – "percentage of input" is defined as a copy number of specific DNA locus in each specific DNA immunoprecipitate normalized on the copy number of the same locus in the same immunoprecipitate sample in dilution 1:100 (1% of DNA input). From the obtained PCR values of "percentage of input" from the specific antibody, the "percentage of input" the control antibody was subtracted.

3.2.7 Isolation of mRNA/miRNA and preparation of cDNA

3.2.7.1 Isolation of mRNA/miRNA from PBMCs, B-cells, Raji cells by TRIzol reagent

Total RNA was extracted from all patients samples (N=239) and control samples (N=22) by TRIzol reagent followed by manufacturer`s protocol with modifications. The precipitation step with isopropanol at -20°C overnight was enhanced by adding linear acrylamide. On the next day, the RNA precipitate was centrifuged at 14000rpm for 30min at 4°C. RNA precipitate was washed with 75% Ethanol, dried on the air and finally resuspended in RNAse free sterile water. The RNA quantity was determined by ND-1000 Spectrophotometer and quality was determined by Agilent 2100 Bioanalyzer. Isolated RNA was stored at -80°C or overwritten into cDNA and run RT-qPCR (see section cDNA and RT-qPCR).

3.2.7.2 Preparation of cDNA (complementary)

For cDNA preparation the TaqMan microRNA Reverse Transcription Kit was used. The manufacturer`s instructions were followed. Single cDNA reaction with components of kit and RNA composed of 15µL (set up of single cDNA reaction is below) and reverse transcription reaction proceed at thermal cycler with program: 30min 16°C, 30min 42°C, 5min 85°C, after hold at 4°C. The 5x primers of specific microRNAs (RNU44, miR-155, miR-150) were as part of specific miRNA assay kit. After reverse transcription reaction complete, sterile H_2O was added to reach the final volume 50µL. The RT-qPCR was performed. The cDNAs were stored at -20°C.

cDNA reaction:	1x
10x RT buffer	1.5µL
25xdNTPs (100mM)	0.4µL
RNAse inhibitors	0.1µL
RT Random primers (10x)	0.5µL
5x primer (for specific miRNA)	1.5µL
Multiscribe Reverse Transcriptase (RT)	1.0µL
RNA (100ng/µL)	1.0µL
ddH_2O	9.0µL
	15.0µL

3.2.7.3 Isolation of miRNAs from B-CLL patient plasma samples by miRNAeasy kit

MicroRNAs (miR-155, miR-24 and let-7a) were isolated from 10 B-CLL plasma samples by miRNA easy kit following the manufacturer`s protocol. Briefly, plasma was lysed and homogenized in QIAzol lysis reagent (monophasic solution of phenol and guanidine thiocyanate). By adding chloroform and centrifugation the plasma lysate separated into aqueous and organic phase. The upper aqueous phase was extracted where the miRNA occurred. By adding ethanol the RNA bonded on the RNAeasy mini elute spin column. From the column was washed out phenol and other contaminants by washing buffers provided by kit. The separated miRNAs were eluted in RNAse free water.

3.2.7.4 Preparation of cDNA (complementary)

The miRNAs from plasma were reverse transcribed by using TaqMan microRNA cDNA Reverse Transcription kit with specific miRNA primers by following the manufacturer`s instructions. Single cDNA reaction composed of 15µL and run at thermal cycler with following program: 30min 16°C, 30min 42°C, 5min 85°C, hold 4°C. After completing, the reverse transcription was proceeded in Real Time qPCR (RT-qPCR). The cDNAs were stored at -20°C.

cDNA reaction:	1x
10x RT buffer	1.5µL
25xdNTPs (100mM)	0.4µL
RNAse inhibitors	0.1µL
5x primer (for specific miRNA)	1.5µL
Multiscribe Reverse Transcriptase (RT)	1.0µL
miRNA	5.0µL
ddH_2O	5.5µL
	15.0µL

3.2.8 Performing of RT-qPCR by TaqMan system and with ROCHE probes

The expression of mRNAs/miRNAs was determined by TaqMan chemistry together with mRNA primers with specific probe and specific miRNA primers provided by microRNA assay kits.

The TaqMan RT-qPCR system is based on fluorogenic-labeled probes that use the 5' nuclease activity of Taq DNA polymerase that detects specific PCR products.

The quantification by the miRNA assays pass over in the two-step RT-qPCR (Figure 4, step 1 and 2). During the reverse transcription (RT) the stem-loop specific miRNA primer (5x) gave rise to the first strand of cDNA (Figure 3.4, step 1). Later, during the qPCR are amplified the PCR products from cDNAs using the TaqMan specific miRNA assay primers (20x) together with the TaqMan Universal PCR Master Mix II that contains the TaqMan probe. TaqMan probes are dual labeled (FAM, NFQ) and hydrolysis of probes increases the specificity of RT-qPCR. TaqMan probes contain a FAM dye label on the 5' end and the minor groove binder (MGB) that increases the melting temperature (Tm). The MGB is attached on

the non-fluorescent quencher (NFQ) localized on the 3' end that inhibits fluorescence when the probe is intact (Figure 3.4, step 3). In the presence of target sequence, the TaqMan probe anneals between the primer sites and the Taq DNA polymerase with 5` nuclease activity cleaves this boundary during the extension of strand. The reporter dye molecules are cleaved from their respective probes with each cycle (Figure 3.4, step 3). The FAM dye separates from NFQ and the reporter signal increases. The removing of the TaqMan probe from target strand allows primer extension and continuing of the polymerization of the template to the end (Figure 3.4, step 4). The increase of fluorescence intensity is equal to the amount of produced amplicons. The higher the starting copy number of the nucleic acid target, the sooner a significant increase in fluorescence is observed. The 5'nuclease assay process (Figure 3.4, steps 4 - 6) takes place during PCR amplification. This process occurs in every cycle and does not interfere with the exponential accumulation of product. During PCR, the TaqMan MGB probe anneals specifically to a complementary sequence between the forward and reverse primer sites (Figure 3.4, step 3). When the probe is intact (Figure 3.4, step 3 and 4), the proximity of the reporter dye to the quencher dye results in suppression of the reporter fluorescence. The Taq polymerase cleaves only probes that are hybridized to the target sequence (Figure 3.4, step 5). Cleavage separates the reporter dye from the quencher dye; the separation of the reporter dye from the quencher dye results in increased fluorescence by the reporter. The increase of fluorescence signal occurs only when the target sequence is complementary to the TaqMan probe and is amplified during qPCR. Because of these requirements, non-specific amplification is not detected. Polymerization of the strand continues, but because the 3' end of the probe is blocked, there is no extension of the probe during PCR (Figure 3.4, step 6).

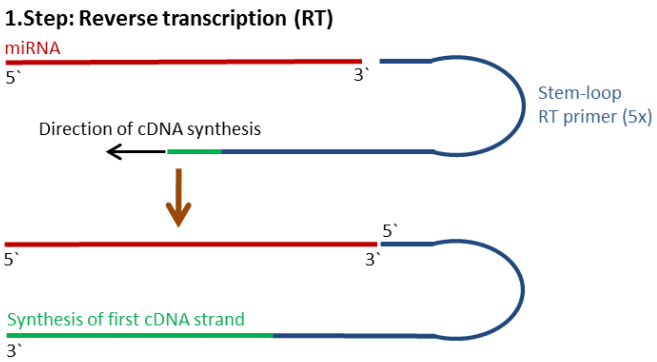

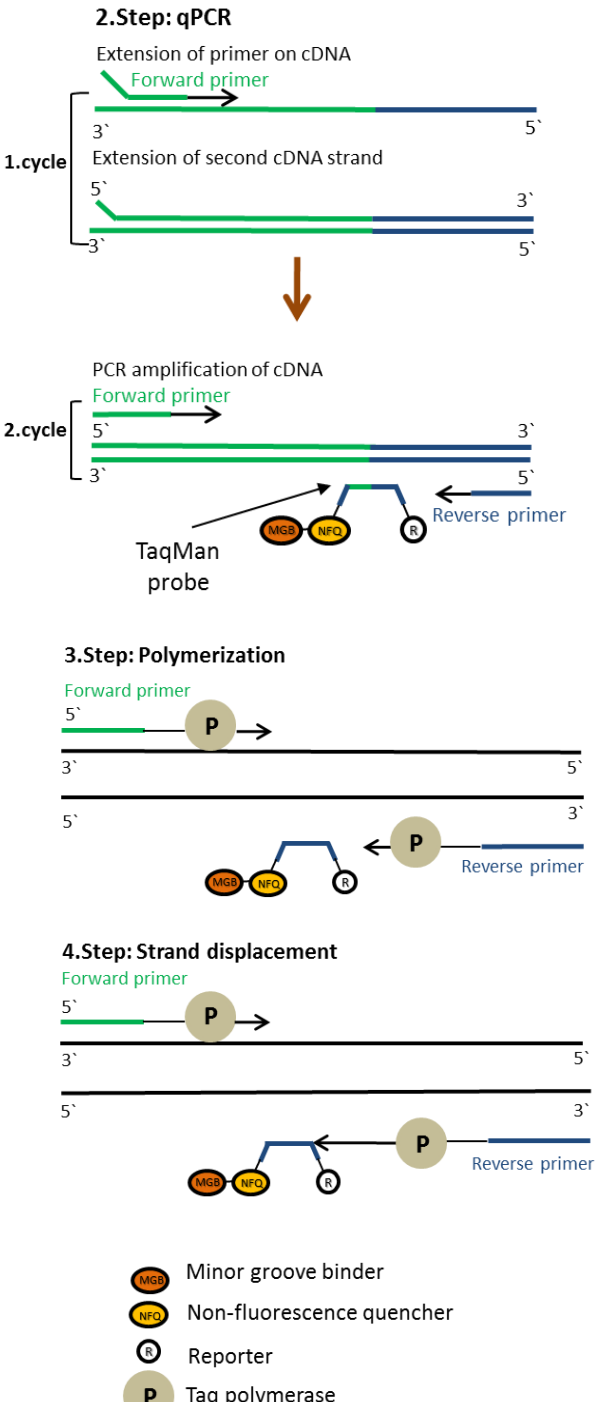
2.Step: qPCR
Extension of primer on cDNA
Forward primer
3`
5`
1.cycle
Extension of second cDNA strand
5`
3`
3`
5`
PCR amplification of cDNA
Forward primer
2.cycle
5`
3`
3`
5`
MGB
NFQ
R
Reverse primer
TaqMan
probe
3.Step: Polymerization
Forward primer
5`
P
3`
5`
5`
3`
P
MGB
NFQ
R
Reverse primer
4.Step: Strand displacement
Forward primer
5`
P
3`
5`
5`
3`
P
MGB
NFQ
R
Reverse primer
MGB
Minor groove binder
NFQ
Non-fluorescence quencher
R
Reporter
P
Taq polymerase

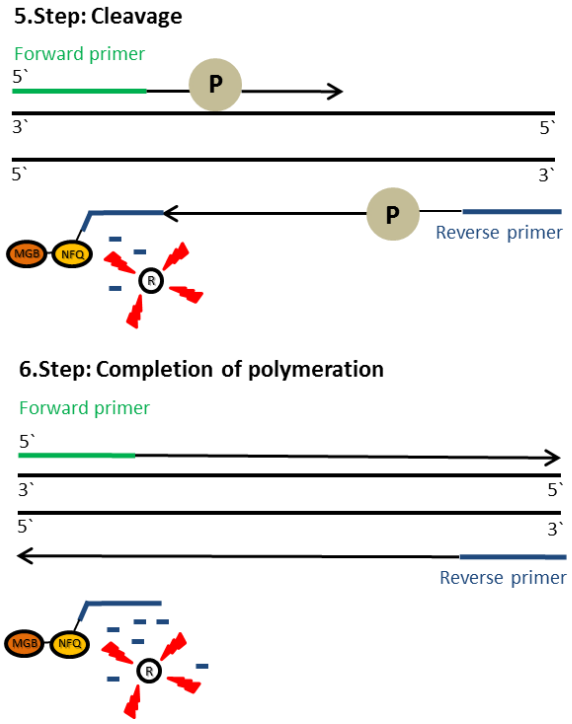

Figure 3.4: Scheme of the TaqMan system RT-qPCR. Scheme describes the preparation of cDNA and process of RT-qPCR. In the first step the miRNA specific primer gave rise to first strand of cDNA, the next steps describes the process of prolongation of strand during qPCR. During the polymerization the FAM and NFQ are attached to the TaqMan probe. During the each extension cycle the reporter dye FAM is cleaved from TaqMan probe. After separation of the FAM from NFQ the reporter dye emits fluorescence that is measured during qPCR. (adapted from http://www3.appliedbiosystems.com/cms/groups/mcb_support/documents/generaldocuments/cms_041461.pdf).

The single reaction RT-qPCR reaction was composed from cDNA master mix (MM) and primer master mix (miRNA primer MM or mRNA primer MM) with the final volume of 8µL. The detailed formula for the single master mix reactions are below:

<u>Single reaction – cDNA master mix:</u>	1x
TaqMan Universal PCR Master Mix II	2.0µL
ddH_2O	1.5µL
cDNA	0.5µL
---	---
	4.0µL
+	
<u>Single reaction – mRNA primer master mix:</u>	1x
TaqMan Universal PCR Master Mix II	2.0µL
Primer F+R (20µM)	0.4µL
Probe (10µM)	0.1µL
ddH_2O	1.5µL
---	---
	4.0µL

or

Single reaction – miRNA primer master mix:	1x
TaqMan Universal PCR Master Mix	2.0µL
miR primer (20x)	0.4µL
ddH_2O	1.6 µL
	4.0µL

The RT-qPCR reactions were applied on the 384 well plates and run on the qPCR instrument according to manufacturer's instructions. Program for cycling of the TaqMan based RT-qPCR reactions was as follows: 95 °C 15s and 60 °C 1´; 40 cycles.

The mRNA primers and specific probes were designed by software ProbeFinder Version 2.45 and Vector NTI Suite 9. The sequences of mRNA primers with specific ROCHE probes are shown in Table 3.3.

Table 3.3: Sequences of mRNA primers with specific ROCHE probes.

Primer name	Probe #	Probe sequence	Primer sequence
GAPDH F	60	CTTCCCCA	AGCCACATCGCTCAGACAC
GAPDH R	60	CTTCCCCA	GCCCAATACGACCAAATCC
PU.1 F	27	CAGGCAGC	CCACTGGAGGTGTCTGACG
PU.1 R	27	CAGGCAGC	CTGGTACAGGCGGATCTTCT
FOS F	67	TGCTGGAG	CTACCACTCACCCGCAGACT
FOS R	67	TGCTGGAG	AGGTCCGTGCAGAAGTCCT
MYB F	56	TGCTGTCC	TGCTCCTAATGTCAACCGAGA
MYB R	56	TGCTGTCC	AGCTGCATGTGTGGTTCTGT
MYC F	34	CTGCCTCT	CACCAGCAGCGACTCTGA
MYC R	34	CTGCCTCT	GATCCAGACTCTGACCTTTTGC

F=Forward; R=Reverse

3.2.8.1 RT-qPCR data analysis and statistics

For the RT-qPCR data analysis the delta-delta Ct method was used, where the Ct (cycle threshold) values of **s**pecific (**s**) were subtracted from Ct values of **r**eference gene (**r**); calculated by $2^{\Delta\Delta(Ctr-Cts)}$ equation. MicroRNA expression levels were normalized on the expression levels of reference gene - RNU44 (small nucleolar RNA, C/D box 44) and mRNA expression levels were normalized on the reference gene GAPDH (glyceraldehyde-3-phosphate dehydrogenase). In case of plasma samples, the normalization was done on average (AVG) of miR-24 and let-7a Ct values. Expression data are presented as mean (two biological duplicates) and error bars indicate the standard error of the mean (SEM).

For statistical analysis of expression data from B-CLL patient samples (PBMCs, CD19+) and controls the Student`s t test and Mann-Whitney test was used (GraphPad software) was used. Any difference for which the P value was <0.05 was regarded as statistically significant (*).

3.2.9 Microarray mRNA profiling

To perform the genome-wide microarray mRNA profiling by the Affymetrix HG-U133 Plus2 GeneChip we separated B-cells from B-CLL peripheral blood patient samples (N=16) and also from peripheral blood samples of healthy donors (N=5). We filtered out 4 B-CLL patient samples due to GeneSpring Quality Control Principal Component Analysis (PCA) analysis.

Briefly, total RNA was purified by TRIzol reagent (see section RNA isolation) followed by preparation of biotin-labeled cRNA (complementary) target population according to 3'-IVT Express Kit protocol. The cRNA probes were used for subsequent hybridization on the gene expression chip containing nearly 50 000 probes followed by fluorescent staining, fluidics processing and scanning according to the Affymetrix recommendations.

3.2.9.1 Microarray data analysis and statistics

High throughput data analyses were performed using GeneSpring GX10 and TIGR MeV4 softwares [242]. GeneSpring software was used for probe level data preprocessing and summarization (using RMA), quality control analysis based primarily on Principal Component

Analysis (PCA) and partially for statistical analysis of microarray data. MeV4 software was used for data visualization, for creating the heat maps.

To determine the expression of **miR-155 targets** in B-CLL patients samples we used the 6 following target prediction tools (data are available on: http://dnasuite.com/gsea/):

PicTar:http://pictar.mdc-berlin.de/

Targetscan:http://www.targetscan.org/

Microrna:http://www.microrna.org/

Microcosm:http://www.ebi.ac.uk/enright-srv/microcosm/

TargetsDiana:http://diana.cslab.ece.ntua.gr/tarbase/

GSEAset:http://www.broadinstitute.org/gsea/msigdb/cards/AGCATTA,MIR-155.html

To determine pattern of expression of **MYB targets** we used 3 different lists of MYB target prediction tools (data are available on: http://dnasuite.com/gsea/):

Set MYB TARGETS GENEGO: http://www.genego.com/

Set MYB TARGETS RULAI.CSHL.EDU:http://rulai.cshl.edu/cgi-bin/TRED/

Set MYB TARGETS LITERATURE is based on the literature search.

To show that notable part of MYB and miR-155 downstream targets are differentially regulated we used GSEA (Gene Set Enrichment Analysis) [243].

GSEA represents the analytical method for interpreting of gene expression data. This method focuses on the gene sets that share common biological function, chromosomal location or regulation pathway. It is a tool how to show significance of a gene list among whole genome expression data of all genes ordered by some significance measure (i.e. t-test p-value of a gene expression between two phenotypes or some other measure of differential regulation). Significant lists are those in which notable part of genes lies at the beginning or at the end of the whole genome ranked list. GSEA scores provided lists of genes by enrichment score (ES) and normalized enrichment score (NES). Primary measurement of the significance of a list is q-value (lower is better). Default GSEA setting marks as significant those list with q-value ≤0.25. The complete GSEA results from our B-CLL patient samples and controls are available on: http://www1.lf1.cuni.cz/~vkulv/gsea.

The detailed protocols are in section 10. Supplement; Supplemental material 10.2.

4. RESULTS

4.1 Expression of candidate oncogenic microRNAs and their targtes in B-CLL

4.1.1 Expression of miR-155, miR-150 and transcription factors PU.1, FOS, MYB and MYC in B-CLL patients and in normal healthy controls

By quantitative PCR and by microarray approach we measured the levels of both: mature form of microRNA-155 (miR-155) ($N_{CD19+/PBMC}$=113; N_{CD19+}=156) and its primary transcript generated from the *MIR155HG* (pri-miR-155) ($N_{B\text{-}cells}$=11; N_{CD19+}=155) (Figure 4.1 and 2).

Our data show significant (P<0.001, Student`s t-test; Mann-Whitney test) increase of mature miR-155 in the circulating leukemic B-cells in comparison to normal B-cells (Figure 4.1A, B). Expression of miR-155 increased from 4-fold up to 32-fold in comparison to the normal CD19+ B-cells in both PBMCs (peripheral blood mononuclear cells) (graph A) and in separated CD19+ B-cells (graph B).

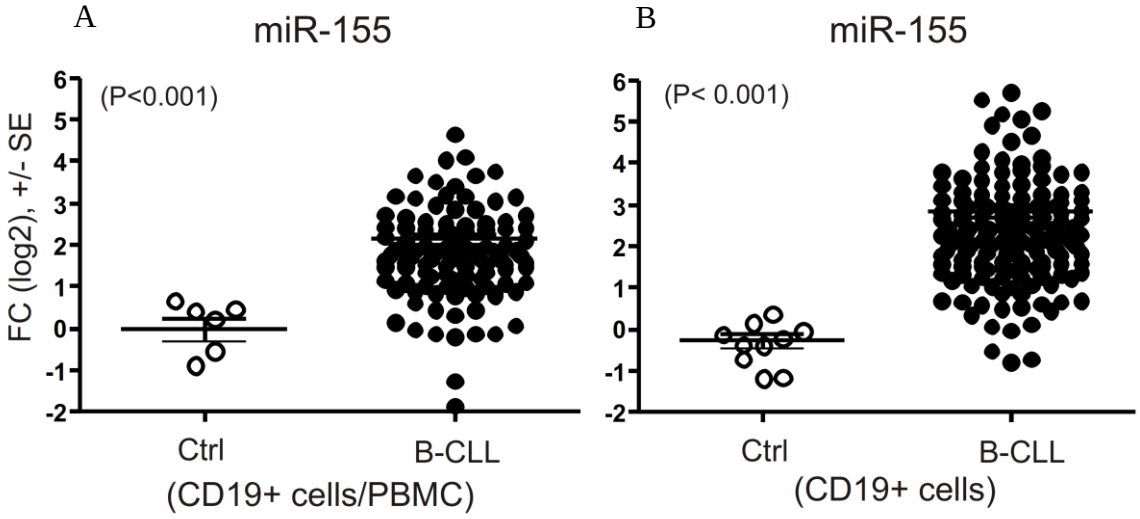

Figure 4.1: Expression of miR-155 in B-CLL patient samples. Results of TaqMan based RT-qPCR showed elevated levels of miR-155 in B-CLL patient samples [(A)$N_{CD19+/PBMC}$=113; (B)N_{CD19+}=156] in comparison with normal CD19+ B-cells [(A)$N_{ctrl\ CD19+}$=6; (B)$N_{ctrl\ CD19+}$=10]. The Y-axis represents relative abundance of mature miR-155 relative to reference gene RNU44. Data are shown as fold change (FC) in log2 scale and baseline normalized to the RNA levels of controls (control measurements were set equal to 1). Error bars represent standard error of the mean (SEM). Statistics was done by Student`s t-test (A) or Mann-Whitney test (B). P values are shown in parentheses.

We detected 16-32 fold over-production of the pri-miR-155 transcript in B-CLL patient cells by RT-qPCR (Figure 4.2A) as well as using a microarray approach (Figure 4.2B) in comparison to normal CD19+ B-cells.

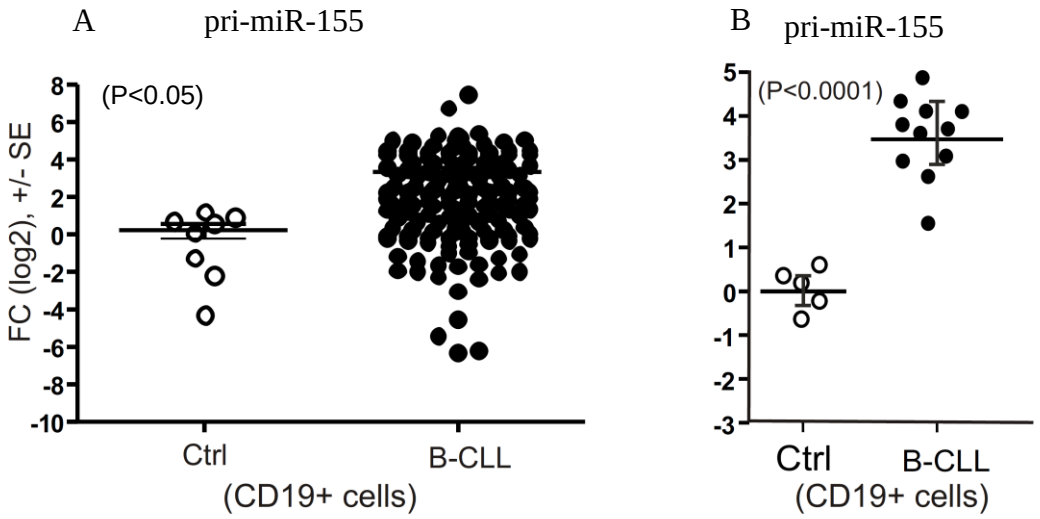

Figure 4.2: Elevated levels of primary transcript (pri-miR-155) a product of *MIR155HG* gene in B-CLL samples. (A) Results of TaqMan based RT-qPCR shown an elevated levels of pri-miR-155 in B-CLL patient samples (N_{CD19+}=155) as compared with normal CD19+ B-cells (N_{CD19+}=8). The Y-axis represents relative abundance of pri-miR-155 relative to GAPDH. Data are shown as fold change (FC) in log2 scale and normalized to the RNA levels of controls (control measurements were set equal to 1). Error bars represent standard error of the mean (SEM). (B) Results from microarrays shown an elevated levels of pri-miR-155 in B-CLL (N_{CD19+}=11) as compared with normal CD19+ B-cells (N_{CD19+}=5). Statistics was done by Student`s t-test (A) or Mann-Whitney test (B). P values are shown in parentheses.

We measured in parallel the expression of mature miR-155 in the peripheral CD19+ B-cells (Figure 4.1) and also in the plasma samples (N=10) (Figure 4.3A). For the measurement of miR-155 level in plasma we selected the samples with the intermediate (~2-fold) and high (~7-fold) expression of mature miR-155 (obtained from measurements in the CD19+ cell population). Indeed, positive correlation between expression of miR-155 in CD19+ B-cells and in plasma (r=0.5) was observed (Figure 4.3B).

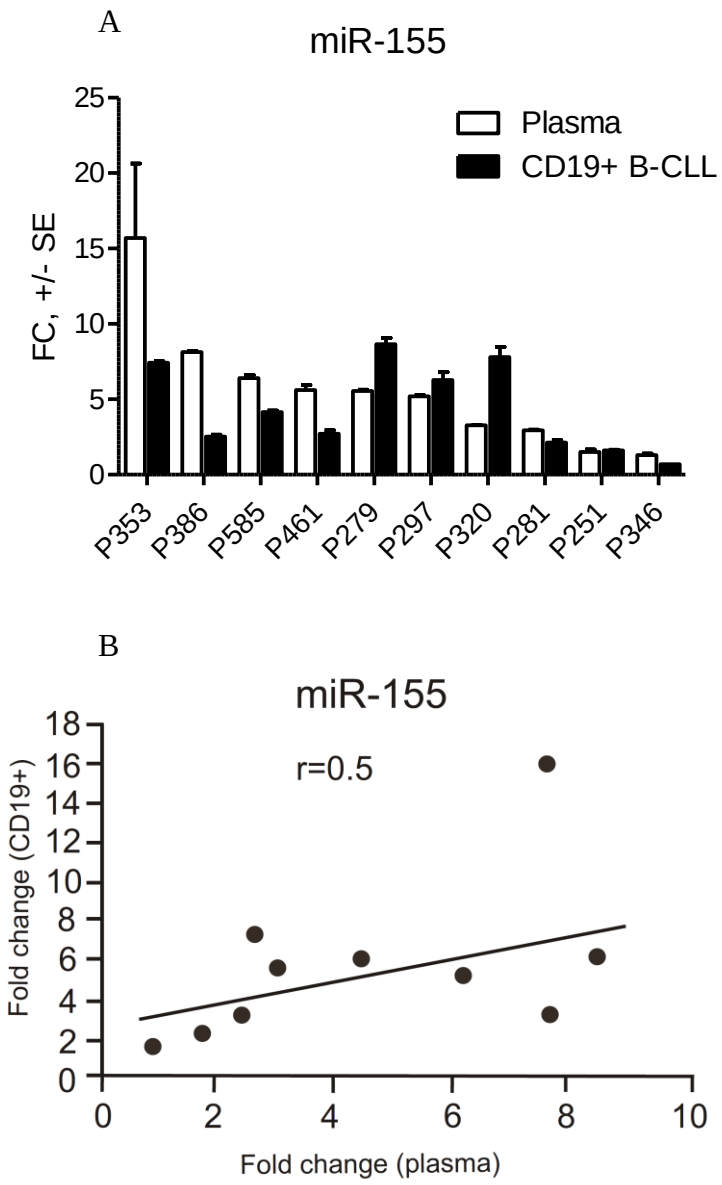

Figure 4.3: Expression of mature miR-155 in plasma samples (N=10) derived from B-CLL patients. Graph A shows results of TaqMan based RT-qPCR of mature miR-155 measured in plasma samples (white box plots) and in separated CD19+ B-CLL samples (black box plots). Expression data are shown as fold change (FC) and in the case of B-CLL CD19+ cells normalized to the RNA levels of controls (control measurements were set equal to 1). Expression data of miR-155 in plasma were normalized on an average of RNA levels of let-7a and miR-24. Error bars represent standard error of the mean (SEM). Graph B shows correlation of miR-155 expression in plasma and separated CD19+ B-CLL cells. We analyzed plasma and peripheral blood samples of 10 B-CLL patients: P353, P386, P585, P461, P279, P297, P320, P281, P251 and P346.

The key hematopoietic transcription factor PU.1 is validated direct target of miR-155 that blocks both RNA stabity as well as translation of PU.1 [157]. miR-155-directed inhibition of PU.1 expression may leads to leukemogenesis [156]. We herein detected 4-32 fold downregulation of mRNA PU.1 in PBMCs (Figure 4.4A) and as well in the purified CD19+ B-CLL separated population (Figure 4.4B). Decreased amount of mRNA PU.1 coincided with decreased PU.1 protein levels (Figure 4.5). The established target of *PU.1* gene is early transcription gene *FOS* (FBJ murine osteosarcoma viral oncogene homolog). Indeed, the mRNA of FOS in B-CLL patient samples was significantly 4-10 fold decreased as shown in Figure 4.6.

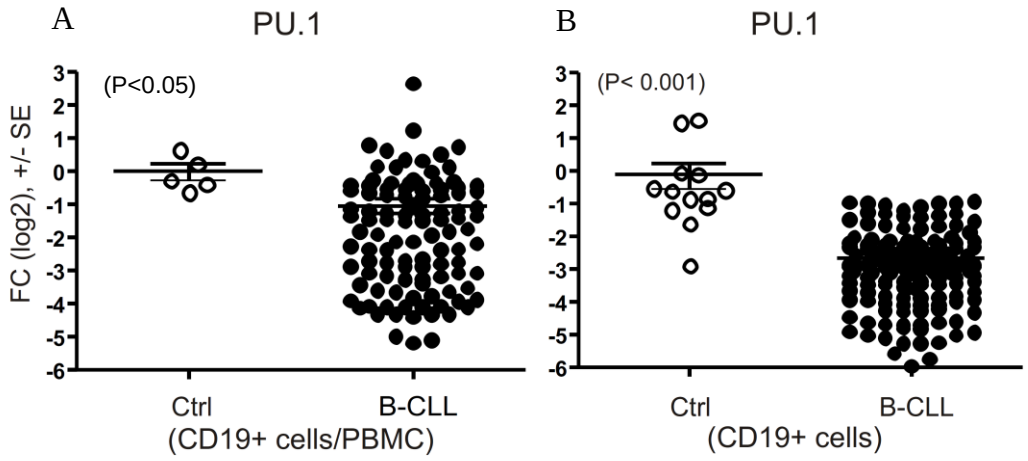

Figure 4.4: Expression of PU.1 in B-CLL patient B-cell samples.
Results of TaqMan based RT-qPCR show decrease in mRNA PU.1 in our B-CLL patient samples ($N_{CD19+/PBMC}$=119; N_{CD19+}=157) in comparison with the PU.1 levels in the control CD19+ B-cells ($N_{ctrl\ CD19+}$=5; $N_{ctrl\ CD19+}$=13). Y-axis represents relative abundance of PU.1 normalized to the levels of the reference gene - GAPDH. Data are shown as fold change (FC) in log2 scale and normalized to mRNA levels of controls (control measurements were set equal to 1). Error bars represent standard error of the mean (SEM). Statistics was done by Student`s t-test (A) or Mann-Whitney test (B). P values are shown in parentheses.

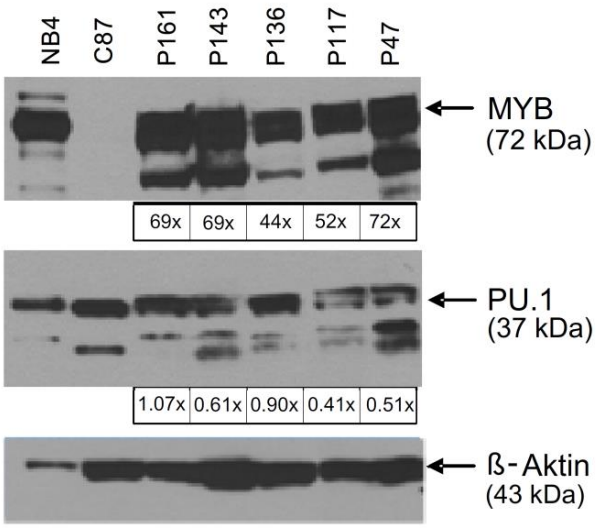

Figure 4.5: Protein levels of PU.1 and MYB in primary B-CLL cells.
Immunoblott analysis of MYB and PU.1 in B-CLL (P161, P143, P136, P117, P47) and control B-cells (C87). The NB4 cell line was used as a positive control. The optical density (below each lane) of each protein band was measured by Scion Image software Beta 4.0.2. The values below the blots represent a fold change of densities of the specific bands (or their expected positions) in the patient samples. Control lanes (NB4 and C87) were normalized to the levels of reference protein - β-actin.

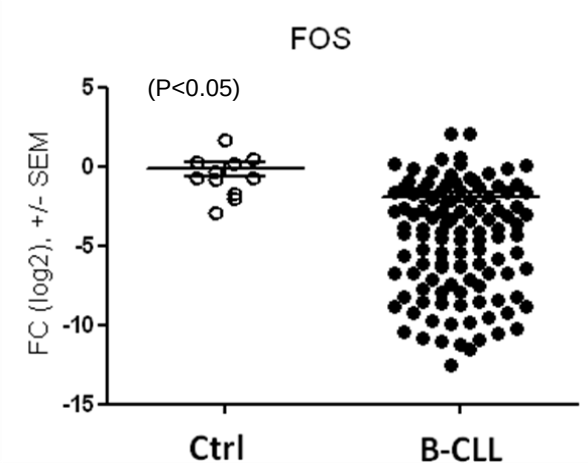

Figure 4.6: Expression of FOS in B-CLL patient B-cell samples. Results of TaqMan based RT-qPCR show decrease of mRNA FOS in separated CD19+ B-CLL cells (N=113) in comparison with the levels of FOS in normal CD19+ B-cells (N=11). The Y-axis represents relative abundance of FOS normalized to the levels of reference gene - GAPDH. Data are shown as fold change (FC) in log2 scale and normalized to mRNA levels in controls (control measurements were set equal to 1). Error bars represent standard error of the mean (SEM). Statistics was done by Student`s t-test. P values are shown in parentheses.

In addition to miR-155, miR-150 is likely related to the pathogenesis of B-CLL [17]. In addition, reviewers of our manuscript [144] asked to determine also miR-150 levels. Our data show, that around 30% of B-CLL samples have elevated miR-150 levels while similar proportion of patients have down- & un-regulated miR-150 levels in both peripheral blood B-CLL cells (Figure 4.7A) and CD19+ B-CLL cells (Figure 4.7B).

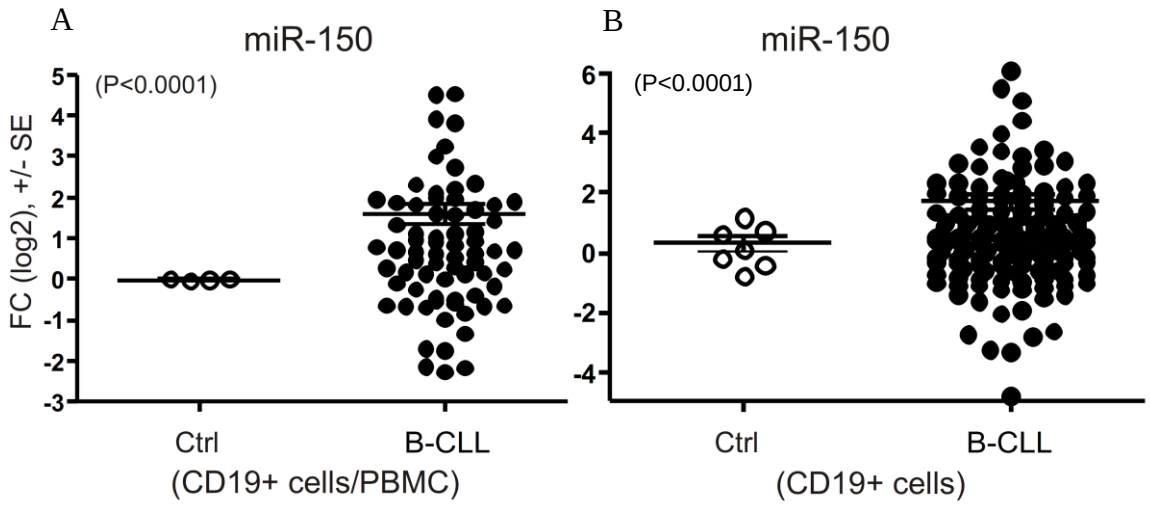

Figure 4.7: Expression of miR-150 in B-CLL patient B-cell samples.
Results of TaqMan based RT-qPCR showed expression of miR-155 in B-CLL patient samples ($N_{CD19+/PBMC}$=71; N_{CD19+}=151) and normal CD19+ B-cells ($N_{ctrl\ CD19+}$=4; $N_{ctrl\ CD19+}$=7). The Y-axis represents relative abundance of miR-150 relative to reference gene - RNU44. Data are shown as fold change and are normalized to RNA levels in controls (control measurements were set equal to 1) and shown in log2 scale. Error bars represent standard error of the mean (SEM). Statistics was done by Student`s t-test (A) or Mann-Whitney test (B). P values are shown in parentheses.

Validated target of both miR-150 and miR-155 is a proto-oncogene and transcription factor *MYB* (v-myb myeloblastosis viral oncogene homolog) that is important for normal B-cells development [72,73,227]. The mRNA levels of MYB showed wide interval of expression levels, starting from 2-32 fold in comparison to normal B-cells. In subset (~40%) of B-CLL patient samples we detected over-produced MYB mRNA and in 20% its down-production (Figure 4.8). The production of MYB protein was in some B-CLL patient samples (N=5) up to 72-fold higher as in the lysates from normal B-cells. MYB protein normally migrates at ~72 kDa (wt form) (Figure 4.5). Additionally, we determined the MYC mRNA levels – an another member of E-box family. In our B-CLL patient samples the MYC mRNA levels were above the levels of normal CD19+ B-cells (Figure 4.9).

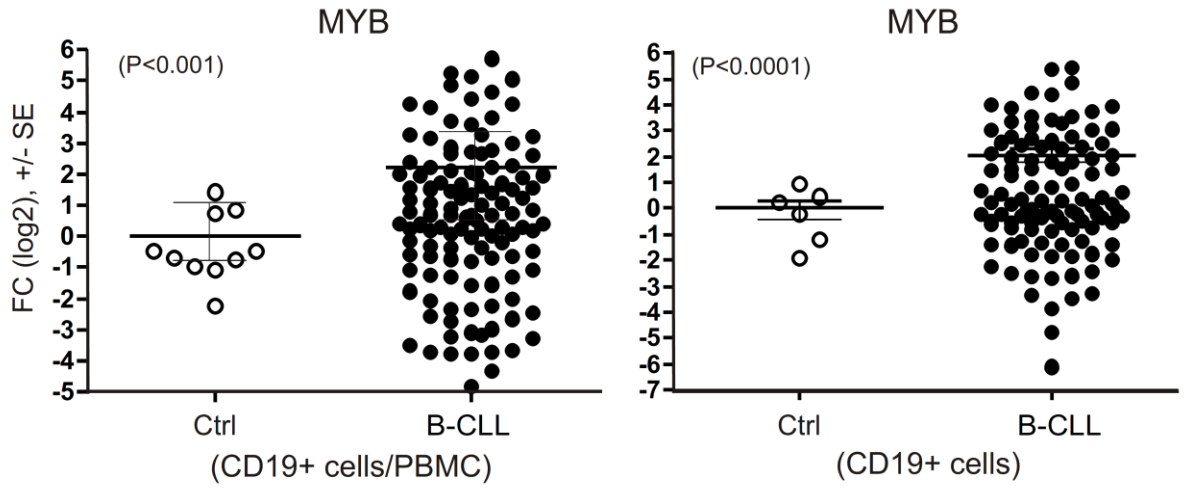

Figure 4.8: Expression of MYB in B-CLL patient B-cell samples.
Results of TaqMan based RT-qPCR showed expression of MYB in B-CLL patient samples ($N_{CD19+/PBMC}$=109; N_{CD19+}=108) and in normal CD19+ B-cells ($N_{ctrl\ CD19+}$=10; $N_{ctrl\ CD19+}$=6). The Y-axis represents relative abundance of MYB relative to reference gene - GAPDH. Data are shown as fold change (in log2 scale) and baseline normalized to the levels of MYB in controls (control measurements were set equal to 1). Error bars represent standard error of the mean (SEM). Statistics was done by Student`s t-test (left graph) or Mann-Whitney test (right graph). P values are shown in parentheses.

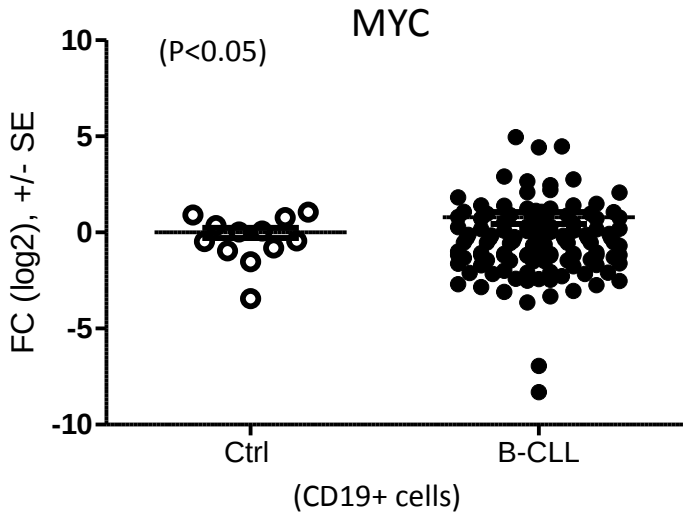

Figure 4.9: Expression of MYC in B-CLL patient B-cell samples.
Results of TaqMan based RT-qPCR shown decrease of MYC in separated CD19+ B-CLL cells (N_{CD19+}=122) and in normal CD19+ B-cells ($N_{ctrl\ CD19+}$=12). The Y-axis represents relative abundance of MYC relative to GAPDH. Data are shown as fold change (in log2 scale) and baseline normalized to the levels of MYB in controls (control measurements were set equal to 1). Error bars represent standard error of the mean (SEM). Statistics was done by Mann-Whitney test. P values are shown in parentheses.

4.1.2 Relationship between expressions of miR-155 – miR-150 - PU.1 – MYB in B-CLL patient samples

Based on our previous expression data (section 4.1.1) we asked if there exists functional relationship between expression patterns of oncomiR miR-155, miR-150, oncogenic transcription factor MYB and tumor supressor transcription factor PU.1 in B-CLL patient samples (N=156). All possible pair combinations within this four molecules demonstrate figures 4.10-12. In the B-CLL patient samples with elevated miR-155 the PU.1 mRNA was decreased (Figure 4.10). Interestingly, expression of miR-155 and miR-150 showed very similar pattern and expression of MYB mRNA in ~30% of B-CLL patients samples overlapped with the elevated expression levels of miR-155 (Figure 4.10).

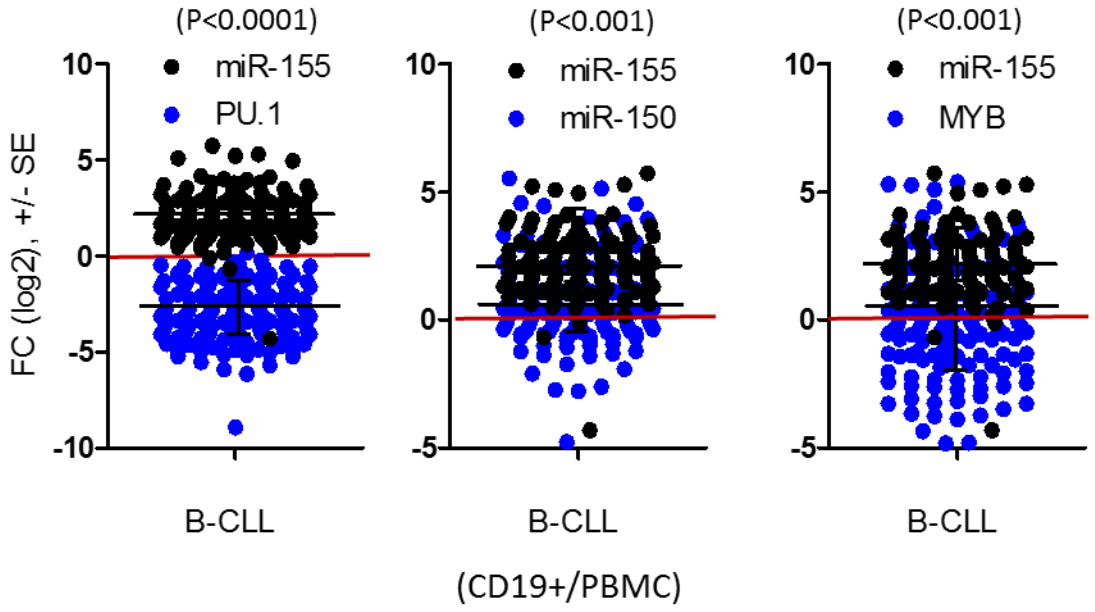

Figure 4.10: Expression of miR-155, PU.1, MYB and miR-150 in B-CLL patient B-cell samples.
Graphs show results of TaqMan based RT-qPCR of B-CLL ($N_{CD19+/PBMC}$=156) patient samples. The dataset contains data that expressed all four genes. The Y-axis represents expression of miR-155 - PU.1, miR-155 – miR-150 and miR-155 – MYB. The expression of miR-155 and miR-150 is relative to the reference gene RNU44 and of PU.1 and MYB relative to the reference gene GAPDH. Data are shown as fold change (in log2 scale) and normalized to the levels of controls (control measurements were set equal to 1 – represented by red line). Error bars represent standard error of the mean (SEM). P values (in parentheses) represent results of Student`s t test.

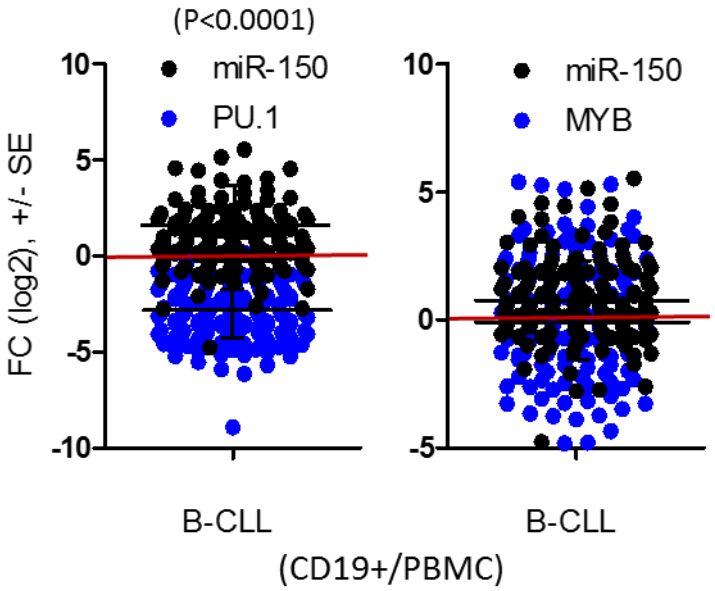

Figure 4.11: Expression of miR-155, miR-150, PU.1 and MYB in B-CLL patient B-cell samples.
Graphs show results of TaqMan based RT-qPCR of B-CLL ($N_{CD19+/PBMC}$=156) patient samples. The dataset contains data that expressed all four genes. The Y-axis shows expression of miR-155 - PU.1, miR-155 – miR-150 and miR-155 – MYB. The expression of miR-155 and miR-150 is relative to reference gene RNU44 and PU.1 and MYB relative to reference gene GAPDH. Data are shown as fold change (in log2 scale) and normalized to the levels of controls (control measurements were set equal to 1 – red line). Error bars represent standard error of the mean (SEM). P values (in parentheses) represent results of Student`s t test.

To see how differed the expression pattern of miR-150 and its target MYB in the same subset of B-CLL patient samples we showed both expression data in one graph (Figure 4.11). Interestingly, MYB and miR-150 showed similar expression pattern (statistically non-significant) and not reciprocal as it would be expected [223]. The expression of PU.1 mRNA was low as compared to expression of miR-150 (Figure 4.11) and MYB mRNA and indeed high levels of MYB showed reciprocal pattern to PU.1 (Figure 4.12).

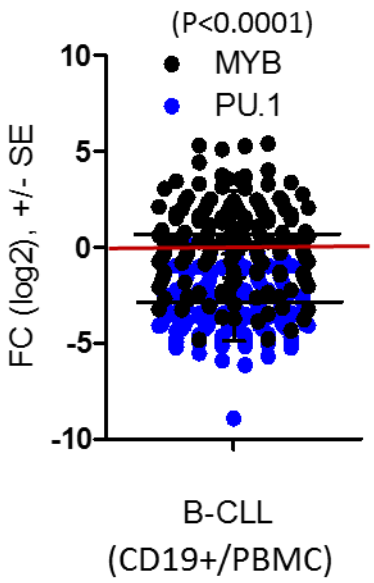

Figure 4.12: Expression of MYB and PU.1 in B-CLL patient B-cell samples.
Graph shows results of TaqMan based RT-qPCR in B-CLL (N_{CD19+}=156). The Y-axis represents expression of MYB, PU.1 relative to GAPDH. Data are shown as fold change (in log2 scale) and normalized to the levels of MYB in controls (control measurements were set equal to 1). Error bars represent standard error of the mean (SEM). Statistics was done by Student`s t test. P values are shown in parentheses.

4.1.3 Clinical and prognostic importance of miR-155, miR-150, MYB and PU.1 expressions in B-CLL patient samples

The progression of B-CLL characterizes Rai stage [44]. Here, we showed analysis of expression of miR-155, PU.1, miR-150 and MYB between different Rai staging categories. We also showed the relationship between mRNA/miRNA expression and overall survival, therapy regimen in B-CLL patient samples (Figure 4.13 - 17). Our data show significantly higher expression of MYB mRNA and lower expression of miR-150 in advanced Rai stages II - IV stages while PU.1 and miR-155 appeared to be similar (Figure 4.13).

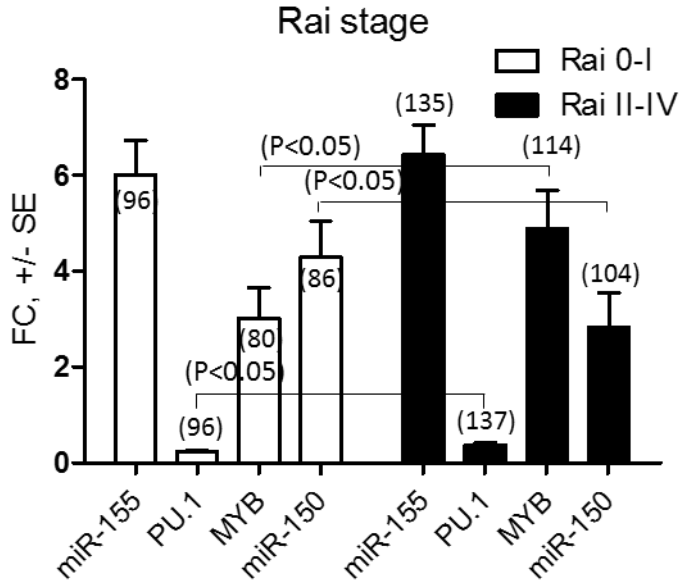

Figure 4.13: Expression of miR-155, PU.1, MYB and miR-150 in B-CLL patient samples based on Rai stage (PBMC/CD19+ B-CLL cells). Graph shows two patient subgroups divided by Rai stage: white bars – represent patients samples with Rai stage 0-I ($N_{miR-155}$=96, $N_{PU.1}$=96, N_{MYB}=80, $N_{miR-150}$=86) and black bars represent patients samples with Rai stage II-IV ($N_{miR-155}$=135, $N_{PU.1}$=137, N_{MYB}=114, $N_{miR-150}$=104). Expressions of miR-155, PU.1, MYB and miR-150 are shown as fold change, each bar represents average of expression. Error bars represent standard error of the mean. P values are shown in parentheses, Student`s t test was used.

We compared expression of miR-155, PU.1, MYB and miR-150 with diferent Rai stages, therapy regimens and overall survival (from diagnosis to the last follow-up) in B-CLL patients. We divided patient samples primarily into two groups based on the Rai staging system – Rai stage 0-I and Rai stage II-IV and secondarily into three subgroups based the number of therapy regimens (1 or more than 1) and on the overall survival status (OS) (0 (live) or 1 (dead)). In the advanced Rai stages (II-IV) we detected an increased expression of MYB compared with Rai 0-I (Figure 4.14). We observed elevated levels of miR-155 in a patient group with advanced Rai stages (II-IV) that underwent at least one line of therapy and are still alive (Figure 4.15; grey bar). The PU.1 mRNA levels increased in the group of patients that underwent more therapy lines (Figure 4.16). The expression of miR-150 decreased in the advanced Rai stages (II-IV) and especially in the group of patients that underwent more therapy lines (Figure 4.17).

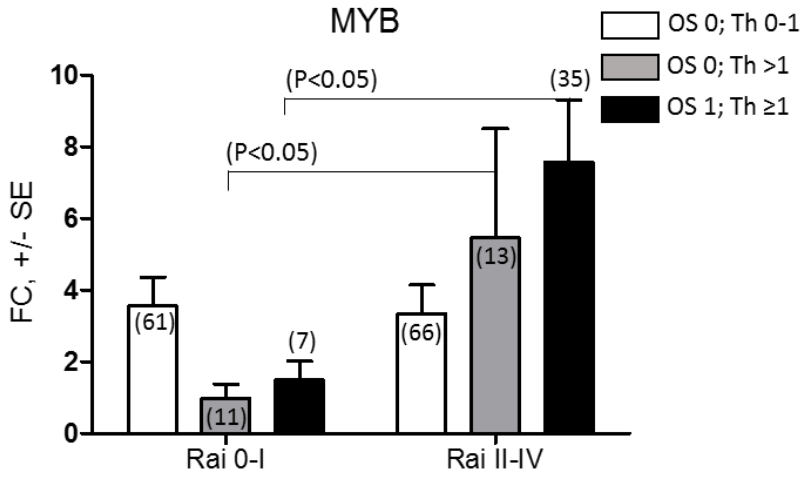

Figure 4.14: Expression of MYB based on the Rai stage, overall survival and therapy regimen in B-CLL patient B-cell samples (PBMC/CD19+ B-CLL cells). Graph shows expression of MYB based on the Rai stage. Three patient subgroups are shown: white bars: currently investigated patients (OS 0) either treated by first line of therapy or untreated (Th 0-1), $N_{Rai\ 0\text{-}I}$=61, $N_{Rai\ II\text{-}IV}$=66; grey bars: currently investigated patients (OS 0) who received second or more lines of therapy (Th>1), $N_{Rai\ 0\text{-}I}$=11, $N_{Rai\ II\text{-}IV}$=13; black bars: previously investigated patients that already died (OS 1) and received at least one line of therapy (Th≥1), $N_{Rai\ 0\text{-}I}$=7, $N_{Rai\ II\text{-}IV}$=35. Error bars represent standard error of the mean. P values are shown in parentheses, Student`s t test was used.

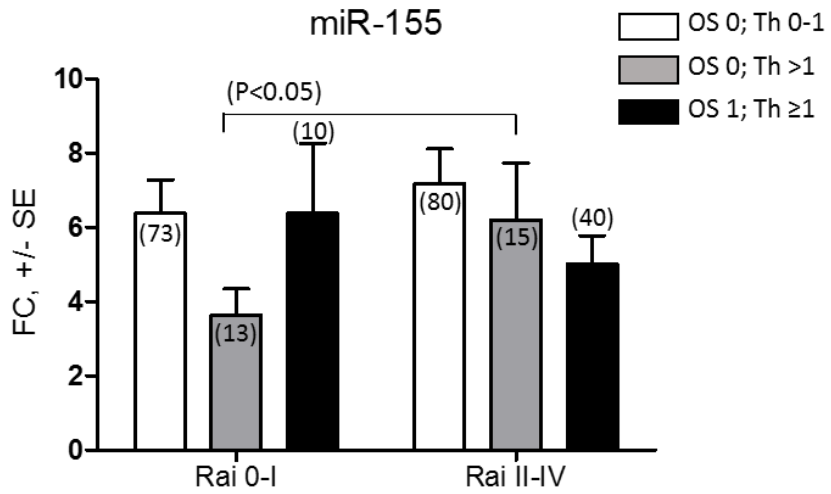

Figure 4.15: Expression of miR-155 based on the Rai stage, overall survival and therapy regimen in B-CLL patient B-cell samples (PBMC/CD19+ B-CLL cells). Graph shows expression of mR-155 based on the Rai stage. Three patient subgroups are shown: white bars: currently investigated patients (OS 0) either treated by first line of therapy or untreated (Th 0-1), $N_{Rai\ 0\text{-}I}$=73, $N_{Rai\ II\text{-}IV}$=80; grey bars: currently investigated patients (OS 0) who received second or more lines of therapy (Th>1), $N_{Rai\ 0\text{-}I}$=13, $N_{Rai\ II\text{-}IV}$=15; black bars: previously investigated patients that already died (OS 1) and received at least one line of therapy (Th≥1), $N_{Rai\ 0\text{-}I}$=10, $N_{Rai\ II\text{-}IV}$=40. Error bars represent standard error of the mean. P values are shown in parentheses, Student`s t test was used.

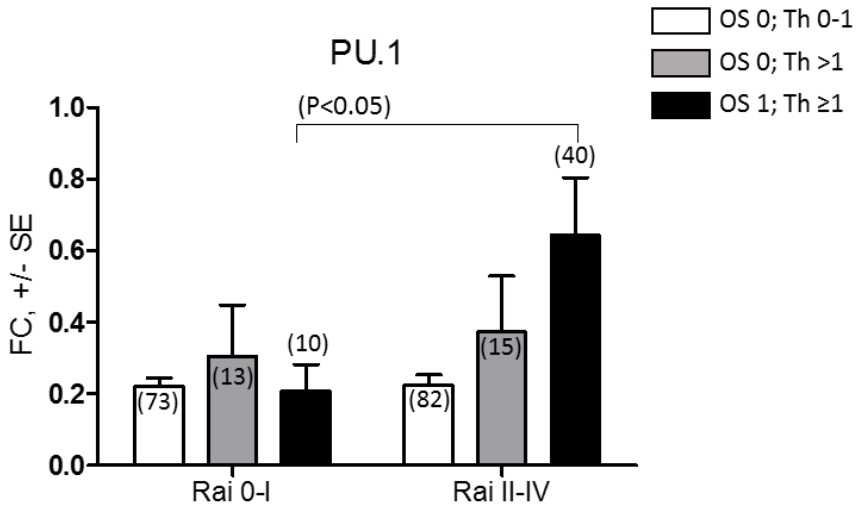

Figure 4.16: Expression of PU.1 based on the Rai stage, overall survival and therapy regimen in B-CLL patient B-cell samples (PBMC/CD19+ B-CLL cells). Graph shows expression of PU.1 based on the Rai stage. Three patient subgroups are shown: white bars: currently investigated patients (OS 0) either treated by first line of therapy or untreated (Th 0-1), $N_{Rai\ 0\text{-}I}$=73, $N_{Rai\ II\text{-}IV}$=82; grey bars: currently investigated patients (OS 0) who received second or more lines of therapy (Th>1), $N_{Rai\ 0\text{-}I}$=13, $N_{Rai\ II\text{-}IV}$=15; black bars: previously investigated patients that already died (OS 1) and received at least one line of therapy (Th≥1), $N_{Rai\ 0\text{-}I}$=10, $N_{Rai\ II\text{-}IV}$=40. Error bars represent standard error of the mean. P values are shown in parentheses, Student`s t test was used.

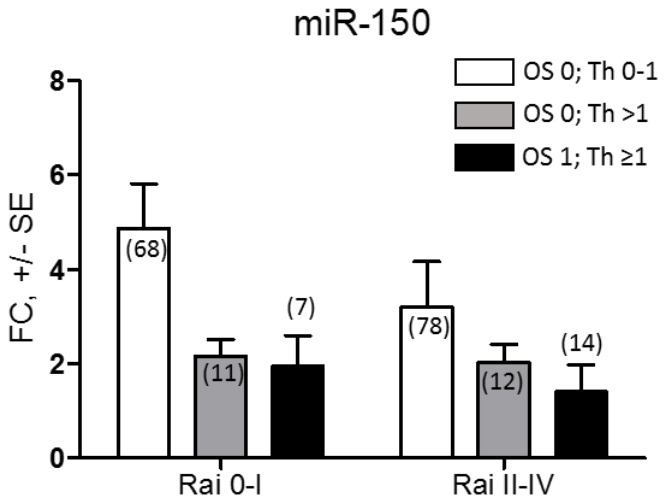

Figure 4.17: Expression of miR-150 based on the Rai stage, overall survival and therapy regimen in B-CLL patient B-cell samples (PBMC/CD19+ B-CLL cells). Graph shows expression of mR-150 based on the Rai stage. Three patient subgroups are shown: white bars: currently investigated patients (OS 0) either treated by first line of therapy or untreated (Th 0-1), $N_{Rai\ 0\text{-}I}$=68, $N_{Rai\ II\text{-}IV}$=78; grey bars: currently investigated patients (OS 0) who received second or more lines of therapy (Th>1), $N_{Rai\ 0\text{-}I}$=11, $N_{Rai\ II\text{-}IV}$=12; black bars: previously investigated patients that already died (OS 1) and received at least one line of therapy (Th≥1), $N_{Rai\ 0\text{-}I}$=7, $N_{Rai\ II\text{-}IV}$=14. Error bars represent standard error of the mean. P values are shown in parentheses, Student`s t test was used.

Prognosis and stage of B-CLL is characterized by Rai staging and also by expression of prognostic markers: ZAP-70, CD38 and IgVH gene mutation status. We further analyzed the expression of miR-155, PU.1, MYB and miR-150 in the relationship with mRNA/miRNA expression with positivity of different prognostic markers (Figures 4.18-20). IgVH – unmutated IgVH versus IgVH mutated B-CLL cells expressed more miR-155 and MYB (not significantly), similar amounts of PU.1 and less miR-150 (Figure 4.18). As pointed in the Introduction, the presence of surface marker ZAP-70 on B-CLL cells categorizes patient into more advanced stage with unfavorable prognosis. We found that patient overexpressing ZAP-70 also expressed more MYB mRNA, less miR-150, while miR-155 and PU.1 expression remained unchanged (Figure 4.19). Presence of another B-CLL prognostic marker, CD38 categorizes patient into more advanced stage with unfavorable prognosis. B-CLL cells expressing the CD38 expressed more miR-155 and mRNA of MYB (significantly), less miR-150, PU.1 remained unchanged (Figure 4.20).

Additionally we divided the patient samples by clinical outcome into two patient groups: 1) favorable (ZAP-70-/CD38-/IgVH mutated) and 2) unfavorable (ZAP-70+/CD38+/IgVH unmutated). This creates highly specifialy and robustly two very distinct group whose prognosis is different and that is not influenced by false positive or false negative outcomes from prognostic determinations. Hence, the expression of miR-155 in group of patients with unfavorable clinical outcome was significantly higher than in group with favorable clinical outcome (Figure 4.21). Furthermore, the expression of PU.1 mRNA was overall decreased in both clinical groups without significant change. Expression of MYB mRNA in unfavorable group of patients was significantly increased (~3-fold). On the other hand, expression of miR-150 decreased (~2-fold) with disease progression (Figure 4.21). Our data points to the relationship between expression of miR-155, PU.1, MYB and miR-150 during the progression of B-CLL. This notion is supported by our data indicating that the studied molecules are likely involved during disease progression and therapy requirement (unpublished, Manuscript *in preparation*).

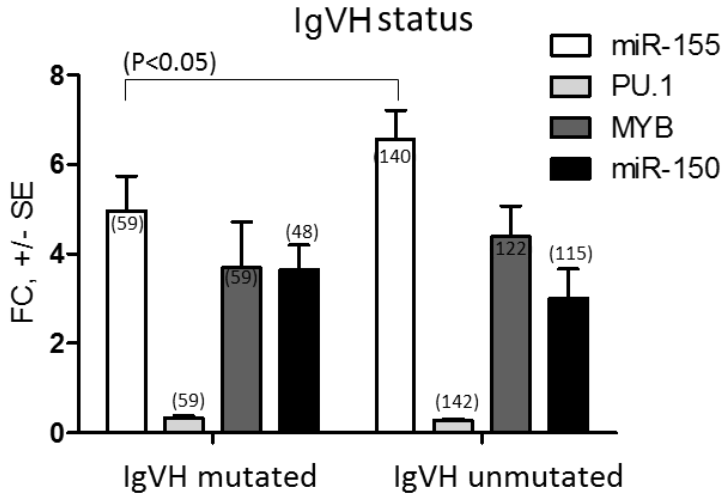

Figure 4.18: Expression of miR-155, PU.1, MYB and miR-150 based on IgVH status of B-CLL (PBMC/CD19+ B-CLL cells). Graph shows expression (shown in fold change) of miR-155, PU.1, MYB and miR-150. B-CLL patient samples were divided into two groups based on the IgVH status: 1, IgVH mutated ($N_{miR-155}$=59, $N_{PU.1}$=59, N_{MYB}=59, $N_{miR-150}$=48) and 2, IgVH unmutated ($N_{miR-155}$=140, $N_{PU.1}$=142, N_{MYB}=122, $N_{miR-150}$=115). Error bars represent standard error of the mean. Number of patients in each group is shown in parentheses above/or in the each bar respectively. P values are shown in parentheses, Student`s t test was used.

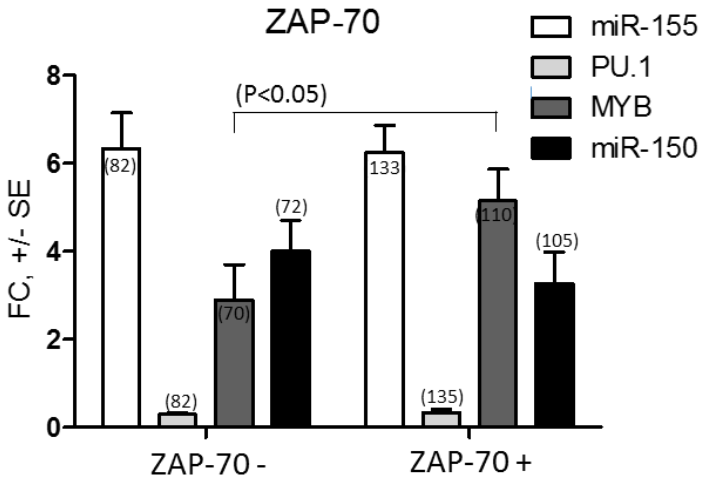

Figure 4.19: Expression of miR-155, PU.1, MYB and miR-150 based on presence of surface marker ZAP-70 in B-CLL patient samples (PBMC/CD19+ B-CLL cells). Graph shows expression (shown in fold change) of miR-155, PU.1, MYB and miR-150. B-CLL patient samples were divided into two groups based on presence of ZAP-70 (sample was assessed as ZAP-70 positive when >20% of cells expressed ZAP-70): 1, ZAP-70 negative ($N_{miR-155}$=82, $N_{PU.1}$=82, N_{MYB}=70, $N_{miR-150}$=72) and 2, ZAP-70 positive ($N_{miR-155}$=133, $N_{PU.1}$=135, N_{MYB}=110, $N_{miR-150}$=105). Error bars represent standard error of the mean. Number of patients in each group is shown in parentheses above/or in the each bar respectively. P values are shown in parentheses, Student`s t test was used.

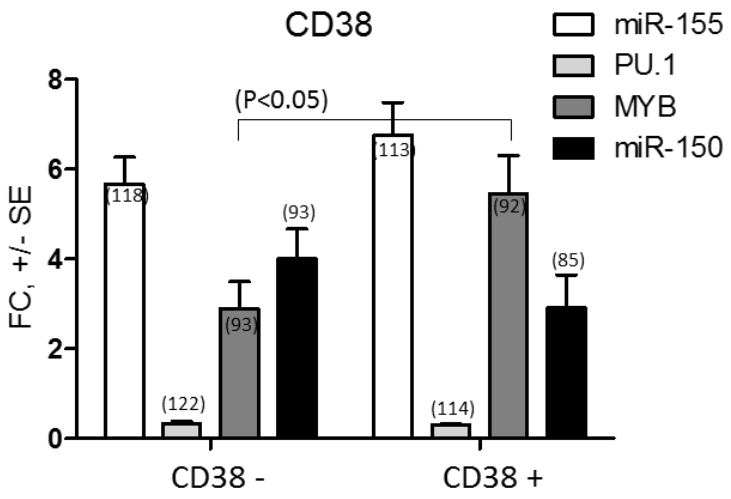

Figure 4.20: Expression of miR-155, PU.1, MYB and miR-150 based on presence of surface marker CD38 in B-CLL patient samples (PBMC/CD19+ B-CLL cells). Graph shows expression (shown in fold change) of miR-155, PU.1, MYB and miR-150. B-CLL patient samples were divided into two groups based on presence of CD38 (sample was assessed as CD38 positive when >30% of cells expressed CD38): 1, CD38 negative ($N_{miR-155}$=118, $N_{PU.1}$=122, N_{MYB}=93, $N_{miR-150}$=93) and 2, CD38 positive ($N_{miR-155}$=113, $N_{PU.1}$=114, N_{MYB}=92, $N_{miR-150}$=85). Error bars represent standard error of the mean. Number of patients in each group is shown in parentheses above/or in the each bar respectively. P values are shown in parentheses, Student`s t test was used.

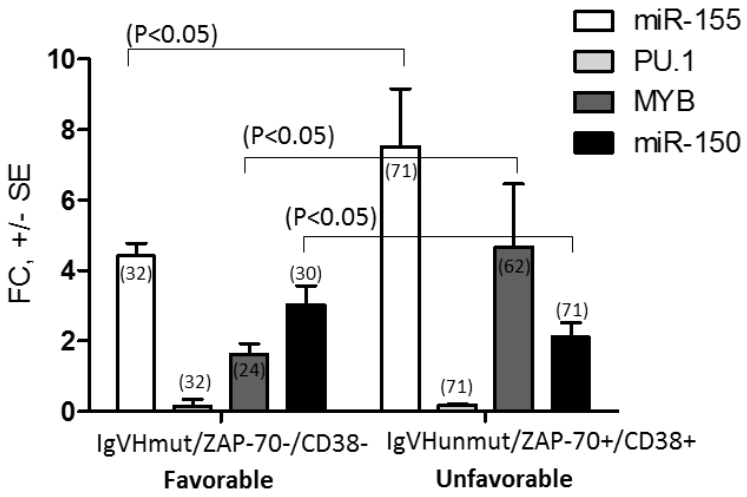

Figure 4.21: Expression of miR-155, PU.1, MYB and PU.1 based on prognostic markers (PBMC/CD19+ B-CLL cells). Graph shows expression (shown in fold change) of miR-155, PU.1, MYB and miR-150. B-CLL patient samples were divided into two groups based on the clinical outcome: 1) favorable clinical outcome = IgVH mutated/CD38-/ZAP-70- ($N_{miR-155}$=32, $N_{PU.1}$=32, N_{MYB}=24, $N_{miR-150}$=30) and 2) unfavorable clinical outcome = IgVH unmutated/CD38+/ZAP-70+ ($N_{miR-155}$=71, $N_{PU.1}$=71, N_{MYB}=62, $N_{miR-150}$=71). Error bars represent standard error of the mean. Number of patients in each group is in parentheses above/or in the each bar respectively. P values are shown in parentheses, Student`s t test was used.

Besides Rai stage and expression of prognostic surface markers, the progression of B-CLL is additionally evaluated by chromosomal aberrations. Among such aberrations belongs deletions of chromosome 13q14, 11q22-23, 17p13 and trisomy of chromosome 12 (see Introduction section). The most frequent aberration of B-CLL cells is deletion of chromosome 13q14 that is also described as a low risk factor of B-CLL. The intermediate risk represents trisomy of chromosome 12 while high risk are deletions of 11q22-23 and 17p13 [13]. We divided our B-CLL patient samples into 5 groups based on the chromosomal aberrations (Figure 4.22-25).

Based on cytogenetics we observed that, expression of miR-155 in the patient samples with deletion of 13q14 or 11q22-23 was interestingly higher as compared to B-CLL patient samples with negative FISH analysis (Figure 4.22). In the B-CLL patient samples with trisomy of chromosome 12 and with the deletion of 17p13 the expression of miR-155 was unchanged (Figure 4.22).

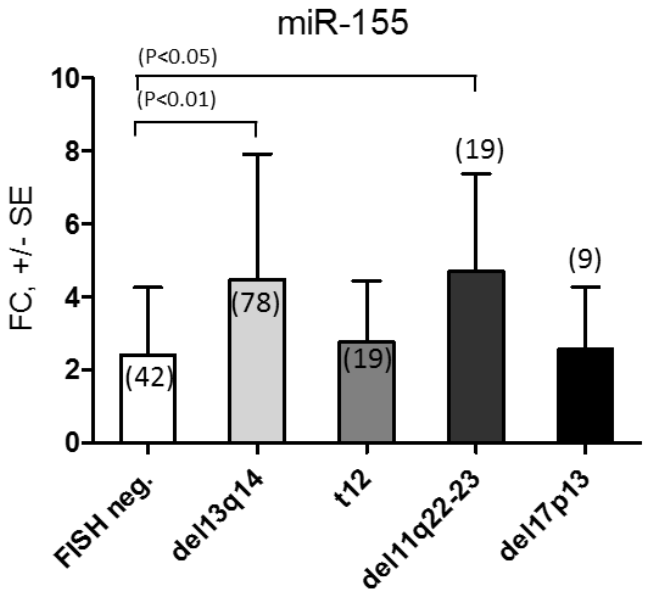

Figure 4.22: Expression of miR-155 in B-CLL samples based on cytogenetics. Graph shows expression (shown in fold change) of miR-155 in the primary B-CLL patient samples (PBMC/CD19+ B-CLL cells) based on the cytogenetics: FISH (B-CLL) negative (N=42); 13q14 (N=78); t12 (N=19); del11q22-23 (N=19); del17p13 (N=9). Error bars represent standard error of the mean. Number of patients in each group is in parentheses above/or in the each bar respectively. P values are shown in parentheses, Student`s t test was used.

Based on cytogenetics we observed that, expression of PU.1 mRNA is not reciprocal to miR-155 (according cytogenetics). In the B-CLL patient samples with deletion of 13q14 and 11q22-23 PU.1 level remains unchanged relative to FISH negative B-CLL, while in the trisomy of chromosome 12 PU.1 was increased (2-fold) and in deletion of 17p13 was signifcantly decreased (Figure 4.23).

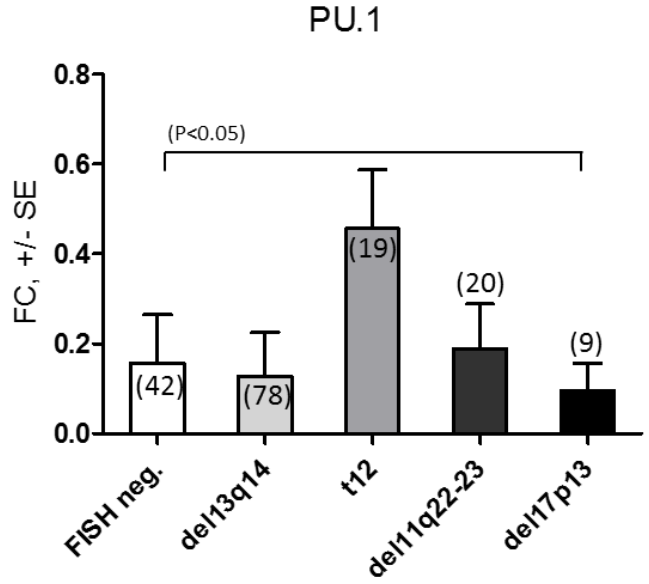

Figure 4.23: Expression of PU.1 in B-CLL samples based on the cytogenetics. Graph shows expression (shown in fold change) of PU.1 in the primary B-CLL patient samples (PBMC/CD19+ B-CLL cells) based on the cytogenetics: FISH (B-CLL) negative (N=42); 13q14 (N=78); t12 (N=19); del11q22-23 (N=20); del17p13 (N=9). Error bars represent standard error of the mean. Number of patients in each group is in parentheses above/or in the each bar respectively. P values are shown in parentheses, Student`s t test was used.

Based on cytogenetics we observed that, levels of MYB mRNA were increased (not significantly) in the B-CLL patient samples with trisomy of chromosome 12 and with 13q14 deletion, but unchanged in the patient samples with deletions 11q22-23, 17p13 (Figure 4.24).

Based on cytogenetics we observed that, interesting expression pattern showed miR-150 regarding to several cytogenetic aberrations (Figure 4.25). Expression of miR-150 was significantly decreased in both high risk groups of B-CLL patient samples: del11q22-23 and del17p13. This suggests potential role of miR-150 in aggressive B-CLL as tumor suppressor. The low risk and intermediate group of B-CLL patient samples was similar to the group of B-CLL patient samples with negative FISH analysis (Figure 4.25).

Cytogenetic data unlike data from prognostic markers as ZAP-70/CD38/IgVH did not overal support conclusion of association between subgroups and expression of miR-155 and its upstream and downstream regulators.

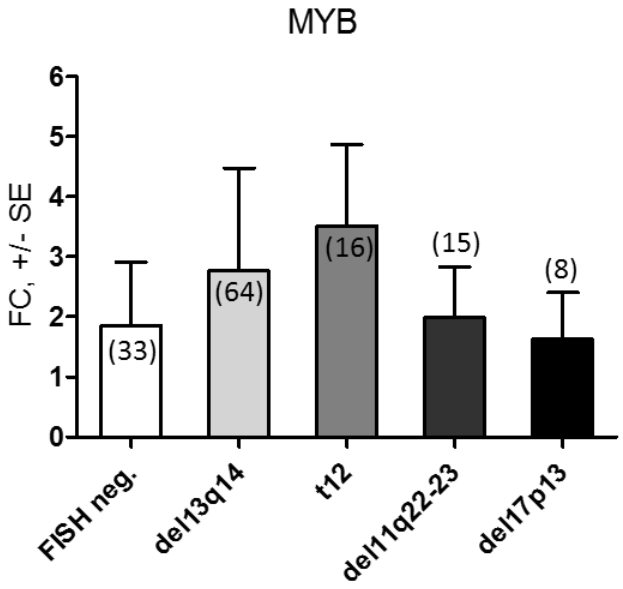

Figure 24: Expression of MYB in B-CLL samples based on the cytogenetics. Graph shows expression (shown in fold change) of MYB in the primary B-CLL patient samples (PBMC/CD19+ B-CLL cells) based on the cytogenetics: FISH (B-CLL) negative (N=33); 13q14 (N=64); t12 (N=16); del11q22-23 (N=15); del17p13 (N=8). Error bars represent standard error of the mean. Number of patients in each group is in parentheses above/or in the each bar respectively. P values are shown in parentheses, Student`s t test was used.

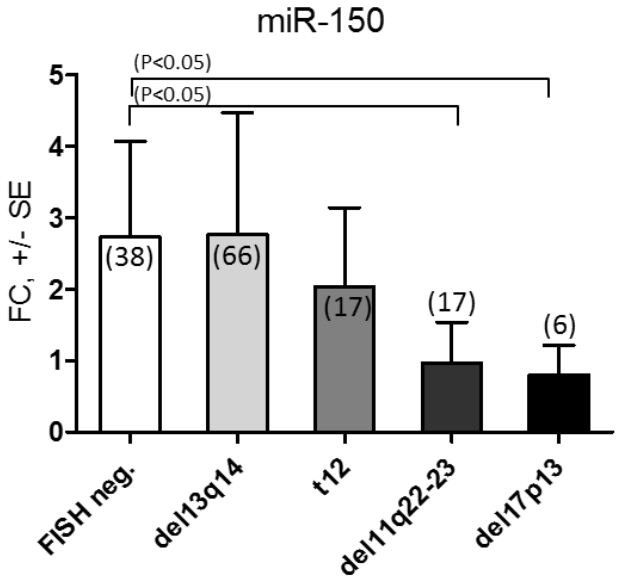

Figure 4.25: Expression of miR-150 in B-CLL samples based on the cytogenetics. Graph shows expression (shown in fold change) of miR-150 in the primary B-CLL patient samples (PBMC/CD19+ B-CLL cells) based on the cytogenetics: FISH (B-CLL) negative (N=38); 13q14 (N=66); t12 (N=17); del11q22-23 (N=15); del17p13 (N=6). Error bars represent standard error of the mean. Number of patients in each group is in parentheses above/or in the each bar respectively. P values are shown in parentheses, Student`s t test was used.

To determine whether there is relationship between expression of MYB mRNA and expressions of miR-155, miR-150 and PU.1, we divided B-CLL patient samples into two groups: 1) samples over expressing MYB (>1.5-fold change) and 2) samples with low expression of MYB (<1.5-fold change). In the MYB-high group we detected increased levels of miR-155 (statistically significant), miR-150 (not significant) and surprisingly also of PU.1 (statistically significant) as compared to MYB-low group (Figure 4.26). Our data indicate on the relationship (yet not always in expected direction) between the levels of studied molecules. We further split B-CLL patient samples into another two groups based on the expression of miR-155 to see the relationship between expression of miR-155 compared to PU.1, MYB and miR-150 (Figure 4.28). In patient group with miR-155> 2.5-fold change, the expression of miR-150 was significantly higher than in second group (miR-155<2.5-fold change). The mRNA of MYB was also increased in group with higher miR-155, but not statistically significant. The PU.1 mRNA level was unchanged (Figure 4.27). Again, this data indicate on the relationship between the four studied molecules.

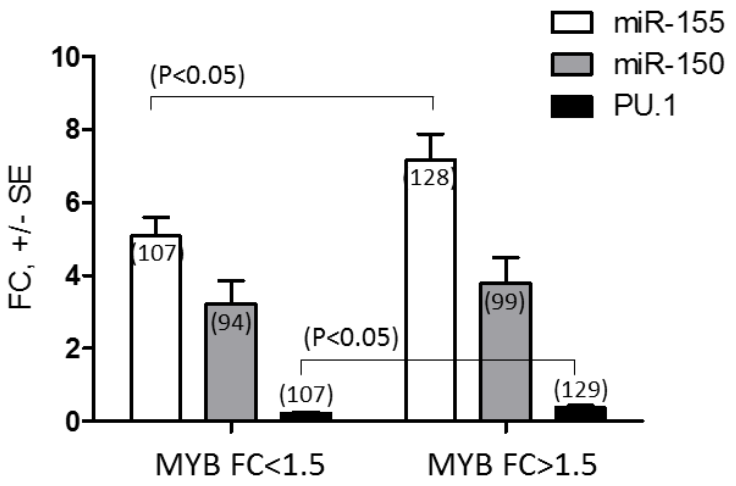

Figure 4.26: Levels of miR-155, miR-150 and PU.1 in B-CLL based on expression of MYB (PBMC/CD19+ B-CLL cells). Graph shows expression of miR-155 (white bars) and miR-150 (grey bars) in MYB under-expressors (<1.5 fold decrease, left) and MYB over-expressors (>1.5 fold increase; right) relative to control B-cells. Error bars represent standard errors of the mean (SEM). Number of patients in each group is in parentheses above/or in the each bar. Statistics was done by Student`s t test and P values are shown in parentheses on top of the brackets indicating the groups being compared.

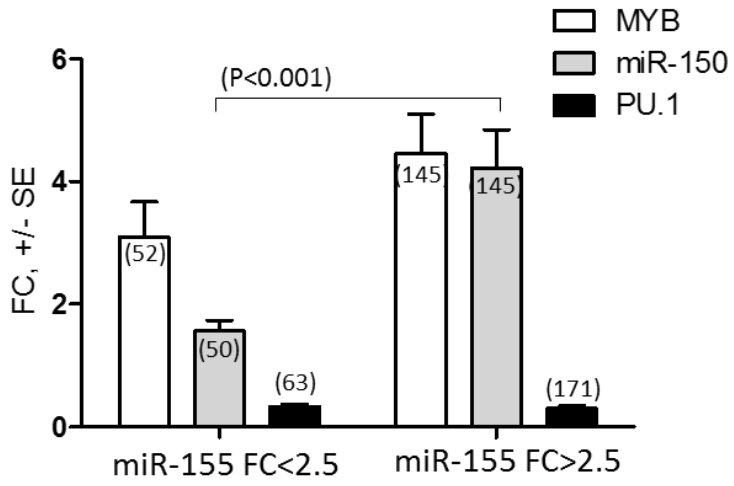

Figure 4.27: Levels of MYB, miR-150 and PU.1 in B-CLL based on the expression of miR-155 (PBMC/CD19+ B-CLL cells). Graph shows expression of miR-155 (white bars) and miR-150 (grey bars) in miR-155 underexpressors (<2.5 fold decrease, left) and miR-155 overexpressors (>2.5 fold increase; right) relative to control B-cells. Error bars represent standard errors of the mean (SEM). Number of patients in each group is in parentheses above/or in the each bar. Statistics was done by Student`s t test and P values are shown in parentheses on top of the brackets indicating the groups being compared.

We hypothetisize, the analysis of expression patterns of miR-155, PU.1 and MYB may reflect the therapy efficacy. Our B-CLL patient cohort include 40% of patients that undergoes therapy prior the study and 49% of patients that undergoes therapy during the study (see Table 3.2 in the section 3. Material and Methods). The therapy as well comprised from Rituximab (anti-CD20 antibody) treatment (375mg/m^2 intravenous infusion D1 of each cycle). To test our hypothesis, the peripheral blood of B-CLL patient was collected before, 24 hrs and 48 hrs after Rituximab treatment. We observed the following expression pattern: miR-155 and MYB were markedly decreased after Rituximab (11- and 6-folds respectively). In contrast, the level of PU.1 mRNA was increased 1-fold (Figure 4.28). Based on these results, the measuring of the levels of miR-155, PU.1 and MYB before and after therapy could help to control success of therapy and can be used as molecular biomarkers of Rituximab efficacy.

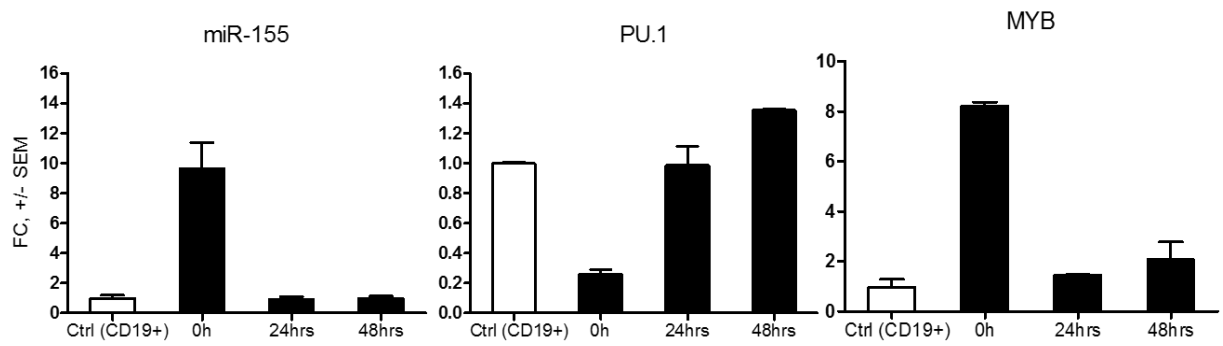

Figure 4.28: Expression of miR-155, PU.1 and MYB in B-CLL patient samples after therapy.
Graphs show expression of miR-155, MYB and PU.1 in the peripheral blood mononuclear cells of B-CLL patient (P143) before and after B-cell specific treatment by Rituximab (antiCD20 antibody) at 0, 24 and 48 hours (X-axis). Expression levels are shown as fold change (Y-axis). Error bars represent standard errors of the mean (SEM).

To summarize this part of results *point-by point*, we found that expression of miR-155 and MYB increased, PU.1 remains unchanged and miR-150 decreased with disease progression in the advanced Rai stages. Moreover, in the B-CLL patient samples with unfavorable clinical outcome (ZAP-70+/CD38+/IgVH unmutated) the levels of miR-155 and MYB were increased; PU.1 was unchanged and miR-150 significantly decreased. Based on the cytogenetic data, we could conclude that expression of miR-155 increased in the B-CLL patient group with deletion 13q14 and 11q22-23 while in other cytogenetic subgroups it was unchanged. The PU.1 expression was significantly low in a group of patients with

deletion of 17p13, and high in a group with trisomy of chromosome 12. Expression of MYB mRNA was higher in patient group with deletion of 13q14 and with trisomy of 12 chromosome. Significantly low expression of miR-150 correlates with high risk of B-CLL based on cytogenetics. The measurement of levels of miR-155, PU.1 and MYB in B-CLL cells after Rituximab therapy underlines the importance of these molecules as potential biomarkers for disease progression and therapy efficacy.

4.2 The occupancy of MYB and epigenetic features at *MIR155HG* promoter region in B-CLL

4.2.1 Occupancy of transcription factor MYB at *MIR155HG* promoter region

To determine whether MYB recruits the *MIR155HG* promoter region we performed the chromatin immunoprecipitation (ChIP) within the *MIR155HG* locus. ChIP was followed by qPCR, where the amplicons ranged from -3.2 kb to 4.4 kb relative to the transcriptional start site (TSS) of *MIR155HG* promoter. Our data shows that in the primary B-CLL cells (N=6) MYB is consistently occupied at the *MIR155HG* promoter region, exclusively at three loci: -0.5kb; +0.1kb and +1.6kb relatively to TSS in comparison to the normal healthy CD19+ B-cells (N=6). While the recruitment was not detected anywhere else upstream or downstream of the studied *MIR155HG* promoter region, we could conclude that MYB recruitment at the *MIR155HG* gene is TSS specific (Figure 4.30A).

To answer the question if MYB has ability to stimulate the transcription of *MIR155HG* we generated luciferase reporter constructs either with mutation in MYB binding site (mut; E-box 1) or without mutation (wt; E-box 1). The putative MYB binding sites (E-box 1-3) sequence A A C T/G G are localized at the positions: 1) -399 – 394bp; 2) +209bp +215bp; 3) +1201bp +1207bp adjacent to the CpG island at *MIR155HG* (Figure 3.3 Section 3. Material and Methods; and schematicaly Figure 4.29). The figure 4.30B shows the relative luciferase activity of HeLa cells measured after 48 hours post transfection with reporter vectors: 1) with mutation in MYB binding site (mut; E-box 1); 2) without mutation in MYB binding site (wt; E-box 1) and 3) control vector (empty vector pGL4.17). Based on our results, only the construct without mutation in MYB binding site was able to bind and stimulate the luciferase activity in HeLa cells. Additionally, we transiently transfected HeLa cells with construct that either carries or not the mutation in MYC binding site. In this case the

luciferase activity was not stimulated neither with unmutated nor mutated binding sites for MYC (data not shown). Based on the ChIP and luciferase assay data we could conclude that MYB specifically binds and stimulates the transcription of *MIR155HG* in B-CLL cells (Figure 4.30).

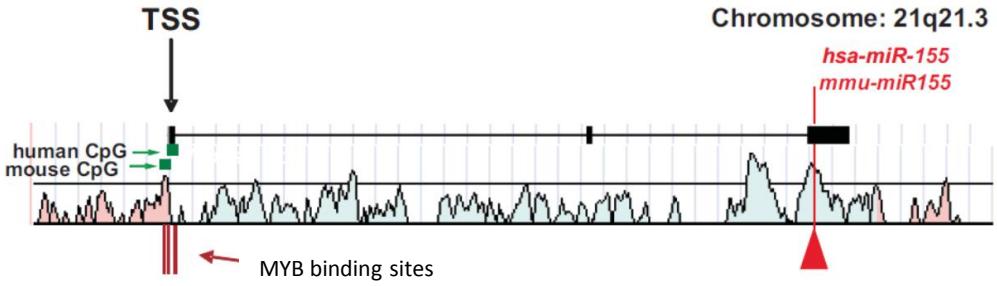

Figure 4.29: Vista plot of MYB binding sites and CpG at *MIR155HG* promoter region. Figure shows presence of MYB binding sites at the *MIR155HG* promoter near the CpG region (-33 – 339bp).

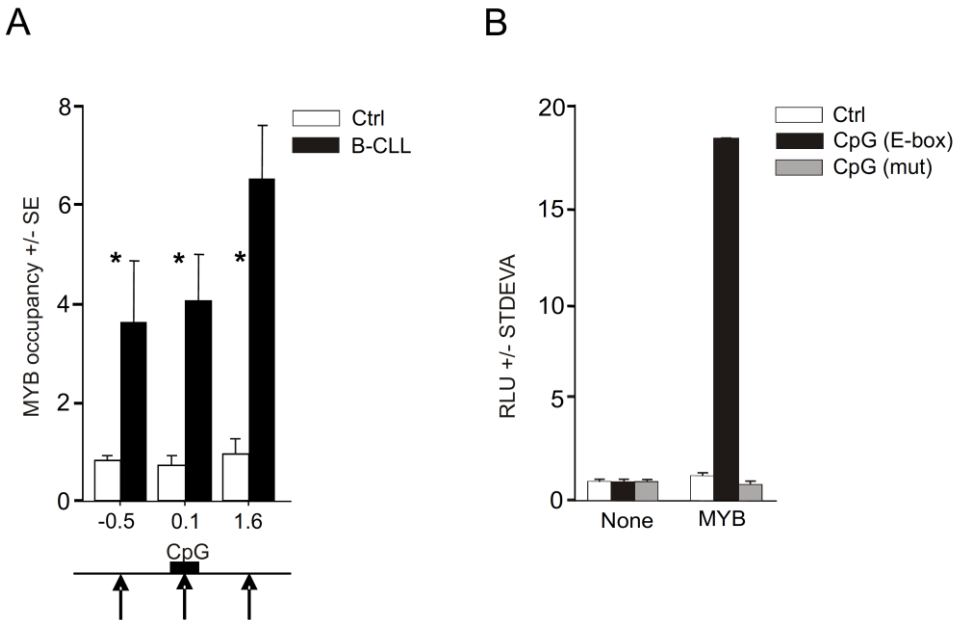

Figure 4.30: Transcription factor MYB binds and stimulates activity of *MIR155HG* promoter.
(A) MYB occupancy within *MIR155HG* was determined by ChIP by using anti-Myb or control antibodies. The ChIP was carried out on cross-linked chromatin isolated from B-CLL cells (N=6, average value indicated by black bars, P40, P39, P47, P250, P254, P255) and normal B-cells (N=6, white bars). The Y-axis indicates the relative occupancy of MYB. The X-axis marks the positions (in kb) of PCR amplicons relative to TSS of *MIR155HG*. The arrows indicate the positions of MYB DNA binding motifs; black box indicates position of the CpG island. Error bars represent standard error of the mean (SEM) of three independent experiments. P values <0.05 are indicated by one asterisk. (B) HeLa cells were transiently transfected with 0.5 µg pGL4.17 reporter vector containing the MYB binding site (-399 bp to -394 bp) (black bars), its deletion mutant (grey bars) or a control reporter plasmid (None (pGL4.17); white bars). Reporter vectors were transfected either alone (left) or co-transfected with 1 µg MYB cDNA expression vector (right). Luciferase activity measured at 48 hrs is shown relative to a control vector, the background activity was subtracted, and data were equalized to the protein content. Average values and standard deviation (STDEVA) of at least two independent experiments are plotted.

4.2.2 Active chromatin marks associates with elevated levels of miR-155 in B-CLL cells

The histone modifications are marks of the transcription activity of chromatin. The actively transcribed DNA contains chromatin (euchromatin) with active epigenetic markers on histones as e.g. H3K9Ac, H3K4Me3. These post translational histone modifications play important role in gene expression, especially in the leukemic cells.

To determine the acetylation status of lysine 9 of histone H3 (H3K9Ac) we performed the ChIP assay on the chromatin of B-CLL patient samples (N=9) and healthy control B-cell samples (N=8). Within the *MIR155HG* promoter region we observed the acetylation peak of H3K9Ac at the loci +0.1kb as compared with healthy control B-cell samples (Figure 4.31; upper graph). In the B-CLL cells we detected spread chromatin H3K9acetylation within the region from -3.2kb to +1.6kb. This epigenetic pattern of H3K9Ac overlapped with the occupied loci (-0.5 - +1.6kb) by MYB at CpG region of *MIR155HG* (Figure 4.31). Moreover, we detected a positive correlation between the MYB mRNA expression and acetylation status (H3K9Ac) at the same three loci: -0.5 kb (r=0.5), +0.1kb (r=0.6) and +1.6 kb (r=0.5) of the *MIR155HG* promoter region (Figure 4.32). Based on our data we could conclude that, transcription factor MYB activates the *MIR155HG* transcription in B-CLL cells.

We further determined another epigenetic mark, the H3K4Me3 at *MIR155HG* promoter region in B-CLL (N=9) and in the normal healthy controls (N=8). The presence of H3K4Me3 mark associated with active gene transcription by DNA dependent RNA polymerase II. Significant enrichment of H3K4Me3 methylation occurred at loci -0.5kb – +1.6kb of *MIR155HG* promoter region (Figure 4.31; lower graph). Taken together, ChIP data: acetylation of H3K9 and methylation (H3K4Me3) at the loci +0.1kb – +1.6kb and positive correlation with expression of MYB mRNA indicates on direct relationship between MYB and transcription activity of *MIR155HG* in B-CLL (Figure 4.31 and 4.32).

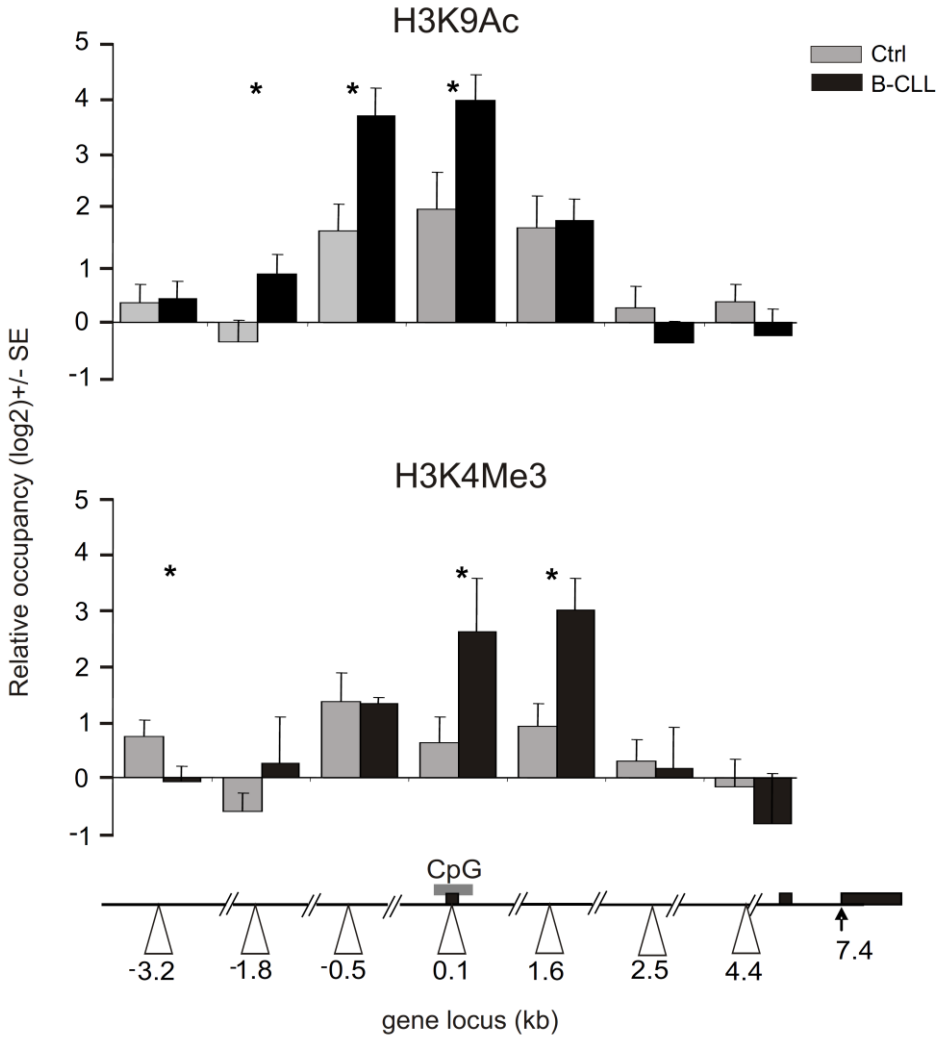

Figure 4.31: Histone modifications at *MIR155HG* promoter in B-CLL cells.
ChIP was performed on cross-linked chromatin from primary B-CLL (N=9: P250, P254, P255, P143, P130, P161, P162, P164, P179, P135, black bars) and control B-cells (N=8, grey bars) using the anti-H3K9Ac, H3K4Me3 and control anti-rabbit IgG antibody as described in section 3. Material and Methods. The level of H3K9 acetylation and H3K4 trimethylation (Y-axis) is expressed relative to control IgG antibody and relative to upstream -4.7kb locus with consistent low H3K9 acetylation and H3K4 methylation patterns. X-axis indicates positions of amplicons (in kb) relative to TSS. Position of CpG is indicated by grey box, exons of human *MIR155HG* indicated as black boxes. Error bars represent standard error of the mean. P values bellow 0.05 are indicated by asterisks.

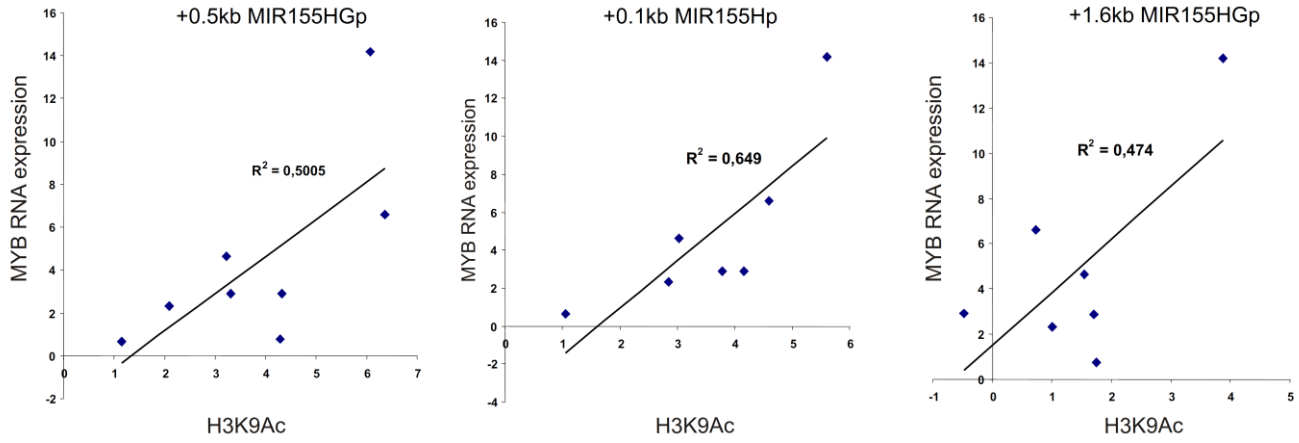

Figure 4.32: Correlation between MYB mRNA level and active chromatin marker H3K9Ac at *MIR155HG* promoter region in B-CLL cells. Scatter plots shows the correlation between MYB mRNA expression (Y-axis) and the levels of H3K9Ac (X-axis) at three amplicons at the CpG island of *MIR155HG*. Correlation coefficient R is shown at the centre of each graph.

4.3 Mutation status of canonical MYB binding motive at the MIR155HG in B-CLL

MIR155HG gene contains highly conserved CpG islands localized -33bp to -349bp upstream of TSS (Figure 3.3 in Section 3. Material and Methods). ChIP data indicated that *MIR155HG* promoter is occupied by MYB (Figure 4.30A) and by luciferase assay we confirmed that MYB by its binding stimulates *MIR155HG* transcription (Figure 4.30B). To test whether are some mutations within the promoter region of *MIR155HG*, we prove the sequence of MYB binding site (E-box 2). Our sequential data showed that the canonical MYB binding motif (E-box 2) within the CpG region at *MIR155HG* is not mutated in B-CLL samples (P89 and P143) in comparison with the sequence from normal healthy control sample (Ctrl; C41) (section 10. Supplement; Supplemental data 10.3).

4.4 Global gene expression profile in B-CLL unrolls deregulation of MYB and miR-155 targets

The mRNA microarray (Affymetrix Human Genome HG-U133 Plus 2.0 Array) was performed on mRNAs isolated from twelve peripheral blood B-CLL samples and five normal healthy donor blood samples (CD19+ separated B-cells) (Figure 4.33).

The clinical characterization of the patients samples is as follows: the most patient samples are in the advanced Rai stage II-IV (P33, P86, P136, P143, P249, P250, P254, 255); more than half of patients express the CD38 surface marker (P33, P86, P137, P138, P143, P155, P250), ZAP-70 (P33, P86, P138, P143, P249, P254, P255) and majority of samples have unmutated IgVH gene (P33, P86, P38, P143, P155, P250, P255, P271). Half of patients have deleted chromosome 11q22-23 (*ATM* gene) (P33, P138, P143, P155, P255, P271) and two patient samples have deleted 17p13 chromosome (*TP53* gene) (P86, P136). The majority of patients have deleted 13q14 chromosome (P33, P86, P136, P143, P155, P249, P250, P255, P271). Transformation into the Richter`s syndrome (DLBCL) occurred in two patient samples (P86 and P143). To summarize this informations, the analyzed patients are in the advanced Rai stage (II-IV) and have poor prognosis that is underlined by elevated levels of miR-155 and MYB and decreased level of PU.1. We detected low expression of miR-155 in only one patient (P155) however this is due to remission.

The target genes of miR-155 and MYB programs in B-CLL is one of our research interest. We used six prediction tools for *in silico* data analysis to determine the miR-155 target genes (for details see section 3. Materials and Methods). The lower part of heat map miR-155 target genes shows significantly decreased levels of many miR-155 targeted mRNAs, among them also a key hematopoietic transcription factor PU.1 (SPI1) and its target *FOS* gene (Figure 4.33A). This is in accordance with our data from RT-qPCR (Figures 4.4 and 4.6). Another important transcription factors that were targeted by miR-155 in B-CLL were: 1) *FOS* (FBJ murine osteosarcoma viral oncogene homolog); 2) *HIF1A* (hypoxia inducible factor 1); 3) *MAFB* (v-maf musculoaponeurotic fibrosarcoma oncogene homolog B (avian)) transcription factor regulates hematopoiesis); 4) *SATB1* (special AT-rich sequence binding protein 1).

We found several genes whose mRNA was up regulated in B-CLL samples and at the same time were targets of miR-155 such as *KRAS* and *SMAD2*. Expression of these genes is

probably regulated by other compensatory mechanism that is dependent or independent on the presence of miR-155.

Three prediction tools were used for construction of MYB target gene list (for details see section: 3. Material and Methods). The MYB target gene list included also typical B-cells and B-CLL genes as *BCL2*, *CD5*, *AICDA* (Figure 4.33B). The over production of Bcl2, an anti-apoptotic protein is due to negative regulation by miR-15/16 cluster that is localized at chromosome 13q14. The surface marker CD5 is expressed by B-CLL cells, therefore it is used for confirmation of B-cell malignancies. Product of gene *AICDA*, the AID protein is involved in two processes that occur during maturation of B-cells: somatic hypermutation and class-switch recombination.

From microarray profiling we conclude, that MYB and miR-155 programs are in B-CLL deregulated.

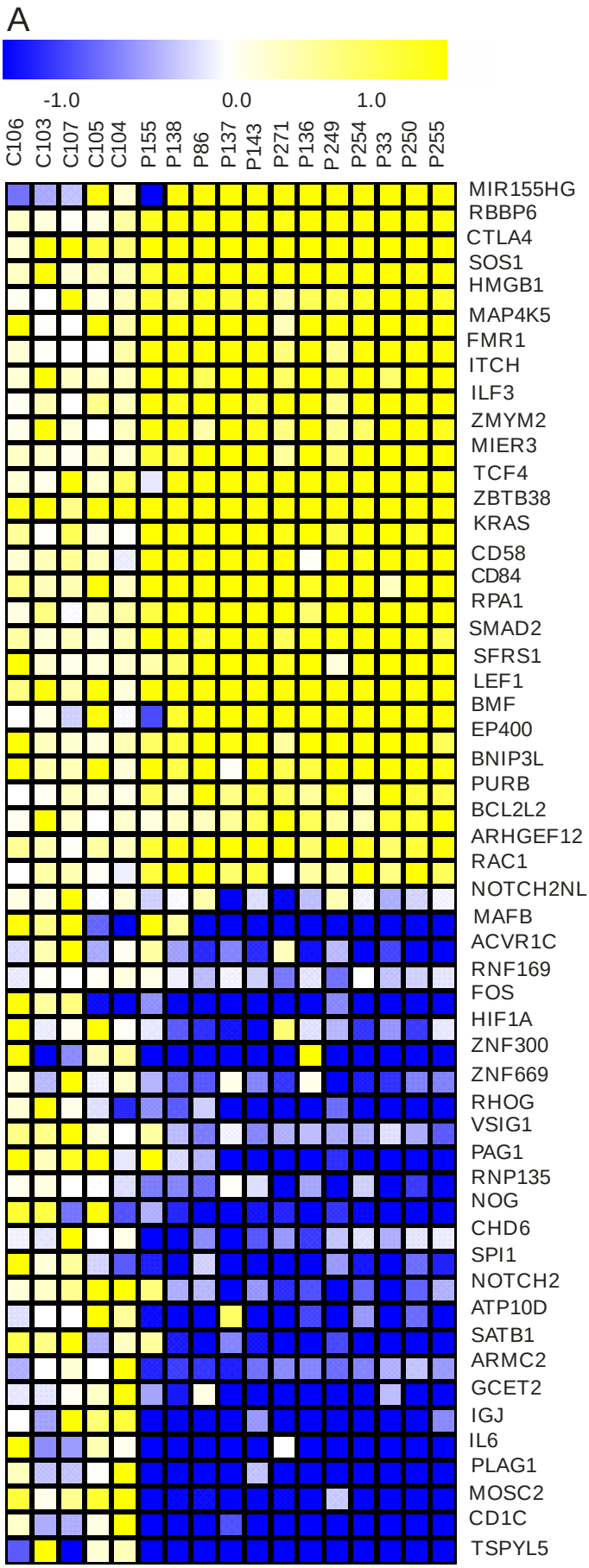
A
-1.0
0.0
1.0
C106
C103
C107
C105
C104
P155
P138
P86
P137
P143
P271
P136
P 249
P254
P33
P250
P255
MIR155HG
RBBP6
CTLA4
SOS1
HMGB1
MAP4K5
FMR1
ITCH
ILF3
ZMYM2
MIER3
TCF4
ZBTB38
KRAS
CD58
CD84
RPA1
SMAD2
SFRS1
LEF1
BMF
EP400
BNIP3L
PURB
BCL2L2
ARHGEF12
RAC1
NOTCH2NL
MAFB
ACVR1C
RNF169
FOS
HIF1A
ZNF300
ZNF669
RHOG
VSIG1
PAG1
RNP135
NOG
CHD6
SPI1
NOTCH2
ATP10D
SATB1
ARMC2
GCET2
IGJ
IL6
PLAG1
MOSC2
CD1C
TSPYL5

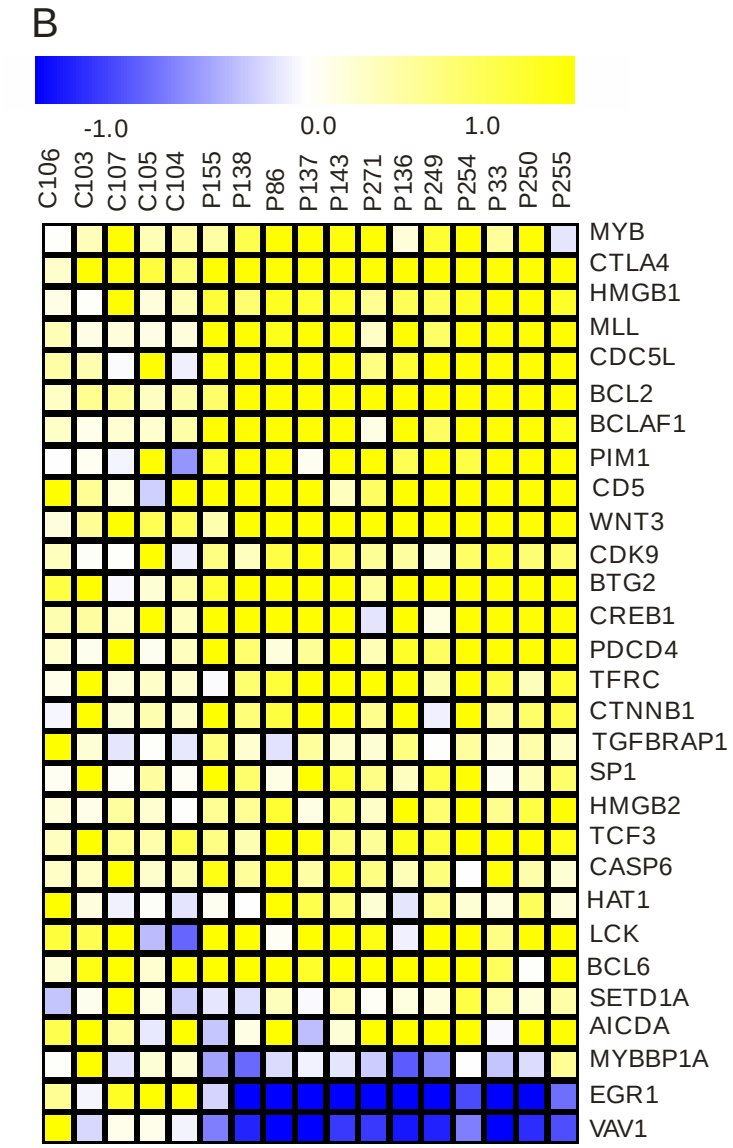

Figure 4.33: Targets of miR-155 and MYB are deregulated in B-CLL.
(A) Heat map shows selected miR-155 target genes which are differentially expressed between B-CLL (N=12; patient codes are indicated on top of the heat maps) and normal B-cells samples (P value of t-test <0.05). Genes were selected from union of six lists of either predicted or experimentally validated target genes of miR-155 (see section 3. Material and Methods/GSEA). (B) Heat map shows selected MYB target genes which are differentially expressed between B-CLL (N=12; patient codes are indicated on top of the heat maps) and normal B cell samples (P value of t-test <0.05). Genes were selected from three independent sources of MYB target genes (see section 3. Material and Methods/GSEA).

4.5 *In vitro* changes at levels of MYB, miR-155 and PU.1 in B-CLL cells show on the tight relationship between these molecules

Our previously published data show, that miR-155 and its validated target gene *PU.1* are in B-CLL are differently expressed [144]. Our data from ChIP and luciferase assay showed that MYB binds and stimulates transcription of *MIR155HG* gene (Figure 4.30). Therefore we performed functional assays where we manipulated the levels of miR-155, PU.1 and MYB to asses the existence of relationship between these molecules *in vitro* (Figures 4.34 – 4.38).

For downregulation of MYB levels we transfected Raji cells and primary B-CLL cells with siRNA MYB. Figure 4.34 indicates on the downregulation of MYB in both Raji and primary B-CLL cells (P88) at 48 hours post transfection. Downregulation of MYB was followed by a decreased level of miR-155 in Raji cell line and in primary B-CLL cells. Reduction of MYB mRNA and afterwards decreased level of miR-155 were concentration dependent (Figure 4.34).

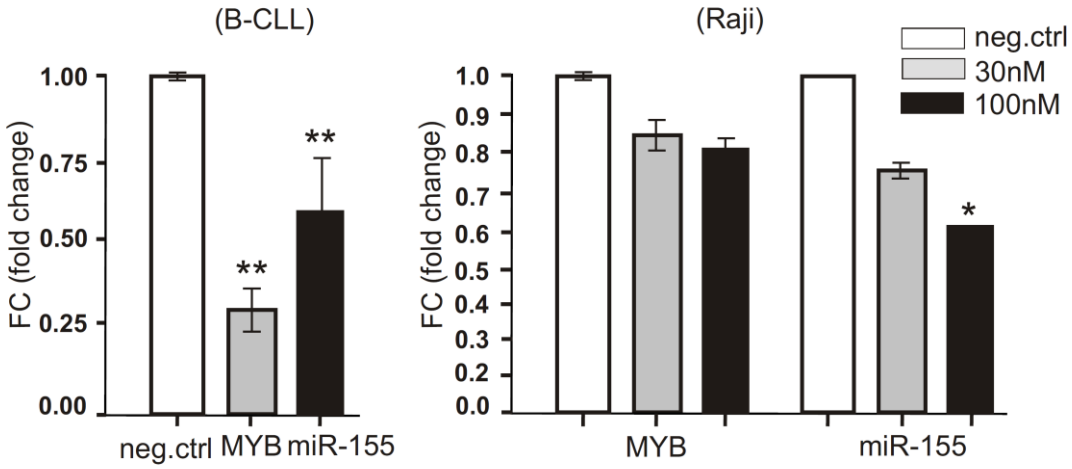

Figure 4.34: Transfection of primary B-CLL cells and Raji cell line with siRNA MYB.
Transfection of primary B-CLL cells (P88) and Raji cell line with siRNA oligonucleotides inhibiting expression of MYB or with negative control oligonucleotides (final concentrations 30 - 100nM). After 48 hours the total RNA was purified, reverse transcribed and measured by quantitative PCR as described in section 3. Material and Methods. The Y-axis represents the relative expression of mRNA of indicated genes relative to reference gene: *GAPDH* (for MYB, PU.1) or *RNU44* (for miR-155). Data are shown as a fold change (FC) and normalized to mRNA levels obtained in negative control transfection experiments (control measurements were set equal to 1). Error bars represent standard errors of the mean (SEM). For statistical analysis we used Student`s t-test, where the P values <0.05 are indicated by one and <0.001 by two asterisks respectively.

To see the effect of *in vitro* increasement of the MYB mRNA and protein level we transiently transfected Raji cells and HeLa cells by expression plasmid that contains MYB

cDNA. After 48 hours post transfection of HeLa cells with MYB pcDNA we detected by western blot 5-fold overproduction of MYB protein (Figure 4.35A) and dose dependent increase of MYB mRNA in Raji cells (Figure 4.35B).

The *in vitro* transient changes of MYB levels leads to corresponding changes of miR-155 expression levels in Raji, HeLa cell line and in primary B-CLL cells (Figure 4.34 and 4.35).

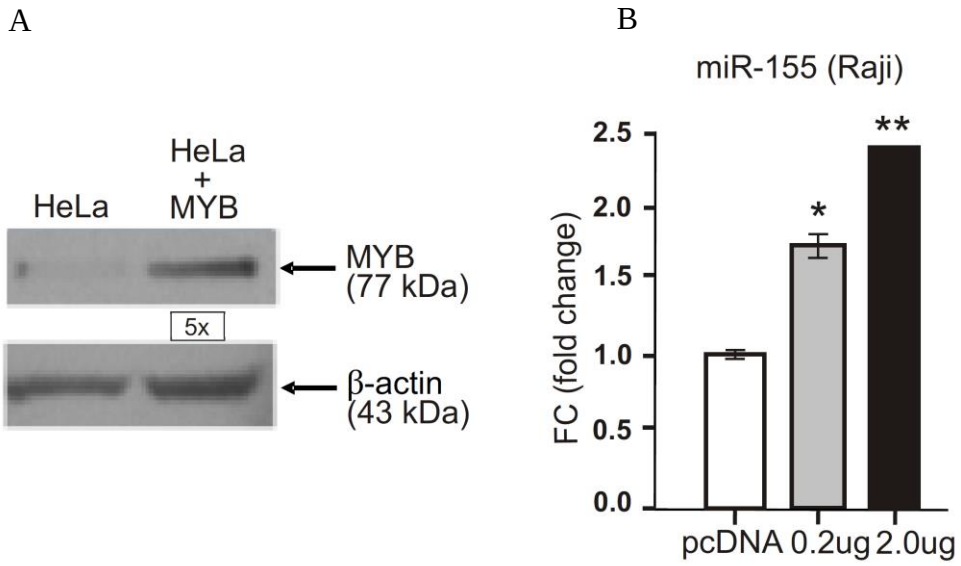

Figure 4.35: Transfection of primary B-CLL cells and Raji cell line with MYB expression plasmid.
(A) The figure shows immunoblotting of MYB protein 48 hours post transfection (HeLa cell line) with MYB cDNA encoding plasmid. Protein level was normalized on the levels of ß-actin protein. The optical density of both proteins is indicated below the blots. (B) The Raji cells were transfected with MYB cDNA encoded by expression plasmid (in two final concentrations: 0.2 µg/µL and 2.0 µg/µL) or with a negative control plasmid (pcDNA 3.1). Cells were harvested 48 hours post transfection and total RNA was extracted and measured by RT-qPCR. Y-axis represents the relative expression of miRNA-155 relative to RNU44 (negative control measurements were set equal to 1). Error bars represent standard error of the mean. We used Student`s t-test, the P values <0.05 are indicated by 1and <0.001 by 2 asterisks respectively.

Silencing of MYB or exogenous over production of MYB mRNA influences expression level of miR-155. Based on this knowledge we silenced or overproduced levels of miR-155 *in vitro* (Figure 4.36 and 4.37).

We transfected Raji cell line and primary B-CLL cells (P161) by anti-miR-155 oligonucleotides at final concentrations 40nM and 100nM. The figure 4.37 indicates on the significant decrease of miR-155 mediated by anti-miR-155 oligonucleotides. This decrease of miR-155 led to a significant PU.1 rescue (3-fold). These results show on the direct effect of miR-155 on the mRNA level of its target gene PU.1 in B-CLL (Figure 4.36).

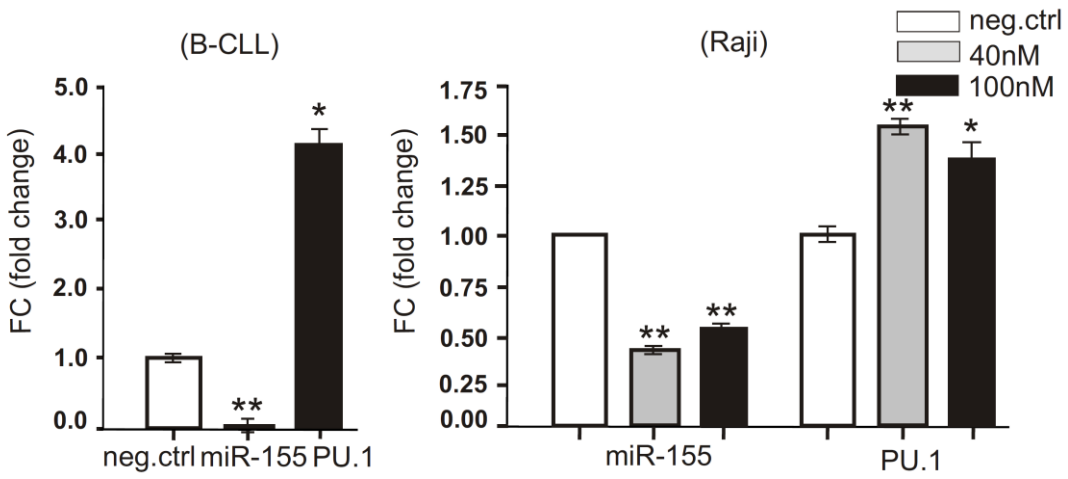

Figure 4.36: Transfection of primary B-CLL cells and Raji cell line with anti-miR-155 oligonucleotides. B-CLL cells (P161) and Raji cell line were transfected with anti-miR-155 oligonucleotides (in the final concentration 40nM, 100nM) and parallel with negative control oligonucleotides (in the final concentration 40nM, 100nM). After 96 hours total RNA was purified, reverse transcribed and measured by quantitative PCR as described in Methods, Y-axis represents the relative expression of mRNA of indicated genes relative to a reference gene *GAPDH* (for PU.1) or *RNU44* (for miR-155). Data are normalized to mRNA levels obtained in negative control transfection experiment (negative control measurements were set equal to 1). Error bars represent standard error of the mean. We used Student`s t-test, the P values <0.05 are indicated by one and <0.01 by two asterisks respectively.

We further tested the effect of aberrant expression of miR-155 on its target gene *PU.1*. The Raji cells were transiently transfected with oligonucleotides of mimic-miR-155 in the final concentrations 40nM and 100nM. After 24 hours post transfection we detected significant increase (~12-32 fold) of miR-155 expression level and corresponding decrease of PU.1 mRNA. Expression changes of miR-155 and PU.1 were concentration dependent (Figure 4.36).

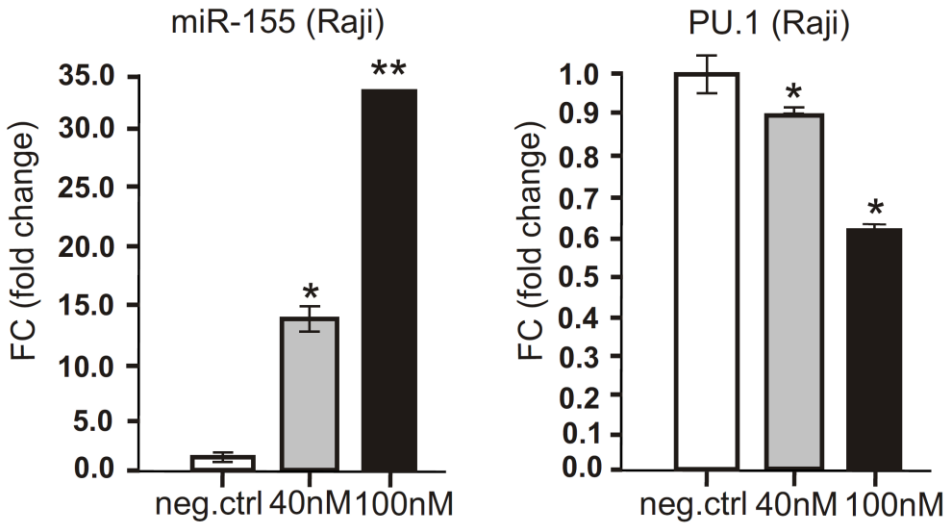

Figure 4.37: Transfection of primary B-CLL cells and Raji cell line with mimic-miR-155 oligonucleotides. Raji cell line was transfected with miR-155 oligonucleotides (in the final concentration 40nM, 100nM) or with negative control oligonucleotides. After 24 hours total RNA was purified, reverse transcribed and measured by quantitative PCR as described in Methods, Y-axis represents the relative expression of mRNA of indicated genes relative to a reference gene *GAPDH* (for PU.1) or *RNU44* (for miR-155). Data are normalized to mRNA levels measured in negative control transfection experiments (negative control measurements were set equal to 1). Error bars represent standard error of the mean. We used Student`s t-test, the P values <0.05 are indicated by one and <0.001 by two asterisks respectively.

The hematopoietic transcription factor PU.1 acts as dose-dependent mediator in maturation of myeloid and lymphoid progenitor cells. Extremely low levels of PU.1 in blood cells leads to leukemia. From literature is known that in mouse progenitor cells the PU.1 expression stimulates production of miR-155 thus initiates differentiation of progenitor cells [157]. We asked whether PU.1 regulates expression of miR-155 in the primary B-CLL cells. B-cells express low levels of PU.1, we next asked: What cause an exogenous increase of PU.1 in B-CLL cells? To answer this question, we transduced the primary B-CLL cells (P40) with lentiviral vector carrying PU.1 and GFP: PU.1-IRES-GFP lentiviral vector. After 72 hours post transduction we sorted out the GFP positive infected cells that contained PU.1-IRES-GFP lentiviral vector (MOI=3) and afterwards we measured changes at mRNA level. The figure 4.38 shows that rescued levels of PU.1 caused an increase of the mRNA of PU.1 (>2-fold) and resulted in decrease of miR-155 and MYB levels. We could conclude: manipulation with PU.1 level significantly decrease miR-155 expression in primary B-CLL cells.

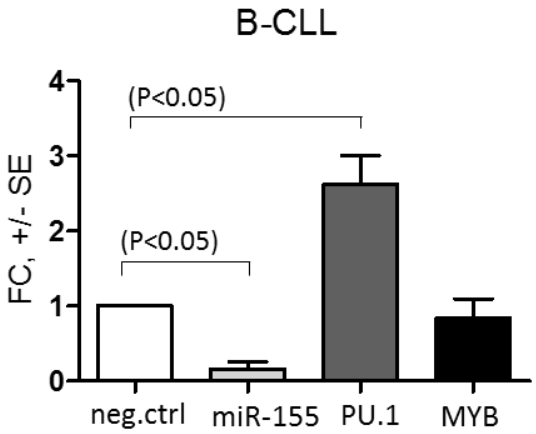

Figure 4.38: Transfection of primary B-CLL cells with PU.1-IRES-GFP lentivirus.
Graph shows results of transduction of primary B-CLL cells (P40) with PU.1-IRES-GFP lentiviral vector. After 72 hours the GFP positivity was measured, GFP positive cells with PU.1-IRES-GFP lentiviral vector were sorted out by FACS AriaIIu cell sorter. From GFP positive sorted cells were purified total RNA, reverse transcribed and measured by quantitative PCR as described in section 3.Material and Methods. The Y-axis represents the relative expression (shown in fold change) of mRNA/miRNA of indicated genes relative to reference gene GAPDH (for PU.1) or RNU44 (for miR-155). Data were normalized to mRNA levels measured in GFP positive sorted cells that do not contain PU.1-IRES and were set equal to 1. Error bars represent standard error of mean. For statistical analysis we used Student`s t-test. The P values lower than 0.05 are indicated by one asterisk.

Based on our data, we suppose that regulatory pathway: MYB→miR-155 —|PU.1 may play a role in reprogramming of gene expression pattern in B-CLL cells. Taken together, in our cohort of B-CLL patients the expression profile of miR-155 and MYB are significantly elevated in subset of patient samples. On the other hand, the production of mRNA and protein of PU.1 were decreased likely by elevated levels of miR-155. We created our working model of B-CLL: the transcription factor MYB stimulates the expression of miR-155 and over production of miR-155 inhibits the production of PU.1 (Figure 4.39). Based on data from PU.1 rescue experiment we could add to our model additional finding: increased level of PU.1 inhibits miR-155 and MYB expression. To this model we could not add miR-150 as we do not have the data from *in vitro* functional assays. Finally, the 20% of our B-CLL patient samples matched the criteria: elevated miR-155 (>2.5-fold), elevated MYB (>1.5-fold) and decreased PU.1 (<0.5-fold) (Figure 4.40).

Figure 4.39: Scheme of our working model in B-CLL. The elevated level of MYB enhances the production of miR-155 that inhibits mRNA and protein production of PU.1 in B-CLL patient samples.

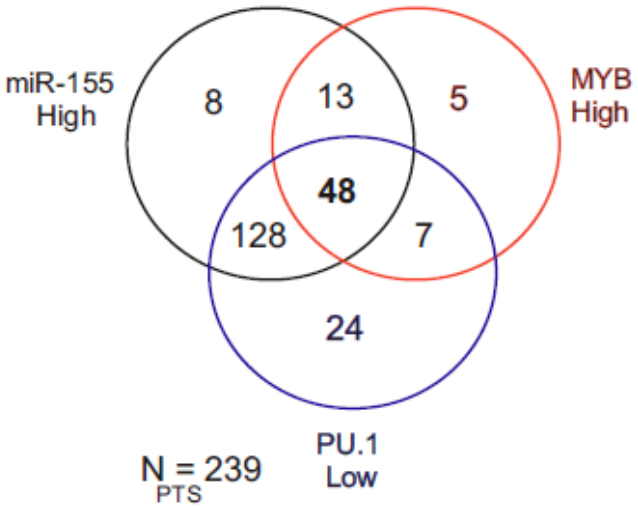

Figure 4.40: Venn diagram of B-CLL patient samples divided accordingly expressions of MYB, PU.1 and miR-155. The patient samples ($N_{CD19+/PBMC}$=239) were divided into three groups – accordingly mRNA/miRNA expression of miR-155 High (FC>2.5), MYB High (FC>1.5) and PU.1 Low (FC<0.5). The 48 patient samples expressed high levels of miR-155, MYB and low PU.1 levels. The 20% of our B-CLL patient samples (20% (48/239)) fit to our working model (Figure 4.39). The Wenn diagram was done using the program by Oliveros, J.C. (2007) VENNY. An interactive tool for comparing lists withVennDiagrams.http://bioinfogp.cnb.csic.es/tools/venny/index.html.

5. DISCUSSION

Chronic lymphocytic leukemia (**B-CLL**) belongs to the most frequent leukemia with recurrent relapses and heterogeneous course. There arise questions as: How to predict in time the disease progression? How to control patient response to the therapy? When to start with therapy? How the normal B-cell transforms into the leukemic cell is under intensive study. *In vitro* studies on the primary leukemic B-cells help us to understand pathogenesis of leukemia in more detail.

5.1 Expression profile of miR-155, PU.1, MYB and miR-150 in relation to the clinical data and epigenetic markers

This Thesis focuses on the role of **miR-155** in B-CLL and on causes of its aberrant expression in B-CLL. The miR-155 was identified by Tam *et al.,* as a B-cell integration cluster, while it is activated by proviral insertions in avian leucosis virus-induced lymphomas [147]. The first report about the elevated level of miR-155 in human leukemia was in Hodgkin's lymphoma cells, described by group of van den Berg [141] and later in B-CLL by Callin *et al.* [145]. Here we found 4-32 fold increase of mature miR-155 in primary B-CLL cells as well as in separated CD19+ B-CLL cells (Figure 4.1A, B). Similar expression pattern described Fulci *et al.* [17]. We ask if there is an association between the expression of primary transcript of miR-155 (pri-miR-155) and its mature form (miR-155). We detected elevated levels of both forms in the primary B-CLL cells, even the primary transcript showed higher expression (Figure 4.2A, B). Our data are in accordance with others [149]. We measured in parallel the levels of miR-155 in plasma of 10 B-CLL patient samples and observed that the levels of miR-155 in plasma and in separated CD19+ B-CLL cells were similar (Figure 4.3A, B). In plasma of B-cell lymphoma patients were described elevated levels of miRNAs as miR-155, miR-210, miR-21 that associated with disease progression [244]. Thus, the measurement of microRNAs in plasma could be used as biomarker of disease and its progression. Callin *et al.,* found a positive association between the high expression of specific miRNAs (miR-155, miR-181a, miR-146, miR-4-2, miR-23b, miR-23a, miR-222, miR-221) and shorter interval from diagnosis to the first therapy in B-CLL patient samples [145]. These findings strongly support importance of miR-155 in B-CLL as a new prognostic marker. Furthermore, others determined the miR-

155 levels in plasma of patients with monoclonal B-lymphocytosis (MBL) that developed into B-CLL and concluded that miR-155 represents prognostic marker of MBL to B-CLL progression [20]. Similarly to this report, we observed that expression of miR-155 during the disease progression fluctuates thus we hypothesize that it could be a useful prediction marker of disease progression and staging [245]. Different levels of miR-155 during disease progression document its higher level in advanced Rai stage (II-IV) (Figure 4.13). In B-CLL patient samples with advanced Rai stage and after therapy, the expression of miR-155 was decreased in dependence on the number of therapy cycles and overall survival (Figure 4.14). Moreover, B-CLL patient samples after Rituximab treatment displayed rapid decrease of miR-155 expression (Figure 4.28). Among the prognostic parameters of B-CLL belong mutation status of IgVH and presence of surface markers ZAP-70 and CD38 [246]. B-CLL cells with unmutated IgVH gene underwent final development prior their entry into the germinal center that correlates with poor prognosis and shorter overall survival of B-CLL patients [246]. We measured the levels of miR-155 in both groups of B-CLL patient samples: unmutated vs. mutated IgVH status (Figure 4.18). B-CLL cells with unmutated IgVH genes expressed significantly higher levels of miR-155 (Figure 4.18). We divided B-CLL patient samples into two groups (favorable and unfavorable) based on the presence of surface markers ZAP-70 and CD38 and on the IgVH status (Figure 4.21). The favorable group is characterized by absence of prognostic surface markers ZAP-70 and CD38 and as well by mutated status of IgVH gene in contrast to unfavorable group (where the surface markers are present and IgVH gene are unmutated). We detected in the B-CLL cells of patient group with unfavorable prognosis IgVH unmutated/CD38+/ZAP-70+ significantly higher expression of miR-155 (Figure 4.21). For additional prognostic evaluation of B-CLL progression the cytogenetic measurement of chromosomal aberrations by FISH is used [28]. In the B-CLL samples with "high risk", carrying the deletion of chromosomal region 11q22-23 or 17p13 respectively, we detected increased expression of miR-155 (Figures 4.24, 4.25).

We can conclude that expression of miR-155 reflects the progression of B-CLL as the levels of miR-155 are higher in advanced Rai stage and in the unfavorable prognostic group. The measurement of miR-155 levels in plasma and in peripheral blood correlates, thus it could be used as biomarker of B-CLL. Moreover, the levels of miR-155 after therapy decreased, that underlines its importance in clinical use.

The validated direct target of miR-155 is a key hematopoietic transcription factor - PU.1 (SPI1) [157]. The role of decreased **PU.1** levels in lymphoid malignancies document data showing its down regulation in multiple myeloma and T-cell lymphoma [204,247]. Here we detected in the primary PBMCs and in CD19+ separated B-CLL cells the 3-4 fold decrease of PU.1 mRNA (Figure 4.4). This is in accordance with data of Dr. Mankai research group, where authors described low levels of PU.1 in B-CLL cells [248]. In the protein lysates of B-CLL patient samples we detected one-fold decrease of PU.1 production (Figure 4.5). An early transcription factor - FOS (FBJ murine osteosarcoma viral oncogene homolog) is a target of PU.1. In our B-CLL patient cohort we found a 4-fold decrease of mRNA FOS (Figure 4.6). The low expressions of FOS and PU.1 support our data from genome-wide arrays, demonstrating their significant down regulation (Figure 4.33A). We detected overall low levels of PU.1 in B-CLL patient samples based on the prognostic markers as IgVH status and expression of ZAP-70, CD38 (Figure 4.18-21). The B-CLL patient samples in advanced Rai stage and after therapy showed increased level of PU.1 as compared with Rai stage 0-I (Figure 4.16). This increase is much stronger when the patients undergo more therapy regimens and displayed more aggressive course of disease (Figure 4.16). Similarly, PU.1 expression decreased 1.5-fold after Rituximab treatment (Figure 4.28). This underlines also fact, that PU.1 expression was significantly decreased in B-CLL patient group with deleted chromosome 17p13 – the patient group with high risk of B-CLL (Figure 4.25). Silenced production of PU.1 mRNA and protein in B-CLL is due to post-transcriptional inhibition mediated by elevated miR-155. Similarly, the mice with low expression of PU.1 (~20%) and with high expression of miR-155 developed more aggressive acute myeloid leukemia in comparison to mice with normal expressions of PU.1 and miR-155 [205]. It was also described an opposite interaction between miR-155 and PU.1 in the myeloid progenitor cells, where PU.1 works as an inhibitor of the miR-155 expression [249].

This data demonstrate that expression of PU.1 is in B-CLL cells inhibited by aberrant expression of oncogenic miR-155. Decrease of PU.1 mRNA level correlates with advanced stages and more aggressive course of B-CLL. Thus, measurement of PU.1 showed prognostic and disease progression potential for B-CLL.

Based on above-mentioned information we asked: What causes this increase of miR-155 expression in B-CLL cells? It is known, that proto-oncogenes stimulate cellular growth and what leads to disease progression [250]. Increased copy numbers of the proto-oncogen

MYC (v-Myc myelocytomatosis viral oncogene homolog) from the E-box family enhance the transformation of B-CLL into Richter`s syndrome [46]. The expression of MYC mRNA in our patient cohort was not up-regulated as reported by others [251]. Since the mRNA level of MYC in our patient cohort was only slightly above the mRNA MYC levels of control CD19+ B-cells (Figure 4.9), we investigated other members of E-box family – *MYB*, *MYBL1* and *MYBL2*. The mRNA levels of MYBL1 and MYBL2 did not show any significant expression changes in B-CLL cells as compared with control B-cells (data not shown). Interestingly, we observed that in a subset of B-CLL patients (~40%) there was a 3-fold up-regulation of **MYB** mRNA (Figure 4.8). We also investigated the protein levels of MYB in primary B-CLL cells. In protein lysates of B-CLL cells we detected up to 72-fold up-regulation of the MYB protein as compared with B-cells from normal healthy donors (Figure 4.5). Here, for the first time we described the role of MYB in B-CLL cells [144]. Moreover, we found three putative MYB binding sites at the *MIR155HG* promoter region (Figure 4.29 and Figure 3.3). MYB binds exclusively at three loci: -0.5kb; +0.1kb and +1.6kb relatively to transcription start site (TSS) of *MIR155HG* gene (Figure 4.30A and section 3. Material and methods, Figure 3.3). Similarly, it was described that MYC binds at the *MIR155HG* promoter region close to TSS and induces development of avian lymphomas [252]. Based on our data and published data we supposed that MYB in B-CLL as MYC in chicken B-cell lymphomas enhances the transcription of *MIR155HG* thus leads to disease progression [144,252]. To answer the question if MYB has ability to stimulate transcription of *MIR155HG*, we generated luciferase reporter constructs either with mutation in MYB binding site (E-box 1) or without such mutation (Figure 4.30B and section 3.Material and Methods; Figure 3.3). The mechanism of activation of *MIR155HG* by MYB is proposed to include acetylation of histone H3K9, a notion supported by others [253]. By ChIP assay we found that active chromatin marks H3K9Ac and H3K4Me3 are recruited at the *MIR155HG* promoter region (Figure 4.31). The enrichment peak of occupancy by H3K9Ac and H3K4Me3 (Figure 4.31) culminated exclusively at three loci (0.5kb; +0.1kb and +1.6kb relative to TSS) and this enrichment peak correlates with the MYB mRNA expression in primary B-CLL cells (Figure 4.32). Next, we asked whether the putative MYB binding site (E-box 2) is not mutated in the primary B-CLL cells. After sequencing of this region we did not observe any mutations in the putative MYB binding site (see the section 10. Supplement; Supplemental data 10.3). The question arises: What causes an aberrant expression of MYB in the leukemic B-cells? The possible answer could be that NFκB by its binding at the first

intron of MYB activates the expression of MYB [254]. Moreover it was shown that NFκB stimulates expression of miR-155 in B-cells [191] and that MYB is a direct target of NFκB [254]. This let us to speculate that initial step in this leukemic process could be some inflammation stimuli that enhance expression of both MYB and miR-155 and let the leukemic cell accumulate/proliferate. It was shown that the expression of MYBL1 correlates with the proliferation of mature B-cells [255] and with the presence of CD38 surface marker on the germinal center B-cells [256]. Presence of surface marker CD38 on B-cells indicates their active proliferation and communication with microenvironment [257]. We observed positive correlation between expression of CD38 marker (CD38+) and the elevated expression of MYB mRNA in B-CLL cells (Figure 4.20). Moreover, we detected elevated expression of MYB mRNA in patient samples with unfavorable prognosis – IgVH unmutated/ZAP-70+/CD38+ (Figure 4.21). The prognosis of B-CLL progression defines Rai staging system (0-IV). We found significantly elevated MYB mRNA in the B-CLL samples with advanced Rai stage (Figure 4.13) and with presence of surface marker ZAP-70 (Figure 4.19). The mutation status of IgVH genes does not correlate with expression of MYB in B-CLL cells (Figure 4.18). Taken together, expression of MYB in B-CLL could be prognostic marker for disease progression as well as for control therapy efficacy.

Between the top 10 MYB targets belongs B-cell specific microRNA - **miR-150** [72,228]. MiR-150 is selectively expressed by mature resting B- and T-cells, but not by their progenitors [227]. MiR-150 regulates differentiation of B-cells through MYB [228]. In our cohort of B-CLL patients we observed in 30% of patient samples elevated miR-150 (2-3 fold); in 40% above control level and in rest 30% decreased miR-150 (Figure 4.7). Our data are in accordance with data of other research groups [17,137,258]. Authors described a negative correlation between expression of miR-150 and prognostic markers IgVH and ZAP-70 (Figures 4.18, 4.19). Wang *et al.,* showed a reciprocal relationship between expressions of miR-155 and miR-150 in the germinal center B-cells, evaluated by *in situ* hybridization [137]. In contrast, we did not found such reciprocal relationship between the expressions of miR-155 and miR-150 in B-CLL samples (Figure 4.10) but we found a rather positive relationship as it show figures 4.27 and 4.10. Since the MYB is a target of miR-150, we assumed between these molecules any relationship. It was described a reciprocal relationship between expression of miR-150 and MYB in the myelodysplastic syndrome (MDS) [259]. We measured

the levels of both, and unfortunately did not find such reciprocal relationship between miR-150 and MYB expressions (Figure 4.11).

5.2 Global gene expression profile: miR-155 and MYB target genes in B-CLL

We performed the global gene expression profiling on the B-CLL patient CD19+ B cell samples (N=12) and the normal healthy control CD19+ B cells (N=5) to assess the behavior of MYB and miR-155 target genes. Our microarray data showed that miR-155 and MYB programs are deregulated in B-CLL (Figure 4.33A, B).

The multifunctional and oncogenic microRNA - miR-155 regulates vast group of targets [73]. We selected a few miR-155 (N=53) target genes using the gene set enrichment analysis (GSEA)(Figure 4.33A). Among the high score validated target of miR-155 belongs the well known hematopoietic transcription factor **PU.1**, that is extremely low in B-CLL (Figure 4.33A; 4.4). The highest levels of PU.1 mRNA are detected in granulocytes, monocytes/macrophages; the lowest levels are in B-cells and practically no expression in erythrocytes and T-cells [204,260]. An upstream regulatory element (URE) is located at -14kb and -17kb upstream of the transcriptional start site of the *PU.1* gene and regulates 80% of PU.1 expression [261]. Mouse model with deleted URE region showed decreased expression of PU.1 levels up to 20% that result into acute myeloid leukemia in mice [247] and in T-lymphoma and multiple myeloma in humans [204]. We moreover observed that PU.1 low (Pu.1 $^{ure/ure}$) mice with increased miR-155 and MYB mRNA levels developed more aggressive acute myeloid leukemia [205]. Due to high methylation of the *PU.1* promoter, expression of PU.1 in Hodgkin`s lymphoma cells is decreased. Further decrease of PU.1 in Hodgkin`s lymphoma cells induces cell growth and blocks apoptosis. Exogenous increase of PU.1 levels led to tumor regression and stabilization of disease in xenograft mouse model just like in primary Hodgkin`s lymphoma cells [262]. This data emphasize that *PU.1* acts as a tumor suppressor in myeloid and lymphoid cells. Rescue of PU.1 is a possible therapeutic option for not only patients with Hodgkin`s lymphoma [262] but probably also for patients with B-cell malignancies. We performed similar experiment, where we exogenously increased the levels of PU.1 in the primary B-CLL cells that resulted in significant increase of mRNA PU.1 and decrease of miR-155 and MYB mRNA levels (Figure 4.38). Based on this data, the *in vitro* manipulation with PU.1 levels in B-cell leukemia/lymphoma provide the PU.1 potentially

useful molecule in the future therapy. The mRNA levels of *PU.1* target gene - *FOS* (FBJ murine osteosarcoma viral oncogene homolog) were in B-CLL also significantly decreased (Figures 4.6 and 4.33A). FOS is an early transcription factor that by interacting with proteins from the JUN family forms a transcription factor complex called AP-1. The AP-1 complex enhances activity of B-cell receptor signaling and possibly stimulates transcription of *MIR155HG* [187]. Upon activation by the BCR authors showed that *JunB* (major activator) and *FosB* (minor activator) recruit *MIR155HG* promoter. Thus, BCR-mediated signaling leads to the induction of *MIR155HG* expression in B-cell line Ramos [187]. It is known that during tumor growth in the hypoxic environment a hypoxia inducible factor 1 (HIF1A) is aberrantly expressed. **HIF1A** regulates vascular endothelial growth factor (VEGF) and thereby is associated with tumor angiogenesis and vascularization. High levels of VEGF were detected in the microvesicles localized in plasma of B-CLL patients [263]. Microvesicles form an important part of the tumor microenvironment and are released by malignant cancer cells. The amount of microvesicles is higher in cancer cells compared with normal healthy cells. Circulating microvesicles in B-CLL patient plasma samples transfer messages to the targeted cells that could be critical for disease progression [263]. Microvesicles enhance expression of **HIF1A** and stimulates AKT signaling pathway and thus leads to activation of tumor environment [263]. Here we detected decreased expression of HIF1A mRNA (Figure 4.33B). Previous studies have shown that microvesicles released from tumor cells into the blood stream of cancer patients contain also miRNAs. Due to abundant presence of RNases in the blood stream, most of the secreted miRNAs are localized in the apoptotic bodies, microvesicles and exosomes or bound to RNA-binding proteins [264]. Zhang Y *et al.*, reported that secreted miR-150 in microvesicles from human blood cells or cultured cells can be taken up by microvascular endothelial cells and these regulate the expression of MYB, which is a known miR-150 target gene [228,265]. Furthermore, Pegtel *et al.*, showed that miRNAs released from exosomes of EBV-infected B-cells can be taken up by the peripheral blood mononuclear cells and then can suppress EBV target genes [266]. These findings strongly support that at least some of the exported miRNAs are used for cell-to-cell communication. Further research is needed to determine the secretory mechanisms of miRNAs; how miRNAs are recognized for uptake and what kind of information can be transferred via this process. Changes in the miRNA expression contribute to the pathogenesis of hematopoietic malignancies, including B-CLL. However, the mechanisms that cause aberrant miRNA

transcription is still poorly described. Among the miR-155 targets we found differentially expressed **MAFB** (viral musculoaponeurotic fibrosarcoma oncogene homolog B) mRNA. *MAFB* is hematopoietic transcription factor that cooperates with MYB [267]. We showed that elevated level of miR-155 decreased the level of MAFB mRNA in B-CLL patients samples (Figure 4.33A). Similarly, it was described decreased expression of MAFB in acute and chronic myeloid leukemia (AML, CML) patient samples [268] and recently also in the B-cell low grade lymphomas [269]. Zhang Y *et al.*, showed the relationship between expression of miR-155 and MAFB in the mouse primary B-lymphoma cells and in the MEC1 B-CLL cell line [269]. Authors moreover showed that after inhibition of miR-155 in the primary B-CLL cells and in the MEC1 cell line cells increased the levels of MAFB mRNA. Thus, miR-155 negatively regulates expression of MAFB in B-cell malignancies [144,269]. Therefore, we can conclude that miR-155 controls proliferation of B-CLL cells through MAFB, which in this case functions as a tumor suppressor. Among miR-155 target genes we also detected the chromatin remodeling factor SATB1. Han *et al.*, observed over produced proto-oncogene **SATB1** (Special AT-rich Binding protein-1) in the breast cancer cells and associated it with poor prognosis of patients. In the breast cancer was proven the oncogenic potential of miR-155 [167,270]. MiR-155 stimulates expression of the tumor suppressor gene *FOXP3*. In breast cancer FOXP3 negatively regulates the expression of SATB1 through miR-155. Collective of authors McInnes recently described the existence of so-called "feed-forward regulatory loop" between FOXP3, miR-155 and SATB1 in human T-cells [271]. Thus, miR-155 negatively regulates many important genes. We also found some miR-155 target genes up-regulated, such as ***KRAS*** and ***SMAD2***. Expression of these genes is probably regulated by other compensatory mechanism that could be dependent or independent on the presence of miR-155. It was described that TGF-β induces *MIR155HG* transcription through binding of SMAD4 to the promoter region [167].

We detected among the **MYB upstream targets** also the typical B-CLL genes such as *BCL2*, *CD5*, *AICDA*, *BCL6* (Figure 4.33B). The product of the gene B-cell lymphoma 2 (**BCL2**) is the anti-apoptotic protein Bcl2 as it blocks the release of mitochondrial cytochrome c and inhibits the activation of initiator caspase 9. Bcl2 by inhibition of programmed cell death prolongs survival of cells [272]. Others and we have reported increased mRNA levels of BCL2 in B-cell malignancies [144,273]. Increased levels of Bcl2 are caused by negative regulation of cluster miR15/16 [274]. Cluster miR-15-16 is localized at 13q14 region, that is often deleted in

B-CLL – therefore the levels of miR-15-16 are very low [16]. There is no effect of miR-15a and miR-16-1 on BCL2 mRNA stability, so the expression of Bcl2 is regulated at the post-transcriptional level [16]. Elevated levels of BCL2 by miR-15-16 cluster down regulation seems to be the main regulatory mechanism involved in the pathogenesis of the major fraction of B-CLL cells. Because the miR-15-16 cluster miRNAs work as the natural inhibitor of Bcl2, this could be used as therapy in cells that over express BCL2 [274]. We detected in our B-CLL patient samples aberrantly expressed the B-CLL surface marker **CD5** [144,275,276] (Figure 4.33B). Presence of CD5 together with CD22 and CD23 markers help to distinguish between MCL and B-CLL [28]. During the maturation process, B-cells undergo somatic hypermutation (SHM) and class-switch recombination (CSR) of immunoglobulin genes [277]. The activation induced cytidine deaminase (**AID**, also known as **AICDA**) is a RNA-editing enzyme that triggers antibody diversification by the deamination of nucleotides within the immunoglobulin locus [277]. Germinal center B-cells after CD40 ligand (CD40L) stimulation express AID [277]. AID plays a key role in maturation of B-cells, where regulates switching between CSR and SHM [278], but the exact mechanisms of how the AID acts remains unclear. It was described that B-CLL cells after CSR have *IgVH* genes unmutated and predominately express AID [279,280]. This is in accordance with our results where the AICDA expression was high in B-CLL patient cells with unmutated *IgVH* genes (Figure 4.33B). Moreover, it was showed in the mouse model that overexpression of Aicda mRNA in B-cells result in T- or B-cell leukemia/lymphoma [281]. Interestingly, the splenic B-cells of miR-155 deficient mice do not expressed Aicda mRNA [157], thus miR-155 is essential for Aicda function. Furthermore, the absence of AID mediated by miR-155 inhibition resulted in imperfect maturation of B-cells [177]. Among the up-regulated MYB targets, we detected ***BCL6*** gene, its mRNA level was increased in B-CLL cells (Figure 4.33B). BCL6 is a multifunctional regulator (mainly repressor) that controls cell cycle, apoptosis, lymphocyte differentiation and immune reactions [273,282]. BCL6 also participates in the chromosomal translocations that occur in DLBCL and in follicular lymphoma [283]. As the highest level of BCL6 was detected in B-cells, its oncogenic properties have been explored mainly in the lymphoid system. Moreover, BCL6 was described as a potential prognostic marker for the diagnosis of B-cell lymphomas [284]. For terminal B-cell differentiation is typical low expression of BCL6, increased level of BLIMP-1 and low level of MYC. This is regulated by an over expression of cell cycle regulating transcription factors MAD1 and MAD4 [282]. Sandhu SK *et al.*, observed contradictory results in Eμ-miR-155 transgenic mice. Authors detected

consistently lower mRNA, protein levels of Bcl6 in mouse splenocytes and purified B-cells in comparison with wild type counterparts. Authors commented such reduction as a result of up-regulation of miR-155 targeted pathway Mxd1/Mad1. Thus transcription of BCL6 is indirectly modulated by miR-155 through the Mxd1/Mad pathway [285]. Human DLBCL is divided into two subtypes: the first subtype is germinal center B-cell (GC) DLBCL, where the BCL6 levels were increased and miR-155 was decreased; and the second subtype is the activated B-cell (ABC) DLBCL that displays an opposite mRNA expression profile [286]. These data underline the importance of BCL6 in B-cell malignancies; until now mainly detected in B-cell lymphomas. We observed that the target of both miR-155 and MYB - the BCL6 mRNA is over produced in the B-CLL cells (Figure 4.33B).

To conclude this paragraph, the miR-155 and MYB program is in B-CLL deregulated based on the GSEA analysis. Among the miR-155 target genes were half (hematopoietic TF – *PU.1*, *FOS, HIF1A*, *SATB1*) down regulated and other half upregulated (Figure 4.33A). Among the MYB targets we detected also the typical B-CLL genes such as CD5 and genes involved in apoptosis as *BCL2* (Figure 4.33B).

5.3 *In vitro* functional assays confirmed relationship between miR-155, PU.1 and MYB in B-CLL cells

We further performed **functional assays** to test the influence of different levels of miR-155, MYB and PU.1 on the primary B-CLL cells and Raji cell line. By *in vitro* manipulations of these molecules we corroborated the existence of a relationship between them (Figures 4.34-4.38). To decrease the elevated levels of miR-155 we transfected Raji and primary B-CLL cells by anti-miR-155 what resulted in significant decrease of miR-155 and increase of PU.1 levels (Figure 4.36). Exogenous increase of miR-155 level by mimic-miR-155 caused an inhibition of PU.1 expression in dose dependent manner (Figure 4.37). The PU.1 rescue experiment showed a direct relationship between levels of PU.1, miR-155 and possibly MYB (Figure 4.38). ChIP data and luciferase assay showed that MYB binds and stimulates *MIR155HG* in B-CLL cells (Figure 4.30A, B). We further asked if there is relationship between MYB and miR-155. Inhibition of MYB mediated by siRNA MYB caused dose dependent decrease of miR-155 levels (Figure 4.34) and transfection of MYB expression plasmid led to increase miR-155 expression in Raji cells (Figure 4.35).

Relationship between expression of miR-155 and MYB further supports significant elevation of miR-155 expression in the B-CLL patients overexpressing MYB (Figures 4.26 and 4.10).

Here we demonstrated that manipulation of miR-155 levels negatively influences PU.1 levels and rescue of PU.1 inhibits expression of miR-155 in B-CLL. We further confirmed that MYB and miR-155 are in tight relationship in B-CLL by either its inhibition or stimulation.

5.4 Working model of B-CLL and future therapy tools

Based on our functional data we designed a **working model for B-CLL**. This model describes relationship between miR-155, MYB and PU.1 (Figure 4.39) verified by our experiments and confronted by published data (Figure 5.1). Here we described for the first time stimulatory role of transcription factor MYB on the *MIR155HG* transcription in primary B-CLL cells (Figures 4.30A, B and 4.39, 5.1). Elevated level of miR-155 inhibits production of both PU.1 mRNA and protein in B-CLL (Figures 4.4, 4.37). Inhibition of miR-155 increased PU.1 mRNA (Figure 4.36). In support of this, Vigorito *et al.,* in miR-155 deficient mice detected elevated levels of PU.1 and after PU.1 rescue the levels of miR-155 decreased in *in vitro* model [157](Figure 5.1). This notion is in accordance with our PU.1 rescue experiment, where we significantly decreased miR-155 (Figures 4.38, 4.39 and 5.1). Interestingly, we found negative relationship between expression of MYB and PU.1, where PU.1 rescue decreased MYB expression in B-CLL (Figure 4.38). Zhao *et al.,* found that MYB inhibits PU.1 expression by ChIP-sequencing method [287]. Elevated expression of miR-150 inhibits MYB expression [228]. Finally, 20% of our patient cohort fit the criteria of described working model: >2.5-fold increase miR-155, >1.5-fold increase MYB and <0.5-fold decrease of PU.1 expression (Figures 4.40; 5.1). Based on these results, therapy of B-CLL could be in future directed to development of synthetic molecules - oligonucleotides that will inhibit production of MYB (siRNA MYB) or miR-155 (anti-miR-155).

Due to aberrant expression of miR-155 in numerous leukemia and cancers and its impact on the prognosis, disease progression, miR-155 could be a key target for future cancer therapy. The first transgenic mouse model (Eμ-mmu-miR-155) confirms that miR-155 acts on development of B-cell leukemia/lymphoma [182]. MiR-155 expressing mice initially displayed pre-leukemic B-cell proliferation in spleen and bone marrow followed by

splenomegaly and progression in B-cell lymphoma within seven months [182]. Recent work on miR-155 knock-in mouse model (tTA-miR-155 ROSA26) with elevated levels of miR-155 proved an anti-miR-155 therapy as possible treatment of B-cell lymphoma [184]. The majority (~60%) of knock-in mice with induced expression of miR-155 developed in five months lymphoma. In contrast, animals without induction of miR-155 expression did not develop aggressive lymphoma. After one week of treatment miR-155 knock-in mice with lymphoma by anti-miR-155 oligonucleotides encapsulated in nanoparticles led to the visible improvement e.g. delay in tumor growth. Efficacy of anti-miR-155 treatment was dose dependent and coated nanoparticles may improve tumor cells uptake that led to increased therapy efficacy [184]. These data underline the anti-cancer potential of anti-miR-155 nanoparticles in therapy of B-cell malignancies. It has been noted that "antagomirs" (the single-stranded RNA analogues complementary to the specific miRNA) or other chemically modified oligonucleotides need an appropriate vehicle to achieve efficient inhibition [288]. Up to now, such experiments with delivery of anti-miR-155 were done only in mice models [184] or *in vitro* on the primary B-CLL cells (Figure 4.36; and [269]). All these data collectively suggest that approaches based on interruption of miR-155 function may have therapeutic ability in treatment of B-cell malignancies.

The miR-155 acts cooperatively with other proto-oncogene or tumor suppressor gene in driving the leukemogenesis; here we found that one such cooperating gene is proto-oncogene MYB in B-CLL [144]. Our data support the importance of MYB proto-oncogene in enhancing the miR-155 production in primary B-CLL cells (Figure 4.30B). In normal hematopoiesis, MYB regulates cell proliferation and differentiation [212]. Higher levels of MYB were observed in acute myeloid [235] and lymphoid leukemia [217] but not in B-CLL. Recently become rediscovered the role of MYB during leukemogenesis. While the mRNA of MYB is often aberrantly produced or duplicated in leukemia – the targeted inhibition of MYB can have wide clinical uses. The importance of the MYB transcription factor can be confirmed by the fact that homozygous null mice die at the embryonic stage due to inability to switch from fetal to adult erythropoiesis; hence, the mice became anemic [224]. Authors Lieu and Reddy demonstrated reduced proliferative capacity, an aberrant, accelerated differentiation of hematopoietic stem cells (HSCs) due to disruption of *MYB* gene in mouse model. Hematopoiesis was also impaired it resulted in decreased production of neutrophils, monocytes, B-cells, erythrocytes and megakaryocytes in mice. These data indicate that MYB

is a key regulator of self-renewal and differentiation of HSCs [289]. Expression of MYB is required for leukemia maintenance while MYB suppression in mice resulted in delayed disease progression, induced by clearance of leukemia cells from all infiltrated organs and led to the complete remission [290]. This sensitivity to MYB inhibition could be applied also to human leukemia cells because the inhibition of MYB in mouse model was much more efficient than mimicking the conventional AML therapy used in humans. The authors found that MYB suppression leads to eradication of aggressive AML without any impact on the normal myelopoiesis [291]. The mRNA and protein half-life should be considered in the target gene selection. The MYB mRNA, as well as its encoded protein, has an estimated half-life of approximately 30 to 50 minutes [292] that is an important factor for efficiency of mRNA targeting. Luger SM *et al.,* showed that mRNA and protein levels correlate. Further, it is clear that in the absence of mRNA to translate, the protein levels of MYB decline rapidly [293]. In 2008, a trial study with official title "Infusional MYB Antisense Oligodeoxynucleotide in Advanced Hematological Malignancies" was started. The aim of the study was evaluation of MYB antisense oligonucleotides in treatment of advanced hematologic malignancies as B-CLL, chronic myeloid leukemia and multiple myeloma (http://clinicaltrialsfeeds.org/clinical-trials/show/NCT00780052). Results of this study have not been published yet, but results seem to be very promising for leukemia patients. Based on all the evidence presented above, anti-microRNA or small interfering mRNA based synthetic molecules seem to be very promising therapy tools in leukemia treatment.

Aim of the Thesis was to explore and understand the molecular mechanism of miR-155 and its target genes: MYB, PU.1 in B-CLL and seek for association between expressions of studied molecules and prognosis/progression of B-CLL. Importance of miR-155 in prognosis/progression confirmes its increased level in advanced Rai stage and in patient group with unfavorable prognosis. We shown that aberrant expression of miR-155 in B-CLL inhibits both mRNA and protein levels of its target gene PU.1. Here we answer the question what causes an aberrant expression of miR-155 in B-CLL and if miR-155 can be used as biomarker of B-CLL progression. We provide evidence that MYB binds and stimulates *MIR155HG* in B-CLL. Moreover, the MYB recruited loci at *MIR155HG* promoter region overlapped with pattern of active epigenetic marks as H3K9Ac and H4K4Me3. It should be noted that the MYB elevation in B-CLL is possibly important not only for the up-regulation of

miR-155 but also for the regulation of additional target genes, including *BCL2* and others known as deregulated in B-CLL. As well as to look on the global gene expression arrays to find out if the miR-155 and MYB programs are deregulated in B-CLL. Finally, we created the working model of B-CLL based on the *in vitro* functional assays on the primary B-CLL cells. The criteria of this model fullfiled 20% of B-CLL patients samples in our cohort.

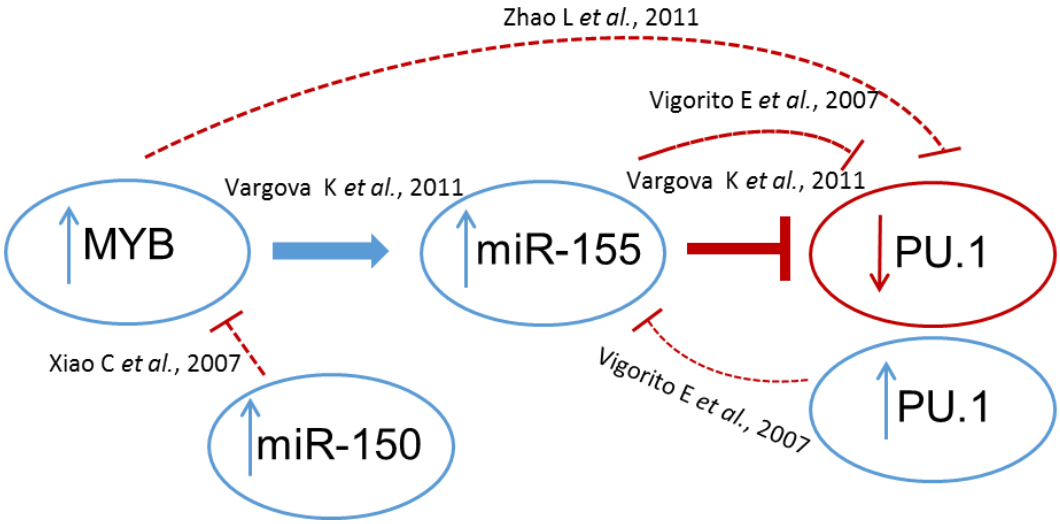

Figure 5.1: Working model of MYB-miR-155-PU.1 in B-CLL. This model describes the relationship between aforementioned molecules based on our results and published data.

6. CONCLUSIONS

- We detected significant overproduction of both primary transcript of miR-155 and its mature form in B-CLL patient cells as compared with the normal healthy B-cells. Expression of miR-155 in the peripheral blood cells and in plasma was similar. The B-CLL patient samples with advanced Rai stage (II-IV) and with unfavorable prognosis (ZAP-70+/CD38+/IgVH unmutated) showed significantly higher expression of miR-155 in comparison with the patient group with favorable prognosis. Further, expression of miR-155 was significantly higher in B-CLL patient group with deletions of chromosome 11q22-23 and 13q14. Expression changes of miR-155 in patient groups with trisomy of chromosome 12 or with deletion of 17p13 chromosome weren't statistically significant.

- In our B-CLL patient samples we detected low levels of PU.1 at both mRNA and protein level. In the group of patient samples with advanced Rai stage (II-IV) and after several therapy regimens, the PU.1 mRNA was significantly increased. Expression of PU.1 mRNA in both (favorable and unfavorable) prognostic patient group remains overal low. Expression of PU.1 mRNA in the B-CLL patient cells with deletion of 17p13 chromosome was significantly decreased, while expression changes of PU.1 in another cytogenetic subgroups weren't statistically significant.

- In subset of ~40% of B-CLL patient samples, we detected elevated level of MYB mRNA. The protein level of MYB was in selected B-CLL patient lysates overproduced as compared to lysates from normal healthy B-cells. The ChIP assay data showed that MYB binds at the three specific loci at the promoter region of *MIR155HG*. Our data from luciferase assay showed that MYB enhances the transcription of miR-155 in B-CLL cells. In the B-CLL patient samples with unfavorable clinical outcome and with advanced Rai stages (II-IV) we detected increased expression of MYB mRNA. The expression changes of MYB mRNA in our B-CLL patient samples based on cytogenetics weren't statistically significant.

- Another B-CLL specific microRNA is miR-150, that is also involed in the maturation of B-cells. In subset of ~30 % of B-CLL patient samples we detected elevated expression of miR-150. We observed significantly decreased expression of miR-150 in B-CLL patient samples with advanced Rai stage (II-IV) and with unfavorable prognosis. Expression of miR-150 was significantly decreased in B-CLL patient samples with deletions of 11q22-23 and 17p13.

- The *in vitro* functional assays on Raji cell line and primary B-CLL patient B-cells (where expression level of miR-155 was manipulated by anti-miR-155 or mimic miR-155 and MYB by siRNA MYB or pcDNA MYB), confirmed dependence of miR-155 expression to MYB and expression of PU.1 to levels of miR-155. Furthermore, we were able to push down the expression level of miR-155 by increasing the level of PU.1 in PU.1 rescue experiment. By microarray approach we have shown that miR-155 and MYB programs are deregulated in B-CLL.

- Generally, our data indicate relationship between miR-155, MYB and PU.1 in B-CLL. We created working model of this relationship in B-CLL patient cells. About 20% of B-CLL patients from our cohort match this model. Finally, it should be concluded that the read out of miR-155, MYB and PU.1 ratio by RT-qPCR could be used as an additional and reliable prognostic marker of B-CLL disorder progression.

7. SUMMARY

This PhD Thesis is focused on the detection of the expression changes of two microRNAs related to B-CLL (miR-155 and miR-150) and two transcription factors (PU.1 and MYB) involved in B-cell maturation process.

Our expression data confirmed elevated levels of miR-155 in the B-CLL patients` peripheral blood mononuclear cells as well as in the blood plasma. We detected increased expression of miR-155 in patient samples with advanced Rai stage (II-IV) and with unfavorable B-CLL clinical outcome. From cytogenetic point of view, the B-CLL cells with deletion of chromosome 17p13 expressed more miR-155.

The expression level of PU.1 fluctuates during the maturation of blood cells; however, when the level of PU.1 expression declines under 20%, the leukemia develops. We detected significant decrease of PU.1 mRNA expression and protein level in B-CLL cells. In B-CLL cells of patients with advanced Rai stage (II-IV), the level of PU.1 mRNA was decreased; however, in cells of patients with therapy regimens, the level of PU.1 mRNA was increased. The difference between expression of PU.1 mRNA in the B-CLL patient samples with favorable and unfavorable prognosis was not statistically significant. Interestingly, B-CLL patient samples with deletion of 17p13 chromosome displayed significantly lower expression of PU.1 mRNA.

Transcription factor MYB plays a crucial role during the development of B-cells. Aberrant expression of MYB leads to lymphoproliferative disorders. Up to now, the role of MYB has been described only in acute and chronic myeloid leukemia but not in B-CLL. We observed increased expression of MYB mRNA and protein in a subset of B-CLL patient samples (~40%). By ChIP assay, we further detected that MYB specifically binds at the promoter region of *MIR155HG* and thereby stimulates the transcription of miR-155 in B-CLL cells. In B-CLL patient samples with advanced Rai stage (II-IV) the expression of MYB was higher as in patients with Rai stage 0-I. The group of B-CLL patient samples with unfavorable prognosis displayed higher expression of MYB in comparison to favorable prognosis group. The expression of MYB mRNA in B-CLL patient samples did not correlate with cytogenetic aberrations.

Another B-CLL specific microRNA is miR-150, that is also involed in the maturation of B-cells. The miR-150 plays role in B-CLL progression. Expression of miR-150 decreased with the disease progression: lower miR-150 expression was detected in cells of patients with advanced Rai stage (II-IV) and with unfavorable prognosis. Similarly, expression of miR-150 was significantly lower in the B-CLL patient samples with deletions of 11q22-23 and 17p13.

Our data, generated from *in vitro* functional assays, indicated the existence of tight relationship between miR-155, PU.1 and MYB molecules in B-CLL cells. We created the working model of such tight relationship. Briefly, the expression of MYB molecule stimulates the expression of miR-155 molecule. The abberantly expressed miR-155 inhibits the PU.1 expression. This leads to B-CLL progression.

The read out of miR-155, MYB and PU.1 ratio by RT-qPCR could be used as an reliable prognostic marker of B-CLL progression. Furthermore, the restoration of the normal balance between studied molecules in leukemic B-cells could be used as an future therapy of B-CLL.

8. AUTHOR CONTRIBUTION

The author wrote the Thesis and, under the kind supervision, performed following experimental procedures: routine cell culture work, patient/control samples preparation (Ficoll-Paque and Rosette separation), mRNA/microRNA extraction, qRT-PCR and delta-delta analysis, transfections (Amaxa, DMRIE-c, JetPEI). Other members of the laboratory helped me with following methods: Pavel Burda with chromatin immunoprecipitations, Nikola Čuřík with western blotting and luciferase assay and Filipp Savvulidi with the flow cytometry analysis and FACS cell sorting. FISH analysis (cytogenetics) was performed by Adela Berková. The patient clinical data was collected by Petra Obrtlíková. The bioinformatical analyses were perfomed by Vojtech Kulvait and Jiří Zavadil (microarrays and GSEA). My mentor, Tomáš Stopka helped me with the experimental design, reviewed the results and revised the PhD Thesis and research publications.

9. REFERENCES

1. Rozman C, Montserrat E. Chronic lymphocytic leukemia. *The New England Journal of Medicine*. 1995;19:1052–1057.

2. Hallek M. Chronic lymphocytic leukemia: 2013 update on diagnosis, risk stratification and treatment. *American Journal of Hematology*. 2013; doi: 10.1002/ajh.23491.

3. Campo E, Swerdlow SH, Harris NL, Pileri S, Stein H, Jaffe ES. The 2008 WHO classification of lymphoid neoplasms and beyond:evolving concepts and practical applications. *Blood*. 2011;117(19):5019–32.

4. Danilov A, Danilova O, Klein AK, Huber BT. Molecular pathogenesis of chronic lymphocytic leukemia. *Curr. Mol. Med*. 2006; (6):665-75.

5. Chiorazzi N. Cell proliferation and death: forgotten features of chronic lymphocytic leukemia B cells. Best practice & research. *Clinical Haematology*. 2007;20(3):399–413.

6. Sieklucka M, Pozarowski P, Bojarska-Junak A, Hus I, Dmoszynska A, Rolinski J. Apoptosis in B-CLL: the relationship between higher ex vivo spontaneous apoptosis before treatment in III-IV Rai stage patients and poor outcome. *Oncology Reports*. 2008;19(6):1611–20.

7. Messmer BT, Messmer D, Allen SL, Kolitz JE, Kudalkar P et al. In vivo measurements document the dynamic cellular kinetics of chronic lymphocytic leukemia B cells. *J. Clin. Invest.* 2005;115:755–764.

8. Willimott S, Baou M, Huf S, Deaglio S, Wagner SD. Regulation of CD38 in proliferating chronic lymphocytic leukemia cells stimulated with CD154 and interleukin-4. *Haematologica*. 2007;92(10):1359–66.

9. Matutes E, Polliack A. Morphological and Immunophenotypic Features of Chronic Lymphocytic Leukemia. *Rev. Clin. Exp. Hematol*. 2000;4.1:22-47.

10. Kikushige Y, Ishikawa F, Miyamoto T, Shima T, Urata S et al. Self-renewing hematopoietic stem cell is the primary target in pathogenesis of human chronic lymphocytic leukemia. *Cancer Cell*. 2011;20(2):246–59.

11. Goldin LR, McMaster ML, Caporaso NE. Precursors to lymphoproliferative malignancies. *Cancer Epidemiol. Biomarkers Prev*. 2013;22(4):533–9.

12. Shanafelt TD, Geyer SM, Kay NE. Prognosis at diagnosis: integrating molecular biologic insights into clinical practice for patients with CLL. *Blood*. 2004;103(4):1202–10.

13. Döhner H, Stilgenbauer S, Benner A, Leupold E, Kröber A et al. Genomic aberrations and survival in chronic lymphocytic leukemia. *The New England Journal of Medicine*. 2000;343(26):1910–6

14. Bertilaccio MTS, Scielzo C, Muzio M, Caligaris-Cappio F. An overview of chronic lymphocytic leukaemia biology. *Clinical Haematology*. 2010;23(1):21–32.

15. Calin GA, Croce CM. Chronic lymphocytic leukemia: interplay between noncoding RNAs and protein-coding genes. *Blood*. 2009;114(23):4761–4770.

16. Calin GA, Dumitru CD, Shimizu M, Bichi R, Zupo S et al. Frequent deletions and down-regulation of micro- RNA genes miR-15 and miR-16 at 13q14 in chronic lymphocytic leukemia. *PNAS*. 2002;99(24):15524–9.

17. Fulci V, Chiaretti S, Goldoni M, Azzalin G, Carucci N et al. Quantitative technologies establish a novel microRNA profile of chronic lymphocytic leukemia. *Blood*. 2007;109(11):4944–51.

18. Srivastava S, Tsongalis GJ, Kaur P. Recent advances in microRNA-mediated gene regulation in chronic lymphocytic leukemia. *Clinical Biochemistry*. 2013;46(10-11):901–8.

19. Visone R, Veronese A, Rassenti LZ, Balatti V, Pearl DK et al. miR-181b is a biomarker of disease progression in chronic lymphocytic leukemia. *Blood*. 2011;118(11):3072–9.

20. Ferrajoli A, Shanafelt TD, Ivan C, Shimizu M, Rabe GK et al. Prognostic value of miR-155 in individuals with monoclonal B-cell lymphocytosis and patients with B-chronic lymphocytic leukemia. *Blood*. 2013; doi:10.1182/blood-2013-01-478222.

21. Dighiero G and Hamblin TJ. Chronic lymphocytic leukaemia. *Lancet*. 2008;371:1017–1029.

22. Ruchlemer R, Polliack A. Geography, ethnicity and “roots” in chronic lymphocytic leukemia. *Leukemia & Lymphoma*. 2013:1142–1150.

23. Watson L, Wyld P, Catovsky D. Disease burden of chronic lymphocytic leukaemia within the European Union. *European Journal of Haematology*. 2008;81(4):253–8.

24. Sellick GS, Catovsky D, Houlston RS. Familial chronic lymphocytic leukemia. *Seminars in oncology*. 2006;33(2):195–201.

25. Rebora P, Lee M, Czene K, Valsecchi MG, Reilly M. High risks of familial chronic lymphatic leukemia for specific relatives: signposts for genetic discovery? *Leukemia*. 2012;26(11):2419–21.

26. Shanshal M, Haddad RY. Chronic lymphocytic leukemia. *Dis. Mon*. 2012;58(4):153–67.

27. Agnew KL, Ruchlemer R, Catovsky D, Matutes E, Bunker CB. Cutaneous findings in chronic lymphocytic leukaemia. *The British Journal of Dermatology*. 2004;150(6):1129–35.

28. Hallek M, Cheson BD, Catovsky D, Caligaris-Cappio F, Dighiero G et al. Guidelines for the diagnosis and treatment of chronic lymphocytic leukemia: a report from the International Workshop on Chronic Lymphocytic Leukemia updating the National Cancer Institute-Working Group 1996 guidelines. *Blood*. 2008;111(12):5446–56.

29. Dighiero G. Unsolved issues in CLL biology and management. *Leukemia*. 2003;17(12):2385–91.

30. Hamblin TJ, Davis Z, Gardiner A, Oscier DG, Stevenson FK. Unmutated Ig V(H) genes are associated with a more aggressive form of chronic lymphocytic leukemia. *Blood*. 1999;94(6):1848–54.

31. Wiestner A, Rosenwald A, Barry TS, Wright G, Davis RE et al. ZAP-70 expression identifies a chronic lymphocytic leukemia subtype with unmutated immunoglobulin genes, inferior clinical outcome, and distinct gene expression profile. *Blood*. 2003;101(12):4944–51.

32. Crespo M, Bosch F, Villamor N, Bellosillo B, Colomer D et al. ZAP-70 expression as a surrogate for immunoglobulin-variable-region mutations in chronic lymphocytic leukemia. *The New England Journal of Medicine*. 2003;348(18):1764–75.

33. Ibrahim S, Keating M, Do K-A, O'Brien S, Huh YO et al. CD38 expression as an important prognostic factor in B-cell chronic lymphocytic leukemia. *Blood*. 2001;98(1):181–186.

34. Chen L, Widhopf G, Huynh L, Rassenti, L, Rai KR et al. Expression of ZAP-70 is associated with increased B-cell receptor signaling in chronic lymphocytic leukemia. *Blood*. 2002;100(13):4609–14.

35. Chan A, Iwashima M, Turck C, Weiss A. ZAP-70: a 70kd protein-tyrosine kinase that associates with the TCR ζ chain. *Cell*. 1992;71:649–62.

36. Smolej L, Vroblova V, Motyckova M, Jankovicova K, Schmitzova D et al. Quantification of ZAP-70 expression in chronic lymphocytic leukemia: T/B-cell ratio of mean fluorescence intensity provides stronger prognostic value than percentage. *Neoplasma*. 2011;58:140–145.

37. Rassenti LZ, Jain S, Keating MJ, Wierda GW, Grever MR et al. Relative value of ZAP-70, CD38, and immunoglobulin mutation status in predicting aggressive disease in chronic lymphocytic leukemia. *Blood*. 2008;112(5):1923–30.

38. Damle RN, Temburni S, Calissano C, Yancopoulos S, Banapou T et al. CD38 expression labels an activated subset within chronic lymphocytic leukemia clones enriched in proliferating B cells. *Blood*. 2007;110(9):3352–9.

39. Chiorazzi N. Implications of new prognostic markers in chronic lymphocytic leukemia. *Hematology Am. Soc. Hematol Educ. Program*. 2012;2012:76–87.

40. Schroers R, Griesinger F, Trümper L, Haase D, Kulle B et al. Combined analysis of ZAP-70 and CD38 expression as a predictor of disease progression in B-cell chronic lymphocytic leukemia. *Leukemia*. 2005;19(5):750–8.

41. Joshi AD, Dickinson JD, Hegde GV, Sanger WG, Armitage JO et al. Bulky lymphadenopathy with poor clinical outcome is associated with ATM downregulation in B-cell chronic lymphocytic leukemia patients irrespective of 11q23 deletion. *Cancer Genetics and Cytogenetics*. 2007;172(2):120–6.

42. Zenz T, Eichhorst B, Busch R, Denzel T, Häbe S et al. TP53 mutation and survival in chronic lymphocytic leukemia. *Journal of Clinical Oncology*. 2010;28(29):4473–9.

43. Binet JL, Auquier A, Dighiero G, Chastang C, Piguet H et al. A New Prognostic Classification of Chronic Lymphocytic Leukemia Derived from a Multivariate Survival Analysis. *Cancer*; 1981*;*48:198-206.

44. Rai KR, Sawitsky A, Cronkite EP, Chanana AD, Levy RN, Pasternack BS. Clinical staging of chronic lymphocytic leukemia. *Blood*. 1975;46(2):219–34.

45. Richter M. Generalized reticular cell sarcoma of lymph nodes associated with lymphatic leukemia. *The American Journal of Pathology*. 1928;IV(4).

46. Tsimberidou A-M, Keating MJ. Richter syndrome: biology, incidence, and therapeutic strategies. *Cancer*. 2005;103(2):216–28.

47. Rai KR, Peterson BL, Appelbaum F, Kolitz J, Elias L et al. Fludarabine compared with chlorambucil as primary therapy for chronic lymphocytic leukemia. *The New England Journal of Medicine*. 2000;343:1750-7.

48. Hallek M, Fischer K, Fingerle-Rowson G, Fink AM, Busch R et al. Addition of rituximab to fludarabine and cyclophosphamide in patients with chronic lymphocytic leukaemia: a randomised, open-label, phase 3 trial. *Lancet*. 2010;376(9747):1164–74.

49. Keating MJ, O'Brien S, Albitar M, Lerner S, Plunkett W et al. Early results of a chemoimmunotherapy regimen of fludarabine, cyclophosphamide, and rituximab as initial therapy for chronic lymphocytic leukemia. *Journal of Clinical Oncology*. 2005;23(18):4079–88.

50. Špaček M, Obrtlíková P, Trněný M. Chronická lymfocytární leukémie – patogeneze, diagnostika, principy terapie. *Postgraduální medicína*. 2013;15:504–510.

51. Laurenti L, Vannata B, Innocenti I, Autore F, Santini F et al. Chlorambucil plus Rituximab as Front-Line Therapy in Elderly/Unfit Patients Affected by B-Cell Chronic Lymphocytic Leukemia: Results of a Single-Centre Experience. *Mediterranean Journal of Hematology and Infectious Diseases*. 2013;5(1):e2013031.

52. Stevenson FK, Krysov S, Davies AJ, Steele AJ, Packham G. B-cell receptor signaling in chronic lymphocytic leukemia. *Blood*. 2011;118(16):4313–20.

53. Wiestner A. Emerging role of kinase-targeted strategies in chronic lymphocytic leukemia. *Hematology Am. Soc. Hematol. Educ. Program*. 2012;2012:88–96.

54. De Weerdt I, Eldering E, van Oers MH, Kater AP. The biological rationale and clinical efficacy of inhibition of signaling kinases in chronic lymphocytic leukemia. *Leukemia research*. 2013;37(7):838–47.

55. Herman SEM, Gordon AL, Hertlein E, Ramanunni A, Zhang X et al. Bruton tyrosine kinase represents a promising therapeutic target for treatment of chronic lymphocytic leukemia and is effectively targeted by PCI-32765. *Blood*. 2011;117(23):6287–96.

56. Advani RH, Buggy JJ, Sharman JP, Smith SM, Boyd TE et al. Bruton tyrosine kinase inhibitor ibrutinib (PCI-32765) has significant activity in patients with relapsed/refractory B-cell malignancies. *Journal of Clinical Oncology.* 2013;31(1):88–94.

57. Chao DT, Korsmeyer SJ. BCL-2 family: regulators of cell death. *Annual Review of Immunology*. 1998;16(1):395–419.

58. Souers AJ, Leverson JD, Boghaert ER, Ackler SL, Catron ND et al. ABT-199, a potent and selective BCL-2 inhibitor, achieves antitumor activity while sparing platelets. *Nature Medicine*. 2013;19(2):202–8.

59. Castelli R, Cassin R, Cannavò A, Cugno M. Immunomodulatory drugs: new options for the treatment of myelodysplastic syndromes. *Clinical lymphoma, myeloma & leukemia*. 2013;13(1):1–7.

60. Davies F, Baz R. Lenalidomide mode of action: linking bench and clinical findings. *Blood*. 2010;24 Suppl 1:S13–9.

61. Strati P, Keating MJ, Wierda WG, Badoux XC, Calin S et al. Lenalidomide induces long-lasting responses in elderly patients with chronic lymphocytic leukemia. *Blood*. 2013;122(5):734–7.

62. Lee RC, Feinbaum RL, Ambros V. The C. elegans heterochronic gene lin-4 encodes small RNAs with antisense complementarity to lin-14. *Cell*. 1993;75(5):843–54.

63. Pasquinelli AE, Reinhart BJ, Slack F, Martindale MQ, Kuroda MI et al. Conservation of the sequence and temporal expression of let-7 heterochronic regulatory RNA. *Nature*. 2000;408(6808):86–9.

64. Lagos-Quintana M, Rauhut R, Lendeckel W, Tuschl T. Identification of novel genes coding for small expressed RNAs. *Science*. 2001;294(5543):853–8.

65. Reinhart BJ, Slack FJ, Basson M, Pasquinelli AE, Bettinger JC et al. The 21-nucleotide let-7 RNA regulates developmental timing in Caenorhabditis elegans. *Nature*. 2000;403(6772):901–6.

66. Griffiths-Jones S, Saini HK, van Dongen S, Enright AJ. miRBase: tools for microRNA genomics. *Nucleic Acids Research*. 2008;36:D154–8.

67. Hsu PWC, Huang H-D, Hsu S-D, et al. miRNAMap: genomic maps of microRNA genes and their target genes in mammalian genomes. *Nucleic Acids Research*. 2006;34:D135–9.

68. Betel D, Wilson M, Gabow A, Marks DS, Sander C. The microRNA.org resource: targets and expression. *Nucleic Acids Research*. 2008;36:D149–53.

69. Maselli V, Di Bernardo D, Banfi S. CoGemiR: a comparative genomics microRNA database. *BMC Genomics*. 2008;9:457.

70. Alexiou P, Vergoulis T, Gleditzsch M, Prekas G, Dalamagas T et al. miRGen 2.0: a database of microRNA genomic information and regulation. *Nucleic Acids Research*. 2010;38:D137–41.

71. Yang J-H, Shao P, Zhou H, Chen Y-Q, Qu L-H. deepBase: a database for deeply annotating and mining deep sequencing data. *Nucleic Acids Research*. 2010;38:D123–30.

72. Lewis BP, Burge CB, Bartel DP. Conserved seed pairing, often flanked by adenosines, indicates that thousands of human genes are microRNA targets. *Cell*. 2005;120(1):15–20.

73. Krek A, Grün D, Poy MN, Wolf R, Rosenberg L et al. Combinatorial microRNA target predictions. *Nature Genetics*. 2005;37(5):495–500.

74. Sethupathy P, Megraw M, Hatzigeorgiou A. A guide through present computational approaches for the identification of mammalian microRNA targets. *Nature methods*. 2006;3(11):1–6.

75. Maragkakis M, Reczko M, Simossis V a, et al. DIANA-microT web server: elucidating microRNA functions through target prediction. *Nucleic Acids Research*. 2009;37:W273–6.

76. Xiao F, Zuo Z, Cai G, Kang S, Gao X, Li T. miRecords: an integrated resource for microRNA-target interactions. *Nucleic Acids Research*. 2009;37:D105–10.

77. Yang J-H, Li J-H, Shao P, Zhou H, Chen Y-Q, Qu L-H. StarBase: a database for exploring microRNA-mRNA interaction maps from Argonaute CLIP-Seq and Degradome-Seq data. *Nucleic acids research*. 2011;39:D202–9.

78. Kozomara A, Griffiths-Jones S. miRBase: integrating microRNA annotation and deep-sequencing data. *Nucleic Acids Research*. 2011;39:D152–7.

79. Lages E, Ipas H, Guttin A, Nesr H, Berger F, Issartel J-P. MicroRNAs: molecular features and role in cancer. *Frontiers in Bioscience*. 2012;17:2508–2540.

80. Griffiths-Jones S. The microRNA Registry. *Nucleic Acids Research*. 2004;32:D109–11.

81. Bartel DP. MicroRNAs: Genomics, Biogenesis, Mechanism, and Function. *Cell*. 2004;116(2):281–297.

82. Ørom UA, Nielsen FC, Lund AH. MicroRNA-10a binds the 5'UTR of ribosomal protein mRNAs and enhances their translation. *Molecular Cell*. 2008;30(4):460–71.

83. Lewis BP, Shih I, Jones-Rhoades MW, Bartel DP, Burge CB. Prediction of mammalian microRNA targets. *Cell*. 2003;115(7):787–98.

84. Rajewsky N. microRNA target predictions in animals. *Nature Genetics.* 2006;38 Suppl:S8–13.

85. Volinia S, Calin G a, Liu C-G, Ambs S, Cimmino A et al. A microRNA expression signature of human solid tumors defines cancer gene targets. *PNAS*. 2006;103(7):2257–61.

86. He L, Thomson JM, Hemann MT, Hernando-Monge E, Mu D et al. A microRNA polycistron as a potential human oncogene. *Nature*. 2005;435(7043):828–33.

87. Zhang L, Coukos G. MicroRNAs: a new insight into cancer genome. *Cell Cycle*. 2006;5(19):2216–2219.

88. Landais S, Landry S, Legault P, Rassart E. Oncogenic potential of the miR-106-363 cluster and its implication in human T-cell leukemia. *Cancer Research*. 2007;67(12):5699–707.

89. Bernstein E, Kim SY, Carmell MA, Murchison EP, Alcorn H et al. Dicer is essential for mouse development. *Nature Genetics.* 2003;35(3):215–7.

90. Calin GA, Liu C-G, Sevignani C, Ferracin M, Felli N et al. MicroRNA profiling reveals distinct signatures in B cell chronic lymphocytic leukemias. *PNAS*. 2004;101(32):11755–60.

91. Kim VN, Han J, Siomi MC. Biogenesis of small RNAs in animals. *Nature reviews*. 2009;10(2):126–39.

92. Lee Y, Kim M, Han J, Yeom K-H, Lee S et al. MicroRNA genes are transcribed by RNA polymerase II. *EMBO*. 2004;23(20):4051–60.

93. Borchert GM, Lanier W, Davidson BL. RNA polymerase III transcribes human microRNAs. *Nature structural & molecular biology*. 2006;13(12):1097–101.

94. Lund E, Güttinger S, Calado A, Dahlberg JE, Kutay U. Nuclear export of microRNA precursors. *Science* (New York, N.Y.). 2004;303(5654):95–8.

95. Tili E, Michaille J-J, Adair B, Alder H, Limaqne E et al. Resveratrol decreases the levels of miR-155 by upregulating miR-663, a microRNA targeting JunB and JunD. *Carcinogenesis*. 2010;31(9):1561–6.

96. Guil S, Cáceres JF. The multifunctional RNA-binding protein hnRNP A1 is required for processing of miR-18a. *Nature structural & molecular biology*. 2007;14(7):591–6.

97. Fukuda T, Yamagata K, Fujiyama S, Matsumoto T, Koshida I et al. DEAD-box RNA helicase subunits of the Drosha complex are required for processing of rRNA and a subset of microRNAs. *Nature Cell Biology*. 2007;9(5):604–11.

98. Han J, Lee Y, Yeom K-H, Nam J-W, Heo I et al. Molecular basis for the recognition of primary microRNAs by the Drosha-DGCR8 complex. *Cell*. 2006;125(5):887–901.

99. Berezikov E, Chung W, Willis J, Cuppen E, Lai EC. Mammalian Mirtron Genes Eugene. *Molecular and Cellular Biology.* 2009;28(2):328–336.

100. Zhou H, Huang X, Cui H, Luo X, Tang Y et al. miR-155 and its star-form partner miR-155* cooperatively regulate type I interferon production by human plasmacytoid dendritic cells. *Blood*. 2010;116(26):5885–94.

101. Bartel DP. MicroRNAs: target recognition and regulatory functions. *Cell*. 2009;136(2):215–33.

102. Breving K, Esquela-Kerscher A. The complexities of microRNA regulation: mirandering around the rules. *The International Journal of Biochemistry & Cell Biology*. 2010;42(8):1316–29.

103. Krol J, Loedige I, Filipowicz W. The widespread regulation of microRNA biogenesis, function and decay. *Nature reviews*. 2010;11(9):597–610.

104. Fabian MR, Sonenberg N, Filipowicz W. Regulation of mRNA translation and stability by microRNAs. *Annual Review of Biochemistry*. 2010;79:351–79.

105. Kulkarni M, Ozgur S, Stoecklin G. On track with P-bodies. *Biochem. Soc. Trans.* 2010;38:242–51.

106. Liu J, Valencia-sanchez MA, Hannon GJ, Parker R. MicroRNA-dependent localization of targeted mRNAs to mammalian P-bodies. *Nat. Cell Biol.* 2007;7(7):719–723.

107. Brengues M, Teixeira D, Parker R. Movement of eukaryotic mRNAs between polysomes and cytoplasmic processing bodies. *Science*. 2005;310(5747):486–9.

108. Iorio MV, Piovan C, Croce CM. Interplay between microRNAs and the epigenetic machinery: an intricate network. *Biochimica et biophysica acta*. 2011;1799(10-12):694–701.

109. Okamura K, Hagen JW, Duan H, Tyler DM, Lai EC. The mirtron pathway generates microRNA-class regulatory RNAs in Drosophila. *Cell*. 2007;130(1):89–100.

110. Kato M and Slack FJ. microRNAs: small molecules with big roles - C. elegans to human cancer. *Biol. Cell*. 2008;100(2):71–81.

111. Ozsolak F, Poling LL, Wang Z, Liu H, Liu XS et al. Chromatin structure analyses identify miRNA promoters. *Genes & Development*. 2008;22(22):3172–83.

112. O'Donnell KA, Wentzel EA, Zeller KI, Dang C V, Mendell JT. c-Myc-regulated microRNAs modulate E2F1 expression. *Nature*. 2005;435(7043):839–43.

113. Lujambio A and Manel E. CpG island hypermethylation of tumor suppressor microRNAs in human cancer. *Cell Cycle*. 2007;6:1455–1459.

114. Libri V, Miesen P, van Rij RP, Buck AH. Regulation of microRNA biogenesis and turnover by animals and their viruses. *Cell. Mol. Life Sci*. 2013. DOI 10.1007/s00018-012-1257-1.

115. Davis B, Hilyard A, Lagna G, Hata A. SMAD proteins control DROSHA-mediated microRNA maturation. *Nature*. 2008;454(7200):56–61.

116. Kawai S, Amano A. BRCA1 regulates microRNA biogenesis via the DROSHA microprocessor complex. *The Journal of Cell Biology*. 2012;197(2):201–8.

117. Zisoulis DG, Kai ZS, Chang RK, Pasquinelli AE. Autoregulation of microRNA biogenesis by let-7 and Argonaute. *Nature*. 2012;486(7404):541–4.

118. Barad O, Mann M, Chapnik E, et al. Efficiency and specificity in microRNA biogenesis. *Nature structural & molecular biology*. 2012;19(6):650–2.

119. Gruber JJ, Zatechka DS, Sabin LR, Yong J, Lum JJ et al. Ars2 links the nuclear cap-binding complex to RNA interference and cell proliferation. *Cell*. 2009;138(2):328–39.

120. Koscianska E, Starega-Roslan J, Krzyzosiak WJ. The role of Dicer protein partners in the processing of microRNA precursors. *PloS one*. 2011;6(12):e28548.

121. Bennasser Y, Chable-Bessia C, Triboulet R, Gibbins D, Gwizdek C et al. Competition for XPO5 binding between Dicer mRNA, pre-miRNA and viral RNA regulates human Dicer levels. *Nature Structural & Molecular Biology*. 2011;18(3):323–7.

122. Iizasa H, Wulff B-E, Alla NR, Mragkakis M, Megraw M et al. Editing of Epstein-Barr virus-encoded BART6 microRNAs controls their dicer targeting and consequently affects viral latency. *The Journal of Biological Chemistry*. 2010;285(43):33358–70.

123. Maas S, Kawahara Y, Tamburro KM, Nishikura K. A-to-I RNA Editing and Human Disease. RNA Biology. 2006;3:1–9.

124. Iwai N, Naraba H. Polymorphisms in human pre-miRNAs. Biochemical and biophysical research communications. 2005;331(4):1439–44.

125. Sun G, Yan J, Noltner K, Feng J, Li H et al. SNPs in human miRNA genes affect biogenesis and function. *RNA*. 2009;15(9):1640–51.

126. Calin GA, Ferracin M, Cimmino A, Di Leva G, Shimizu M et al. A MicroRNA signature associated with prognosis and progression in chronic lymphocytic leukemia. *The New England Journal of Medicine*. 2005;353(17):1793–801.

127. Klein U, Lia M, Crespo M, Siegel R, Shen Q et al. The DLEU2/miR-15a/16-1 cluster controls B cell proliferation and its deletion leads to chronic lymphocytic leukemia. *Cancer Cell*. 2010;17(1):28–40.

128. Migliazza A, Bosch F, Komatsu H, Cayanis E, Martinotti S et al. Nucleotide sequence, transcription map, and mutation analysis of the 13q14 chromosomal region deleted in B-cell chronic lymphocytic leukemia. *Blood*. 2001;97(7):2098–2104.

129. Pfeifer D, Pantic M, Skatulla I, Rawluk J, Kreutz C et al. Genome-wide analysis of DNA copy number changes and LOH in CLL using high-density SNP arrays. *Blood*. 2007;109(3):1202–10.

130. Cimmino A, Calin GA, Fabbri M, Iorio MV, Ferracin M et al. miR-15 and miR-16 induce apoptosis by targeting BCL2. *PNAS*. 2005;102(39):13944–9.

131. Masood A, Chitta K, Paulus A, Khan NH, Sher T et al. Downregulation of BCL2 by AT-101 enhances the antileukaemic effect of lenalidomide both by an immune dependant and independent manner. *British Journal of Haematology*. 2012;157(1):59–66.

132. Zanette DL, Rivadavia F, Molfetta GA, Barbuzzano FG, Proto-Siqueira R et al. miRNA expression profiles in chronic lymphocytic and acute lymphocytic leukemia. *Brazilian Journal of Medical and Biological Research.* 2007;40(11):1435–40.

133. Asslaber D, Piñón JD, Seyfried I, Desch P, Stöcher M et al. microRNA-34a expression correlates with MDM2 SNP309 polymorphism and treatment-free survival in chronic lymphocytic leukemia. *Blood.* 2010;115(21):4191–7.

134. Fabbri M, Bottoni A, Shimizu M, Spizzo R, Nicoloso MS et al. Association of a microRNA/TP53 feedback circuitry with pathogenesis and outcome of B-cell chronic lymphocytic leukemia. *JAMA*. 2011;305(1):59–67.

135. Zenz T, Häbe S, Denzel T, Mohr J, Winkler D et al. Detailed analysis of p53 pathway defects in fludarabine-refractory chronic lymphocytic leukemia (CLL): dissecting the contribution of 17p deletion, TP53 mutation, p53-p21 dysfunction, and miR34a in a prospective clinical trial. *Blood*. 2009;114(13):2589–97.

136. Rossi S, Shimizu M, Barbarotto E, Nicoloso MS, Dimitri F et al. microRNA fingerprinting of CLL patients with chromosome 17p deletion identify a miR-21 score that stratifies early survival. *Blood*. 2010;116(6):945–52.

137. Wang M, Tan LP, Dijkstra MK, van Lom K, Robertus JL et al. miRNA analysis in B-cell chronic lymphocytic leukaemia:proliferation centres characterized by low miR-150 and high BIC/miR-155 expression. *Journal of Pathology*. 2008;215:13–20.

138. Zhu D-X, Zhu W, Fang Ch, Fan L, Zou Z-J et al. miR-181a/b significantly enhances drug sensitivity in chronic lymphocytic leukemia cells via targeting multiple anti-apoptosis genes. *Carcinogenesis*. 2012;33(7):1294–301.

139. Ventura A, Young AG, Winslow MM, Lintault L, Meissner A et al. Targeted deletion reveals essential and overlapping functions of the miR-17 through 92 family of miRNA clusters. *Cell*. 2008;132(5):875–86.

140. Xiao C, Srinivasan L, Calado DP, Patterson HCh, Zhang B et al. Lymphoproliferative disease and autoimmunity in mice with increased miR-17-92 expression in lymphocytes. *Nature Immunology*. 2008;9(4):405–14.

141. Van den Berg A, Kroesen B-J, Kooistra K, de Jong D, Briggs J et al. High expression of B-cell receptor inducible gene BIC in all subtypes of Hodgkin lymphoma. *Genes, Chromosomes & Cancer*. 2003;37(1):20–8.

142. Gibcus JH, Tan LP, Harms G, Schakel RN, de Jong D et al. Hodgkin Lymphoma Cell Lines Are Characterized by a Specific. *Neoplasia*. 2009;11(2):167–176.

143. Marton S, Garcia MR, Robello C, Persson H, Trajtenberg F et al. Small RNAs analysis in CLL reveals a deregulation of miRNA expression and novel miRNA candidates of putative relevance in CLL pathogenesis. *Leukemia.* 2008;22(2):330–8.

144. Vargova K, Curik N, Burda P, Basova P, Kulvait V et al. MYB transcriptionally regulates the miR-155 host gene in chronic lymphocytic leukemia. *Blood.* 2011;117(14):3816–25.

145. Calin GA, Ferracin M, Cimmino A, di Leva G, Shimizu M et al. A MicroRNA signature associated with prognosis and progression in chronic lymphocytic leukemia. *The New England Journal of Medicine*. 2005;353(17):1793–801.

146. Zhong H, Xu L, Zhong J-H, Fei X, Liu Q et al. Clinical and prognostic significance of miR-155 and miR-146a expression levels in formalin-fixed/paraffin-embedded tissue of patients

with diffuse large B-cell lymphoma. *Experimental and therapeutic medicine*. 2012;3(5):763–770.

147. Tam W, Ben-Yehuda D, Hayward WS. bic , a novel gene activated by proviral insertions in avian leukosis virus-induced lymphomas, is likely to function through its noncoding RNA. *Molecular and cellular biology*. 1997;17:1490.

148. Tam W. Identification and characterization of human BIC, a gene on chromosome 21 that encodes a noncoding RNA. *Gene*. 2001;274(1-2):157–67.

149. Eis PS, Tam W, Sun L, Chadburn A, Li Z et al. Accumulation of miR-155 and BIC RNA in human B cell lymphomas. *PNAS*. 2005;102(10):3627–32.

150. Faraoni I, Antonetti FR, Cardone J, Bonmassar E. miR-155 gene: a typical multifunctional microRNA. *Biochimica et biophysica acta*. 2009;1792(6):497–505.

151. Elton TS, Selemon H, Elton SM, Parinandi NL. Regulation of the MIR155 host gene in physiological and pathological processes. *Gene*. 2012; S0378-1119(12)01512-0. doi: 10.1016/j.gene.2012.12.009. [Epub ahead of print].

152. Georgantas III RW, Hildreth R, Morisot S, Alder J, Liu Ch-G et al. CD34+ hematopoietic stem-progenitor cell microRNA expression and function: a circuit diagram of differentiation control. *PNAS*. 2007;104(8):2750-2755.

153. Ramkissoon S, Mainwaring L, Oquasawara Y, Keyvanfar K, McCoy JP et al. Hematopoietic-specific microRNA expression in human cells. *Leukemia research*. 2006;30(5):643-7.

154. Fernando TR, Rodriguez-Malave NI, Rao DS. MicroRNAs in B cell development and malignancy. *Journal of Hematology & Oncology*. 2012;5(1):1-10.

155. Calame K. MicroRNA-155 function in B Cells. *Immunity*. 2007;27(6):825–7.

156. O'Connell RM, Rao DS, Chaudhuri AA, Boldin MP, Taganov TK et al. Sustained expression of microRNA-155 in hematopoietic stem cells causes a myeloproliferative disorder. *The Journal of Experimental Medicine*. 2008;205(3):585–94.

157. Vigorito E, Perks KL, Abreu-Goodger C, Bunting S, Xiang Z et al. microRNA-155 regulates the generation of immunoglobulin class-switched plasma cells. *Immunity*. 2007;27(6):847–59.

158. Vigorito E, Kohlhaas S, Lu D, Leyland R. miR-155: an ancient regulator of the immune system. *Immunological reviews*. 2013;253(1):146–57.

159. Ma X, Ma C, Zheng X. MicroRNA-155 in the Pathogenesis of Atherosclerosis: A Conflicting Role? *Heart, lung & circulation*. 2013. S1443-9506(13)01029-9. doi: 10.1016/j.hlc.2013.05.651. [Epub ahead of print].

160. Trotta R, Chen L, Ciarlariello D, Josyula S, Mao Ch et al. miR-155 regulates IFN-γ production in natural killer cells. *Blood*. 2012;119(15):3478–85.

161. Huang R, Hu G, Lin B, Lin Z, Sun C. MicroRNA-155 silencing enhances inflammatory response and lipid uptake in oxidized low-density lipoprotein-stimulated human THP-1 macrophages. *J. Invest. Med.* 2010;58(8):961–7.

162. Leng R-X, Pan H-F, Qin W-Z, Chen G-M, Ye D-Q. Role of microRNA-155 in autoimmunity. *Cytokine & growth factor reviews*. 2011;22(3):141–7.

163. Zhu G-F, Yang L-X, Guo R-W, Liu H, Shi Y-K et al. miR-155 inhibits oxidized low-density lipoprotein-induced apoptosis of RAW264.7 cells. *Mol. Cell. biochem*. 2013. DOI:1007/s11010-013-1741-4.

164. Haasch D, Chen Y-W, Reilly RM, Chiou GX, Koterski S et al. T cell activation induces a noncoding RNA transcript sensitive to inhibition by immunosuppressant drugs and encoded by the proto-oncogene, BIC. *Cellular Immunology*. 2002;217(1-2):78–86.

165. Corsten MF, Papageorgiou A, Verhesen W, Carai P, Lindou M et al. MicroRNA profiling identifies microRNA-155 as an adverse mediator of cardiac injury and dysfunction during acute viral myocarditis. *Circulation research*. 2012;111(4):415–25.

166. Dudda JC, Salaun B, Ji Y, Palmer DC, Monnot GC et al. MicroRNA-155 is required for effector CD8+ T cell responses to virus infection and cancer. *Immunity*. 2013;38(4):742–53.

167. Kong W, Yang H, He L, Zhao JJ, Coppola D et al. MicroRNA-155 is regulated by the transforming growth factor beta/Smad pathway and contributes to epithelial cell plasticity by targeting RhoA. *Mol. Cell. Biol*. 2008;28(22):6773–84.

168. Chang S, Sharan SK. Epigenetic control of an oncogenic microRNA, miR-155, by BRCA1. *Oncotarget*. 2012;3(1):5–8.

169. Wang X, Tang S, Le S-Y, Lu R, Zheng Z-M et al. Aberrant expression of oncogenic and tumor-suppressive microRNAs in cervical cancer is required for cancer cell growth. *PloS one*. 2008;3(7):e2557.

170. Zhu Y-D, Wang L, Sun C, Fun L, Zhu DX et al. Distinctive microRNA signature is associated with the diagnosis and prognosis of acute leukemia. *Medical Oncology*. 2012;29(4):2323–31.

171. Canale S, Cocco C, Frasson C, Seganfreddo E, di Carlo E et al. Interleukin-27 inhibits pediatric B-acute lymphoblastic leukemia cell spreading in a preclinical model. *Leukemia*. 2011;25(12):1815–24.

172. Metzler M, Wilda M, Busch K, Viehmann S, Borkhardt A. High expression of precursor microRNA-155/BIC RNA in children with Burkitt lymphoma. *Genes, Chromosomes and Cancer.* 2004;39(2):167–169.

173. Kluiver J, Poppema S, de Jong D, Blokzjil T, Harms G et al. BIC and miR-155 are highly expressed in Hodgkin, primary mediastinal and diffuse large B cell lymphomas. *The Journal of Pathology*. 2005;207(2):243–9.

174. Li S, Moffett HF, Lu J, Werner L, Zhang H et al. MicroRNA expression profiling identifies activated B cell status in chronic lymphocytic leukemia cells. *PloS one*. 2011;6(3):e16956.

175. Fabbri M, Croce CM. Role of microRNAs in lymphoid biology and disease. *Current opinion in hematology*. 2011;18(4):266–72.

176. Thai T-H, Calado DP, Casola S, Ansel KM, Xiao Ch et al. Regulation of the germinal center response by microRNA-155. *Science*. 2007;316(5824):604–8.

177. Teng G, Hakimpour P, Landgraf P, Rice A, Tuschl T et al. MicroRNA-155 is a negative regulator of activation-induced cytidine deaminase. *Immunity.* 2008;28(5):621–629.

178. O'Connell RM, Zhao JL, Rao DS. MicroRNA function in myeloid biology. *Blood*. 2011; 118(11):2960-9.

179. Helgason CD, Kalberer CP, Damen JE, Chappel SM, Pineault N et al. A dual role for Src homology 2 domain-containing inositol-5-phosphatase (SHIP) in immunity: aberrant development and enhanced function of b lymphocytes in ship -/- mice. *The Journal of Experimental Medicine*. 2000;191(5):781–94.

180. Yin Q, Wang X, McBride J, Fewell C, Flemington E. B-cell receptor activation induces BIC/miR-155 expression through a conserved AP-1 element. T*he Journal of biological chemistry*. 2007;283(5):2654–62.

181. Mraz M, Kipps TJ. MicroRNAs and B cell receptor signaling in chronic lymphocytic leukemia. *Leukemia & lymphoma*. 2013;54(8):1836–9.

182. Costinean S, Zanesi N, Pekarsky Y, et al. Pre-B cell proliferation and lymphoblastic leukemia/high-grade lymphoma in E(mu)-miR155 transgenic mice. *PNAS*. 2006;103(18):7024–9.

183. Rodriguez A, Vigorito E, Clare S, Warren MV, Couttet P et al. Requirement of bic/microRNA-155 for normal immune function. *Science*. 2007; 316(5824): 608–611.

184. Babar IA, Cheng CJ, Booth CJ, Liang X, Weidhaas JB et al. Nanoparticle-based therapy in an in vivo microRNA-155 (miR-155)-dependent mouse model of lymphoma. *PNAS*. 2012;109(26):E1695–704.

185. O'Connell RM, Taganov KD, Boldin MP, Cheng G, Baltimore D. MicroRNA-155 is induced during the macrophage inflammatory response. *PNAS*. 2007;104(5):1604–9.

186. Tili E, Michaille J-J, Cimino A, Costinean S, Dumitru CD et al. Modulation of miR-155 and miR-125b levels following lipopolysaccharide/TNF-alpha stimulation and their possible roles in regulating the response to endotoxin shock. *Journal of Immunology*. 2007;179(8):5082–9.

187. Yin Q, McBride J, Fewell C, Lacey M, Wang X et al. MicroRNA-155 is an Epstein-Barr virus-induced gene that modulates Epstein-Barr virus-regulated gene expression pathways. *Journal of Virology*. 2008;82(11):5295–306.

188. Zuo T, Wang L, Morrison C, Chang X, Zhang H et al. FOXP3 Is an X-Linked Breast Cancer Suppressor Gene and an Important Repressor of the HER-2/ErbB2 Oncogene. *Cell*. 2007;129(7):1275–1286.

189. McInnes N, Sadlon TJ, Brown CY, Pederson S, Beyer M et al. FOXP3 and FOXP3-regulated microRNAs suppress SATB1 in breast cancer cells. *Oncogene*. 2012;31(8):1045–54.

190. Li P, Grgurevic S, Liu Z, Harris D, Rozovski U et al. Signal transducer and activator of transcription-3 induces MicroRNA-155 expression in chronic lymphocytic leukemia. *PloS one*. 2013;8(6):e64678. doi: 10.1371/journal.pone.0064678.

191. Gatto G, Rossi A, Rossi D, Kroening S, Bonatti S, Mallardo M. Epstein-Barr virus latent membrane protein 1 trans-activates miR-155 transcription through the NF-kappaB pathway. *Nucleic Acids Research*. 2008;36(20):6608–19.

192. Linnstaedt SD, Gottwein E, Skalsky RL, Luftig MA CB. Virally induced cellular miR-155 plays a key role in B cell immortalization by EBV. *Journal of Virology*. 2010:11670–8.

193. Gottwein E, Mukherjee N, Sachse C, et al. A viral microRNA functions as an ortholog of cellular miR-155. *Nature*. 2009;450(7172):1096–1099.

194. Skalsky RL, Samols M a, Plaisance KB, Boss IW, Riva A et al. Kaposi's sarcoma-associated herpesvirus encodes an ortholog of miR-155. *Journal of Virology*. 2007;81(23):12836–45.

195. Moreau-Gachelin F, Tavitian A, Tambourin P. PU.1 is aputative oncogene in virally induced murine erytroleukemias. *Nature*. 1988;331:277–280.

196. Klemsz MJ, McKercher SR, Celada A, Van Beveren C, Maki RA. The macrophage and B cell-specific transcription factor PU.1 is related to the ets oncogene. *Cell*. 1990;61(1):113–24.

197. Oikawa T, Yamada T, Kihara-Negishi F,Yamamoto H, Kondoh N et al. The role of Ets family transcription factor PU.1 in hematopoietic cell differentiation, proliferation and apoptosis. *Cell Death and Differentiation.* 1999;6(7):599–608.

198. Scott E, Simon MC, Singh H. Requirement of transcription factor PU. 1 in the development of multiple hematopoietic lineages. *Science*. 1994;265(5178):1573–1577.

199. DeKoter RP, Kamath MB, Houston IB. Analysis of concentration-dependent functions of PU.1 in hematopoiesis using mouse models. *Blood cells, molecules & diseases*. 2007;39(3):316–20.

200. Singh H, Pongubala JMR, Medina KL. Gene Regulatory Networks that Orchestrate the Development of B Lymphocyte. Mechanisms of Lymphocyte Activation and Immune Regulation XI (Gupta S, Alt F, Cooper M, Melchers F, Rajewsky K, eds.). Boston, MA: Springer US; 2007:57.

201. Rosenbauer F, Wagner K, Kutok JL, Iwasaki H, Le Beau MM et al. Acute myeloid leukemia induced by graded reduction of a lineage-specific transcription factor, PU.1. *Nature Genetics*. 2004;36(6):624–30.

202. Cook W, McCaw B, Herring C, John DL, Foote SJ et al. PU. 1 is a suppressor of myeloid leukemia, inactivated in mice by gene deletion and mutation of its DNA binding domain. *Blood*. 2004;104:3437–3444.

203. Koschmieder S, Rosenbauer F, Steidl U, Owens BM, Tenen DG. Role of transcription factors C/EBPα and PU. 1 in normal hematopoiesis and leukemia. *Int. J. Hematol*. 2005;81(5):368–377.

204. Tatetsu H, Ueno S, Hata H, Yamada Y, Takeya M et al. Down-regulation of PU.1 by methylation of distal regulatory elements and the promoter is required for myeloma cell growth. *Cancer Research*. 2007;67(11):5328–36.

205. Vlckova P, Pospisil V, Stanek L, Burda P, Savvulidi F et al. Aggressive acute myeloid leukaemia in PU.1/p53 double mutant mice. *Oncogene*. 2013 (*submitted*).

206. Roussel M, Saule S, Laqrou C, Rommens C, Beuq H et al. Three new types of viral oncogene of cellular origin specific for hematopoietic cell transformation. *Nature*. 1979;281:452–455.

207. Oh IH, Reddy EP. The myb gene family in cell growth, differentiation and apoptosis. *Oncogene*. 1999;18(19):3017–33.

208. Pattabiraman DR, Gonda TJ. Role and potential for therapeutic targeting of MYB in leukemia. *Leukemia*. 2013;27(2):269–77.

209. Biedenkapp H, Borgmeyer U, Sippel A, Klempnauer KH. Viral myb oncogene encodes a sequence-specific DNA-binding activity. *Nature*. 1988;335(27):835–837.

210. O'Rourke JP, Ness SA. Alternative RNA splicing produces multiple forms of c-Myb with unique transcriptional activities. *Molecular and Cellular Biology*. 2008;28(6):2091–101.

211. Nakata Y, Shetzline S, Sakashita C, Kalota A, Rallapalli R et al. c-Myb contributes to G2/M cell cycle transition in human hematopoietic cells by direct regulation of cyclin B1 expression. *Molecular and Cellular Biology*. 2007;27(6):2048–58.

212. Ramsay RG, Gonda TJ. MYB function in normal and cancer cells. *Nature reviews*. 2008;8(7):523–34.

213. Greig KT, Carotta S, Nutt SL. Critical roles for c-Myb in hematopoietic progenitor cells. *Seminars in immunology*. 2008;20(4):247–56.

214. Fahl SP, Crittenden RB, Allman D, Bender TP. c-Myb is required for pro-B cell differentiation. *Journal of Immunology*. 2009;183(9):5582–92.

215. Thomas MD, Kremer CS, Ravichandran KS, Rajewsky K, Bender TP. c-Myb is critical for B cell development and maintenance of follicular B cells. *Immunity*. 2005;23(3):275–86.

216. Carvalho TL, Mota-Santos T, Cumano A, Demengeot J, Vieira P. Arrested B lymphopoiesis and persistence of activated B cells in adult interleukin 7(-/)- mice. *The Journal of Experimental Medicine*. 2001;194(8):1141–50.

217. Ferrari S, Torelli U, Serelli L, Donelli A, Wenturelli D et al. Study of the levels of expression of two in acute and chronic leukemias of both lymphoid and lineage. *Leukemia research*. 1985;9(7):833–842.

218. Rosson D, Tereba A. Transcription of Hematopoietic-associated Oncogenes in Childhood Leukemia. *Cancer research*. 1983;43:3912–3918.

219. Sarvaiya PJ, Schwartz JR, Hernandez CP, Rodriguez PC, Vedeckis W V. Role of c-Myb in the survival of pre B-cell acute lymphoblastic leukemia and leukemogenesis. *American Journal of Hematology.* 2012;87(10):969–76.

220. Clappier E, Cuccuini W, Kalota A, Crinquette A, Cayuela JM et al. The C-MYB locus is involved in chromosomal translocation and genomic duplications in human T-cell acute leukemia (T-ALL), the translocation defining a new T-ALL subtype in very young children. *Blood*. 2007;110(4):1251–61.

221. Lahortiga I, De Keersmaecker K, Van Vlierberghe P, Graux C, Cauwelier B et al. Duplication of the MYB oncogene in T cell acute lymphoblastic leukemia. *Nature Genetics*. 2007;39(5):593–5.

222. Lidonnici MR, Corradini F, Waldron T, Bender TP, Calabretta B. Requirement of c-Myb for p210(BCR/ABL)-dependent transformation of hematopoietic progenitors and leukemogenesis. *Blood*. 2008;111(9):4771–9.

223. Machová-Poláková K, Lopotová T, Klamová H, Burda P, Trnený M et al. Expression patterns of microRNAs associated with CML phases and their disease related targets. *Molecular Cancer Research*. 2011;10:41.

224. Mucenski ML, McLain K, Kier AB, Swerdlow SH, Schreiner CM et al. A functional c-myb gene is required for normal murine fetal hepatic hematopoiesis. *Cell*. 1991;65(4):677–89.

225. Greig KT, de Graaf CA, Murphy JM, Carpinelli MR, Pang SHM et al. Critical roles for c-Myb in lymphoid priming and early B-cell development. *Blood*. 2010;115(14):2796.

226. Waldron T, De Dominici M, Soliera AR, Audia A, Iacobucci I et al. c-Myb and its target Bmi1 are required for p190BCR/ABL leukemogenesis in mouse and human cells. *Leukemia*. 2012;26(4):644–53.

227. Monticelli S, Ansel KM, Xiao C, Socci ND, Krichevski AM et al. MicroRNA profiling of the murine hematopoietic system. *Genome Biology*. 2005;6(8):R71.

228. Xiao C, Calado DP, Galler G, Thai T-H, Patterson HCh et al. MiR-150 controls B cell differentiation by targeting the transcription factor c-Myb. *Cell*. 2007;131(1):146–59.

229. Chen S, Wang Z, Dai X, Pan J, Ge J et al. Re-expression of microRNA-150 induces EBV-positive Burkitt lymphoma differentiation by modulating c-Myb in vitro. *Cancer Science*. 2013;104(7):826–34.

230. Lin Y-C, Kuo M-W, Yu J, Kuo H-H, Lin R-J et al. c-Myb is an evolutionary conserved miR-150 target and miR-150/c-Myb interaction is important for embryonic development. *Molecular Biology and Evolution*. 2008;25(10):2189–98.

231. Kastner P, Chan S. PU.1: a crucial and versatile player in hematopoiesis and leukemia. *The International Journal of Biochemistry & Cell Biology*. 2008;40(1):22–7.

232. Qiu C, Wang J, Yao P, Wang E, Cui Q. microRNA evolution in a human transcription factor and microRNA regulatory network. *BMC systems biology*. 2010;4:90.

233. Chen J, Wang B-C, Tang J-H. Clinical significance of microRNA-155 expression in human breast cancer. *Journal of Surgical Oncology*. 2012;106(3):260–6.

234. Emambokus N, Vegiopoulos A, Harman B, Jenkinson E, Anderson G, Frampton J. Progression through key stages of haemopoiesis is dependent on distinct threshold levels of c-Myb. *EMBO*. 2003;22(17):4478–88.

235. Westin E, Gallo R, Arya S, Eva A, Souza LM et al. Differential expression of the amv gene in human hematopoietic cells. *Proc. Nati Acad. Sci*. 1982;79:2194–2198.

236. Jin S, Zhao H, Yi Y, Nakata Y, Kalota A, Gewirtz AM. c-Myb binds MLL through menin in human leukemia cells and is an important driver of MLL-associated leukemogenesis. *J. Clin. Invest*. 2010;120(2):593-606.

237. Pulvertaft R. Cytology of Burkitt's tumour (African lymphoma). *Lancet*. 1964:238–40.

238. Scherer WF, Syverton JT, Gey GO. Studies on the propagation in vitro of poliomyelitis viruses. *J. Exp. Med.* 1953;97(5):695-710.

239. Drexler H, Quentmeier H, MacLeod R, Uphoff CC, Hu ZB. Leukemia cell lines: In vitro models for the study of acute promyelocytic leukemia. *Leukemia research*. 1995; (10):681-91.

240. Rekhtman N, Choe K, Matushansky I, Murray S, Stopka T, Skoultchi AI. PU. 1 and pRB interact and cooperate to repress GATA-1 and block erythroid differentiation. *Molecular and Cellular Biology*. 2003;23(21):7460–7474.

241. Stopka T, Amanatullah DF, Papetti M, Skoultchi AI. PU.1 inhibits the erythroid program by binding to GATA-1 on DNA and creating a repressive chromatin structure. *EMBO*. 2005;24(21):3712–23.

242. Saeed A, Sharov V, White J, Li J, Liang W et al. TM4: a free, open-source system for microarray data management and analysis. *Biotechniques.* 2003;34(2):374–8.

243. Subramanian A, Tamayo P, Mootha VK, Mukherjee S, Ebert BL et al. Gene set enrichment analysis: a knowledge-based approach for interpreting genome-wide expression profiles. *PNAS*. 2005;102(43):15545–50.

244. Ge T, Liang Y, Fu R, Wang G, Ruan EB et al. Expressions of miR-21, miR-155 and miR-210 in plasma of patients with lymphoma and its clinical significance. *Zhongguo Shi Yan Xue Ye Xue Za Zhi*. 2012;2:305–9.

245. Pesta M, Vargova K, Vargova J, Dusilkova N, Kulvait V et al. Model to understand clinical relevance of prognostics of CLL in real time. *Blood*. 2013 (*in prep.*).

246. Hamblin TJ, Davis Z, Gardiner A, Oscier DG, Stevenson FK. Unmutated Ig V(H) genes are associated with a more aggressive form of chronic lymphocytic leukemia. *Blood*. 1999;94(6):1848–54.

247. Rosenbauer F, Owens BM, Yu L, Tumang JR, Steidl U et al. Lymphoid cell growth and transformation are suppressed by a key regulatory element of the gene encoding PU.1. *Nature Genetics*. 2006;38(1):27–37.

248. Mankaï A, Buhé V, Hammadi M, Youinou P, Ghedira I et al. Improvement of rituximab efficiency in chronic lymphocytic leukemia by CpG-mediated upregulation of CD20 expression independently of PU.1. *Annals of the New York Academy of Sciences*. 2009;1173:721–8.

249. Ghani S, Riemke P, Schönheit J, Lenze D, Stumm J et al. Macrophage development from HSCs requires PU.1-coordinated microRNA expression. *Blood*. 2011;118(8):2275–84.

250. O'Neil J, Look A. Mechanisms of transcription factor deregulation in lymphoid cell transformation. *Oncogene*. 2007;26(47):6838–49.

251. Tam W, Hughes SH, Hayward WS, Besmer P. Avian bic , a Gene Isolated from a Common Retroviral Site in Avian Leukosis Virus-Induced Lymphomas That Encodes a Noncoding RNA, Cooperates with c-myc in Lymphomagenesis and Erythroleukemogenesis. *Journal of Virology*. 2002;76(9):4275–4286.

252. Neiman PE, Elsaesser K, Loring G, Kimmel R. Myc oncogene-induced genomic instability: DNA palindromes in bursal lymphomagenesis. *PLoS Genetics*. 2008;4(7):e1000132.

253. Mo X, Kowenz-Leutz E, Laumonnier Y, Xu H, Leutz A. Histone H3 tail positioning and acetylation by the c-Myb but not the v-Myb DNA-binding SANT domain. *Genes Dev*. 2005;19(20):2447–57.

254. Toth CR, Hostutler RF, Baldwin AS, Bender TP. Members of the nuclear factor kappa B family transactivate the murine c-myb gene. *J. Biol. Chem.* 1995;270(13):7661-71.

255. Golay J, Capucci A, Arsura M, Castellano M, Rizzo V, Introna M. Expression of c-myb and B-myb, but not A-myb, correlates with proliferation in human hematopoietic cells. *Blood.* 1991;77(1):149–58.

256. Golay J, Loffarelli L, Luppi M, Castellano M, Introna M. The human A-myb protein is a strong activator of transcription. *Oncogene*. 1994;9:2469-79.

257. Malavasi F, Deaglio S, Damle R, Cutrona G, Ferrarini M, Chiorazzi N. CD38 and chronic lymphocytic leukemia: a decade later. *Blood*. 2011;118(13):3470–8.

258. Moussay E, Wang K, Cho J-H, van Moer K, Pierson S et al. MicroRNA as biomarkers and regulators in B-cell chronic lymphocytic leukemia. *PNAS*. 2011;108(16):6573–8.

259. Hussein K, Theophile K, Büsche G, Schlegelberger B, Göhring G et al. Significant inverse correlation of microRNA-150/MYB and microRNA-222/p27 in myelodysplastic syndrome. *Leukemia research*. 2010;34(3):328–34.

260. Iwasaki H, Somoza C, Shigematsu H, Duprez EA, Iwasaki-Arai J et al. Distinctive and indispensable roles of PU.1 in maintenance of hematopoietic stem cells and their differentiation. *Blood*. 2005;106(5):1590–600.

261. Okuno Y, Huang G, Rosenbauer F, et al. Potential autoregulation of transcription factor PU. 1 by an upstream regulatory element. *Molecular and Cellular Biology*. 2005;25(7):2832–2845.

262. Yuki H, Ueno S, Tatetsu H, Niiro H, Iino T et al. PU.1 is a potent tumor suppressor in classical Hodgkin lymphoma cells. *Blood*. 2013;121(6):962–70.

263. Ghosh AK, Secreto CR, Knox TR, Ding W, Mukhopadhyay D, Kay NE. Circulating microvesicles in B-cell chronic lymphocytic leukemia can stimulate marrow stromal cells: implications for disease progression. *Blood*. 2010;115(9):1755–64.

264. Kosaka N, Ochiya T. Unraveling the Mystery of Cancer by Secretory microRNA: Horizontal microRNA Transfer between Living Cells. *Frontiers in Genetics*. 2011;2:97.

265. Zhang Y, Liu D, Chen X, et al. Secreted monocytic miR-150 enhances targeted endothelial cell migration. Molecular cell. 2010;39(1):133–44.

266. Pegtel DM, Cosmopoulos K, Thorley-Lawson DA, van Eijndhoven MA, Hopmans ES et al. Functional delivery of viral miRNAs via exosomes. *PNAS*. 2010;107(14):6328–33.

267. Hegde SP, Kumar A, Kurschner C, Shapiro L. c-Maf Interacts with c-Myb To Regulate Transcription of an Early Myeloid Gene during Differentiation c-Maf Interacts with c-Myb To Regulate Transcription of an Early Myeloid Gene during Differentiation. *Molecular and Cellular Biology*. 1998;18(5): 2729–2737.

268. Fan LP and Shen JZ. Expression of Maf-b mRNA in de novo leukemia patients and its clinical significance. *Zhongguo Shi Yan Xue Ye Xue Za Zhi.* 2010;18:1147–50.

269. Zhang Y, Roccaro AM, Rombaoa C, Flores L, Obad S et al. LNA-mediated anti-miR-155 silencing in low-grade B-cell lymphomas. *Blood*. 2012;120(8):1678–86.

270. Han H-J, Russo J, Kohwi Y, Kohwi-Shigematsu T. SATB1 reprogrammes gene expression to promote breast tumour growth and metastasis. *Nature*. 2008;452(7184):187–93.

271. McInnes N, Sadlon TJ, Brown CY, Pederson S, Beyer M et al. FOXP3 and FOXP3-regulated microRNAs suppress SATB1 in breast cancer cells. *Oncogene*. 2012: 1045–1054.

272. Cory S, Huang DCS, Adams JM. The Bcl-2 family: roles in cell survival and oncogenesis. *Oncogene*. 2003;22(53):8590–607.

273. Sánchez-Beato M, Sánchez-Aguilera A, Piris MA. Cell cycle deregulation in B-cell lymphomas. *Blood*. 2003;101(4):1220–35.

274. Cimmino A, Calin GA, Fabbri M, Iorio MV, Ferracin M et al. miR-15 and miR-16 induce apoptosis by targeting BCL2. *PNAS*. 2005;102(39):13944–9.

275. Chiorazzi N, Rai KR, Ferrarini M. Chronic lymphocytic leukemia. *The New England Journal of Medicine*. 2005;352(8):804–15.

276. García-Muñoz R, Galiacho VR, Llorente L. Immunological aspects in chronic lymphocytic leukemia (CLL) development. *Ann. Hematol*. 2012;91(7):981–96.

277. Honjo T, Kinoshita K, Muramatsu M. Molecular mechanism of class switch recombination: linkage with somatic hypermutation. *Annual Review of Immunology*. 2002;20:165–96.

278. Muramatsu M, Kinoshita K, Fagarasan S, Yamada S, Shinkai Y, Honjo T. Class switch recombination and hypermutation require activation-induced cytidine deaminase (AID), a potential RNA editing enzyme. *Cell*. 2000;102(5):553–63.

279. Oppezzo P, Dighiero G. What do somatic hypermutation and class switch recombination teach us about chronic lymphocytic leukaemia pathogenesis? *Current Top Microbiol. Immunol*. 2005;294:71–89.

280. Marantidou F, Dagklis A, Stalika E, Korkolopoulou P, Saetta A et al. Activation-induced cytidine deaminase splicing patterns in chronic lymphocytic leukemia. *Blood cells, molecules & diseases*. 2010;44(4):262–7.

281. Komeno Y, Kitaura J, Watanabe-Okochi N, Kato N, Oki T et al. AID-induced T-lymphoma or B-leukemia/lymphoma in a mouse BMT model. *Leukemia*. 2010;24(5):1018–24.

282. Lee SC, Bottaro A, Chen L, Insel RA. Mad1 is a transcriptional repressor of Bcl-6. *Molecular Immunology*. 2006;43(12):1965–71.

283. Dent AL, Vasanwala FH, Toney LM. Regulation of gene expression by the proto-oncogene BCL-6. *Critical Reviews in Oncology/Hematology*. 2002;41(1):1–9.

284. Dogan A, Bagdi E, Munson P, Isaacson PG. CD10 and BCL-6 expression in paraffin sections of normal lymphoid tissue and B-cell lymphomas. *The American Journal of Surgical Pathology*. 2000;24(6):846–852.

285. Sandhu SK, Volinia S, Costinean S, Galasso M, Neinast R et al. miR-155 targets histone deacetylase 4 (HDAC4) and impairs transcriptional activity of B-cell lymphoma 6 (BCL6) in the Eμ-miR-155 transgenic mouse model. *PNAS*. 2012;109(49):20047–52.

286. Rai D, Karanti S, Jung I, Dahia PLM, Aguiar RCT. Coordinated expression of microRNA-155 and predicted target genes in diffuse large B-cell lymphoma. *Cancer genetics and cytogenetics*. 2008;181(1):8–15.

287. Zhao L, Glazov EA, Pattabiraman DR, Al-Owaidi F, Zhang P et al. Integrated genome-wide chromatin occupancy and expression analyses identify key myeloid pro-differentiation transcription factors repressed by Myb. *Nucleic Acids Research*. 2011;39(11):4664–79.

288. Krützfeldt J, Rajewsky N, Braich R, Rajeev KG, Tuschl T et al. Silencing of microRNAs in vivo with “antagomirs”. *Nature*. 2005;438(7068):685–9.

289. Lieu YK, Reddy EP. Conditional c-myb knockout in adult hematopoietic stem cells leads to loss of self-renewal due to impaired proliferation and accelerated differentiation. *PNAS*. 2009;106(51):21689–94.

290. Zuber J, Rappaport AR, Luo W, Wanq E, Chen C et al. An integrated approach to dissecting oncogene addiction implicates a Myb-coordinated self-renewal program as essential for leukemia maintenance. *Genes dev*. 2011;25(15):1628–40.

291. Zuber J, Brodin-Sartorius A, Lapidus N, Patey N, Tosolini M et al. FOXP3-enriched infiltrates associated with better outcome in renal allografts with inflamed fibrosis. *Nephrology, dialysis, transplantation*. 2009;24(12):3847–54.

292. Baer MR, Augustinos P, Kinniburgh AJ. Defective c-myc and c-myb RNA turnover in acute myeloid leukemia cells. *Blood.* 1992;79(5):1319–26.

293. Luger SM, O`Brien SG, Ratajczak J, Mick R, Stadtmauer EA et al. Oligodeoxynucleotide-mediated inhibition of c-myb gene expression in autografted bone marrow: a pilot study. *Blood*. 2002;99(4):1150–1158.

Other sources of literature (internet links):

[1] http://moon.ouhsc.edu/kfung/jty1/HemeLearn/HemeCase/PB-001-Ans.htm (B-CLL cells blood smear picture)

[2] http://www.ncbi.nlm.nih.gov/gene/114614 (*MIR155HG* gene)

[3]http://www.ebi.ac.uk/ebisearch/search.ebi?query=MYB&db=allebi&requestFrom=searchBox&submit=Search (*MYB* gene)

[4] http://ncicll.com/(WHO B-CLL classification)

[5]http://www.stemcell.com/en/Products/All-Products/RosetteSep-Human-B-Cell-Enrichment-Cocktail.aspx (Rosette separtion scheme)

[6]http://www3.appliedbiosystems.com/cms/groups/mcb_support/documents/generaldocuments/cms_041461.pdf (TaqMan qRT-PCR)

[7] http://bioinfogp.cnb.csic.es/tools/venny/index.html (Wenn diagram)

[8] http://clinicaltrialsfeeds.org/clinical-trials/show/NCT00780052 (MYB trial study, 2008)

miR-155 target gene databases:

PicTar: http://pictar.mdc-berlin.de/

Targetscan: http://www.targetscan.org/

Microrna: http://www.microrna.org/

Microcosm: http://www.ebi.ac.uk/enright-srv/microcosm/

TargetsDiana: http://diana.cslab.ece.ntua.gr/tarbase/

GSEAset: http://www.broadinstitute.org/gsea/msigdb/cards/AGCATTA,MIR-155.html

MYB target gene databases:

Set MYB TARGETS GENEGO: http://www.genego.com/

Set MYB TARGETS RULAI.CSHL.EDU: http://rulai.cshl.edu/cgi-bin/TRED/

Our GSEA data are available at: http://www1.lf1.cuni.cz/~vkulv/gsea

10. SUPPLEMENT

Supplemental table 10.1: Clinical and expression data of patient cohort from General Faculty Hospital in Prague (at the last page of the Thesis).

Supplemental table 10.2: Clinical and expression data of patient cohort from University Hospital and Medical Faculty Brno (at the last page of the Thesis).

Supplemental table 10.3: Clinical and expression data of healthy donors (controls) from Institute of Hematology and Blood Transfusion in Prague.

Sample info					Expression (fold change)						
Code of sample	Date of sample	Gender	Donors age at the date of sample	Sample origin (PBMC or CD19+)	miR-155	PU.1	MYB	miR-150	pri-miR-155	FOS	MYC
C63	24.8.2009	M	36	PBMC	NA	NA	0,51	NA	ND	ND	ND
C76	10.9.2010	M	22	PBMC	0,61	NA	1,68	NA	ND	ND	ND
C77	10.9.2010	M	20	PBMC	1,17	1,17	1,78	NA	ND	ND	ND
C83	27.10.2010	M	22	PBMC	NA	NA	NA	NA	ND	ND	ND
C81	26.10.2010	M	31	PBMC	NA	NA	0,21	NA	ND	ND	ND
C84	27.10.2010	M	22	PBMC	NA	NA	0,61	NA	ND	ND	ND
C93	6.2.2010	M	31	PBMC	0,44	0,83	0,72	0,99	ND	ND	ND
C94	6.2.2010	M	29	PBMC	0,34	1,58	0,73	0,98	ND	ND	ND
C95	6.9.2010	M	38	PBMC	0,46	0,77	0,60	1,01	ND	ND	ND
C96	7.9.2010	M	38	PBMC	0,42	0,65	0,47	1,02	ND	ND	ND
C51	14.7.2010	M	38	CD19+	1,11	0,44	NA	1,53	0,04	0,61	0,74
C52	20.7.2009	M	28	CD19+	0,87	0,33	NA	NA	NA	0,58	1,05
C53	20.7.2009	M	35	CD19+	0,98	0,66	0,00	0,76	0,01	0,77	0,72
C55	27.7.2009	M	30	CD19+	0,62	2,78	0,00	0,59	0,02	3,23	2,07
C56	8.3.2009	M	35	CD19+	2,40	0,93	0,06	2,30	0,06	0,31	1,29
C57	8.3.2009	M	29	CD19+	1,30	0,56	NA	1,69	0,03	0,13	1,71
C58	8.10.2009	M	31	CD19+	0,44	0,47	0,01	1,07	0,00	1,16	1,88
C60	17.8.2009	F	29	CD19+	NA	0,70	NA	NA	0,38	0,25	0,35
C62	24.8.2009	M	43	CD19+	0,77	0,67	0,01	0,89	0,03	1,34	0,51
C75	10.6.2009	F	25	CD19+	0,93	0,55	0,01	NA	0,70	0,57	1,01
C46	29.6.2009	M	35	CD19+	0,46	2,95	0,01	NA	1,45	NA	0,57
C47	29.6.2009	M	28	CD19+	0,78	0,97	0,00	NA	0,13	1,18	0,09

Supplemental material 10.1: Restriction maps of plasmids

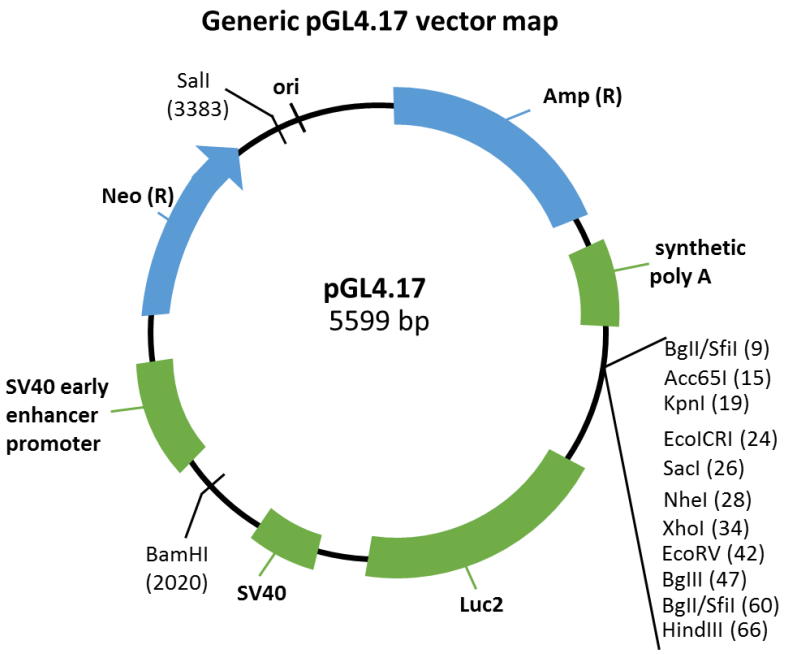

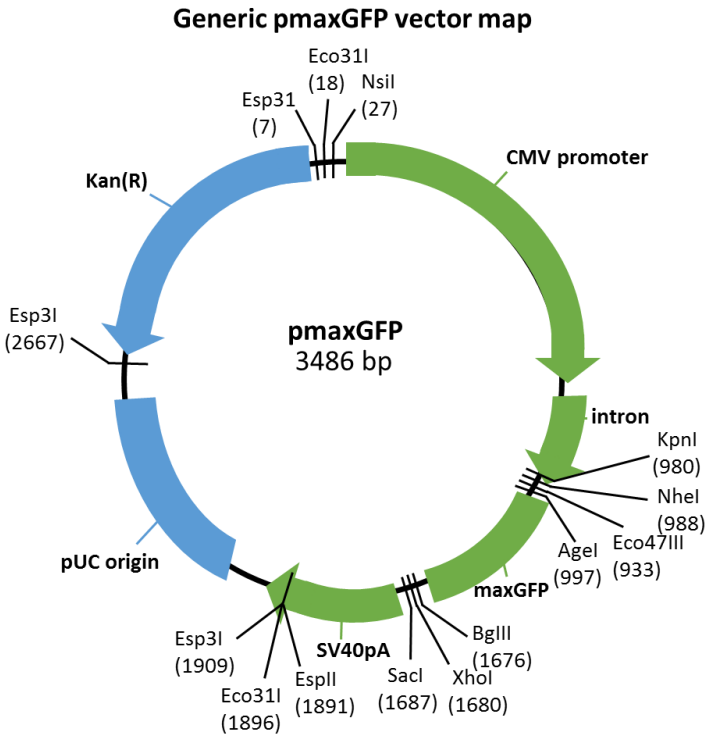

Generic pcDNA3.1 (+/-) vector map

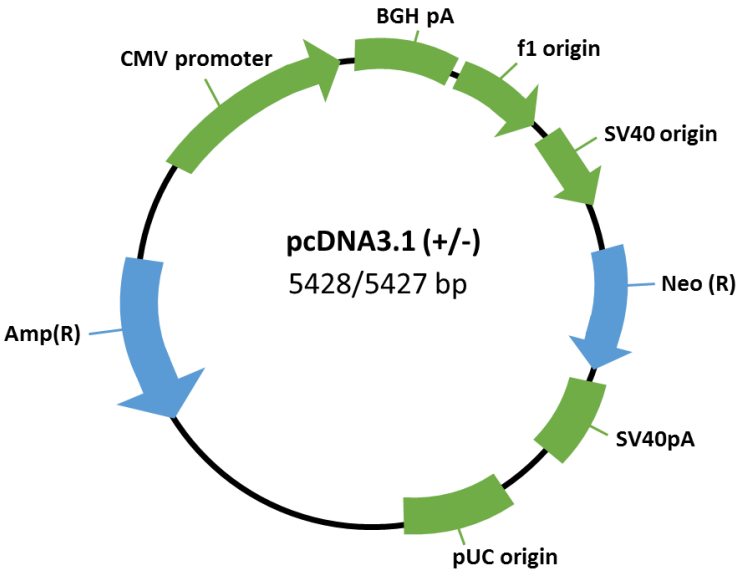

Generic PU.1-IRES-GFP vector map

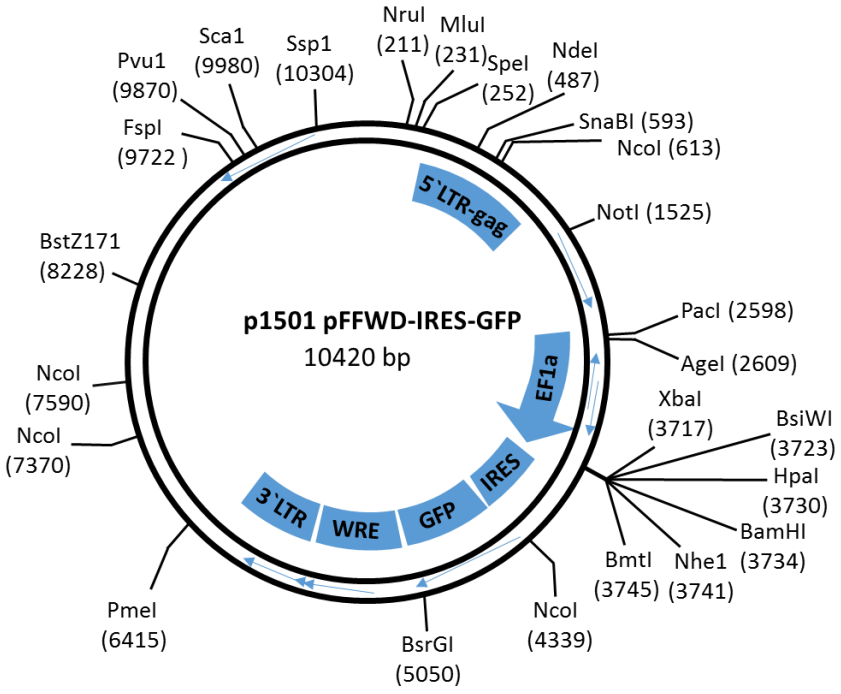

Generic pcDNA3.1 (+) c-myb vector map

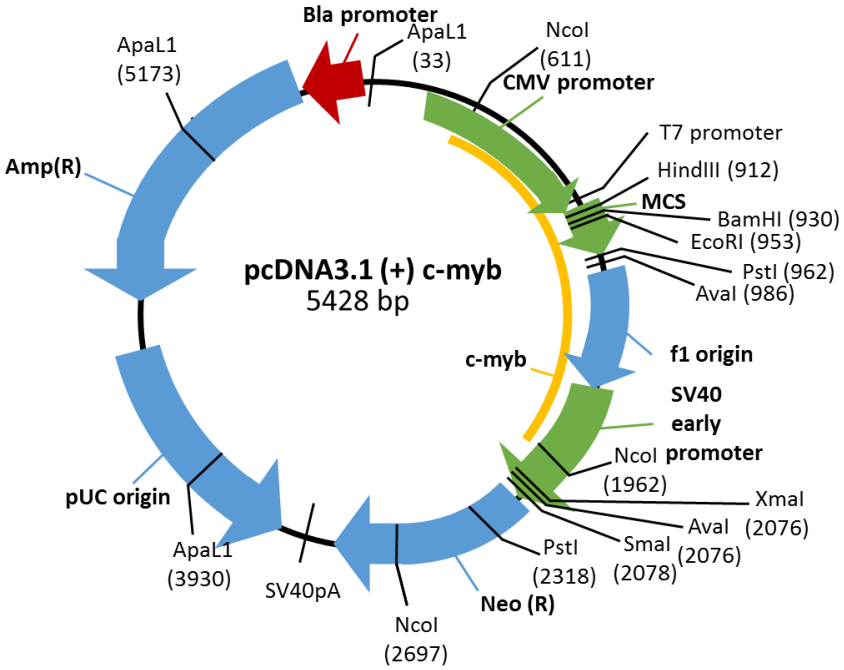

Supplemental material 10.2: Detailed protocols.

Isolation of peripheral blood mononuclear cells (PBMCs) by Ficoll – Paque:

1) Dilute the peripheral anti-coagulated blood with sterile 1xPBS in ratio 1:1.

2) Load carefully diluted blood sample on the Ficoll-Paque PREMIUM layer in ratio 1:1.

3) Centrifuge at 2000rpm for 25min at 18-20°C; with brake off and use swing out rotor.

4) Harvest and wash the PBMCs ("foggy ring") with sterile 1xPBS (3x volume) at 1500rpm for 6min at 4°C.

5) The separated PBMCs can be now used for culturing or RNA/miRNA or DNA isolating or can be frozen for future experiments.

Isolation of CD19+ B-cells by RosetteSep kit:

1) To the 1mL of the whole anti-coagulated blood add 50µL of RosetteSep®Human B Cell Enrichment Cocktail and incubate for 20min at room temperature. (NOTE: If you have frozen blood cells, thaw the cells and wash with sterile 1xPBS supplemented with 2% of FBS; then follow the protocol).

2) Dilute the sample with sterile 1xPBS with 2% of FBS in ratio 1:1 and mix gently.

3) Load carefully the diluted blood sample on the Ficoll-Paque PREMIUM layer in ratio 1:1.

4) Centrifuge at 2000rpm for 20min at 18-20°C; with brake off; with swing out rotor.

5) The desired CD19+ B-cells will be at the interlayer between Ficoll-Paque and plasma.

6) Wash desired CD19+ B-cells with sterile 1xPBS (3x volume) at 1500rpm for 6min at 4°C.

6) The desired CD19+ B-cells (untouched) can be used for culturing or RNA/miRNA/DNA isolation or can be frozen for future experiments.

Lysis of erythrocytes by ammonium chloride (NH_4Cl):

1) Warm the solution of NH_4Cl up to 37°C.

2) To the 1mL of peripheral blood add 49mL (50x) of warmed up NH_4Cl and invert the tube several times, incubate at 37°C for 15-20min (in shaking incubator).

3) Centrifuge the cells after lysis at 1500rpm for 10min at 4°C.

4) Aspirate the supernatant and the cell pellet resuspend in 10mL of 1xPBS and centrifuge as in the step 3.

5) Resuspend the cell pellet in the appropriate culture medium or start the isolation of RNA, DNA or just freeze the cell pellet for later analysis. (NOTE: freezing medium contains 90% of FBS and 10% of DMSO).

Magnetic separation of CD19+ B-cells by MACS magnetic beads:

1) Determine the cell number and wash cells with MACS buffer (5mL).

2) Pellet the cells by centrifuging at 1500rpm for 10min at 4°C.

3) To the cell pellet add 7µL of anti-CD19 FITC antibody and incubate on ice for 20min.

4) Wash out the unbound antibody by MACS buffer (3mL), centrifuge at 1500rpm for 10min at 4°C.

5) Add 80µL of MACS buffer to the cell pellet and 20µl of FITC beads per 10^7 cells.

6) Mix well and incubate for 15min in the refrigerator by occasional vortexing.

7) Wash with 3mL of MACS buffer 1500rpm for 10min at 4°C.

8) Aspirate the supernatant completely and resuspend the cell pellet in 500µL of MACS buffer.

9) Prepare appropriate magnetic separator and magnetic column.

10) Rinse the column with appropriate volume of MACS buffer (LS column with 3mL of MACS buffer) and apply the cell suspension onto the empty column reservoir.

11) The fraction of unlabeled cells will pass through the column; collect this fraction into appropriate tube.

12) Wash the column with MACS buffer 3 times (LS column with 3x3mL of MACS buffer).

13) Apply 5mL of MACS buffer onto empty column reservoir and flush out the labeled CD19+ B cell fraction.

14) Centrifuge both fractions (labeled, unlabeled) at 1500rpm for 10min at 4°C and prepare aliquots ($10x10^3$ cells) for flow cytometry measurement.

Transfection of primary B-CLL cells by lipofection reagent DMRIE-c:

1) Grow the cells to ~80% of confluency and determine the cell number.

2) Prior the transfection with DMRIE-c wash the cells ($0.8x10^6$ cells/mL/6 well) with OPTI-MEM medium (2mL).

3) Centrifuge the cells at 1500rpm for 6min at 18-20°C and resuspend in 400µL of OPTI-MEM medium/well.

4) Prepare transfection reactions with the final volume 100µL/well. Transfection reaction contains: DMRIE-c (2µL/reaction) + oligonucleotides (MYB siRNA (30nM) or anti-miR-155 (40nM) or negative control oligonucleotides) + pmaxGFP plasmid (2µg/reaction). Fill up the reaction with OPTI-MEM medium to get the final volume 100µL/well.

5) Apply the transfection reactions on the cells and incubate for 5hrs in humidified atmosphere with 5% CO_2 at 37°C. (NOTE: the transfection reactions should by applied very slowly – by drop-wise).

6) After 5hrs of incubation add the equal volume of cultivation IMDM medium supplemented with 20% FBS and 1% of MEM non-essential amino acids (500µl).

7) After 48-96hrs harvest the cells, isolate RNA and perform RT-qPCR.

Transfection of HeLa cells by lipofection reagent JetPEI:

1) Grow the cells in confluence ~60% and seed $80x10^3$ cells per 24 well tissue plate in 1mL of culture medium (RPMI-1640 supplemented with 10% of FBS).

2) Prepare transfection reactions in the final volume of 100µL.

3) To the 50µL of 150mM NaCl solution add 1.5µg of plasmid DNA. Vortex gently and spin down briefly.

4) To the 50µL of 150mM NaCl solution add 2µL of jetPEI solution. Vortex gently and spin down briefly.

5) Mix the prepared solutions, vortex and spin down. Incubate for 25min at room temperature.

6) Apply 100µL of the prepared solution drop-wise onto the cells and culture cells in humidified atmosphere with 5% CO_2 at 37°C.

7) After 48hrs harvest the cells, prepare cell lysates and perform the reporter gene assay and western blot.

Transfection of Raji cells by Amaxa nucleofector:

1) 24hrs prior to transfection determine the cell number, seed in concentration $2x10^6$ cells per 1/6 well plate and culture in IMDM medium supplemented with 10% of FBS, 1% of MEM non-essential amino acids, but without antibiotics!

2) On the next day, wash the cells with 1xPBS (2mL).

3) Centrifuge the cells at 400g for 6min at 18-20°C and resuspend in 2mL/well of IMDM medium supplemented with 10% of FBS and 1% of MEM non-essential amino acids.

4) Prepare the working nucleofection solution by mixing the nucleofection solution and supplement in ratio 4.5:1.

5) Combine the 100µl of nucleofection solution with: oligonucleotides [MYB siRNA (30nM, 100nM)/anti-miR-155 (40nM, 100nM)/mimic-miR-155 (40nM, 100nM) and appropriate

negative control oligonucleotides] + pmaxGFP plasmid (2µg/reaction) or MYB and control pcDNA plasmids (0.2µg, 2µg).

6) Transfer the cell/RNA/DNA suspension into certified cuvette (sample must cover the bottom of the cuvette without air bubbles), close the cuvette with the cap, insert into nucleofector and select the appropriate nucleofector program M-013 for Raji cell line.

7) Take the cuvette out of the holder once the program is finished and transfer cells immediately into prepared warmed up IMDM medium.

8) Incubate cells in humidified atmosphere with 5% CO_2 at 37°C until analysis.

9) Harvest the cells after 24hrs for mimic hsa-miR-155 transfection and 48hrs for siRNA MYB, anti-miR-155 and plasmid MYB transfections. Isolate RNA and perform RT-qPCR.

Transduction of primary B-CLL cells with lentivirus:

1) Plate $1x10^6$ B-CLL cells* in 24 well plates.

2) For sensitizing of cells add polybrane in the final concentration 8µg/ml.

3) Add the lentivirus with 3 MOI (MOI in range 3-10).

4) Spin the plate for 30min at 1000g 32°C, incubate overnight in the 37°C incubator.

5) Change the culture medium for cells on the next day.

6) After 72hrs harvest cells, isolate RNA and perform RT-qPCR.

* Cell concentration depends on the cell type, lower is better, because lower cell concentration could increase the MOI.

Calculation of MOI: If 60µL of virus (virus titer: $5x10^7$ TU/mL (transduction unit/mL)) was added to $1x10^6$ cells, the MOI will be 3.

MOI = virus amount (mL) x virus titer (TU/mL)/cell number
MOI = 0.06 mL x $5x10^7$TU/mL /$1x10^6$=3 (e.g.).

Luciferase reporter assay:

1) Prepare the luciferase reagent by combining the Dual-Glo® Luciferase buffer with Dual-Glo Luciferase substrate in the ratio 1:100. Mix by inversion until the substrate is thoroughly dissolved.

2) Resuspend the cells in the prepared reagent (75µL/well). (NOTE: Reagents should be added 10min before quantifying the luminescence. For the maximal light intensity, samples should be measured within 2hrs of reagent addition.)

3) In 10min measure the luminiscence on the luminometer.

Control measurements for CD19 purity after MACS separation:

1) Wash the cells ($10x10^3$ cells) with 1xPBS/1% BSA buffer; centrifuge at 400g for 6min at 4°C.

2) Add 7µL/tube of CD19 FITC antibody to the cell pellet and incubate on ice for 20min.

3) Wash the cells with 3mL of 1xPBS/1% BSA buffer; centrifuge at 400g for 6min at 4°C.

4) Resuspend the cell pellet in 300 µL of 1xPBS/1% BSA buffer.

5) Add 1µL of PI and immediately measure on FACS.

AnnexinV staining:

1) Harvest cells (~$1x10^6$ cells) and wash in 1xPBS; centrifuge at 400g for 6min at 4°C.

2) Resuspend the cell pellet in 3mL of 10x diluted binding buffer; centrifuge at 400g for 6min at 4°C.

3) Resuspend cell pellet in 100µL of 1x diluted binding buffer and add 5µL of FITC conjugated AnnexinV, incubate at room temprature for 10-15min in dark.

4) Wash cells in 1x binding buffer and centrifuge at 400g for 6min at 4°C.

5) Resuspend cells in 200 µL of 1x binding buffer and proced FACS analysis.

Western blot:

1) Harvest cells ($3x10^6$); centrifuge at 2000rpm for 5min at RT.

2) Wash the cells with 1xPBS (500µl); centrifuge at 2000rpm for 5min at RT.

3) Lyse the cells in RIPA buffer (200µl) and incubate on ice for 12min. In time intervals 3, 6, 9 and 12min during the incubation time vortex the samples for 15sec.

4) Sonicate the protein lysates on the Sonic Dismembrator with a micro tip (50% amplitude, 3 cycles for 1sec, pause 5sec). Immediately after sonication procedure place the samples on ice for 10min.

5) Determine the protein concentration on Biophotometer. Use Bradford reagent for protein measurement and construct the calibration curve.

6) To the 20ng protein lysate add 6µL of NuPAGE LDS sample buffer (4x) and fill up with the NuPAGE MOPS SDS buffer to the final volume 24µL.

7) Denaturate proteins at 70°C for 10min and immediately load (20ng per lane) on the NuPAGE 10% Bis-Tris gel in NuPAGE MOPS SDS (1x) running buffer. The running conditions are as follows: 80V (15min) - 120V (1hr), 125mA, for 90min.

8) After running the gel, transfer gel into prepared iBlot gel transfer stacks and blot the gel on the PVDF membrane (program: P2, blotting time 7min).

9) To block the unspecific binding, incubate the membrane with 7.5% non-fat milk in PBS/0.1% Tween 20 for 45min on the shaking platform.

10) Incubate with primary antibody (anti-PU.1, anti-MYB, anti-actin) in concentration 1:600 (PU.1, c-MYB) and 1:100 (β-actin) diluted in 7.5% non-fat milk in PBS/0.1% Tween 20 at 4°C overnight.

11) Wash the membrane 3x with 7.5% non-fat milk in PBS/0.1% Tween 20 for 20min on the shaking platform.

12) Incubate with secondary antibody in concentration 1:4000 diluted in 7.5% non-fat milk in PBS/0.1% Tween 20 at room temperature for 1hour on the shaking platform.

13) Wash the membrane 3x with 7.5% non-fat milk in PBS/0.1% Tween 20 for 20min on the shaking platform.

14) For detection of signal use ECLPlus Western blot system; mix an equal volume of detection solution 1 with detection solution 2 allowing sufficient total volume to cover the membrane.

15) Dry the excess of wash buffer from the membrane and place with protein side up on wrap; pipette the mixed detection reagent on to the membrane and incubate for 1min at room temperature.

16) Dry the excess of detection buffer from membrane and place with protein side down on to a fresh piece of wrap; wrap up the blots and gently smooth out any air bubbles. Place the wrapped blots with the protein side up in an X-ray film cassette.

17) Place a sheet of autoradiography film (Hyperfilm ECL) on top of the membrane, close the cassette and expose for e.g. 15 sec. Develop the first piece of film immediately, and on the

basis of its appearance estimate how long to continue the exposure of the second piece of film.

18) After developing of film store the membrane wet and wrapped in a refrigerator at 4°C.

Chromatin immunoprecipitation (ChIP):

1) Harvest the cells (~$1x10^6$) and crosslink with formaldehyde in the final concentration 1% (3mL into 30mL of medium) for 15min at room temperature.

2) Stop the crosslink reaction by adding 2.5M glycine to a final concentration of 0.15M (2.6ml to 50ml mixture); incubate on ice for 5min.

3) Centrifuge the cells at 1900g for 4min at 4°C, remove supernatant and leave on ice for 5 min. Resuspend and rinse the pellets in pre-cold 1xPBS (app. 7.5ml) by up and down pipetting several times and leave on ice for about 30min.

4) Centrifuge at 4000g for 3min to collect pellets. Prepare fresh lysis buffer I, II, III and keep them on ice. (NOTE: during all following steps the cell pellets should be done on ice!)

5) Add to the pellet 10mL of lysis buffer I; mix and centrifuge at 400g for 10min at 4°C.

6) Add to the pellet 10mL of lysis buffer II; mix and leave on ice for10min.

7) Centrifuge at 400g for 10min at 4°C; add 2mL of lysis buffer III to the pellet, mix by short vortex and transfer into 15mL polypropylene tube and follow to sonication step or freeze at -80°C.

8) Sonicate the samples in a dry ice-ethanol cooling bath with 40% intensity (amplitude) in 500 cycles of 2sec of pulses to yield the 200-600bp DNA fragments. Centrifuge at 400g for 10min at 4°C.

9) Add proteinase K buffer (170µL to 20µL of sonicated aliquot), 10µg/tube of RNAse, 10mg/mL of proteinase K and incubate overnight at 37°C.

10) Add 20µL of 3M sodium acetate (pH=7), 2µL of glycogen, 500µL of 96% ethanol and incubate at -20°C for 15min.

11) Centrifuge at max. speed for 15min at 4°C, carefully remove supernatant, wash the pellets with 500µL of 70% ethanol; Centrifuge at max. speed for 10min at 4°C and dry the DNA pellets on air.

12) Dissolve DNA pellets in 25µL of TE buffer by incubating at 37°C for 30min at shaking platform. Run an aliquot of sample on 1% agarose gel to check for presence of 200-300bp DNA bands.

13) Add 5µL of protein A and G beads to the 90µL of immunoprecipitation buffer (IP); centrifuge at 5000g for 5min at room temperature. Resuspend pellet with beads in 150µL of IP buffer and add 30µL of BSA (10mg/mL). Incubate for 2hrs at 4°C on shaking platform.

14) Clear the chromatin by adding 105µL of IP buffer and 10µL of protein A and G beads, gently shake and centrifuge at 400g for 5min at 4°C.

15) To the pellet add 30µL of IP buffer and incubate for 4 hrs (or overnight) at 4°C on shaking platform.

16) Add 1-2µg of antibody per tube (MYB, H3K9acetyl, H3K4methyl and control antibody (IgG)) and incubate for 2hrs at 4°C on shaking platform.

17) Centrifuge at 14000g for 10min at 4°C. Take out 100µL of supernatant as "DNA input" control.

18) Add 100µL of chromatin per 100µL of antibody-beads and add 800µL of IP buffer, incubate overnight at 4°C on shaking platform.

19) On the next day continue the incubation at room temperature for 1hour on the shaking platform.

20) Centrifuge at 5000g for 5min at 4°C, remove supernatant. Add 900µL of IP buffer and centrifuge again.

21) Remove 950µL of supernatant and add 1mL of wash buffer.

22) Centrifuge at 6000g for 6min at 4°C, remove supernatant. Add 900µL of IP buffer and centrifuge again. Repeat step 21 an 22.

23) Add 1mL of wash buffer II and centrifuge at 6000g for 6 at 4°C, remove supernatant.

24) Resuspend pellet in 100µL of proteinase K buffer and add 1µL of proteinase K, 10µL of RNAse per 100µL of buffer. Incubate at 37°C for 30min, overnight at 55°C and 2hrs at 65°C to reverse crosslink.

25) Dilute 10% of input into 2%, 1%, 0.5% ,0.25%, 0.125% and 0.0625% for the preparation of standard curve. Perform the qPCR.

Isolation of mRNA/miRNA from PBMCs, B-cells, Raji cells by TRIzol reagent:

1) Harvest the cells (~$5x10^6$) and centrifuge at 1500rpm for 6min at room temperature.

2) Decant the supernatant completely and resuspend (by up and down pipetting) the cell pellet in 1mL of TRIzol reagent until it´s clear (use syringe with needle), leave for 5 min on the bench to complete the cell lysis. In this step you can stop and store the sample at -80°C or continue RNA isolation.

3) To the TRIzol cell suspension add 200µL of chloroform (CH_3Cl) (20% of the total volume), cap the tube securely and vortex for 20sec. Centrifuge at 11000rpm for 15min at 4°C.

4) Aspirate the clear upper phase (~500µL) into a new eppendorf tube and mix with the same volume of CHCl3, vortex and centrifuge at 11000rpm for 10min at 4°C.

5) Aspirate the upper aqueous clear phase and transfer into new eppendorf tube and add 1µL of linear acrylamid, 500µL of isopropanol, vortex and spin shortly, and precipitate at -20°C overnight.

6) On the next day vortex the tube/s shortly and centrifuge at max. speed (14000rpm) for 30min at 4°C.

7) Decant the supernatant, add 1mL of 75% ethanol, vortex gently and centrifuge at max speed (14000rpm) for 5min at 4°C.

8) Decant the supernatant, spin down shortly and decant the rest of liquid completely, leave the pellet to dry on the air for 3-5 min covered with a paper towel. (NOTE: do not over dry the RNA pellet!).

9) Resuspend the RNA pellet in 10-20µL of nuclease free water with RNAse inhibitors (1%) and analyze the RNA quantity by Nanodrop and quality by Bioanalysator Agilent. Store the RNA at -80%. The good quality RNA should have following parameters: OD A260/A280 as well as the OD A260/A230 ratio=2.0 (or close to 2.0), the RIN (RNA Integrity Number) should be more >7.

Isolation of miRNAs from B-CLL patient plasma samples by miRNAeasy kit:

1) Thaw the plasma on ice. (NOTE: The plasma samples should be kept on ice until step 6!).

2) Cool down the centrifuge for 4°C. Replace 250µl of plasma into 1.5 ml sterile tube. Spin down at 3000g (5500rpm) for 5min at 4°C (keep the supernatant).

3) Transfer 200µl of plasma to a new sterile 1.5 ml tube and add 1mL of QIAzol (5x volume) and vortex for 30sec.

4) Incubate for 5min at room temperature (RT) (20-25°C).

5) Add 200µl of chloroform (in the equal volume to the starting material), vortex and incubate for 2min at RT.

6) Centrifuge at 12000g (10500rpm) for 15min at 4°C.

7) Heat the centrifuge to RT.

8) Transfer the upper aqueous phase (~600µL) into 2ml tube.

9) Add 900µL of ethanol (1.5 volume of obtained aqueous phase) and 25µl of glycogen, mix by pipetting. Incubate the samples for 10min at 4°C.

10) Transfer the 750µl to the RNAeasy mini spin column, centrifuge at 13000g (11500rpm) for 30sec at RT, discard the flow-through. Repeat this step until whole sample is used – remix the suspension by pipetting before loading it again.

11) Discard the flow-through. Wash the column with 700µl of RWT, centrifuge at 13000g (11500rpm) for 1min at RT.

12) Discard the flow-through. Wash the column 3x with 500µl of RPE, centrifuge at 13000g (11500rpm) for 1min at RT. (NOTE: repeat this step 3x).

13) Transfer the column into a new collection tube and spin down at 16000g (14000rpm) for 2min at RT. Leave the tubes open for 2min.

14) Transfer column to the new 1.5 mL eppendorf tube and carefully add 50µl of RNase-free water, the liquid should be centered on the membrane!

15) Incubate for 2min at RT, then centrifuge at 16000g (14000rpm) for 2min at RT.

16) Store the isolated miRNA at -80°C.

The isolated miRNA can be directly used for reverse transcription reaction and followed by TaqMan RT-qPCR.

Supplemental material 10.3: Data from sequencing of B-CLL patient samples and control sample.

MYB F in E-box 2 (from +128bp to +607bp): ACCAAGGAGACGCTCCTGGCACTG

```
C41 (+128) GTCTCGCGCT-CCGCCCGCCTTTCCTCTCTTGAACGTGGCAGGGACGCCGGGGGACTTCS
P89          GTCTCGCGCTCCCGCCCGCCTTTCCTCTCTTGAACGTGGCAGGGACGCCGGGGGACTTCS
P143         -TCTCGCGCT-CCGCCCGCCTTTCCTCTCTTGAACGTGGCAGGGACGCCGGGGGACTTCS

C41      GTGCGAGGGTCACCGCCGGGTTAACTGGCGAGGCAAGGCGGGGGCAGCGCGCACGTGGCC
P89      GTGCKAGGGTCACCGCCGGGTTAACTGGCGAGGCAAGGCGGGGGCAGCGCGCACGTGGCC
P143     YTGCGAGGGTCACCGCCGGGTTAACTGGCGAGGCAAGGCGGGGGCAGCGCGCACGTGGCC

C41      GTGRAGCCCGGCCTGGTCCCGCGCGCGCCTGCGGGTGCCCCCTGGGGACTCAGTGGTGTC
P89      GTGGAGCCCGGCCTGGTCCCGCGCGCGCCTGCGGGTGCCCCCTGGGGACTCAGTGGTGTC
P143     GTGGAGCCCGGCCTGGTCCCGCGCGCGCCTGCGGGTGCCCCCTGGGGACTCAGTGGTGYC

C41      SCCTCGCCCGGGACCAGAGATTGCGCTGGATGGATTCCCGCGGGCAGAGGCAGGGGGAAG
P89      GCCTCGCCCGGGACCAGAGATTGCGCTGGATGGATTCCCGCGGGCAGAGGCAGGGGGAAG
P143     GCCTCGCCCGGGACCAGAGATTGCGCTGGATGGATTCCCGCGGGCAGAGGCAGGGGGAAG

C41       GAGGGGTGTTCGAAACCTAATACTTGAGCTTCTTTGCAAAGTTTCCTTGGATGGTTGGGG
P89       GAGGGGTGTTCRAAACCTAATACTTGAGCTTCTTTGCAAAGTTTCCTTGGAKGGTTGGGG
P143      GAGGGGTGTTCGAAACCTAATACTTGAGCTTCTTTGCAAAGTTTCCTTGGATGGTTGGGG

C41      ACGTACCTGTATAATGGCCCTGGACCAGCTTCCCTGTTGGAGTGGCCAGAGAAGTGTGTA
P89      ACGTACCTGTATAATGGCCCTGGACCASCTTCCCTGTTGGAGTGGCCAGAGAAGTGTGTA
P143     ACGTACCTGTATAATGGCCCTGGACCAGCTTCCCTGTTGGAGTGGCCAGAGAAGTGTGTA

C41      AAACACACTAGAGGGGCAGGGTGGAAAAAGAGACTGCCTTCAAAACTTGTATCTTTTCGA
P89      AAACACACTAGAGGGGCAGGGTGGAAAAAGAGACTGCCTTCAAAACTTGTATCTTTTCWA
P143     AAACACACTAGAGGGGCAGGGTGGAAAAAGAGACTGCCTTCAAAACTTGTATCTTTTCGA

C41 (+548) TTTCATTTTGAAAAATAACTACAAATCTATTTTAATTTTACAAAGTTAGACTCATAGCAT
P89          TTTCATTTTGAAAAW-AACTA-AA-TCTATTTTAATTTTACAAAGTTR-ACTC-TAGY-T
P143         TTTCATTTTGAAAAATAACTACAAATCTATTTTAATTTTACAAAGTTAGACTCATAGCAT
```

Mutations:
+188 (P143)
+546 (P89)

MYB R in E-box 2 (from +119 to -361bp): **CGTCCCTGCCACGTTCAAGAGAGG**

C41 (+119) GCGTACCTGCAGTGCCAGGAGCGTCTCCTTGGTTCCCCGCGCTTGCTCTGCGGGCGGCTC
P89 G-G-AC-TGCAG-G-CA-GA-CGTCTCCTTGGTTCCCCGCGCTTGCTCTGCGGGCGGCTC
P143 GCGTACCTGCAGTGCCAGGAGCGTCTCCTTGGTTCCCCGCGCTTGCTCTGCGGGCGGCTC

C41 GGGGCTCCGCTATCCGCTCCCTTCCCGAGGCTGCAGGCGGCGCTGGGCCCGGGCTCGGCC
P89 GGGGCTCCGCTATCCGCTCCCTTCCCGAGGCTGCAGGCGGCGCTGGGCCCGGGCTCGGCC
P143 GGGGCTCCGCTATCCGCTCCCTTCCCGAGGCTGCAGGCGGCGCTGGGCCCGGGCTCGGCC

C41 GCGCACAGGAAGCCCGCGCCTGCGAACGTGCGACCCTTTTATAACTCACTTGTGACTCAT
P89 GCGCACAGGAAGCCCGCGCCTGCGAACGTGCGACCCTTTTATAACTCACTTGTGACTCAT
P143 GCGCACAGGAAGCCCGCGCCTGCGAACGTGCGACCCTTTTATAACTCACTTGTGACTCAT

C41 AACCGACCAGGCGCCTTTTCTGCAACCCCCCCCCCCTTCYCCCCCCYCCKGCCKGTTYTK
P89 AACCGACCAGGGGCCTTTTCTGCAACCCCCCCCCCCTTCTCTCCCCCCCTC---------
P143 AACCGACCAGGCGCCTTTTCTGCAACCCCCCCCCCCTTYYCCCCCCYCCKGCYKGTTYTK

C41 GGAACCWAMAGYTKGAAAAAYTTTTTTYTTTTWAAAGRAAAARYCAAAAAASCCCMSCSC
P89 ----------
P143 GGAACCWAMAGYTTGAAAAAWTTTTTTCTTTTWAAAGRAAAAGYCRAAAAAGCCCASSSC

C41 CSGGGWAGKKGGGGTTTYCCCCTTTCCCTTTCCCGGGGGGYCWTGGGGGGGGGGTTTTTTT
P89 ----------
P143 CCGGGRAGKKGGGGTTTYCCCCTTTCCCTTTCYCGGGGGKCATTGSGKGGGTGRTTTTTT

C41 TTTCTCCCAACMCMCSCCGGGTACTTTCCTGCCCCGCGCCSCAGGGYTTGGGCTCCAACC
P89 ----------
P143 TTTCTCCCAACMCMCSCCGGGTACTTTCCTGCCCCGCGCCSCARGGSTTGGGCTCCCACC

C41 (-311) TTTGTTCTTAAAAAAAAGGAAACSCCTTCAAAKGASGGCCCAAASGTCSCCCGAACTTTC
P89 ----------
P143 TTTGTTCTTAAAAAAAAGGAAACSCCTTCAAAKGACGGCCCAAAMGTCSCCCGAACTTTC

Mutations:
-234 (P143)
-242 (P143)
-244 (P143)
-307 (P143)

11. LIST OF PUBLICATIONS

Related to the Thesis:

M Pesta, **K Vargova**, J Vargova, N Dusilkova, V Kulvait, P Obrtlikova, A Berkova, K Michalova, M Trneny and T Stopka. Model to understand the clinical relevance of prognostics of CLL in the real time. ***Blood***. 2013. (*in prep.*).

Vargova K, Curik N, Burda P, Basova P, Kulvait V, Pospisil V, Savvulidi F, Kokavec J, Necas E, Berkova A, Obrtlikova P, Karban J, Mraz M, Pospisilova S, Mayer J, Trneny M, Zavadil J, Stopka T. MYB transcriptionally regulates the miR-155 host gene in chronic lymphocytic leukemia. ***Blood.*** 2011 Apr 7; 117(14):3816-25. IF=10.5

Unrelated to the Thesis:

Petra Vlckova, Vit Pospisil, Libor Stanek, Pavel Burda, Filipp Savvulidi, **Karina Vargova**, Martina Kapalova, Erika Kuzmova, Anna Jonasova, Ulrich Steidl, Peter Laslo and Tomas Stopka. Aggressive acute myeloid leukaemia in PU.1/p53 double mutant mice. ***Oncogene***. 2013 (*submitted*).

N Curik, P Burda, **K Vargova**, V Pospisil, M Belickova, P Vlckova, F Savvulidi, E Necas, H Hajkova, C Haskovec, J Cermak, M Krivjanska, M Trneny, P Laslo, A Jonasova and T Stopka. 5-Azacitidine in aggressive myelodisplastic syndromes regulates chromatin structure at *PU.1* gene and cell differentiation cpacity. Luekemia, 2012 Aug; 26(8):1804-11. IF=9.51

Pospisil V, **Vargova K**, Kokavec J, Rybarova J, Savvulidi F, Jonasova A, Necas E, Zavadil J, Laslo P, and Stopka T. Epigenetic silencing of the oncogenic miR-17-92 cluster during PU.1-directed macrophage differentiation. ***EMBO J***. 2011 Sep 6. IF=10.1

Vargova J, **Vargova K**, and Stopka T. Nuclear Localization of Chromatin Remodeling ISWI ATPase Smarca5 (Snf2h) in Mouse. ***Front Biosci.*** E1, 553-559, June 1, 2009. IF=3.308

Kokavec J, Vargova J, Burda P, **Vargova K**, Necas E, Zavadil J, and Stopka T. SWI/SNF2 proteins in germinal and early embryonic development. ***Folia Zool.*** – 58 (Suppl. 1), 2009. IF=0.522